The Geology and Petrology of Mauna Kea Volcano, Hawaii— A Study of Postshield Volcanism

U.S. GEOLOGICAL SURVEY PROFESSIONAL PAPER 1557

AVAILABILITY OF BOOKS AND MAPS OF THE U.S. GEOLOGICAL SURVEY

Instructions on ordering publications of the U.S. Geological Survey, along with prices of the last offerings, are given in the current-year issues of the monthly catalog "New Publications of the U.S. Geological Survey." Prices of available U.S. Geological Survey publications released prior to the current year are listed in the most recent annual "Price and Availability List." Publications that may be listed in various U.S. Geological Survey catalogs (**see back inside cover**) but not listed in the most recent annual "Price and Availability List" may no longer be available.

Reports released through the NTIS may be obtained by writing to the National Technical Information Service, U.S. Department of Commerce, Springfield, VA 22161; please include NTIS report number with inquiry.

Order U.S. Geological Survey publications **by mail** or **over the counter** from the offices listed below.

BY MAIL

Books

Professional Papers, Bulletins, Water-Supply Papers, Techniques of Water-Resources Investigations, Circulars, publications of general interest (such as leaflets, pamphlets, booklets), single copies of Earthquakes & Volcanoes, Preliminary Determination of Epicenters, and some miscellaneous reports, including some of the foregoing series that have gone out of print at the Superintendent of Documents, are obtainable by mail from

U.S. Geological Survey, Information Services
Box 25286, Federal Center
Denver, CO 80225

Subscriptions to periodicals (Earthquakes & Volcanoes and Preliminary Determination of Epicenters) can be obtained ONLY from the

Superintendent of Documents
Government Printing Office
Washington, DC 20402

(Check or money order must be payable to Superintendent of Documents.)

Maps

For maps, address mail orders to

U.S. Geological Survey, Information Services
Box 25286, Federal Center
Denver, CO 80225

Residents of Alaska may order maps from

U.S. Geological Survey, Earth Science Information

OVER THE COUNTER

Books and Maps

Books and maps of the U.S. Geological Survey are available over the counter at the following U.S. Geological Survey offices, all of which are authorized agents of the Superintendent of Documents.

- **ANCHORAGE, Alaska**–Rm. 101, 4230 University Dr.
- **LAKEWOOD, Colorado**–Federal Center, Bldg. 810
- **MENLO PARK, California**–Bldg. 3, Rm. 3128, 345 Middlefield Rd.
- **RESTON, Virginia**–USGS National Center, Rm. 1C402, 12201 Sunrise Valley Dr.
- **SALT LAKE CITY, Utah**–Federal Bldg., Rm. 8105, 125 South State St.
- **SPOKANE, Washington**–U.S. Post Office Bldg., Rm. 135, West 904 Riverside Ave.
- **WASHINGTON, D.C.**–Main Interior Bldg., Rm. 2650, 18th and C Sts., NW.

Maps Only

Maps may be purchased over the counter at the following U.S. Geological Survey offices:

- **FAIRBANKS, Alaska**–New Federal Bldg, 101 Twelfth Ave.
- **ROLLA, Missouri**–1400 Independence Rd.
- **STENNIS SPACE CENTER, Mississippi**–Bldg. 3101

The Geology and Petrology of Mauna Kea Volcano, Hawaii— A Study of Postshield Volcanism

By Edward W. Wolfe, William S. Wise, *and* G. Brent Dalrymple

U.S. GEOLOGICAL SURVEY PROFESSIONAL PAPER 1557

A detailed investigation of the growth and magmatic history of a Hawaiian volcano in its postshield stage

UNITED STATES GOVERNMENT PRINTING OFFICE, WASHINGTON : 1997

U.S. DEPARTMENT OF THE INTERIOR
BRUCE BABBITT, Secretary

U.S. GEOLOGICAL SURVEY
GORDON P. EATON, Director

For sale by U.S. Geological Survey, Information Services
Box 25286, Federal Center, Denver, CO 80225

Published in the Western Region, Menlo Park, Calif.
Manuscript approved for publication July 13, 1994.

Text edited by George A. Havach
Illustrations edited by Taryn A. Lindquist

Library of Congress Cataloging-in-Publication Data

The geology and petrology of Mauna Kea volcano, Hawaii: A study of postshield volcanism / by Edward W. Wolfe, William S. Wise, and G. Brent Dalrymple
p. cm. -- (U.S. Geological Survey professional paper ; 1557)
Includes bibliographical references.
Supt. of Docs. no.: I 19.16:1557
1. Geology--Hawaii--Mauna Kea. 2. Rocks, Igneous--Hawaii--Mauna Kea. I. Wise, William S., 1933- . II. Dalrymple, G. Brent. III. Title. IV. Series.
QE523.M37W65 1997
559.69'1--dc21 97-18869
CIP

CONTENTS

PLATES

FIGURES

TABLES

The Geology and Petrology of Mauna Kea Volcano, Hawaii—A Study of Postshield Volcanism

By Edward W. Wolfe, William S. Wise,[1] and G. Brent Dalrymple

ABSTRACT

The subaerially exposed lavas of Mauna Kea form a cap that conceals the underlying tholeiitic basalts of the volcano's shield stage. Our geologic mapping shows that this postshield cap consists of older basaltic lavas overlain by younger hawaiitic lavas. Thus, the postshield eruptive stage consisted of basaltic and hawaiitic substages. Lavas of the basaltic substage compose the Hamakua Volcanics, which were erupted between approximately 250 and 70–65 ka, whereas those of the hawaiitic substage compose the Laupahoehoe Volcanics, which were erupted between approximately 65 and 4 ka.

Hamakua lavas were erupted both from fissure vents near the summit and from point-source vents marked by cinder cones that are scattered over the flanks of Mauna Kea. Lithologic distinctions and an intercalated glacial deposit permit stratigraphic subdivision of the Hamakua Volcanics on the upper flanks of the volcano. Lower and upper volcanic units, herein named the Hopukani Springs and Liloe Spring Volcanic Members, are separated by the Pohakuloa Glacial Member. A younger glacial deposit, the Waihu Glacial Member, occurs as a lens enclosed, at least in part, within the Liloe Spring Volcanic Member. No consistent criteria exist for stratigraphic subdivision of the Hamakua lavas exposed on the lower slopes.

Laupahoehoe lavas issued from numerous point-source vents, most of which are marked by scoria cones mainly on the upper flanks and summit of the volcano. Air-fall ash and lapilli from the Laupahoehoe eruptions mantle much of the upper slopes, forming scattered tephra blankets and ash dunes. Reworked ash is the dominant component of local slope deposits.

A final glaciation of Mauna Kea's summit occurred between approximately 40 and 13 ka. Till and outwash deposited at that time compose the Makanaka Glacial Member of the Laupahoehoe Volcanics. Laupahoehoe eruptions occurred before, during, and after the Makanaka glacial episode.

The Hamakua Volcanics consist of alkali basalt, transitional basalt, and, among the oldest lavas, rare tholeiitic basalt. Evolved basalts are common, apparently derived by crystal fractionation of olivine-controlled parental magma in reservoirs within the volcano, mostly at shallow levels. Petrologic considerations suggest that these parental magmas originated from partial melting of peridotite at approximately 30-kbar pressure and that the degree of silica saturation reflects the degree of partial melting: Alkali basalt originates from a lesser degree of partial melting, and tholeiitic basalt from a greater degree. Alkali basalt is common on the lower flanks of the volcano but rare on the upper flanks, a difference suggesting that the degree of partial melting decreased outward from beneath the center of the volcano during Hamakua time.

A distinct compositional gap separates the Hamakua and Laupahoehoe lavas. The Laupahoehoe lavas consist mostly of felsic hawaiite to mugearite but include some benmoreite. They are aphyric to somewhat plagioclase phyric and, unlike the underlying basaltic lavas, commonly contain xenoliths of gabbro, peridotite, or pyroxenite. We interpret these hawaiitic magmas as derived from fractionation of basaltic magma in reservoirs below the base of the crust. Little or no additional fractionation occurred during ascent.

The estimated total volume of Mauna Kea is more than 30,000 km^3. Shield-stage lavas represent the bulk of the volcano; the volume of postshield lavas is less than 1,000 km^3. The transition from the shield to the postshield stage occurred before approximately 250 to 200 ka, and we estimate that Mauna Kea volcanism began about 1 Ma. Decreasing magma supply provides a context for the magmatic and volcanic evolution of the volcano. The decreasing supply was accompanied by changing lava composition, from tholeiitic basalt that dominated the shield stage, through transitional and alkali basalt that dominated the postshield basaltic substage, to hawaiitic lava of the postshield hawaiitic substage.

[1] Department of Geological Sciences, University of California, Santa Barbara, CA 93106.

INTRODUCTION

Mauna Kea and Mauna Loa, both volcanoes that rise more than 4,000 m above sea level, dominate the landscape of the Island of Hawaii (fig. 1). Offshore soundings led early students of the Hawaiian volcanoes (Dana, 1890) to realize that these volcanoes were built on a sea floor 5 km deep and are each, therefore, at least 9 km high. Recent seismic-refraction studies, however (summarized by Moore, 1987), have shown that as these piles of lava accumulated, they depressed the sea floor by as much as another 6 km (fig. 1). Thus, the summits of Mauna Kea and Mauna Loa are approximately 15 km above the downwarped substrate, and the volume of each volcano exceeds 32,000 km^3, representing enormous outpourings of magma from localized sources.

Evidence from volcanoes of differing ages suggests that an idealized Hawaiian volcano evolves through a sequence of four eruptive stages—preshield, shield, postshield, and rejuvenated (Clague and Dalrymple, 1987, 1989)—distinguished on the bases of lava composition, eruptive rate and style, and stage of development. No preshield lavas are exposed on the Hawaiian islands. However, dredge samples from the active Loihi Seamount include alkalic basalt and basanite, which led Moore and others (1982) to conclude that Loihi Seamount and, possibly, all Hawaiian volcanoes initially erupt alkalic basalt. Loihi Seamount represents the preshield stage. The shield stage is marked by rapid eruption of tholeiitic basalt. Kilauea and Mauna Loa are vigorously active shield-stage volcanoes; their lavas consist, with rare exception, of tholeiitic basalt, which contains a relatively low concentration of alkalis and, relative to postshield-stage basalt, a relatively high concentration of SiO_2 (Wolfe and Morris, 1996). We infer that the shield-stage lavas of Mauna Kea are composed predominantly of tholeiitic basalt similar to that of Kilauea and Mauna Loa. Postshield volcanism is characterized by relatively slow eruption of alkalic and transitional basalt. Hualalai, Mauna Kea, and Kohala are all capped by postshield lavas, which are more alkalic than the shield-stage basalt (Wolfe and Morris, 1996). The rejuvenated stage, during which small amounts of SiO_2-poor lava are erupted, occurs after as much as a few million years of volcanic quiescence; no volcanoes of the Island of Hawaii have reached this stage.

R.A. Daly, the first petrologist to study the rocks of Mauna Kea (Daly, 1911), realized that the lavas erupted near the summit are distinctly andesitic (we use the term "hawaiitic"; see subsection below entitled "Major Rock Classes and Petrographic Groups"), compositionally more evolved than those of Mauna Loa or the lower flanks of Mauna Kea. All subsequent petrologic investigations of the two volcanoes have concluded that although Mauna Loa is still actively building a shield of tholeiitic basalt with summit and rift-zone eruptions, Mauna Kea had evolved to a later stage with its own characteristic eruptive style and more alkalic lava compositions. On the basis of their reconnaissance mapping, Stearns and Macdonald (1946) described this postshield activity of Mauna Kea, and it became the type example of the "postcaldera stage" of Hawaiian volcanoes (Stearns, 1946).

Postshield lavas cover the entire subaerial surface of Mauna Kea. Recent detailed geologic mapping of these postshield lavas and intercalated sedimentary deposits, and new K-Ar and ^{14}C radiometric data on selected lava flows, provide a new stratigraphic framework for refinement of our ideas concerning the volcanic and petrologic evolution of the volcano. This report presents a detailed analysis of the geologic and magmatic evolution of Mauna Kea Volcano during its postshield stage, which had begun by about 250–200 ka, and an interpretative synthesis of the development of the volcano from its inception to the present.

PREVIOUS MAJOR CONTRIBUTIONS

Previous studies of the geology of Mauna Kea focused primarily on two aspects: the composition and petrology of the lavas, and the glacial deposits and their interrelations with the lavas. We mention briefly here only the major contributions to our geologic understanding of Mauna Kea and elaborate further elsewhere in this report.

R.A. Daly set the stage for subsequent study of Mauna Kea by recognizing that the summit has been glaciated (Daly, 1910) and that the volcano is basaltic on its lower flanks and consists of "andesite" and "trachydolerite" (both hawaiitic in our terminology) on its upper flanks and summit (Daly, 1911). He attributed this apparent stratification to "gravitative differentiation." Daly's analyses of two samples of hawaiite from the upper slopes provided the first compositional data from Mauna Kea. Washington (1923) described and analyzed an additional nine Mauna Kea rocks, including both basalt and hawaiite. These 11 analyses constituted the entire compositional data set for Mauna Kea when Stearns and Macdonald (1946) published their classic volume on the geology of the Island of Hawaii.

Gregory and Wentworth (1937) published an excellent description of the glacial features of the most recent glacial episode; they pointed out that some postglacial volcanic activity had occurred. Wentworth and Powers (1941) recognized that several separate glacial episodes have occurred on Mauna Kea and that the various glacial deposits are interleaved with volcanic rocks. Stearns (1945) clarified the aerial distribution of these glacial deposits. He concluded, however, that only the youngest, his Makanaka Drift, is a glacial deposit; he viewed the other deposits as volcanic explosion breccias or fanglomerates.

Macdonald (1945, 1949) and Stearns and Macdonald (1946) established the fundamental volcanic framework for Mauna Kea. Their geologic map (Stearns and Macdonald,

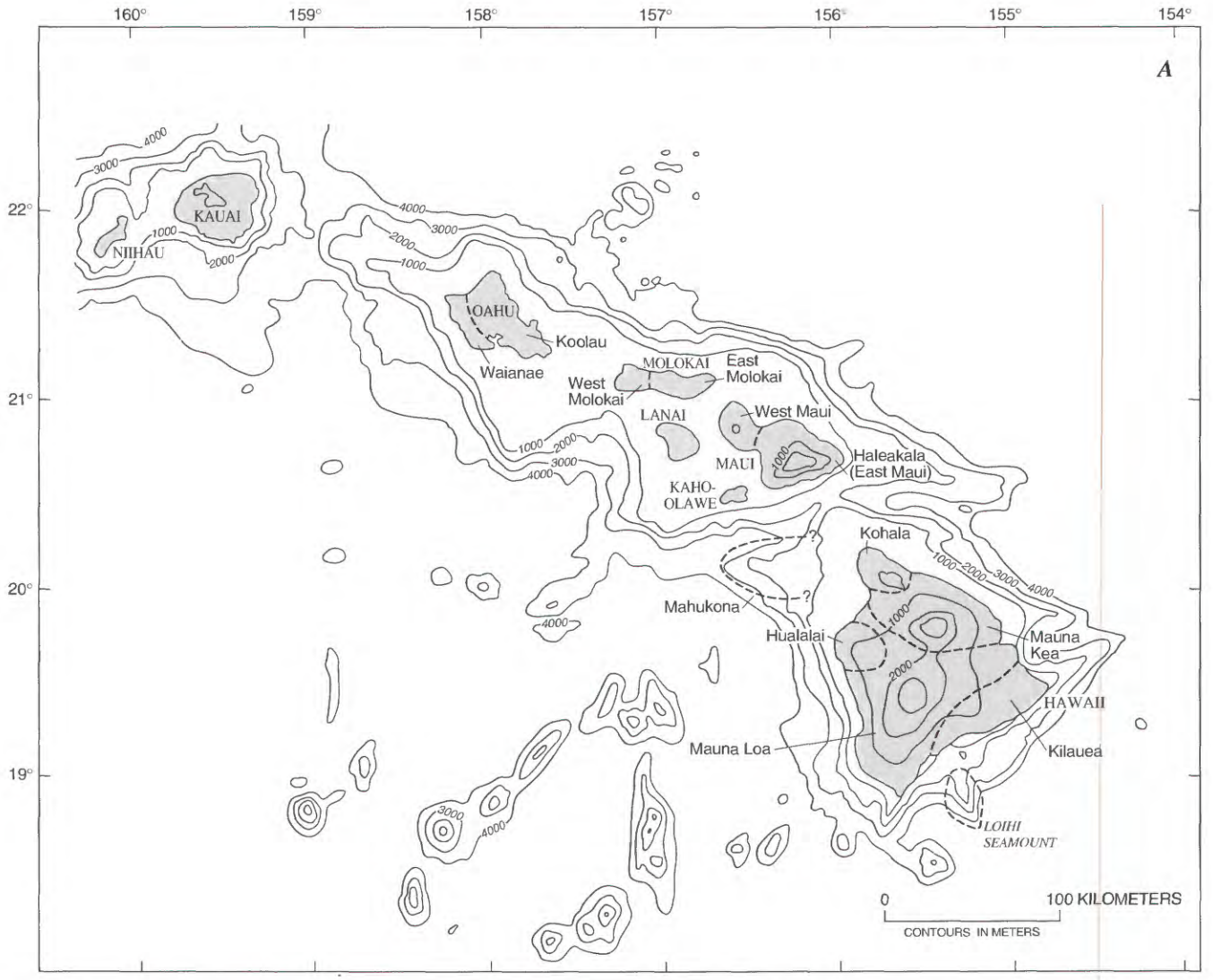

Figure 1. Location, topography, bathymetry, and geographic features of Mauna Kea Volcano. *A*, Generalized topography and bathymetry of southeastern part of the Hawaiian Ridge (Mark and Moore, 1987). Individual volcanoes are identified for those islands composed of more than one shield volcano. Extinct Mahukona Volcano (Clague and Moore, 1991) and youthful Loihi Volcano are identified on submarine flanks of the Island of Hawaii. *B*, Topography and bathymetry of Island of Hawaii, showing areal extent of Mauna Kea Volcano, locations of nearby volcanoes, and contour of surface of oceanic crust beneath volcanoes. Topography modified from U.S. Geological Survey, 1:250,000, Hawaii, 1975; contour interval, 1,000 ft. Bathymetry modified from Chase and others (1980); contour interval, 300 m. Dashed lines represent 100-m contours; hachures point into closed depressions. Structure-contour values calculated by subtracting thickness of crust (5 km; Hill and Zucca, 1987) from structure-contour values for base of crust (in kilometers below sea level) from Moore (1987); in addition, 7-km contour is shifted northwestward to avoid its near-coincidence with surface of oceanic crust on sea floor adjacent to steep flanks of volcanic pile at a depth of approximately 5 km. *A–A′* marks position of cross section shown in figure 3. *C*, Geographic features of Mauna Kea discussed in text. Topographic contours from U.S. Geological Survey, Hawaii County, Sheets 1 and 2, 1980; 4,000-m contour omitted. ag, the aqueduct gulch; HS, Hopukani Springs; HSS, Humuula Sheep Station; LS, Liloe Spring; WS, Waihu Spring.

1946), showing the distribution of their Hamakua and Laupahoehoe Volcanic Series, is a major milestone in the study of Mauna Kea geology. Subsequently, Macdonald and Katsura (1964) and Macdonald (1968) significantly amplified the compositional data set for Mauna Kea and definitively characterized the compositional evolution of Hawaiian volcanoes.

S.C. Porter reexamined the glacial deposits and their relations to the volcanic rocks. He presented compelling evidence that the explosion breccias and fanglomerates of Stearns (1945) are, in fact, glacial deposits. Porter was the first to recognize subglacially erupted lavas on Mauna Kea. He emphasized the importance of the various glacial deposits as markers for subdividing the volcanic rocks, and he

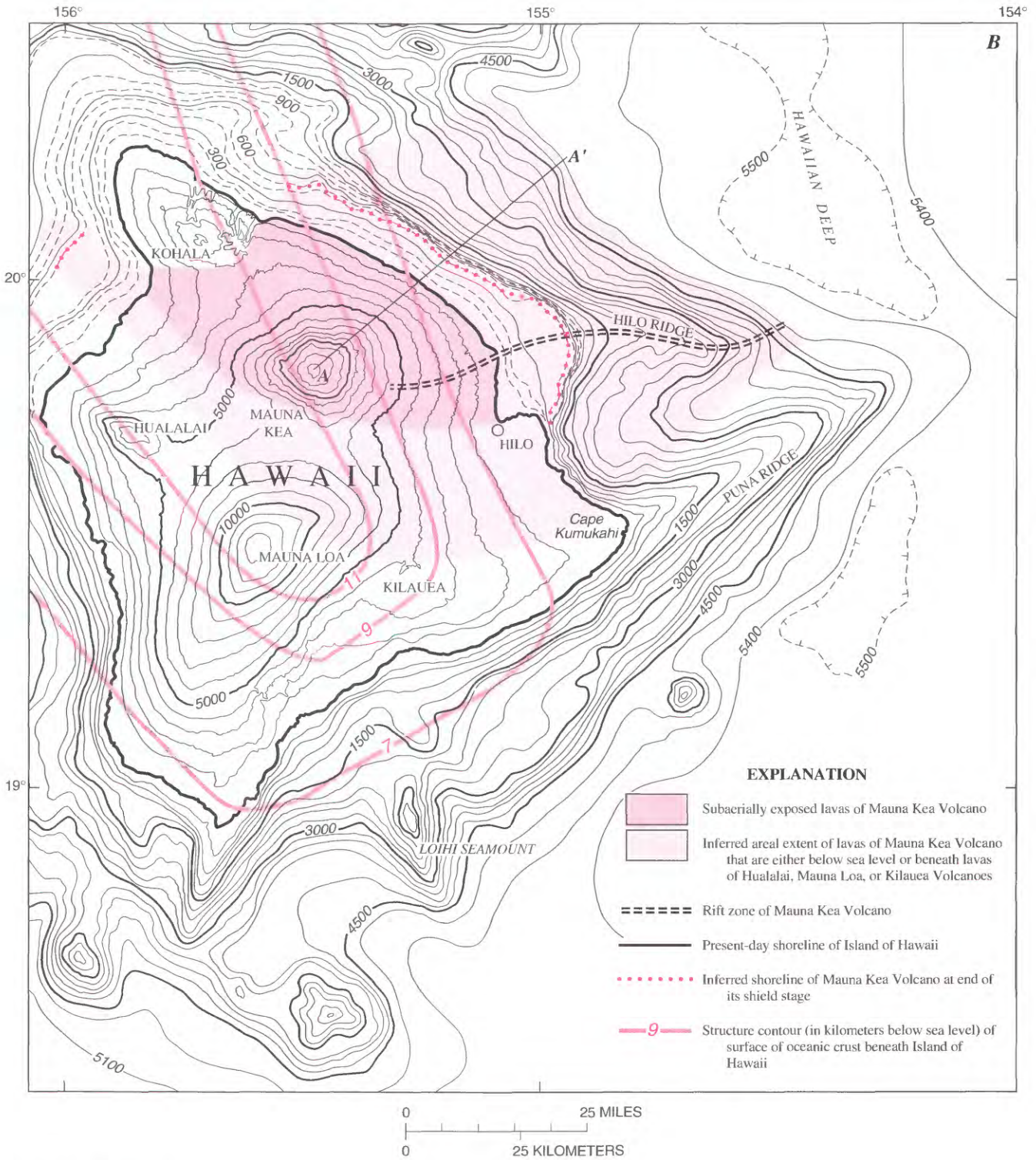

Figure 1. Continued.

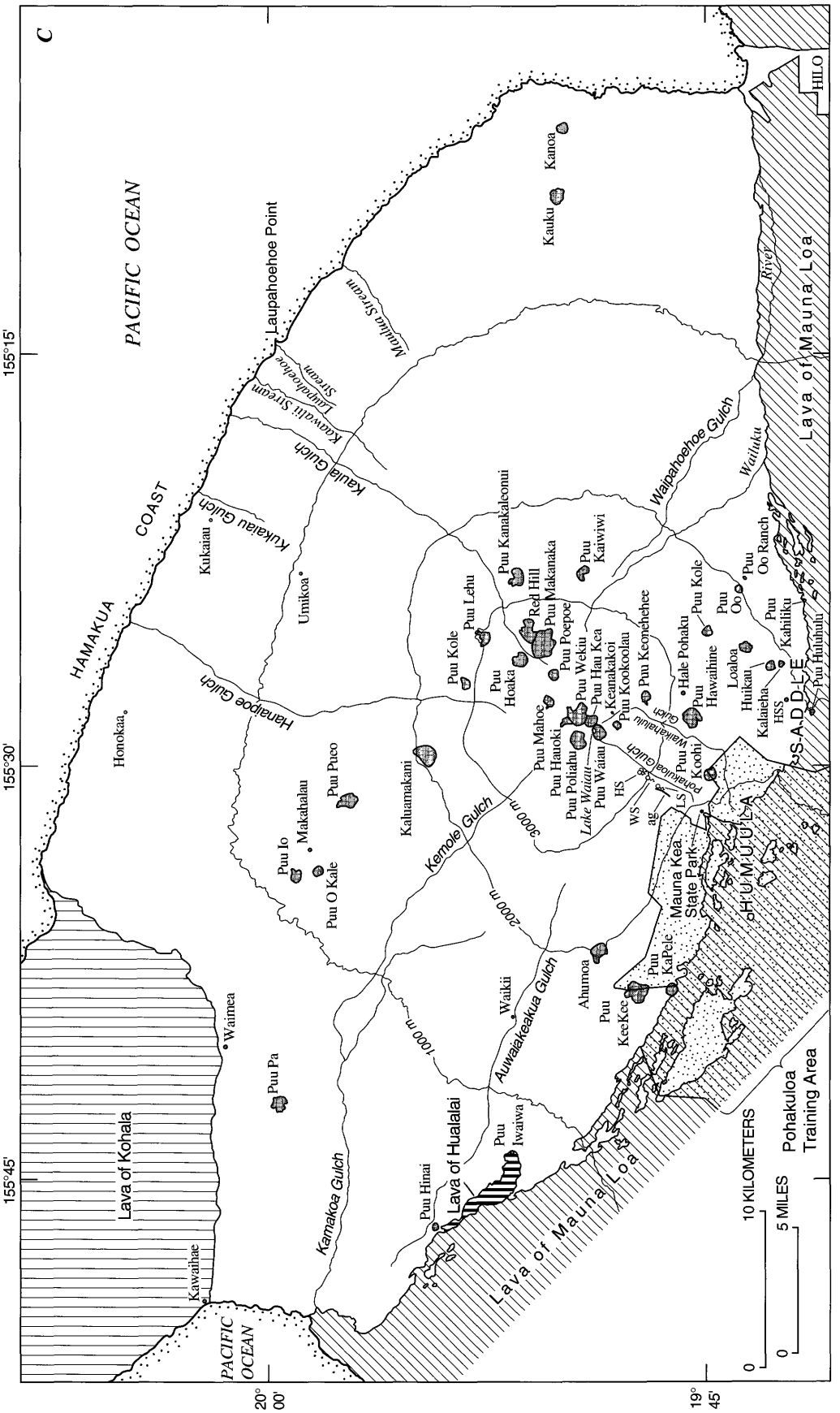

Figure 1. Continued.

also was the first to use isotopic dating to relate the sequence to global glacial events. Porter's studies resulted in a geologic map of the upper parts of Mauna Kea (Porter, 1979a) and a series of published reports treating various aspects of the geology (Porter, 1971, 1972a, b, 1973, 1975, 1979a–d, 1987; Porter and others, 1977).

CURRENT WORK

This report is the culmination of detailed mapping of the entire volcano by Wolfe and Wise (see pls. 1, 2; figs. 12, 22; Wolfe and Morris, 1996), new K-Ar dating by Dalrymple, and assembly of a comprehensive set of major-oxide analyses (table 1) of samples tied to the mapping (see pls. 3, 4). These three components together constitute a powerful data set for evaluating the growth of the volcano in its postshield stage; we examine the volcanic and magmatic record with well-understood stratigraphic and chronologic constraints.

Wise began his new work on Mauna Kea in 1981, spending a total of 8 months during summer field seasons through 1987. During that period, his effort was focused on mapping and sampling the Hamakua Volcanics of the lower flanks to study the petrology of the Hamakua lavas. In addition, he mapped the geology of the southwest and upper west flanks in fall 1987. Wolfe began mapping on the upper south and east flanks and in the summit area in 1986, working there intermittently through 1987. Dalrymple began collecting and dating samples closely tied to the mapping in 1985; that effort continued throughout the remaining period of our study.

Preparation of this report has been a mutual effort in which Wise took the lead in petrologic analysis and in discussion of the Hamakua Volcanics of the lower flanks, Wolfe focused primarily on geologic evaluation of the upper flanks and summit, and Dalrymple was responsible for discussion of the K-Ar dating.

ACKNOWLEDGMENTS

M.A. Kuntz mapped much of the geology of the Umikoa and Makahalau quadrangles, both of which are on the upper north flank of Mauna Kea (fig. 2). Meyer Rubin determined ^{14}C ages on charcoal samples from beneath several lava flows of the younger volcanic rocks member of the Laupahoehoe Volcanics. B.D. Turrin collected samples of and determined K-Ar ages on several lava flows of the Hamakua Volcanics and the older volcanic rocks member of the Laupahoehoe Volcanics. J.C. Dohrenwend gave useful counsel on surficial processes and deposits during the early stages of our mapping on the upper flanks of the volcano, and provided results of a morphometric reconnaissance of Mauna Kea's cinder cones. T.E.C. Keith graciously analyzed alteration minerals in samples from Puu Waiau and Puu Poliahu. F.A. Frey supplied major- and trace-element analyses of selected Mauna Kea lavas. K.J. Murata provided important major-element analyses, notes, and thin sections for lavas he had examined along the lower northeast flank of Mauna Kea. Cartographer Jean Morris was an indispensable colleague in preparation of the map illustrations.

We also thank the managements of the Parker Ranch, the Hamakua Sugar Co., and the Hilo Coast Processing Co. and personnel of the Hawaii Division of Forestry for their helpful cooperation in permitting access to ranchland, plantations, and forestland not normally open to the public.

Finally, we thank M.A. Mangan and W.E. Scott for their helpful reviews.

GEOLOGIC SETTING

The subaerial and submarine contours of the upper surface of the volcano indicate that most of the mass of Mauna Kea lies to the east of the present summit and that the shield apparently had a shape and orientation similar to those of the present-day Kilauea (fig. 1). The central conduit system for Mauna Kea's shield was probably beneath the present summit area, and the only major rift zone extended eastward, where it formed Hilo Ridge. The older Mahukona and Kohala shields and the largely concurrent Hualalai shield buttressed the growing Mauna Kea shield from northwest to southwest, inhibiting the development of a rift zone extending westerly. Conversely, because of the assumed younger age of Mauna Loa, we show Mauna Kea extending beneath the adjacent Mauna Loa shield. Eruptive activity of Mauna Kea was partly contemporaneous with that at Kohala, Hualalai, and Mauna Loa, and the volcano boundaries are undoubtedly complex. Field evidence indicates that lavas of Mauna Kea are intercalated with those of all three of its subaerial neighbors.

Cross sections of volcanoes during their shield stages have a characteristic shape (Moore and Fiske, 1969): Fluid, subaerial flows originating from summit or rift-zone vents slope gently, whereas the submarine slopes, composed of submarine flows and clastic debris fans that form where subaerial flows reached the shoreline, slope more steeply. The average subaerial slope from the shoreline of Kilauea and Mauna Loa up to about 2,000-m elevation is about 4°, whereas below sea level this slope increases abruptly to an average of 13° at 500-m depth (Mark and Moore, 1987). Moore and Fiske (1969) showed that the break in slope at the shoreline is a feature only of shield-stage volcanoes, on which upward growth at the shoreline is sufficiently rapid to keep pace with the subsidence that records isostatic adjustment of the growing volcanic mass (Moore, 1987). Postshield lavas apparently are insufficiently fluid or voluminous to consistently reach the shoreline and maintain the slope break at sea level. Thus, continuing subsidence during the postshield stage progressively submerges the

Table 1. Chemical analyses and normative ne, ol, hy, and q in Mauna Kea lavas

[Major-oxide compositions and partial Cross, Iddings, Pirsson, and Washington (CIPW) norms in weight percent; nd, not determined. Norms were computed from analyses recalculated to 100 percent dry weight after removal of normative calcite and partitioning of Fe to FeO and Fe_2O_3 in the ratio 88:12. Units: h, undivided Hamakua Volcanics; hh, Hopukani Springs Volcanic Member of the Hamakua Volcanics; hl, Liloe Spring Volcanic Member of the Hamakua Volcanics; lo, older volcanic rocks member of the Laupahoehoe Volcanics; ly, younger volcanic rocks member of the Laupahoehoe Volcanics. Rock types (see table 2 and fig. 5): ank, ankaramite; ben, benmoreite; bs, phenocryst-poor basalt; gm, mechanically separated sample of groundmass; h/m, hawaiite or mugearite; olbs, olivine basalt; pic, picrite; plbs, plagioclase basalt; ppbs, porphyritic basalt. Most sample localities are grouped by quadrangle identifier (for example, GQ–18; see pls. 3 and 4 for locations of samples and explanation of locality-numbering system); most others are traverses (for example, La–7) along stratigraphic sections exposed in gulches (Ki, Kaawalii; La, Laupahoehoe; Ma, Maulua; Wa, Waikahalulu; see pls. 3 and 4 for locations of traverses); the remaining samples (for example, Er–21; not plotted) were dredged from Hilo Ridge. Suffix "G" identifies mechanically separated groundmass from the same flow as the sample with otherwise-identical sample-locality number. do, ditto. The data of this table are available as a digital electronic file (Wolfe, 1997)]

Remarks: a, Dredged from Hilo Ridge (D.L. Peck, unpub. data, 1965). Collection depths: Er–20, 1,650 m; Er–21, 2,740 m; Er–22, 3,200 m. Classical chemical analyses; analyst, E.S. Daniels, U.S. Geological Survey, Denver, Colo.

b, X-ray-fluorescence analyses. H_2O specifically determined only for those samples analyzed for CO_2; otherwise, H_2O content is loss on ignition. Analysts: A.J. Bartel, E. Robb, D. Siems, K. Stewart, and J.E. Taggart, U.S. Geological Survey, Denver, Colo.

c, X-ray-fluorescence analyses. H_2O content is loss on ignition. Analysts: R. Johnson and J. Evans, U.S. Geological Survey, Reston, Va.

d, X-ray-fluorescence analyses; analyst, F.A. Frey, Massachusetts Institute of Technology, Cambridge, Mass.

e, Collected by K.J. Murata (unpub. data, 1961–66). Classical chemical analyses; analysts: P. Buschman, E.S. Daniels, E.L. Munson, D.F. Powers, and R.T. Okamura, U.S. Geological Survey, Denver, Colo.

Sample Locality No.	Unit	Feature	Type	Laboratory No.	Remark	Major oxides													Partial CIPW norm			
						SiO_2	Al_2O_3	Fe_2O_3	FeO	MgO	CaO	Na_2O	K_2O	H_2O	TiO_2	P_2O_5	MnO	CO_2	Total	ne	ol	hy	q
Er-20	--	Flow	pic	D100696	a	47.94	10.43	2.03	9.54	17.34	7.42	1.99	0.39	0.58	1.98	0.24	0.17	0.02	100.07	0.00	23.02	19.20	0.00
Er-21	--	do-	pic	D100697	a	47.28	10.00	2.30	9.05	19.82	7.55	1.59	.26	.51	1.46	.14	.17	.01	100.14	.00	28.65	17.82	.00
Er-22	--	do-	olbs	D100698	a	47.01	12.12	2.86	9.29	12.61	8.98	2.36	.72	1.07	2.48	.27	.17	.02	99.96	.00	21.90	6.96	.00
GP-36	lo	do-	h/m	D-276075	b	49.10	17.00	12.40	nd	4.46	7.35	4.51	1.76	.00	3.09	.84	.21	nd	100.72	2.70	14.11	.00	.00
GP-37	lo	Cone	h/m	D-276073	b	49.80	16.90	11.80	nd	4.03	7.04	4.56	1.90	.00	2.76	.96	.22	nd	99.97	1.36	13.66	.00	.00
GQ-9	lo	do-	h/m	D-276026	b	50.20	17.00	12.00	nd	4.13	7.09	4.16	1.84	.00	2.91	.89	.22	nd	100.44	.00	10.66	4.91	.00
GQ-11	lo	Flow	h/m	W-235826	c	49.25	17.59	11.54	nd	4.17	6.99	4.86	1.86	nd	2.67	.77	.22	nd	99.92	4.42	13.68	.00	.00
GQ-18	lo	Cone	h/m	D-276061	b	50.20	17.00	11.60	nd	4.16	7.03	4.67	1.88	.00	2.79	.88	.22	nd	100.43	1.72	13.41	.00	.00
GQ-19	lo	do-	h/m	D-276060	b	50.00	17.00	11.80	nd	4.18	7.08	4.82	1.88	.00	2.83	.90	.22	nd	100.71	3.07	13.31	.00	.00
GQ-21	lo	Flow	h/m	D-276074	b	48.50	16.70	12.30	nd	4.60	7.42	4.51	1.70	.24	3.13	.79	.21	nd	100.10	3.38	13.93	.00	.00
GQ-22	lo	do-	h/m	D-284775	b	49.10	16.80	12.30	nd	4.47	7.37	4.29	1.72	.00	3.11	.81	.21	nd	100.18	1.13	14.15	.00	.00
GQ-23	lo	Cone	h/m	D-276063	b	48.60	16.80	12.40	nd	4.66	7.45	4.15	1.67	.00	3.09	.82	.21	nd	99.85	.92	14.82	.00	.00
GR-12	lo	do-	h/m	D-276026	b	49.30	16.90	12.00	nd	4.19	7.18	4.30	1.77	.35	2.94	.89	.22	nd	100.04	.32	14.12	.00	.00
GR-13	lo	Flow	h/m	D-276025	b	48.50	16.80	12.50	nd	4.60	7.30	4.25	1.69	.00	3.16	.79	.21	nd	99.80	1.54	14.73	.00	.00
GR-14	lo	Cone	h/m	D-276036	b	49.20	17.10	11.90	nd	3.87	6.95	4.20	1.77	1.16	2.76	.94	.22	nd	100.07	.00	12.27	3.06	.00
GR-15	ly	Flow	h/m	D-276035	b	50.60	17.00	11.60	nd	3.96	6.77	4.82	1.93	.00	2.67	.93	.22	nd	100.50	1.72	13.41	.00	.00
GR-16	ly	do-	h/m	D-276034	b	50.40	17.00	11.50	nd	4.02	6.81	4.60	1.90	.00	2.67	.91	.22	nd	100.03	.56	13.71	.00	.00
GR-17	lo	Cone	h/m	D-276024	b	49.30	16.90	12.10	nd	4.35	7.30	4.40	1.80	.05	3.05	.87	.22	nd	100.34	1.45	13.90	.00	.00
GR-18	lo	Flow	h/m	D-276041	b	50.60	17.40	10.70	nd	3.32	6.47	4.80	2.08	.71	2.29	1.26	.22	nd	99.85	.21	13.34	.00	.00
GR-19	lo	do-	h/m	D-276027	b	48.70	17.00	12.10	nd	4.31	7.35	4.35	1.68	.25	3.02	.90	.22	nd	99.88	1.40	14.19	.00	.00
GR-20	lo	do-	h/m	D-276042	b	50.50	17.00	11.30	nd	3.78	6.72	4.80	2.00	.00	2.58	1.03	.22	nd	99.93	1.36	13.23	.00	.00
GR-21	lo	Cone	h/m	D-284786	b	50.30	17.10	11.90	nd	4.06	6.95	4.35	1.88	.00	2.79	.91	.22	nd	100.46	.00	12.83	1.89	.00
GR-22	lo	Flow	h/m	D-276043	b	49.80	16.90	11.80	nd	4.12	7.01	4.64	1.85	.00	2.83	.89	.22	nd	100.06	1.85	13.57	.00	.00
GR-23	lo	do-	h/m	D-276029	b	49.80	17.00	11.90	nd	4.17	7.09	4.48	1.81	.00	2.88	.90	.22	nd	100.25	.85	13.92	.00	.00
GR-24	lo	Cone	h/m	D-276044	b	50.80	17.50	11.00	nd	3.28	6.33	4.73	2.04	.28	2.33	1.15	.22	nd	99.66	.00	12.28	1.93	.00
GR-25	ly	Flow	h/m	D-276037	b	50.70	17.00	11.60	nd	3.99	6.82	4.64	1.94	.21	2.67	.92	.22	nd	100.71	.58	13.62	.00	.00
GR-26	lo	do-	h/m	D-276030	b	49.40	16.90	12.20	nd	4.42	7.26	4.38	1.79	.00	3.05	.85	.22	nd	100.47	1.29	14.15	.00	.00
GR-27	lo	do-	h/m	D-276028	b	49.80	17.00	12.10	nd	4.27	7.13	4.36	1.82	.00	2.95	.89	.22	nd	100.54	.35	14.23	.00	.00
GR-28	lo	Cone	h/m	D-276048	b	50.00	17.90	10.90	nd	3.39	6.56	4.50	1.74	1.24	2.34	1.28	.23	nd	100.08	.00	9.83	6.66	.00
GR-29	lo	do-	h/m	D-284782	b	49.70	16.90	11.70	nd	4.09	7.05	4.45	1.85	.58	2.77	.89	.22	nd	100.20	.76	13.75	.00	.00
GR-30	ly	Flow	h/m	D-276040	b	50.30	16.90	11.60	nd	3.97	6.77	4.81	1.92	.00	2.66	.92	.22	nd	100.07	1.97	13.42	.00	.00
GR-31	lo	do-	h/m	D-276049	b	51.10	17.20	11.00	nd	3.34	6.43	4.98	2.14	.10	2.28	1.20	.23	nd	100.00	1.10	13.11	.00	.00
GR-32	lo	Cone	h/m	D-276031	b	49.40	16.90	12.00	nd	4.27	7.20	4.54	1.78	.04	2.96	.88	.22	nd	100.19	1.91	13.77	.00	.00
GR-33	lo	do-	h/m	D-284783	b	49.80	17.00	11.90	nd	4.07	7.03	4.40	1.88	.05	2.81	.88	.22	nd	100.04	.54	13.95	.00	.00
GR-34	ly	Flow	h/m	D-276039	b	50.70	17.00	11.50	nd	3.97	6.87	4.67	1.95	.00	2.68	.93	.22	nd	100.49	.87	13.37	.00	.00
GR-35	lo	do-	h/m	D-276032	b	50.80	17.00	11.60	nd	3.95	6.95	4.66	1.94	.00	2.72	.94	.22	nd	100.78	.72	13.26	.00	.00
GR-36	lo	do-	h/m	D-276033	b	50.10	16.90	11.40	nd	3.96	6.92	4.70	1.96	.04	2.69	.93	.22	nd	99.82	1.81	13.11	.00	.00
GR-37	ly	do-	h/m	D-276038	b	50.70	16.90	11.50	nd	3.95	6.82	4.62	1.96	.00	2.66	.93	.22	nd	100.26	.47	13.44	.00	.00
GR-38	lo	Cone	h/m	D-276047	b	50.40	17.10	11.20	nd	3.81	6.85	4.82	2.00	.02	2.62	1.02	.22	nd	100.06	1.95	12.94	.00	.00
GR-39	lo	do-	h/m	D-284781	b	50.50	17.10	11.60	nd	3.87	7.01	4.56	1.94	.00	2.67	.96	.22	nd	100.43	.50	13.39	.00	.00

Table 1. Chemical analyses and normative ne, ol, hy, and q in Mauna Kea lavas—Continued.

Sample Locality No.	Unit	Feature	Type	Laboratory No.	Remark	Major oxides												Partial CIPW norm			
						SiO_2	Al_2O_3	Fe_2O_3	FeO	MgO	CaO	Na_2O	K_2O	H_2O	TiO_2	P_2O_5	MnO	CO_2	Total	ne	ol	hy	q
GR-40	lo	Flow	h/m	D-284780	b	50.30	16.90	11.40	nd	3.96	6.95	4.35	1.91	0.00	2.73	0.94	0.22	nd	99.66	0.00	11.57	2.69	0.00
GR-41	lo	do-	h/m	D-284779	b	50.80	17.20	11.20	nd	3.88	6.89	4.63	1.95	.00	2.69	.92	.22	nd	100.38	.39	13.08	.00	.00
GR-42	lo	Cone	h/m	D-284784	b	50.40	17.40	10.70	nd	3.56	6.73	4.55	2.04	.88	2.48	1.05	.21	nd	100.00	.00	12.59	.66	.00
GR-43	ly	Flow	h/m	D-278148	b	52.00	17.20	10.80	nd	3.61	6.48	4.90	2.10	.00	2.36	.98	.23	nd	100.66	.14	12.78	.00	.00
GR-44	lo	Cone	h/m	D-284778	b	50.00	16.90	11.90	nd	4.21	6.90	4.42	1.83	.19	2.79	.88	.22	nd	100.24	.08	14.35	.00	.00
GR-45	lo	Flow	h/m	D-284785	b	48.70	17.10	12.10	nd	4.03	7.32	4.20	1.86	.65	2.94	.93	.22	nd	100.05	.90	14.08	.00	.00
GR-46	lo	Cone	h/m	D-284777	b	50.20	17.10	11.60	nd	3.82	6.89	4.40	1.85	.22	2.66	.96	.22	nd	99.92	.00	12.05	2.49	.00
GS-9	h	Flow	bs	D-276045	b	46.40	14.10	14.80	nd	6.21	10.30	2.96	.99	.10	4.05	.56	.20	nd	100.67	.17	14.02	.00	.00
GS-11	h	do-	bs	D-276046	b	44.80	14.60	13.20	nd	7.90	12.30	1.97	.22	1.84	3.08	.37	.18	nd	100.46	.00	12.34	5.18	.00
GS-15	lo	do-	h/m	D-276050	b	50.50	17.20	11.20	nd	3.56	6.70	4.92	2.06	.06	2.42	1.14	.22	nd	99.98	1.96	13.13	.00	.00
HP-1	lo	Cone	h/m	D-276070	b	50.00	17.40	11.20	nd	3.39	6.69	4.56	1.98	.82	2.59	.91	.22	nd	99.76	.39	13.02	.00	.00
HP-4	lo	do-	h/m	D-276068	b	50.20	17.10	11.30	nd	3.96	6.88	4.83	1.96	.10	2.59	1.01	.22	nd	100.15	2.33	13.30	.00	.00
HP-5	lo	do-	h/m	D-276069	b	49.40	17.10	11.90	nd	4.05	7.05	4.63	1.90	.00	2.84	.99	.21	nd	100.07	2.33	13.79	.00	.00
HP-9	lo	Flow	h/m	D-260896	b	49.30	16.90	12.50	nd	4.51	7.17	4.48	1.74	.00	3.01	.85	.22	.00	100.68	1.89	14.69	.00	.00
HP-11	lo	do-	h/m	D-260899	b	49.90	17.10	12.00	nd	4.09	7.05	4.68	1.85	.00	2.85	.90	.22	.00	100.64	2.11	13.69	.00	.00
HP-13	h	do-	bs	81-36	d	45.99	13.65	14.14	nd	8.32	10.84	2.48	.82	.16	3.23	.42	.20	nd	100.25	.14	17.69	.00	.00
HP-14	h	do-	plbs	81-46	d	45.36	14.81	14.11	nd	7.45	10.55	2.49	.94	.19	3.46	.46	.18	nd	100.00	.27	17.15	.00	.00
HP-15	lo	do-	h/m	81-32	d	49.82	16.97	11.72	nd	4.04	6.88	4.32	1.84	.10	2.76	.83	.22	nd	99.50	.00	13.10	1.36	.00
HP-17	lo	do-	h/m	D-260883	b	49.90	16.90	12.00	nd	4.18	6.96	4.46	1.82	.00	2.81	.88	.22	.00	100.13	.50	14.23	.00	.00
HP-18	h	do-	bs	KM-9	d	47.75	13.64	14.95	nd	5.31	10.00	2.72	.95	.22	3.63	.46	.20	nd	99.83	.00	3.31	13.58	.00
HP-19	h	do-	ppbs	81-19	d	47.48	14.21	14.15	nd	6.42	10.99	2.41	.79	.21	3.24	.40	.20	nd	100.50	.00	6.47	10.84	.00
HQ-2	lo	Cone	h/m	D-284764	b	52.40	17.60	10.30	nd	2.97	6.12	4.74	2.24	.32	2.09	1.24	.23	nd	100.25	.00	6.76	8.50	.00
HQ-3	hh	Flow	pic	H-1	d	43.79	9.57	13.77	nd	17.84	9.91	1.20	.47	nd	2.41	.30	.19	nd	99.45	.00	33.25	3.37	.00
HQ-4	lo	Cone	h/m	D-276056	b	52.20	17.40	10.10	nd	3.00	6.11	5.13	2.33	.39	2.05	1.24	.23	nd	100.18	.43	12.18	.00	.00
HQ-5	hl	Flow	bs	D-276057	b	46.80	14.00	15.10	nd	5.75	10.70	2.88	.71	.05	3.88	.44	.20	nd	100.51	.00	10.42	3.63	.00
HQ-6	lo	Cone	h/m	D-276065	b	50.20	17.00	11.40	nd	3.83	6.79	4.47	1.99	.11	2.64	1.01	.21	nd	99.65	.00	13.31	.52	.00
HQ-7	hl	do-	bs	D-284765	b	47.30	14.20	14.60	nd	6.19	11.20	2.69	.80	.00	3.65	.48	.20	nd	101.31	.00	10.07	4.36	.00
HQ-8	hl	Flow	plbs	D-284774	b	48.00	14.40	13.70	nd	6.67	11.40	2.56	.75	.00	3.23	.38	.19	nd	101.28	.00	8.47	7.08	.00
HQ-9	lo	Cone	h/m	D-276067	b	49.70	17.00	11.40	nd	3.84	6.92	4.73	1.99	.00	2.66	1.01	.21	nd	99.46	2.30	13.15	.00	.00
HQ-10	hl	do-	bs	D-284766	b	47.70	14.00	14.60	nd	6.25	11.00	2.78	.86	.00	3.64	.47	.20	nd	101.50	.00	10.03	4.48	.00
HQ-11	lo	do-	h/m	D-276066	b	49.70	17.10	11.40	nd	3.78	6.97	4.70	1.94	.34	2.69	.99	.21	nd	99.82	2.03	13.06	.00	.00
HQ-12	lo	Flow	h/m	D-292989	b	49.80	17.20	11.50	nd	3.86	6.95	4.67	1.96	.19	2.74	1.02	.21	nd	100.10	1.81	13.36	.00	.00
HQ-13	hl	Cone	bs	D-284773	b	48.10	13.90	15.30	nd	5.48	10.40	2.71	.88	.00	3.83	.47	.21	nd	101.28	.00	3.93	12.66	.00
HQ-14	hl	do-	plbs	D-284772	b	48.20	14.40	13.90	nd	6.25	11.30	2.60	.79	.00	3.31	.40	.19	nd	101.34	.00	6.97	8.31	.00
HQ-15	hl	Flow	bs	D-284771	b	48.00	13.90	14.80	nd	5.81	10.70	2.76	.83	.00	3.73	.44	.20	nd	101.17	.00	6.14	9.31	.00
HQ-16	hh	do-	olbs	D-284770	b	48.70	13.30	13.60	nd	7.29	11.60	2.43	.67	.00	3.40	.35	.18	nd	101.52	.00	4.96	11.70	.00
HQ-17	hl	do-	bs	D-284767	b	48.10	14.00	14.70	nd	5.64	10.50	2.94	.98	.00	3.73	.45	.20	nd	101.24	.00	8.31	5.80	.00
HQ-18	hh	do-	plbs	D-284768	b	48.40	13.30	13.40	nd	8.05	11.60	2.26	.63	.00	2.95	.35	.18	nd	101.12	.00	6.82	11.96	.00
HQ-19	hh	do-	olbs	D-284769	b	48.80	13.50	13.40	nd	6.97	11.90	2.41	.69	.00	2.99	.36	.19	nd	101.21	.00	5.07	10.81	.00
HQ-20	lo	do-	h/m	D-292990	b	50.70	17.30	11.30	nd	3.62	6.74	4.61	2.04	.00	2.43	1.11	.21	nd	100.06	.00	13.58	.19	.00
HQ-21	hl	do-	bs	D-292944	b	47.60	14.10	14.80	nd	5.65	10.40	3.13	1.10	.00	3.96	.56	.20	nd	101.50	.00	12.45	.06	.00
HQ-22	lo	do-	h/m	D-292986	b	50.20	17.10	11.10	nd	3.59	6.79	4.91	2.02	.43	2.51	1.11	.22	nd	99.98	2.28	12.77	.00	.00
HQ-23	lo	do-	h/m	D-292994	b	52.80	17.30	9.47	nd	3.11	5.98	5.20	2.36	.23	1.94	1.01	.21	nd	99.61	.48	11.41	.00	.00
HQ-24	hl	do-	bs	D-292947	b	47.00	14.10	14.60	nd	5.85	10.80	2.96	1.04	.00	3.94	.53	.19	nd	101.01	.33	12.36	.00	.00
HQ-25	hl	do-	bs	D-292948	b	47.10	14.20	14.60	nd	5.81	10.80	3.00	1.02	.00	3.96	.53	.19	nd	101.21	.36	12.29	.00	.00
HQ-26	hl	do-	bs	D-292949	b	47.00	14.50	14.80	nd	5.99	11.20	2.57	.68	.00	3.47	.43	.20	nd	100.84	.00	8.82	6.76	.00
HQ-27	hl	do-	plbs	D-292943	b	47.70	14.30	14.70	nd	5.85	11.20	2.66	.83	.00	3.39	.42	.20	nd	101.25	.00	8.60	6.02	.00
HQ-28	lo	do-	h/m	D-292993	b	51.00	17.40	11.00	nd	3.47	6.83	4.94	2.10	.00	2.38	1.15	.21	nd	100.48	1.79	12.67	.00	.00
HQ-29	lo	do-	h/m	D-292945	b	50.70	16.90	10.90	nd	3.55	6.63	5.01	2.11	.00	2.40	1.12	.22	nd	99.54	2.23	12.52	.00	.00
HQ-30	lo	do-	h/m	D-292946	b	51.20	17.20	10.90	nd	3.50	6.67	5.02	2.12	.00	2.43	1.14	.23	nd	100.41	1.82	12.50	.00	.00
HQ-31	lo	do-	h/m	D-292991	b	50.50	17.10	11.40	nd	4.01	6.88	4.48	1.98	.00	2.65	.95	.22	nd	100.17	.04	13.76	.00	.00
HQ-32	lo	do-	h/m	D-292961	b	51.90	17.30	10.40	nd	3.33	6.56	4.94	2.18	.00	2.32	1.16	.23	nd	100.32	.20	12.18	.00	.00
HQ-33	lo	do-	h/m	D-292957	b	50.60	17.00	11.30	nd	3.87	6.88	4.78	1.99	.00	2.63	.97	.22	nd	100.24	1.64	12.95	.00	.00
HQ-34	lo	do-	h/m	D-292960	b	51.60	17.20	10.50	nd	3.67	6.51	4.77	2.16	.00	2.38	.99	.21	nd	99.99	.04	12.73	.00	.00
HQ-35	lo	do-	h/m	D-292966	b	52.60	17.60	9.70	nd	3.04	5.94	5.06	2.37	.02	2.14	1.06	.22	nd	99.75	.00	11.12	.96	.00
HQ-36	lo	do-	h/m	D-292958	b	51.00	17.10	11.10	nd	3.72	6.67	4.74	2.05	.00	2.53	.98	.22	nd	100.11	.57	13.04	.00	.00
HQ-37	lo	do-	h/m	D-292983	b	52.90	17.30	9.49	nd	3.05	6.16	5.03	2.34	.14	2.08	1.05	.22	nd	99.76	.00	9.47	2.31	.00
HQ-38	lo	do-	h/m	D-292956	b	50.40	17.20	11.40	nd	3.92	7.00	4.58	1.95	.00	2.66	.98	.22	nd	100.31	.71	13.43	.00	.00

Table 1. Chemical analyses and normative ne, ol, hy, and q in Mauna Kea lavas—Continued.

Sample Locality No.	Unit	Feature	Type	Laboratory No.	Remark	Major oxides													Partial CIPW norm			
						SiO_2	Al_2O_3	Fe_2O_3	FeO	MgO	CaO	Na_2O	K_2O	H_2O	TiO_2	P_2O_5	MnO	CO_2	Total	ne	ol	hy	q
HQ-39	lo	do-	h/m	D-292959	b	51.60	17.40	10.40	nd	3.50	6.55	4.82	2.17	0.00	2.38	0.98	0.21	nd	100.01	0.32	12.31	0.00	0.00
HQ-40	lo	do-	h/m	D-292955	b	50.90	17.20	11.00	nd	3.87	6.94	4.58	2.02	.00	2.59	.97	.22	nd	100.29	.17	13.01	.00	.00
HQ-41	lo	do-	h/m	D-292984	b	50.80	17.20	11.10	nd	3.62	6.77	4.85	2.05	.00	2.49	1.11	.22	nd	100.21	1.36	12.94	.00	.00
HQ-42	lo	do-	h/m	D-292967	b	51.00	17.10	10.90	nd	3.55	6.70	4.97	2.11	.00	2.46	1.11	.22	nd	100.12	1.82	12.45	.00	.00
HQ-43	lo	do-	h/m	D-284763	b	50.70	17.20	11.40	nd	3.59	6.92	4.65	2.06	.00	2.52	1.12	.22	nd	100.38	.54	13.20	.00	.00
HQ-44	lo	do-	h/m	D-292965	b	51.30	17.40	10.70	nd	3.30	6.53	4.94	2.15	.24	2.27	1.26	.22	nd	100.31	.62	12.87	.00	.00
HQ-45	lo	do-	h/m	D-292964	b	51.50	17.30	10.50	nd	3.41	6.77	4.72	2.11	.21	2.30	1.13	.22	nd	100.17	.00	11.51	1.25	.00
HQ-46	lo	do-	h/m	D-292968	b	50.10	17.40	11.20	nd	3.73	6.72	4.63	1.96	.57	2.59	1.05	.22	nd	100.17	.68	13.68	.00	.00
HQ-47	lo	do-	h/m	D-292962	b	50.80	17.10	11.10	nd	3.69	6.81	4.85	2.03	.00	2.52	1.04	.22	nd	100.16	1.54	12.75	.00	.00
HQ-48	h	Cone	plbs	D-292992	b	46.00	14.80	14.30	nd	5.88	11.10	2.48	.71	.94	3.38	.42	.19	nd	100.20	.00	9.89	5.42	.00
HQ-49	lo	Flow	h/m	D-292963	b	50.70	16.80	10.90	nd	3.68	6.90	4.56	1.92	.89	2.49	1.03	.22	nd	100.09	.00	11.18	2.20	.00
HQ-50	lo	do-	h/m	D-292985	b	50.20	17.20	11.40	nd	3.55	6.82	4.63	2.03	.24	2.52	1.14	.22	nd	99.95	.64	13.48	.00	.00
HQ-51	lo	do-	h/m	D-278155	b	49.80	17.00	11.80	nd	4.06	7.10	4.67	1.91	.00	2.82	.95	.21	nd	100.32	2.20	13.42	.00	.00
HQ-52	lo	do-	h/m	D-292976	b	49.80	17.00	11.80	nd	4.33	7.01	4.55	1.82	.01	2.72	.91	.22	nd	100.17	1.34	14.37	.00	.00
HQ-53	lo	do-	h/m	D-292977	b	50.20	16.90	11.40	nd	4.10	6.90	4.77	1.99	.00	2.57	1.04	.22	nd	100.09	2.08	13.62	.00	.00
HQ-54	lo	do-	h/m	D-292979	b	49.70	16.80	11.70	nd	4.49	7.02	4.50	1.84	.00	2.68	.90	.22	nd	99.85	1.29	14.49	.00	.00
HQ-55	lo	do-	h/m	D-292971	b	50.30	17.10	11.50	nd	3.96	6.89	4.66	1.94	.00	2.63	.92	.22	nd	100.12	1.32	13.54	.00	.00
HQ-56	lo	do-	h/m	D-292982	b	48.80	17.20	11.80	nd	4.07	7.03	4.50	1.79	.90	2.78	.98	.22	nd	100.07	1.77	14.33	.00	.00
HQ-57	lo	do-	h/m	D-292978	b	50.10	16.80	11.50	nd	4.63	6.86	4.72	1.95	.00	2.56	1.02	.22	nd	100.36	2.17	14.69	.00	.00
HQ-58	lo	do-	h/m	D-292975	b	51.30	17.10	10.90	nd	3.55	6.44	4.83	2.11	.00	2.36	1.01	.22	nd	99.82	.39	12.98	.00	.00
HQ-59	lo	do-	h/m	D-292972	b	50.60	17.20	11.40	nd	3.88	6.81	4.64	1.98	.00	2.61	.93	.22	nd	100.27	.71	13.51	.00	.00
HQ-60	lo	do-	h/m	D-292973	b	50.50	16.90	11.30	nd	3.72	6.68	4.68	1.98	.32	2.54	.94	.22	nd	99.78	.60	13.21	.00	.00
HQ-61	lo	do-	h/m	D-292974	b	50.10	16.60	11.90	nd	5.20	7.04	4.32	1.82	.00	2.61	.85	.22	nd	100.66	.49	15.90	.00	.00
HQ-62	lo	do-	h/m	D-292969	b	49.40	17.00	11.60	nd	3.94	6.75	4.60	1.89	.35	2.67	.93	.21	nd	99.34	1.52	13.94	.00	.00
HQ-63	lo	do-	h/m	D-278154	b	50.30	17.00	11.90	nd	4.18	7.03	4.65	1.83	.00	2.79	.90	.22	nd	100.80	1.33	13.81	.00	.00
HQ-64	lo	do-	h/m	D-292970	b	50.10	17.00	11.60	nd	3.99	6.83	4.40	1.94	.25	2.72	.93	.22	nd	99.98	.00	13.49	.67	.00
HQ-65	lo	do-	h/m	D-292980	b	49.90	17.00	11.90	nd	4.22	7.13	4.66	1.86	.00	2.84	.89	.22	nd	100.62	2.27	13.65	.00	.00
HQ-66	lo	do-	h/m	D-292981	b	49.80	16.90	11.90	nd	4.22	7.10	4.60	1.87	.00	2.83	.89	.22	nd	100.33	1.89	13.73	.00	.00
HQ-67	lo	do-	h/m	D-292987	b	49.60	17.10	11.70	nd	4.14	7.20	4.53	1.88	.00	2.76	.97	.21	nd	100.09	1.71	13.74	.00	.00
HQ-68	lo	do-	h/m	D-292988	b	50.50	17.00	11.30	nd	3.96	6.68	4.71	1.97	.08	2.64	.88	.22	nd	99.94	1.09	13.40	.00	.00
HR-1	lo	Cone	h/m	D-284758	b	50.10	17.00	11.80	nd	4.06	6.99	4.60	1.89	.00	2.76	.91	.23	nd	100.34	1.26	13.72	.00	.00
HR-2	lo	Flow	h/m	D-278094	b	50.40	17.10	11.30	nd	3.93	6.91	4.55	1.95	.00	2.71	.88	.21	nd	99.94	.55	13.20	.00	.00
HR-3	lo	do-	h/m	D-276054	b	51.00	17.40	10.80	nd	3.68	6.72	4.83	2.08	.21	2.53	1.03	.22	nd	100.50	1.16	12.75	.00	.00
HR-4	lo	do-	h/m	D-278093	b	50.20	16.90	11.10	nd	3.74	6.80	4.55	1.97	.00	2.58	.96	.22	nd	99.02	.22	13.09	.00	.00
HR-5	lo	Dike	h/m	D-284757	b	50.60	17.20	11.70	nd	4.05	7.06	4.48	1.95	.00	2.75	.99	.22	nd	101.00	.14	13.83	.00	.00
HR-6	lo	Cone	h/m	D-284756	b	49.80	17.10	11.70	nd	4.09	7.21	4.45	1.87	.02	2.84	.93	.22	nd	100.23	1.00	13.56	.00	.00
HR-7	lo	Flow	h/m	D-276051	b	51.40	17.30	10.90	nd	3.44	6.58	4.99	2.11	.00	2.30	1.15	.22	nd	100.39	1.17	12.83	.00	.00
HR-8	hl	do-	bs	D-284759	b	48.30	14.00	13.90	nd	7.02	11.80	2.31	.68	.00	2.92	.36	.19	nd	101.48	.00	6.67	10.42	.00
HR-9	hh	do-	bs	D-284750	b	48.30	12.90	13.60	nd	7.47	12.30	2.21	.59	.25	2.89	.34	.19	nd	101.04	.00	5.72	10.66	.00
HR-10	hh	do-	olbs	D-271469	b	49.00	12.90	13.10	nd	7.81	12.50	2.27	.61	.00	2.89	.32	.18	.00	101.58	.00	5.91	9.91	.00
HR-11	ly	do-	h/m	D-284748	b	51.40	17.20	11.00	nd	3.74	6.66	4.78	2.04	.00	2.56	.89	.21	nd	100.48	.50	12.76	.00	.00
HR-12	hh	do-	plbs	D-284751	b	48.40	14.50	13.40	nd	6.78	12.10	2.37	.62	.00	2.80	.34	.18	nd	101.49	.00	6.83	8.97	.00
HR-13	hl	do-	bs	D-284752	b	48.40	14.40	13.60	nd	5.99	10.90	2.63	.69	.00	3.74	.34	.18	nd	100.87	.00	2.46	13.50	.00
HR-14	lo	Cone	h/m	D-278118	b	51.50	17.10	10.80	nd	3.49	6.52	5.01	2.13	.14	2.25	1.15	.22	nd	100.31	1.14	12.78	.00	.00
HR-15	ly	Flow	h/m	D-284755	b	53.40	17.20	10.10	nd	2.84	5.90	4.94	2.33	.00	1.99	1.16	.24	nd	100.10	.00	5.74	8.68	.00
HR-16	hl	do-	bs	D-284753	b	47.40	14.40	14.60	nd	5.64	10.90	2.59	.80	.26	3.69	.45	.20	nd	100.93	.00	5.85	9.66	.00
HR-17	hl	do-	bs	D-284754	b	47.00	14.00	15.50	nd	5.60	10.70	2.67	.69	.00	3.81	.48	.21	nd	100.66	.00	6.85	9.22	.00
HR-18	lo	do-	h/m	D-278081	b	50.50	17.10	11.30	nd	3.77	6.85	4.84	1.99	.00	2.61	1.07	.22	nd	100.25	1.78	13.04	.00	.00
HR-19	lo	do-	h/m	D-278082	b	51.10	17.20	10.80	nd	3.68	6.51	4.87	2.11	.02	2.55	.93	.21	nd	99.98	1.23	12.61	.00	.00
HR-20	lo	do-	h/m	D-276053	b	50.20	17.50	11.00	nd	3.61	6.77	4.74	1.95	.55	2.53	1.09	.23	nd	100.17	1.07	13.32	.00	.00
HR-21	lo	do-	h/m	LOF	d	49.55	17.10	11.52	nd	4.20	7.04	5.06	1.87	nd	2.84	.86	.20	nd	100.24	5.01	12.84	.00	.00
HR-22	lo	do-	h/m	D-276055	b	50.80	17.30	11.00	nd	3.70	6.84	5.01	2.06	.00	2.56	1.07	.22	nd	100.56	2.68	12.51	.00	.00
HR-23	lo	do-	h/m	D-284747	b	50.40	17.00	11.80	nd	4.06	7.08	4.57	1.87	.00	2.79	.92	.22	nd	100.71	.84	13.53	.00	.00
HR-24	hl	do-	bs	D-284749	b	47.60	13.70	15.90	nd	5.51	10.60	2.86	.85	.00	3.77	.48	.21	nd	101.48	.00	8.75	6.22	.00
HR-25	lo	Cone	h/m	D-278080	b	50.60	17.20	10.70	nd	3.67	6.73	4.86	2.04	.35	2.48	.99	.21	nd	99.83	1.72	12.50	.00	.00
HR-26	lo	do-	h/m	D-276052	b	51.00	17.30	10.80	nd	3.37	6.37	5.11	2.13	.38	2.26	1.16	.22	nd	100.10	2.01	12.87	.00	.00
HR-27	lo	do-	h/m	D-278119	b	50.90	17.10	11.20	nd	3.56	6.76	4.86	2.05	.00	2.45	1.13	.22	nd	100.23	1.21	12.94	.00	.00
HR-28	lo	Flow	h/m	D-284746	b	50.10	16.90	11.80	nd	4.14	7.06	4.61	1.83	.00	2.78	.90	.22	nd	100.34	1.26	13.65	.00	.00

Table 1. Chemical analyses and normative ne, ol, hy, and q in Mauna Kea lavas—Continued.

Sample Locality No.	Unit	Feature	Type	Laboratory No.	Remark	Major oxides													Partial CIPW norm			
						SiO_2	Al_2O_3	Fe_2O_3	FeO	MgO	CaO	Na_2O	K_2O	H_2O	TiO_2	P_2O_5	MnO	CO_2	Total	ne	ol	hy	q
HR-29	ly	do-	h/m	D-284739	b	52.20	17.20	10.80	nd	3.36	6.36	4.95	2.11	0.00	2.24	1.08	0.23	nd	100.53	0.00	11.88	1.22	0.00
HR-30	lo	do-	h/m	D-284745	b	50.20	17.00	11.80	nd	4.11	7.07	4.55	1.89	.00	2.84	.89	.22	nd	100.57	1.07	13.56	.00	.00
HR-31	hl	do-	bs	D-284742	b	47.70	13.80	15.30	nd	5.53	10.50	2.91	.87	.00	3.93	.49	.21	nd	101.24	.00	7.76	6.87	.00
HR-32	lo	do-	h/m	D-278083	b	51.50	17.20	10.80	nd	3.38	6.49	5.04	2.16	.00	2.25	1.19	.23	nd	100.24	1.27	12.71	.00	.00
HR-33	lo	do-	h/m	D-278117	b	50.60	17.10	11.20	nd	3.85	6.98	4.89	2.00	.00	2.68	1.02	.22	nd	100.54	2.36	12.58	.00	.00
HR-34	hl	do-	bs	D-284741	b	47.90	14.10	15.00	nd	5.46	10.70	2.90	.91	.00	3.76	.49	.21	nd	101.43	.00	8.10	5.91	.00
HR-35	hl	do-	bs	D-284740	b	48.20	13.80	15.10	nd	5.65	10.70	2.93	.87	.00	3.71	.47	.21	nd	101.64	.00	7.90	6.46	.00
HR-36	lo	Cone	h/m	D-278144	b	50.40	17.00	11.40	nd	3.93	7.02	4.54	1.91	.43	2.66	.96	.22	nd	100.47	.33	13.33	.00	.00
HR-37	lo	Flow	h/m	D-278116	b	49.60	17.20	11.10	nd	3.79	6.93	4.35	1.95	.95	2.68	1.02	.22	nd	99.79	.00	13.01	.70	.00
HR-38	hl	Dike	bs	D-278147	b	48.30	14.60	13.80	nd	6.03	11.50	2.49	.61	.00	3.25	.40	.19	nd	101.17	.00	3.54	12.63	.00
HR-39	hl	do-	bs	D-284731	b	47.30	14.00	15.20	nd	6.00	11.00	2.59	.53	.00	3.60	.43	.21	nd	100.86	.00	5.97	10.99	.00
HR-40	lo	Cone	h/m	D-278135	b	51.40	17.00	11.00	nd	3.36	6.29	5.09	2.20	.00	2.21	1.34	.23	nd	100.12	1.04	13.32	.00	.00
HR-41	hl	Flow	bs	D-278145	b	48.70	13.50	15.40	nd	5.17	9.87	3.06	1.10	.00	4.08	.54	.21	nd	101.63	.00	4.85	10.22	.00
HR-42	hh	do-	plbs	D-278146	b	48.30	13.90	14.20	nd	6.69	12.00	2.22	.60	.00	3.12	.36	.19	nd	101.58	.00	3.97	13.05	.00
HR-43	hh	Cone	plbs	D-278111	b	47.00	16.30	11.40	nd	7.09	12.40	2.25	.40	.72	2.73	.31	.16	nd	100.76	.00	8.93	6.35	.00
HR-44	hh	Flow	ank	D-292954	b	47.60	10.60	13.10	nd	14.00	10.80	1.84	.43	.00	2.32	.26	.18	nd	101.13	.00	19.41	9.64	.00
HR-45	lo	do-	h/m	D-284743	b	50.60	17.20	11.20	nd	3.89	6.94	4.86	1.97	.11	2.61	1.00	.22	nd	100.60	2.09	12.94	.00	.00
HR-46	hh	do-	pic	65-1	d	46.38	8.94	13.34	nd	17.93	9.65	1.43	.35	.17	1.86	.23	.18	nd	100.46	.00	27.45	10.92	.00
HR-47	hh	do-	plbs	D-284737	b	48.30	12.70	13.20	nd	8.86	11.70	2.17	.57	.08	2.79	.33	.18	nd	100.88	.00	8.02	11.76	.00
HR-48	hl	Dike	bs	D-292951	b	47.30	13.10	16.30	nd	5.83	10.30	2.71	.87	.00	4.06	.42	.22	nd	101.11	.00	7.50	8.92	.00
HR-49	hl	do-	bs	D-292952	b	49.40	13.20	15.10	nd	5.29	9.59	3.06	1.04	.00	4.16	.58	.21	nd	101.63	.00	.65	16.12	.00
HR-50	lo	Flow	h/m	D-284762	b	51.10	17.20	11.10	nd	3.60	6.70	5.04	2.09	.00	2.42	1.10	.22	nd	100.57	2.27	12.73	.00	.00
HR-51	hh	do-	bs	D-284734	b	47.80	14.80	13.90	nd	6.31	12.20	2.48	.62	.00	2.96	.35	.19	nd	101.61	.00	9.43	4.58	.00
HR-52	hl	do-	bs	D-284733	b	47.60	14.20	13.80	nd	6.59	12.00	2.46	.69	.00	3.15	.38	.19	nd	101.06	.00	9.12	5.13	.00
HR-53	hh	do-	bs	D-284735	b	48.10	13.70	15.50	nd	5.38	10.20	2.91	.97	.00	3.80	.52	.21	nd	101.29	.00	6.34	9.27	.00
HR-54	hh	do-	bs	D-284736	b	48.00	13.50	14.90	nd	6.41	10.90	2.71	.88	.00	3.47	.45	.20	nd	101.42	.00	9.01	6.64	.00
HR-55	lo	do-	h/m	D-278112	b	49.10	16.80	12.30	nd	4.52	7.34	4.47	1.75	.00	3.06	.86	.21	nd	100.41	2.23	14.17	.00	.00
HR-56	hl	do-	bs	D-284738	b	48.60	13.60	15.50	nd	5.07	9.85	3.10	1.07	.00	4.02	.56	.21	nd	101.58	.00	5.31	9.72	.00
HR-57	hh	do-	olbs	D-292953	b	48.60	13.10	12.90	nd	7.84	12.00	2.23	.59	.06	2.87	.33	.18	nd	100.70	.00	4.94	12.60	.00
HR-58	lo	do-	h/m	D-284744	b	51.00	17.00	10.90	nd	3.34	6.77	5.06	2.15	.00	2.41	1.35	.22	nd	100.20	1.90	12.25	.00	.00
HR-59	hh	do-	plbs	D-278113	b	46.30	13.50	14.00	nd	9.04	11.40	2.10	.26	1.11	3.03	.36	.19	nd	101.29	.00	11.80	9.96	.00
HR-60	lo	Cone	h/m	D-284760	b	49.90	16.90	11.10	nd	3.67	6.44	4.27	2.01	1.79	2.35	1.12	.21	nd	99.76	.00	9.41	7.05	.00
HR-61	hh	Flow	bs	D-278114	b	47.70	13.70	13.50	nd	7.86	10.50	2.62	.74	.19	3.11	.42	.19	nd	100.53	.00	10.75	8.16	.00
HR-62	hh	do-	bs	D-278115	b	50.10	14.00	13.80	nd	3.88	8.06	3.96	1.49	.00	3.45	1.28	.22	nd	100.24	.00	2.34	13.54	.00
HR-63	lo	do-	h/m	D-278142	b	50.00	17.00	11.90	nd	4.23	7.20	4.70	1.83	.00	2.87	.89	.21	nd	100.83	2.35	13.44	.00	.00
HR-64	lo	Cone	h/m	D-278141	b	49.80	16.80	11.00	nd	3.86	6.41	4.35	2.15	1.80	2.40	1.10	.21	nd	99.88	.00	12.45	2.75	.00
HR-65	lo	Flow	h/m	D-278110	b	48.30	16.80	12.70	nd	4.94	7.41	4.35	1.68	.00	3.21	.82	.21	nd	100.42	2.81	15.21	.00	.00
HR-66	lo	do-	h/m	D-284761	b	50.90	17.10	11.00	nd	3.40	6.66	5.02	2.11	.07	2.35	1.22	.23	nd	100.06	1.87	12.65	.00	.00
HR-67	lo	do-	h/m	D-278108	b	48.20	16.80	12.50	nd	4.95	7.56	4.15	1.63	.00	3.19	.80	.20	nd	99.98	1.80	15.11	.00	.00
HR-68	lo	do-	h/m	D-278143	b	49.70	16.80	11.60	nd	4.33	7.50	4.53	1.81	.29	2.90	.87	.21	nd	100.54	2.10	12.94	.00	.00
HR-69	lo	do-	h/m	D-278140	b	50.40	17.00	11.60	nd	4.14	7.10	4.70	1.88	.00	2.83	.88	.21	nd	100.74	1.77	13.10	.00	.00
HR-70	lo	do-	h/m	D-278109	b	48.10	16.80	12.60	nd	4.83	7.44	4.30	1.70	.00	3.19	.83	.21	nd	100.00	2.75	14.98	.00	.00
HR-71	lo	do-	h/m	D-284732	b	50.70	17.20	11.10	nd	3.69	7.05	4.75	2.06	.00	2.56	1.08	.22	nd	100.41	1.50	12.59	.00	.00
HR-72	lo	do-	h/m	D-278139	b	51.20	17.00	10.90	nd	3.55	6.67	4.86	2.04	.14	2.47	1.01	.22	nd	100.06	.74	12.43	.00	.00
HR-73	lo	do-	h/m	D-278138	b	50.40	17.20	11.60	nd	4.13	7.17	4.51	1.91	.00	2.86	.91	.21	nd	100.90	.82	13.40	.00	.00
HR-74	lo	Cone	h/m	D-278107	b	49.00	17.00	12.10	nd	4.29	7.20	4.37	1.77	1.29	2.97	.88	.22	nd	101.09	1.37	14.29	.00	.00
HR-75	ly	Flow	h/m	D-278095	b	50.20	17.00	11.60	nd	4.03	6.98	4.80	1.93	.00	2.75	.95	.22	nd	100.46	2.39	13.20	.00	.00
HR-76	lo	do-	h/m	D-278137	b	50.60	17.00	11.50	nd	4.01	6.97	4.68	1.94	.00	2.70	.95	.22	nd	100.57	1.16	13.29	.00	.00
HR-77	lo	do-	h/m	D-278098	b	50.70	17.00	11.20	nd	3.80	6.79	4.81	1.99	.00	2.58	.98	.22	nd	100.07	1.44	12.93	.00	.00
HR-78	lo	do-	h/m	D-278136	b	51.30	17.10	10.70	nd	3.51	6.60	4.68	2.14	.41	2.32	1.17	.22	nd	100.15	.00	11.56	1.97	.00
HR-79	lo	do-	h/m	D-278097	b	49.50	16.90	11.60	nd	4.22	7.22	4.63	1.84	.00	2.86	.95	.21	nd	99.93	2.32	13.35	.00	.00
HR-80	lo	do-	h/m	D-278096	b	51.10	17.30	10.90	nd	3.71	6.73	4.99	2.07	.00	2.55	.98	.21	nd	100.54	2.22	12.43	.00	.00
HR-81	lo	do-	h/m	D-278099	b	50.90	16.90	11.10	nd	3.69	6.77	4.87	2.01	.00	2.56	.99	.21	nd	100.00	1.42	12.50	.00	.00
HR-82	lo	Cone	h/m	D-278106	b	49.80	17.10	11.40	nd	3.81	6.79	4.27	1.93	1.90	2.65	.99	.22	nd	100.86	.00	11.32	3.79	.00
HR-83	ly	Bomb	h/m	D-278105	b	50.30	17.00	11.80	nd	4.06	6.90	4.62	1.88	.00	2.72	.91	.22	nd	100.41	.98	13.88	.00	.00
HR-84	lo	Flow	h/m	D-278084	b	49.60	16.90	11.70	nd	4.04	7.03	4.50	1.78	.06	2.78	.92	.22	nd	99.53	.76	13.74	.00	.00
HR-85	lo	do-	h/m	D-278100	b	50.30	17.10	11.20	nd	3.75	7.01	4.48	1.94	.51	2.58	1.01	.22	nd	100.10	.00	12.95	.32	.00
HR-86	lo	do-	h/m	D-278085	b	50.80	17.20	11.20	nd	3.87	6.81	4.69	2.01	.00	2.64	.95	.22	nd	100.39	.81	13.15	.00	.00

Table 1. Chemical analyses and normative ne, ol, hy, and q in Mauna Kea lavas—Continued.

Sample Locality No.	Unit	Feature	Type	Laboratory No.	Remark	Major oxides													Partial CIPW norm			
						SiO_2	Al_2O_3	Fe_2O_3	FeO	MgO	CaO	Na_2O	K_2O	H_2O	TiO_2	P_2O_5	MnO	CO_2	Total	ne	ol	hy	q
HR-87	ly	do-	h/m	D-278101	b	50.70	17.20	11.00	nd	3.71	6.81	4.64	2.03	0.17	2.53	1.01	0.22	nd	100.02	0.37	13.03	0.00	0.00
HR-88	lo	Cone	h/m	D-278088	b	51.20	17.10	10.80	nd	3.50	6.49	4.94	2.11	.27	2.42	1.05	.23	nd	100.11	1.09	12.59	.00	.00
HR-89	lo	Flow	h/m	D-278089	b	50.80	17.20	11.20	nd	3.83	6.86	4.57	1.99	.00	2.60	.98	.22	nd	100.25	.00	13.27	.08	.00
HR-90	lo	do-	h/m	D-278102	b	51.10	17.00	10.70	nd	3.31	6.61	4.89	2.17	.51	2.24	1.38	.22	nd	100.13	.40	12.79	.00	.00
HR-91	ly	do-	h/m	D-278104	b	49.60	17.10	12.20	nd	4.36	7.24	4.32	1.75	.04	2.91	.83	.21	nd	100.56	.57	14.47	.00	.00
HR-92	lo	do-	h/m	D-278090	b	50.40	16.90	11.50	nd	3.99	6.94	4.87	1.96	.00	2.69	.96	.22	nd	100.43	2.53	12.97	.00	.00
HR-93	lo	do-	h/m	D-278091	b	51.00	17.00	11.10	nd	3.73	6.69	4.85	2.03	.00	2.51	.97	.22	nd	100.10	1.22	12.81	.00	.00
HR-94	lo	do-	h/m	D-278086	b	50.30	16.90	11.80	nd	4.00	6.90	4.70	1.89	.00	2.68	.91	.22	nd	100.30	1.47	13.62	.00	.00
HR-95	lo	Cone	h/m	D-278103	b	50.60	17.10	11.50	nd	3.80	6.63	4.71	1.93	.00	2.54	.97	.23	nd	100.01	.54	13.80	.00	.00
HR-96	lo	do-	h/m	D-278087	b	50.90	17.00	11.20	nd	3.78	6.72	4.87	2.02	.00	2.56	.97	.22	nd	100.24	1.59	12.87	.00	.00
HR-97	ly	Flow	h/m	D-278092	b	51.00	17.10	11.30	nd	3.90	6.80	4.68	1.96	.00	2.61	.92	.22	nd	100.49	.41	13.27	.00	.00
HS-1	lo	do-	h/m	D-277509	b	48.60	16.90	12.20	nd	4.44	7.22	4.30	1.74	.26	3.02	.89	.22	nd	99.79	1.41	14.65	.00	.00
HS-2	lo	do-	h/m	D-277508	b	48.40	16.90	12.50	nd	4.56	7.40	4.28	1.70	.06	3.16	.85	.21	nd	100.02	1.92	14.63	.00	.00
HS-3	lo	do-	h/m	D-277507	b	48.20	16.90	12.60	nd	4.80	7.51	4.33	1.66	.00	3.25	.82	.21	nd	100.28	2.79	14.77	.00	.00
HS-4	lo	do-	h/m	D-277506	b	49.70	17.00	11.70	nd	4.02	6.95	4.60	1.86	.05	2.79	.95	.22	nd	99.84	1.40	13.70	.00	.00
HS-5	ly	do-	h/m	D-277505	b	49.40	16.90	12.00	nd	4.29	7.09	4.62	1.82	.00	2.87	.85	.22	nd	100.06	2.53	13.89	.00	.00
HT-1	lo	do-	h/m	D-277499	b	50.10	17.10	11.50	nd	3.71	6.59	4.55	1.99	.12	2.59	1.03	.23	nd	99.51	.04	14.02	.00	.00
HT-2	h	do-	plbs	D-277498	b	47.20	13.80	15.00	nd	5.62	10.60	2.78	.84	.00	3.83	.49	.20	nd	100.36	.00	7.60	7.25	.00
HU-1	h	do-	bs	D-277500	b	45.90	14.70	14.50	nd	6.39	10.50	2.54	.62	.46	3.83	.35	.19	nd	99.98	.00	10.02	7.00	.00
HU-2	h	do-	bs	D-277497	b	46.80	13.60	15.50	nd	5.69	10.30	2.69	.71	.00	4.12	.44	.20	nd	100.05	.00	5.84	10.66	.00
HU-3	h	do-	plbs	D-277501	b	47.20	14.80	13.50	nd	6.57	11.30	2.29	.35	.34	3.13	.34	.19	nd	100.01	.00	3.69	15.07	.00
HU-4	h	do-	bs	D-277493	b	46.90	14.10	14.80	nd	6.61	11.30	2.26	.31	.01	3.32	.34	.20	nd	100.15	.00	4.59	14.64	.00
HU-5	lo	do-	h/m	D-277495	b	49.40	17.10	11.80	nd	3.95	6.90	4.51	1.85	.04	2.78	.96	.22	nd	99.51	1.01	14.08	.00	.00
HU-6	h	Cone	olbs	D-277496	b	40.20	13.20	18.00	nd	8.19	8.94	3.81	1.28	.00	6.04	.80	.20	nd	100.66	12.71	18.84	.00	.00
HU-7	h	Flow	ank	D-277491	b	46.00	10.10	12.60	nd	16.10	10.80	1.67	.47	.00	2.08	.26	.17	nd	100.25	.00	28.59	1.88	.00
HU-8	h	do-	bs	D-277492	b	46.00	13.80	15.20	nd	5.08	9.26	3.01	1.20	.50	4.85	.65	.20	nd	99.75	.00	8.63	5.58	.00
IO-1	lo	do-	h/m	PH-1	d	49.48	16.91	11.85	nd	4.17	6.98	4.62	1.81	.08	2.85	.78	.21	nd	99.74	2.25	13.62	.00	.00
IO-2	lo	do-	h/m	D-260903	b	49.90	17.00	12.00	nd	4.26	7.14	4.74	1.82	.00	2.92	.84	.22	.00	100.84	2.76	13.49	.00	.00
IO-3	h	do-	bs	115-3	d	47.79	14.07	14.60	nd	5.17	10.24	2.83	1.00	.31	3.54	.49	.20	nd	100.24	.00	5.40	9.83	.00
IO-4	h	do-	bs	115-20	d	47.01	13.73	13.67	nd	7.26	11.16	2.43	.82	.17	3.30	.42	.18	nd	100.15	.00	10.31	6.18	.00
IO-5	h	do-	olbs	115-4	d	47.23	12.64	12.20	nd	11.23	11.63	1.68	.50	.13	2.13	.27	.16	nd	99.80	.00	12.82	12.05	.00
IO-6	h	do-	bs	115-6	d	45.73	14.61	15.83	nd	5.05	8.28	3.32	1.41	.10	4.57	.75	.22	nd	99.87	.00	15.30	.09	.00
IO-7	h	do-	plbs	D-260901	b	48.80	14.90	13.30	nd	5.81	10.50	2.96	.93	.00	3.44	.47	.18	.00	101.29	.00	6.38	8.47	.00
IO-8	h	do-	bs	115-23	d	47.60	14.21	13.30	nd	6.05	11.15	2.51	.81	.07	3.28	.42	.19	nd	99.59	.00	4.90	10.47	.00
IO-9	h	do-	ank	115-12	d	45.17	10.20	12.44	nd	15.06	10.98	1.66	.55	.16	1.91	.27	.18	nd	98.58	.16	28.44	.00	.00
IO-10	h	do-	bs	115-14	d	45.24	14.32	16.56	nd	5.09	8.13	3.34	1.43	.15	4.71	.74	.23	nd	99.94	.64	16.00	.00	.00
IO-11	h	do-	bs	115-37	d	47.60	13.52	14.44	nd	6.31	10.55	2.48	.89	.38	3.43	.44	.20	nd	100.24	.00	5.09	12.62	.00
IO-12	h	do-	bs	D-260902	b	44.80	14.20	17.30	nd	5.16	8.29	3.31	1.38	.31	4.93	.74	.23	.07	100.72	1.08	16.43	.00	.00
IO-13	h	do-	bs	115-25	d	47.84	13.77	14.81	nd	5.57	10.37	2.52	.96	.00	3.62	.47	.20	nd	100.13	.00	2.47	14.98	.00
IO-14	h	do-	ppbs	115-36	d	47.96	14.27	12.56	nd	7.20	11.76	2.13	.67	.11	2.77	.32	.18	nd	99.93	.00	4.42	13.31	.00
IO-15	h	do-	bs	115-35	d	48.26	14.32	12.34	nd	6.80	11.81	2.25	.71	.00	2.81	.35	.17	nd	99.82	.00	3.55	12.87	.00
IO-16	h	do-	plbs	115-11	d	47.50	15.42	13.67	nd	5.25	11.02	2.74	.83	.17	3.38	.40	.19	nd	100.57	.00	7.41	6.26	.00
IP-1	h	do-	plbs	D-260897	b	46.70	13.90	15.90	nd	5.60	10.70	2.83	.74	.00	3.96	.41	.21	.00	100.95	.00	10.74	3.60	.00
IP-2	h	do-	ppbs	NO-9	d	50.01	14.29	13.52	nd	4.26	8.78	3.29	1.35	.29	3.11	.75	.21	nd	99.86	.00	.00	16.75	.50
IP-3	h	do-	olbs	D-260887	b	46.60	14.20	14.10	nd	5.72	11.00	2.90	.97	.29	3.78	.52	.18	.00	100.26	.33	11.83	.00	.00
IP-4	lo	do-	ben	D-260888	b	54.70	17.60	9.13	nd	2.25	4.96	5.73	2.60	.15	1.60	.98	.23	.00	99.93	.06	10.72	.00	.00
IP-5	h	do-	ppbs	73-4	d	45.39	14.38	13.71	nd	8.04	10.93	2.54	.85	.20	3.26	.42	.19	nd	99.91	1.33	17.11	.00	.00
IP-6	h	do-	plbs	NO-11	d	47.34	15.74	13.09	nd	5.63	11.69	2.42	.72	.13	2.96	.36	.17	nd	100.25	.00	6.73	7.71	.00
IP-7	h	do-	ppbs	NO-5	d	47.52	13.88	13.48	nd	6.91	11.35	2.57	.82	.07	3.32	.40	.19	nd	100.51	.00	9.96	4.85	.00
IP-8	h	do-	bs	83-17	d	46.10	14.86	15.69	nd	5.15	8.31	3.13	1.42	.34	4.56	.75	.22	nd	100.53	.00	12.31	4.71	.00
IP-9	h	do-	plbs	NO-13	d	45.54	14.44	13.81	nd	8.16	10.90	2.59	.90	.13	3.24	.42	.19	nd	100.32	1.83	17.37	.00	.00
IP-10	lo	do-	h/m	D-260882	b	49.90	17.10	12.10	nd	3.99	6.99	4.68	1.91	.00	2.79	1.05	.21	.00	100.72	1.88	13.98	.00	.00
IP-11	h	do-	olbs	D-260889	b	47.30	13.60	14.50	nd	6.54	10.80	2.73	.92	.00	3.48	.44	.19	.00	100.50	.00	11.31	3.64	.00
IP-12	h	do-	bs	NO-14	d	46.97	14.44	13.86	nd	5.74	10.73	2.93	.98	.19	3.71	.49	.19	nd	100.23	.00	11.65	.77	.00
IP-13	h	do-	bs	D-260884	b	47.20	14.10	14.00	nd	6.14	10.90	3.00	.99	.00	3.75	.51	.18	.00	100.77	.45	12.37	.00	.00
IP-14	h	do-	ppbs	D-260885	b	47.30	13.20	13.00	nd	9.73	11.80	2.23	.66	.00	2.76	.34	.17	.00	101.19	.00	16.29	2.41	.00
IP-15	h	do-	bs	71-9	d	47.47	13.98	13.91	nd	5.81	10.72	2.47	.87	.25	3.46	.46	.19	nd	99.59	.00	3.28	13.31	.00
IP-16	h	do-	ppbs	97-2	d	47.48	14.14	12.82	nd	7.46	11.56	2.23	.75	.31	2.98	.38	.18	nd	100.29	.00	7.84	9.41	.00

Table 1. Chemical analyses and normative ne, ol, hy, and q in Mauna Kea lavas—Continued.

Sample Locality No.	Unit	Feature	Type	Laboratory No.	Remark	Major oxides													Partial CIPW norm			
						SiO_2	Al_2O_3	Fe_2O_3	FeO	MgO	CaO	Na_2O	K_2O	H_2O	TiO_2	P_2O_5	MnO	CO_2	Total	ne	ol	hy	q
IP-17	h	do-	bs	D-260892	b	47.40	14.00	15.00	nd	5.61	10.80	2.79	.93	0.00	3.56	0.45	0.20	0.01	100.75	0.00	9.58	4.48	0.00
IP-18	h	do-	ppbs	D-260893	b	48.00	14.20	13.10	nd	6.60	11.60	2.53	.80	.19	3.17	.40	.18	.00	100.77	.00	7.40	7.20	.00
IP-19	lo	do-	ben	NO-10	d	54.17	17.11	9.58	nd	2.63	5.00	5.48	2.55	.14	1.60	1.07	.22	nd	99.55	.00	9.70	3.14	.00
IP-20	h	do-	bs	83-27	d	47.11	13.76	13.33	nd	7.79	10.92	2.53	.83	.13	3.27	.44	.18	nd	100.29	.00	12.37	4.65	.00
IP-21	h	do-	bs	D-260898	b	47.40	13.90	12.60	nd	7.98	11.90	2.24	.57	.00	2.84	.34	.17	.00	99.94	.00	9.35	7.78	.00
IP-22	lo	do-	h/m	D-271468	b	50.30	17.00	11.70	nd	4.00	6.99	4.80	1.96	.00	2.76	.96	.22	.00	100.69	2.42	13.17	.00	.00
IP-23	h	do-	olbs	D-260895	b	47.70	12.90	12.80	nd	9.84	11.70	2.14	.69	.00	2.60	.31	.17	.00	100.85	.00	14.17	5.63	.00
IP-24	h	do-	bs	85-2		47.51	13.75	13.17	nd	7.70	10.95	2.38	.81	.00	3.27	.45	.18	nd	100.17	.00	8.42	9.85	.00
IP-25	h	do-	olbs	D-260185	b	46.80	14.10	13.70	nd	6.69	11.50	2.49	.85	.41	3.38	.43	.18	.00	100.53	.00	11.21	2.94	.00
IP-26	h	do-	bs	D-260186	b	47.50	13.40	13.00	nd	8.30	11.30	2.30	.77	.35	2.90	.35	.17	.00	100.34	.00	10.83	7.33	.00
IQ-1	lo	do-	ben	D-276005	b	54.20	17.70	2.62	5.85	2.26	4.93	5.67	2.59	.00	1.58	.98	.23	.00	98.61	.22	11.07	.00	.00
IQ-2	lo	do-	h/m	D-276004	b	49.40	17.00	6.42	4.66	4.00	7.04	4.66	1.92	.04	2.75	.95	.22	.00	99.06	2.55	13.38	.00	.00
IQ-3	hl	do-	bs	D-276023	b	47.10	14.50	4.03	8.70	6.74	12.00	2.44	.52	.00	3.27	.37	.18	.00	99.85	.00	9.52	5.23	.00
IQ-4	lo	do-	h/m	D-276000	b	50.60	17.10	4.31	6.10	3.74	6.82	4.86	2.04	.08	2.60	1.03	.21	.00	99.49	1.89	12.69	.00	.00
IQ-5	lo	do-	h/m	D-276003	b	49.00	17.00	4.91	6.29	4.27	7.20	4.43	1.81	.15	2.97	.88	.21	.00	99.12	1.82	13.92	.00	.00
IQ-6	hl	do-	bs	D-276002	b	48.00	14.20	4.73	8.70	4.51	9.07	3.67	1.47	.00	4.18	.76	.21	.00	99.50	.22	11.26	.00	.00
IQ-7	h	do-	olbs	D-275999	b	46.70	14.20	3.08	9.47	6.85	10.90	2.53	.91	.20	3.58	.45	.18	.00	99.05	.00	10.79	4.80	.00
IQ-8	lo	do-	h/m	D-275998	b	49.80	17.00	7.76	3.46	4.00	7.10	4.75	1.92	.26	2.74	.95	.21	.02	99.97	2.70	13.14	.00	.00
IQ-9	lo	do-	h/m	D-276001	b	52.90	17.60	3.20	6.39	2.61	5.10	5.23	2.49	.25	1.76	1.16	.24	.00	98.93	.00	11.08	3.19	.00
IQ-10	h	Cone	olbs	D-260890	b	47.50	12.60	13.00	nd	9.95	11.90	2.12	.59	.26	2.66	.32	.17	.00	101.07	.00	14.26	5.40	.00
IQ 11	lo	Flow	h/m	D-275992	b	49.20	17.00	4.31	6.92	4.34	7.23	4.57	1.82	.24	2.97	.92	.21	.00	99.73	2.55	13.93	.00	.00
IQ-12	lo	Cone	ben	D-275991	b	54.50	17.40	5.12	3.86	2.20	4.60	5.58	2.72	.25	1.46	1.03	.23	.00	98.95	.00	9.50	3.07	.00
IQ-13	lo	Flow	h/m	D-275996	b	49.90	17.00	5.91	5.12	3.97	6.98	4.78	1.94	.00	2.75	.98	.22	.00	99.55	2.53	13.25	.00	.00
IQ-14	h	do-	bs	D-275997	b	47.40	14.00	4.94	7.97	6.34	11.50	2.55	.84	.00	3.40	.41	.18	.00	99.53	.00	8.85	5.03	.00
IQ-15	h	Cone	olbs	D-275994	b	45.80	12.20	4.23	7.44	12.40	11.80	1.81	.29	.40	2.36	.24	.17	.00	99.14	.00	20.97	2.98	.00
IQ-16	h	do-	plbs	D-260177	b	47.60	15.20	13.20	nd	6.09	11.30	2.57	.79	.02	3.08	.40	.18	.00	100.43	.00	8.21	6.75	.00
IQ-17	h	do-	olbs	D-260176	b	46.80	13.40	12.60	nd	9.79	12.00	1.96	.39	.49	2.63	.32	.17	.00	100.55	.00	12.75	7.99	.00
IQ-18	h	Flow	bs	D-260188	b	47.30	14.30	13.40	nd	6.33	11.50	2.46	.84	.00	3.21	.40	.18	.00	99.92	.00	8.08	6.43	.00
IQ-20	lo	do-	h/m	D-275990	b	52.30	18.40	4.30	5.13	2.21	4.75	5.11	2.24	1.19	1.57	1.10	.25	.00	98.55	.00	4.94	10.86	.00
IQ-21	h	do-	olbs	D-275995	b	45.10	11.30	3.77	8.11	13.70	12.00	1.39	.22	.66	2.29	.24	.17	.00	98.95	.00	21.78	5.25	.00
IR-1	lo	do-	h/m	D-278153	b	50.70	17.20	11.10	nd	3.77	6.75	4.58	1.92	.56	2.57	1.04	.22	nd	100.41	.00	12.14	1.88	.00
IR-2	lo	do-	h/m	D-276013	b	49.90	17.10	2.98	7.67	4.11	7.09	4.45	1.82	.00	2.83	.87	.21	.01	99.04	.49	13.59	.00	.00
IR-3	hl	do-	bs	D-278150	b	47.40	13.50	15.50	nd	5.33	10.10	2.88	1.01	.13	4.21	.61	.21	nd	100.88	.00	6.30	8.85	.00
IR-4	hl	do-	bs	D-278149	b	47.30	14.30	14.70	nd	6.00	11.10	2.83	.75	.00	3.58	.45	.19	nd	101.20	.00	11.04	2.87	.00
IR-5	hl	do-	bs	D-278151	b	48.60	13.50	15.70	nd	5.04	9.67	3.19	1.02	.00	4.30	.52	.21	nd	101.75	.00	5.24	9.57	.00
IR-6	hl	do-	bs	D-278152	b	47.70	13.50	15.50	nd	5.24	9.93	2.97	1.01	.00	4.22	.54	.21	nd	100.82	.00	6.13	8.82	.00
IR-7	lo	do-	h/m	D-276012	b	50.70	17.10	3.75	6.88	3.92	6.73	4.77	1.95	.00	2.62	.90	.22	.00	99.54	1.23	13.39	.00	.00
IR-8	lo	do-	h/m	D-276014	b	49.50	16.90	3.54	7.43	4.22	7.34	4.55	1.83	.00	2.89	.87	.22	.00	99.29	2.27	13.28	.00	.00
IR-9	lo	do-	h/m	D-276018	b	50.00	17.10	3.33	6.90	3.61	6.73	4.75	1.86	.75	2.49	1.01	.22	.00	98.75	.98	13.08	.00	.00
IR-10	lo	do-	h/m	D-276011	b	50.40	17.10	2.71	7.46	3.46	6.76	4.65	2.07	.00	2.37	1.25	.22	.00	98.45	.13	13.28	.00	.00
IR-11	lo	do-	h/m	D-276015	b	50.70	17.00	2.80	7.20	3.51	6.68	4.73	2.02	.00	2.45	1.06	.22	.00	98.37	.31	12.67	.00	.00
IR-12	lo	do-	h/m	D-276016	b	51.20	17.20	3.39	6.58	3.50	6.71	4.97	2.12	.00	2.48	1.08	.22	.00	99.45	1.66	12.13	.00	.00
IR-13	lo	Cone	ben	D-276019	b	55.10	17.40	2.71	5.87	2.18	4.34	5.51	2.73	.00	1.37	.97	.23	.00	98.41	.00	5.97	8.18	.00
IR-14	lo	Flow	h/m	D-276021	b	49.60	17.00	4.25	6.79	4.23	7.13	4.76	1.89	.00	2.84	.93	.21	.00	99.63	3.21	13.50	.00	.00
IR-15	lo	do-	h/m	D-276020	b	49.90	17.00	2.20	8.37	4.12	7.02	4.65	1.91	.00	2.85	.88	.21	.00	99.11	2.01	13.22	.00	.00
IR-16	h	do-	bs	D-276022	b	46.80	13.80	4.84	8.96	6.11	9.74	3.20	1.21	.00	4.07	.60	.20	.00	99.53	.80	13.96	.00	.00
IR-17	ly	do-	h/m	D-276017	b	50.70	17.00	3.69	7.03	3.86	6.71	4.77	1.98	.00	2.60	.94	.22	.00	99.50	1.22	13.41	.00	.00
IR-18	lo	do-	h/m	D-276006	b	50.30	17.00	4.07	6.51	3.85	6.88	4.61	1.94	.00	2.65	.95	.22	.00	98.98	.73	13.21	.00	.00
IR-19	lo	do-	h/m	D-276008	b	48.70	17.00	6.78	4.52	3.93	7.07	4.37	1.84	.49	2.81	.95	.21	.00	98.67	1.25	13.95	.00	.00
IR-20	lo	do-	h/m	D-276009	b	49.30	17.10	5.56	5.62	3.87	7.01	4.54	1.87	.24	2.77	.99	.22	.00	99.09	1.47	13.78	.00	.00
IR-21	lo	do-	h/m	D-276010	b	49.50	17.10	2.64	8.33	3.94	7.04	4.49	1.89	.15	2.82	.98	.22	.00	99.10	1.15	13.89	.00	.00
IS-1	lo	do-	h/m	D-277503	b	51.30	17.00	11.10	nd	3.55	6.43	4.85	2.07	.00	2.41	1.02	.23	nd	99.96	.32	13.10	.00	.00
IS-2	lo	do-	h/m	D-277504	b	51.40	17.20	11.00	nd	3.60	6.54	4.78	2.04	.00	2.42	1.02	.23	nd	100.23	.00	13.04	.17	.00
IS-3	h	do-	olbs	D-277502	b	45.40	13.50	14.20	nd	8.69	11.60	2.04	.25	1.00	3.18	.39	.20	nd	100.45	.00	12.58	8.01	.00
IS-4	ly	do-	h/m	D-271467	b	50.40	16.90	11.80	nd	3.81	6.79	4.68	1.90	.12	2.67	.92	.23	.00	100.22	.86	13.50	.00	.00
IT-1	h	do-	plbs	D-271471	b	46.20	14.90	14.50	nd	6.73	10.80	2.57	.61	.20	3.86	.34	.19	.00	100.90	.00	11.89	4.55	.00
IT-2	lo	do-	h/m	D-271470	b	49.30	17.00	12.10	nd	4.09	7.02	4.49	1.80	.24	2.86	.93	.22	.00	100.05	1.29	14.23	.00	.00
IT-3	h	do-	olbs	D-271473	b	47.00	13.10	13.40	nd	9.70	11.10	2.18	.68	.45	2.93	.36	.18	.00	101.08	.00	14.65	6.43	.00

Table 1. Chemical analyses and normative ne, ol, hy, and q in Mauna Kea lavas—Continued.

Sample Locality No.	Unit	Feature	Type	Laboratory No.	Remark	Major oxides												Partial CIPW norm			
						SiO_2	Al_2O_3	Fe_2O_3	FeO	MgO	CaO	Na_2O	K_2O	H_2O	TiO_2	P_2O_5	MnO	CO_2	Total	ne	ol	hy	q
IT-4	h	do-	olbs	D-271472	b	47.00	12.20	14.00	nd	11.30	9.73	2.37	0.62	0.01	2.98	0.39	0.18	0.00	100.78	0.00	18.28	7.68	0.00
IT-5	h	do-	plbs	D-271476	b	47.40	14.40	14.80	nd	6.17	10.90	2.63	.67	.00	3.51	.43	.20	.00	101.11	.00	8.08	8.49	.00
IT-6	h	do-	olbs	D-271474	b	46.50	14.30	15.50	nd	5.87	10.30	2.59	.73	.64	3.74	.46	.21	.00	100.84	.00	8.10	9.70	.00
IT-7	h	do-	bs	D-271478	b	47.20	14.00	14.50	nd	5.20	10.20	3.16	1.11	.00	4.84	.63	.20	.00	101.04	.00	8.83	2.47	.00
IT-8	h	do-	olbs	D-271475	b	47.70	13.90	12.70	nd	8.43	12.50	2.24	.57	.00	2.65	.32	.17	.00	101.18	.00	12.47	3.60	.00
IT-9	h	do-	bs	D-271477	b	44.60	16.30	16.00	nd	5.61	8.39	3.05	1.17	.20	4.22	.62	.21	.00	100.37	.41	18.56	.00	.00
JO-1	h	do-	ank	114-9	d	47.82	12.60	12.07	nd	10.66	11.72	1.71	.54	.23	2.40	.30	.16	nd	100.21	.00	9.09	14.79	.00
JO-2	h	do-	bs	D-260900	b	48.50	14.20	13.60	nd	6.56	11.50	2.56	.71	.00	3.09	.37	.18	.00	101.27	.00	6.43	9.28	.00
JO-5	h	do-	olbs	KW-1	d	47.06	13.54	13.25	nd	7.68	11.34	2.46	.84	.09	3.12	.43	.19	nd	100.00	.00	12.26	3.74	.00
JO-7	h	do-	olbs	D-260744	b	47.90	14.00	14.40	nd	5.58	10.10	3.13	1.13	.00	4.06	.55	.20	.00	101.05	.00	9.70	3.40	.00
JP-1	h	do-	olbs	85-10	d	47.10	10.12	12.72	nd	14.35	10.83	1.63	.57	.07	2.32	.30	.18	nd	100.19	.00	19.39	10.10	.00
JP-2	h	do-	olbs	D-260187	b	47.90	14.20	13.80	nd	6.20	11.20	2.56	.70	.00	3.17	.38	.19	.00	100.30	.00	5.86	10.06	.00
JP-7	h	do-	bs	D-277461	b	48.70	13.90	13.10	nd	6.99	11.50	2.33	.64	.05	2.84	.35	.17	nd	100.57	.00	3.20	14.77	.00
JQ-1	h	do-	bs	D-260179	b	45.70	13.90	14.70	nd	7.68	10.60	2.19	.50	.86	3.48	.43	.20	.00	100.24	.00	9.71	11.54	.00
JQ-2	h	do-	olbs	D-260178	b	45.50	11.50	13.10	nd	13.50	10.60	1.76	.55	.00	2.54	.31	.17	.00	99.53	.00	23.49	4.40	.00
JQ-3	h	do-	olbs	D-260180	b	47.10	12.90	13.70	nd	9.29	11.30	2.24	.56	.00	3.00	.38	.18	.00	100.65	.00	13.09	7.29	.00
JQ-4	lo	do-	ben	D-260173	b	54.70	18.10	8.99	nd	2.25	3.82	5.25	2.75	.96	1.25	.88	.21	.00	99.16	.00	.58	15.75	.00
JQ-5	h	do-	ank	D-260181	b	46.30	12.60	13.20	nd	11.50	11.10	2.02	.54	.00	2.58	.32	.18	.00	100.34	.00	20.07	3.70	.00
JQ-6	lo	do-	ben	D-260191	b	54.70	17.40	9.49	nd	2.20	4.62	5.42	2.67	.34	1.49	1.06	.24	.00	99.63	.00	6.10	8.12	.00
JQ-8	h	do-	ppbs	D-260172	b	46.20	12.70	13.50	nd	10.40	10.80	2.20	.73	.60	2.91	.37	.18	.00	100.59	.00	19.09	2.50	.00
JQ-9	h	do-	bs	D-260171	b	45.90	14.80	14.20	nd	6.61	10.90	2.36	.56	.99	3.44	.43	.19	.00	100.38	.00	9.30	8.68	.00
JQ-10	lo	do-	ben	D-260175	b	54.90	17.40	9.17	nd	2.22	4.46	5.60	2.74	.00	1.39	.98	.23	.00	99.09	.00	8.33	4.58	.00
JQ-13	h	do-	ank	D-260174	b	46.10	10.70	12.60	nd	15.40	10.60	1.74	.51	.10	2.06	.25	.17	.00	100.23	.00	27.57	2.43	.00
JQ-16	h	do-	olbs	D-260192	b	46.10	12.70	13.60	nd	9.79	11.00	2.26	.75	.26	2.99	.39	.18	.00	100.02	.00	18.39	1.55	.00
JQ-17	h	do-	olbs	D-260184	b	45.10	11.00	13.10	nd	14.50	10.60	1.72	.43	.73	2.45	.29	.17	.00	100.09	.00	26.33	2.81	.00
JQ-20	h	do-	olbs	D-260190	b	46.90	13.50	13.80	nd	7.97	11.20	2.59	.84	.09	3.23	.42	.19	.00	100.73	.03	15.79	.00	.00
JQ-21	h	do-	bs	D-260182	b	45.30	14.70	13.60	nd	6.74	11.20	2.27	.57	1.52	3.42	.41	.18	.00	99.91	.00	10.29	6.47	.00
JQ-22	h	do-	olbs	D-277473	b	44.90	12.40	13.80	nd	11.90	10.20	1.68	.55	1.59	2.92	.34	.19	nd	100.47	.00	18.68	9.60	.00
JQ-23	h	do-	ank	D-277460	b	46.40	11.70	13.10	nd	12.20	11.00	1.93	.62	.71	2.73	.33	.17	nd	100.89	.00	19.81	4.75	.00
JQ-25	h	do-	ank	D-260183	b	46.40	11.80	12.60	nd	13.30	11.10	1.93	.52	.04	2.26	.26	.17	.00	100.38	.00	23.86	1.78	.00
JR-1	h	do-	bs	D-271452	b	46.80	14.40	14.20	nd	6.20	11.40	2.73	.78	.40	3.52	.44	.19	.00	101.06	.00	12.56	.44	.00
JR-2	h	do-	bs	D-271451	b	46.70	13.90	15.30	nd	5.26	9.36	3.26	1.23	.68	4.33	.65	.21	.00	100.88	.00	12.83	.60	.00
JR-3	h	do-	bs	D-271454	b	47.30	14.40	13.40	nd	6.80	11.80	2.49	.75	.18	3.41	.43	.18	.00	101.14	.00	10.09	4.02	.00
JR-4	h	do-	olbs	D-271455	b	46.50	14.60	12.60	nd	8.84	12.40	2.01	.27	.97	2.50	.28	.17	.00	101.14	.00	12.97	5.90	.00
JR-5	h	do-	bs	D-271445	b	46.40	14.50	14.50	nd	6.33	11.30	2.49	.75	.50	3.56	.42	.19	.00	100.94	.00	11.11	3.83	.00
JR-6	lo	do-	h/m	D-271446	b	48.90	17.10	12.30	nd	4.14	7.13	4.24	1.80	.72	2.94	.97	.22	.00	100.46	.40	14.78	.00	.00
JR-7	h	do-	bs	D-271447	b	48.40	13.70	15.30	nd	4.46	8.38	3.25	1.32	1.03	4.10	.67	.23	.00	100.84	.00	2.51	14.77	.00
JR-8	h	do-	bs	D-271449	b	45.00	15.00	16.70	nd	4.48	7.12	3.22	1.56	1.05	5.17	.85	.24	.00	100.39	.00	12.10	6.57	.00
JR-9	h	do-	bs	D-271448	b	47.30	14.00	14.60	nd	5.78	10.50	3.19	1.03	.00	3.88	.54	.20	.00	101.02	.73	12.40	.00	.00
JR-10	h	do-	bs	D-271450	b	47.90	13.80	13.80	nd	6.75	11.20	2.71	.83	.00	3.34	.42	.18	.00	100.93	.00	9.97	4.71	.00
JR-11	h	do-	olbs	D-271453	b	46.90	13.20	14.90	nd	7.50	9.92	2.98	1.06	.01	3.82	.55	.20	.00	101.04	.24	16.43	.00	.00
JR-12	h	do-	plbs	D-271456	b	47.60	14.20	14.70	nd	6.07	10.60	2.93	.80	.18	3.75	.52	.21	.00	101.56	.00	10.05	4.94	.00
JR-13	h	do-	plbs	D-260189	b	46.20	14.70	15.10	nd	5.24	9.58	2.59	.85	.93	3.62	.52	.21	.00	99.54	.00	5.29	13.82	.00
JS-1	h	do-	bs	D-271466	b	46.50	13.70	15.20	nd	5.27	9.78	3.26	1.30	.00	4.88	.71	.20	.00	100.80	.68	11.68	.00	.00
JS-2	h	do-	bs	D-271457	b	46.50	13.70	15.40	nd	5.15	9.54	3.15	1.34	.25	5.00	.75	.21	.00	100.99	.00	10.90	1.61	.00
JS-3	h	do-	bs	D-271463	b	45.90	13.30	14.90	nd	5.40	9.51	3.08	1.30	.92	4.79	.73	.20	.00	100.03	.00	11.30	1.38	.00
JS-4	h	do-	plbs	D-271464	b	46.60	14.80	14.30	nd	6.17	10.50	2.70	.66	.76	3.75	.34	.19	.00	100.77	.00	9.57	6.53	.00
JS-5	h	do-	olbs	D-271465	b	46.60	12.90	14.60	nd	8.23	10.00	2.94	1.00	.67	3.54	.52	.19	.00	101.19	.87	17.57	.00	.00
JS-6	h	do-	bs	D-271462	b	47.40	12.70	13.80	nd	9.52	11.00	2.66	.86	.00	3.22	.44	.18	.00	101.78	.64	18.04	.00	.00
JS-7	h	do-	olbs	D-271461	b	48.60	13.40	13.30	nd	7.89	11.30	2.37	.51	.13	3.08	.34	.18	.00	101.10	.00	5.01	14.33	.00
JS-8	h	do-	bs	D-271459	b	46.70	13.70	14.50	nd	7.25	9.64	3.53	1.22	.00	3.83	.64	.19	.00	101.20	3.64	15.66	.00	.00
JS-9	h	do-	ank	D-271460	b	47.40	10.60	12.70	nd	14.40	11.40	1.74	.43	.09	2.21	.26	.18	.00	101.41	.00	21.37	6.46	.00
JS-10	h	do-	olbs	D-271458	b	48.90	13.30	14.30	nd	7.02	10.80	2.50	.61	.21	3.27	.39	.19	.00	101.49	.00	2.75	16.81	.00
Ki-1	h	do-	olbs	Ki-1	d	45.73	13.06	13.79	nd	9.82	10.82	2.23	.64	nd	3.09	.36	.18	nd	99.72	.00	18.48	2.45	.00
Ki-2	h	do-	olbs	Ki-2	d	45.48	12.78	13.90	nd	10.20	10.77	2.42	.64	nd	3.11	.35	.18	nd	99.83	.91	20.63	.00	.00
Ki-3	h	do-	pic	Ki-3	d	44.38	7.63	13.30	nd	24.24	7.38	1.08	.08	nd	1.55	.16	.19	nd	99.99	.00	42.24	10.42	.00
Ki-4	h	do-	pic	Ki-4	d	45.99	9.99	13.40	nd	17.22	9.47	1.40	.21	nd	2.17	.21	.17	nd	100.23	.00	24.87	13.94	.00
Ki-5	h	do-	pic	Ki-5	d	46.78	9.76	12.90	nd	16.91	9.39	1.25	.39	nd	2.09	.21	.19	nd	99.87	.00	20.27	19.15	.00

Table 1. Chemical analyses and normative ne, ol, hy, and q in Mauna Kea lavas—Continued.

Sample Locality No.	Unit	Feature	Type	Laboratory No.	Remark	Major oxides													Partial CIPW norm			
						SiO_2	Al_2O_3	Fe_2O_3	FeO	MgO	CaO	Na_2O	K_2O	H_2O	TiO_2	P_2O_5	MnO	CO_2	Total	ne	ol	hy	q
Ki-6	h	do-	olbs	Ki-6	d	45.65	13.10	13.89	nd	9.14	10.84	2.45	0.70	nd	3.28	0.39	0.18	nd	99.62	0.30	18.62	0.00	0.00
Ki-6G	h	do-	gm	D101088	e	46.65	14.23	3.15	9.27	6.50	11.91	3.03	.79	.14	3.88	.43	.18	.00	100.16	2.72	10.92	.00	.00
Ki-7	h	do-	olbs	Ki-7	d	45.71	13.41	13.93	nd	8.68	11.08	2.17	.66	nd	3.41	.38	.19	nd	99.62	.00	14.37	4.88	.00
Ki-8	h	do-	pic	Ki-8	d	46.25	8.78	12.71	nd	17.89	10.29	1.76	.12	nd	1.81	.19	.16	nd	99.96	.00	30.58	3.95	.00
Ki-9	h	do-	bs	Ki-9	d	47.22	13.57	13.76	nd	8.60	11.23	2.27	.17	nd	2.76	.29	.19	nd	100.06	.00	9.10	12.67	.00
Ki-10	h	do-	bs	Ki-10	d	48.19	14.14	13.24	nd	6.38	11.25	2.55	.70	nd	3.03	.35	.18	nd	100.01	.00	5.16	10.80	.00
Ki-11	h	do-	ank	Ki-11	d	46.23	7.61	12.31	nd	20.13	10.66	.95	.23	nd	1.46	.15	.16	nd	99.89	.00	29.29	10.70	.00
Ki-11G	h	do-	gm	?	e	49.36	14.88	3.25	6.12	7.66	12.43	2.46	.62	.09	2.67	.31	.14	.01	100.00	.00	5.02	9.16	.00
Ki-101	h	do-	pic	I3730	e	47.07	9.73	2.52	9.31	18.68	8.48	1.59	.32	.21	1.90	.20	.18	.01	100.20	.00	27.23	14.79	.00
Ki-101G	h	do-	gm	D101089	e	49.42	12.64	2.89	8.64	9.13	11.11	2.52	.30	.23	2.67	.27	.17	nd	99.99	.00	5.82	15.41	.00
La-1	h	do-	olbs	La-1	d	45.97	13.82	14.00	nd	8.49	10.35	2.74	.55	.70	3.26	.49	.20	nd	100.57	.00	18.06	.97	.00
La-2	h	do-	bs	La-2	d	47.72	14.60	14.20	nd	6.62	10.84	2.44	.19	.82	3.17	.34	.19	nd	101.13	.00	2.28	18.49	.00
La-3	h	do-	bs	La-3	d	49.37	13.24	13.20	nd	6.61	10.68	2.32	.54	.38	2.93	.30	.17	nd	99.74	.00	.00	19.29	1.70
La-4	h	do-	ank	La-4	d	47.16	10.32	12.89	nd	14.20	10.79	1.84	.45	.11	2.31	.25	.18	nd	100.50	.00	20.79	7.90	.00
La-4G	h	do-	gm	D101083	e	48.31	14.16	2.25	9.11	7.21	12.10	2.40	.62	.46	2.92	.32	.17	.01	100.04	.00	6.66	8.45	.00
La-5	h	do-	ank	La-5	d	46.72	10.66	14.40	nd	12.57	9.62	2.20	.71	.30	2.83	.34	.20	nd	100.55	.00	21.12	6.57	.00
La-6	h	do-	pic	La-6	d	44.43	10.47	14.34	nd	15.90	8.82	1.74	.32	.43	2.53	.31	.19	nd	99.48	.00	29.07	7.43	.00
La-7	h	do-	bs	La-7	d	47.62	13.34	13.56	nd	7.77	9.73	3.13	1.05	.81	3.17	.50	.19	nd	100.87	.15	16.64	.00	.00
La-7G	h	do-	gm	D101087	e	47.83	13.99	6.02	6.77	6.31	10.14	2.97	1.02	.71	3.54	.52	.18	.01	100.01	.00	9.55	5.62	.00
La-8	h	do-	olbs	La-8	d	46.58	13.20	13.80	nd	8.55	9.92	3.17	.92	.32	3.17	.48	.19	nd	100.30	2.25	17.98	.00	.00
La-9	h	do-	olbs	La-9	d	45.56	12.97	14.00	nd	9.66	10.74	2.85	.72	.26	3.20	.38	.19	nd	100.53	3.43	19.15	.00	.00
La-10	h	do-	bs	La-10	d	45.49	13.03	14.00	nd	9.64	10.74	2.44	.69	.44	3.19	.38	.19	nd	100.23	.75	19.82	.00	.00
La-11	h	do-	bs	La-11	d	49.46	13.43	13.58	nd	6.05	10.30	2.51	.60	.14	3.02	.32	.19	nd	99.60	.00	.00	18.82	1.67
La-101	h	do-	olbs	I4174	e	45.50	13.56	5.22	7.85	9.88	9.66	2.33	.47	1.81	3.20	.39	.18	.01	100.06	.00	16.70	8.28	.00
La-102	h	do-	olbs	I3726	e	47.28	13.98	3.27	9.00	8.07	11.25	2.40	.43	.70	3.03	.34	.18	.00	99.93	.00	9.82	9.20	.00
La-102G	h	do-	gm	D101084	e	47.34	14.49	3.44	9.16	6.57	11.44	2.61	.50	.58	3.40	.33	.18	.01	100.05	.00	8.30	6.95	.00
La-103	h	do-	bs	I3727	e	45.32	14.86	3.90	11.25	4.96	7.89	3.41	1.65	.75	4.79	.88	.22	.01	99.89	1.04	16.21	.00	.00
La-103G	h	do-	gm	D101085	e	44.04	14.32	4.31	12.15	5.05	7.56	3.18	1.71	1.11	5.24	.92	.23	.01	99.83	.87	17.76	.00	.00
La-104	h	do-	bs	I3728	e	47.93	14.44	3.16	10.35	5.79	10.58	2.89	.84	.11	3.37	.42	.20	.01	100.09	.00	9.33	5.88	.00
La-104G	h	do-	gm	D101086	e	48.01	14.31	3.32	10.55	5.29	10.20	3.07	.95	.09	3.65	.41	.20	.01	100.06	.00	9.27	4.89	.00
La-105	h	do-	pic	K3580	e	44.70	8.42	3.40	8.86	22.03	8.22	1.17	.14	.86	1.79	.18	.18	.04	99.99	.00	37.50	10.20	.00
La-105G	h	do-	gm	D101082	e	46.63	12.34	4.58	7.18	9.99	11.73	1.84	.19	1.72	2.97	.27	.16	.00	99.60	.00	7.81	14.76	.00
Mu-2	h	do-	bs	Mu-2	d	47.68	14.98	13.25	nd	6.82	11.91	2.14	.20	.29	2.62	.27	.19	nd	100.35	.00	2.91	16.43	.00
Mu-3	h	do-	plbs	Mu-3	d	47.83	14.35	14.52	nd	5.93	10.79	2.52	.31	.31	3.32	.35	.19	nd	100.42	.00	.96	18.24	.00
Mu-4	h	do-	olbs	Mu-4	d	46.65	13.96	13.73	nd	8.05	11.51	2.04	.19	.49	3.03	.31	.17	nd	100.13	.00	6.27	15.03	.00
Mu-5	h	do-	olbs	Mu-5	d	45.93	14.32	13.49	nd	7.93	10.18	2.80	.88	.09	3.28	.41	.17	nd	99.48	.85	17.36	.00	.00
Mu-6	h	do-	bs	Mu-6	d	44.28	15.24	16.22	nd	5.76	9.29	2.84	.67	.80	4.73	.70	.20	nd	100.73	.00	13.49	4.90	.00
Mu-7	h	do-	bs	Mu-7	d	47.47	14.28	14.55	nd	6.28	11.13	2.36	.40	.38	3.25	.34	.19	nd	100.63	.00	3.17	15.69	.00
Mu-8	h	do-	bs	Mu-8	d	47.02	12.19	13.76	nd	10.76	11.24	1.39	.18	.71	2.74	.29	.19	nd	100.47	.00	4.64	24.52	.00
Mu-9	h	do-	ank	Mu-9	d	45.93	9.62	13.53	nd	15.93	10.80	1.26	.22	.53	2.04	.22	.19	nd	100.27	.00	22.32	12.18	.00
Mu-10	h	do-	olbs	Mu-10	d	45.48	11.58	14.01	nd	14.28	9.75	1.71	.21	.43	2.53	.29	.18	nd	100.45	.00	22.35	11.25	.00
Mu-11	h	do-	bs	Mu-11	d	46.18	14.61	15.74	nd	5.15	8.57	2.90	1.20	1.56	4.83	.61	.21	nd	101.56	.00	7.28	10.70	.00
Mu-13	h	do-	bs	Mu-13	d	47.12	14.82	14.41	nd	6.03	10.62	2.66	.22	.85	3.29	.33	.19	nd	100.54	.00	4.67	14.18	.00
Mu-14	h	do-	bs	Mu-14	d	46.85	15.01	14.96	nd	6.25	10.01	2.61	.21	1.30	3.42	.35	.20	nd	101.17	.00	4.69	16.83	.00
Mu-15	h	do-	bs	Mu-15	d	46.57	14.48	14.46	nd	6.74	11.42	2.18	.18	.54	3.32	.32	.20	nd	100.41	.00	4.21	15.51	.00
Wa-4	hh	do-	olbs	H-4	d	48.08	11.96	13.06	nd	9.98	11.51	1.75	.56	.30	2.56	.31	.18	nd	100.25	.00	6.16	17.87	.00
Wa-6	hh	do-	bs	H-6	d	47.35	14.10	13.79	nd	6.15	11.04	3.14	.96	.17	3.58	.50	.19	nd	100.97	1.36	12.00	.00	.00
Wa-7	hh	do-	olbs	H-7	d	48.72	13.99	12.47	nd	7.07	11.79	2.18	.60	.15	2.81	.32	.19	nd	100.29	.00	1.28	16.66	.00
Wa-8	hh	do-	olbs	H-8	d	48.63	12.50	12.66	nd	8.31	12.27	1.82	.55	.54	2.66	.31	.18	nd	100.43	.00	.97	18.95	.00
Wa-9	hh	do-	bs	H-9	d	48.80	13.27	12.06	nd	7.90	12.51	2.00	.51	.36	2.53	.28	.17	nd	100.39	.00	2.16	15.62	.00
Wa-10	hh	do-	bs	H-10	d	48.53	12.77	12.72	nd	7.96	12.24	1.98	.57	.24	2.74	.32	.19	nd	100.26	.00	2.41	16.07	.00
Wa-11	hh	do-	bs	H-11	d	48.01	14.23	13.94	nd	5.66	11.18	2.21	.75	.29	3.12	.38	.19	nd	99.96	.00	.00	17.66	.23
Wa-13	hh	do-	bs	H-13	d	47.50	14.55	13.79	nd	5.91	11.00	2.56	.67	.24	3.31	.40	.19	nd	100.12	.00	5.17	10.99	.00
Wa-14	hh	do-	bs	H-14	d	47.21	13.95	15.06	nd	5.64	10.51	2.55	.72	.37	3.67	.46	.21	nd	100.35	.00	4.02	13.42	.00
Wa-16	hl	do-	bs	H-16	d	47.13	14.05	14.49	nd	5.83	10.82	3.21	.73	nd	3.49	.40	.20	nd	100.35	.98	12.45	.00	.00
Wa-17	hl	do-	bs	H-17	d	48.36	13.80	14.77	nd	4.80	9.40	3.35	1.07	nd	3.76	.70	.21	nd	100.22	.00	6.04	8.77	.00

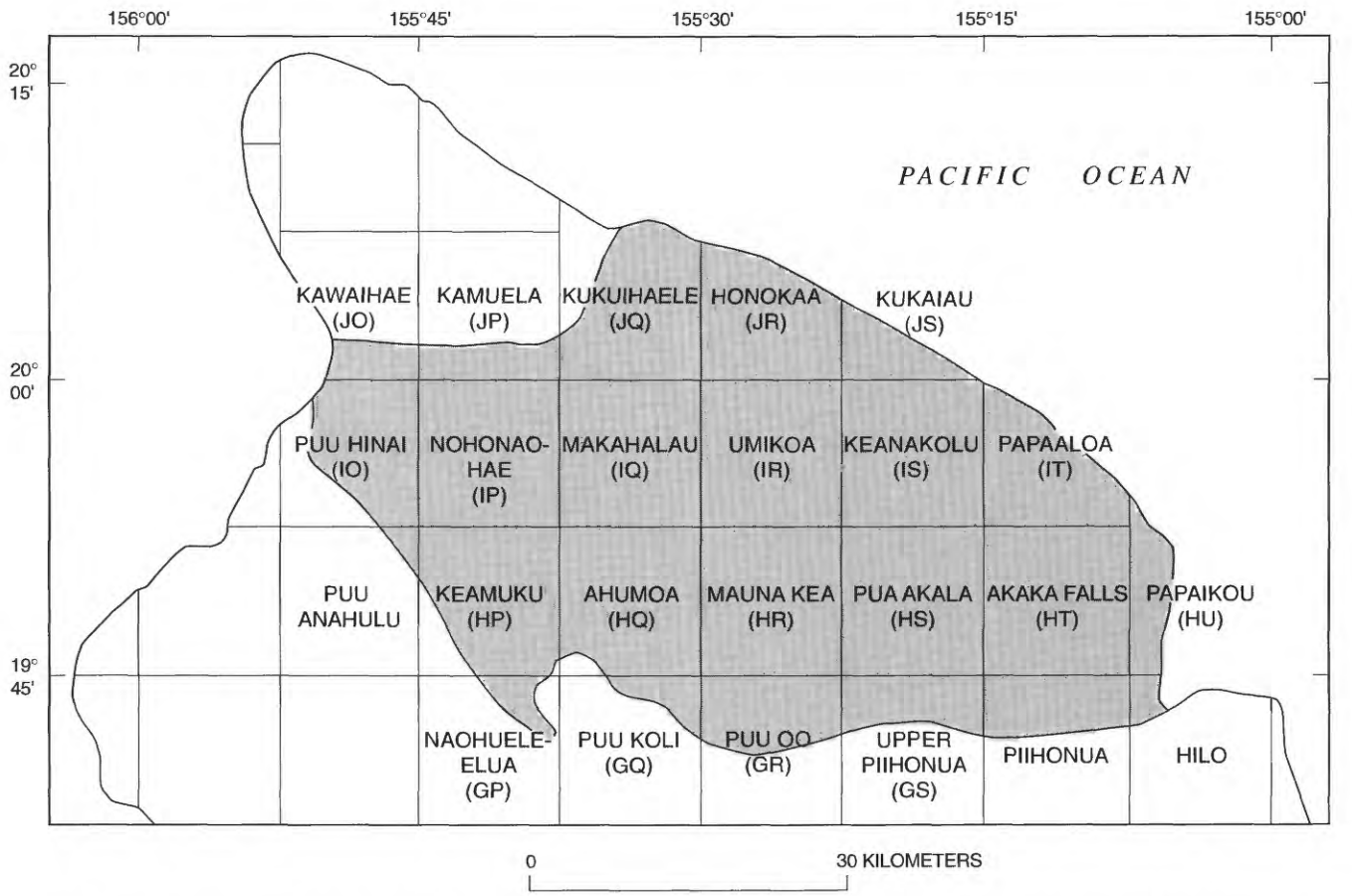

Figure 2. Index map of north half of Island of Hawaii, showing approximate area of Mauna Kea lavas (shading) and locations of U.S. Geological Survey 7½′ quadrangles that cover that area. Also shown are quadrangle-identifier codes (in parentheses), which, in combination with locality numbers, give sample-locality numbers used in tables, figures, and text; see plates 3 and 4 for explanation of sample-locality-numbering system.

break in slope that had previously been maintained at the shoreline of the active shield.

A section through the summit and northeast flank of Mauna Kea (fig. 3) reveals the shield-stage slope break at a depth of approximately 400 m. This submerged slope break shows that subsidence continued after the end of shield growth and that the gently sloping nearshore bench is essentially a relic of the final surface of the subaerial shield-stage lavas. Although there are no subaerial exposures of this shield, we approximate its profile by analogy with Mauna Loa (fig. 1*B*).

Our view that the gently sloping nearshore bench approximately represents the final surface of the subaerial tholeiitic shield differs from a recent hypothesis of Moore and Clague (1992), who inferred, on the basis of subsidence rates estimated from the submergence of dated coral-reef deposits, that the voluminous shield-building eruptions of Mauna Kea ceased at about 130 ka. By 130 ka, eruptions of alkalic and transitional basalt had been occurring for about 100,000 yr or more (since before eruption of the lava flow dated at 237±31 ka; see section below entitled "Geochronology"). Subsidence of approximately 400 m in 130,000 yr indicates an average subsidence rate of 3 mm/yr. Extrapolated to the period between 130 ka and the end of predominantly tholeiitic-lava production before 237±31 ka, the 3-mm/yr subsidence rate implies that an average thickness of at least 300 m of alkalic and transitional basalt would have had to accumulate above the predominantly tholeiitic shield lavas at the present position of the submerged slope break to maintain the slope break at sea level until 130 ka. Yet, in present seacliff exposures, the lava flow dated at 237±31 ka (pl. 4; see fig. 13) occurs only about 100 m below the relict, onshore, subaerial surface of the volcano; and lava flows as old as 187±40, 149±23, and 153±22 ka (pl. 4; tables 4, 5) form parts of the relict subaerial surface of the north and northwest flanks. As noted below (see section entitled "Hamakua Volcanics"), the lava flows of both the coastal sections and the subaerial flanks are predominantly aa flows, each representing an individual eruption from a single isolated vent. Large lava shields with extensive flow

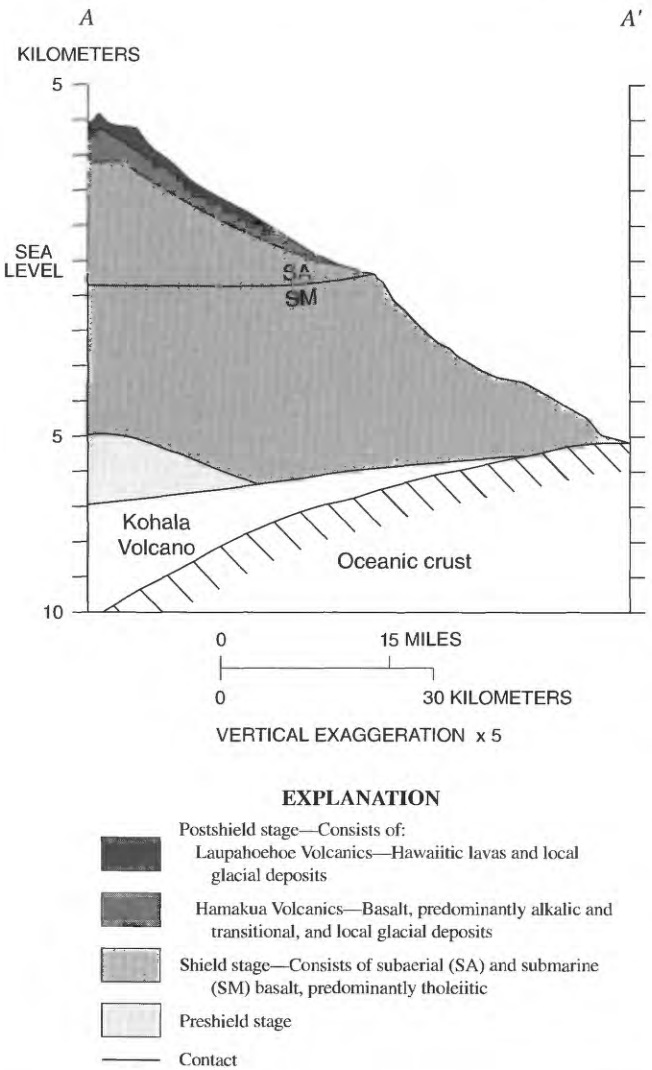

Figure 3. Cross section through northeast flank of Mauna Kea (line *A–A'*, fig. 1*B*), illustrating relations between preshield, shield, and postshield lavas. Cross section based in part on Moore and Fiske (1969, fig. 3). Note downwarping of oceanic crust and lavas of Kohala Volcano, preshield stage, and shield stage.

fields of tube-fed pahoehoe, such as those that comprise two-thirds of Kilauea's surface (Holcomb, 1987) and represent the sustained eruptions which are largely responsible for maintenance or extension of Kilauea's shoreline, are not exposed on Mauna Kea. Therefore, we doubt that the eruptions of alkalic and transitional basalt were able to sustain shield growth, as proposed by Moore and Clague (1992), and we regard the gently sloping nearshore bench as approximately representing the final surface of the predominantly tholeiitic subaerial shield. Because postshield lavas are truncated by the coastal seacliffs, the shield-stage lavas underlying the nearshore bench evidently are at least partly mantled by postshield lava flows.

Postshield lava flows and pyroclastic rocks overlie the Mauna Kea shield and form the volcano's present subaerial surface. Our geologic mapping shows that during the early part of this stage only basaltic lavas were erupted (Hamakua Volcanics), and during the later part only hawaiitic lavas (Laupahoehoe Volcanics). On this basis, we divide the postshield stage of Mauna Kea into two parts: the basaltic and hawaiitic substages.

It is instructive to consider the construction of the entire volcanic pile in terms of volume versus time (fig. 4). Swanson (1972) estimated the average modern magma-supply rate for Kilauea Volcano at approximately 0.1 km^3/yr. If that rate applied throughout most of the Mauna Kea shield stage, a shield as large as that of Mauna Kea could be built in 320,000 yr. More likely, however, the rate of 0.1 km^3/yr is a maximum, appropriate for episodes of sustained eruption, and the average long-term magma-supply rate at Kilauea ranges from 0.01 to 0.1 km^3/yr (Dvorak and Dzurisin, 1993). Using an intermediate value of approximately 0.05 km^3/yr as our estimate for the average supply rate, we illustrate a 650,000-yr duration for the shield stage in figure 4. The relatively small volume of the postshield lavas of Mauna Kea, erupted over a period of about 250,000 yr, indicates that postshield magma supply was far less, averaging about 0.004 km^3/yr.

Decreasing magma supply provides a context for interpreting the magmatic and volcanic evolution of Mauna Kea during its shield and postshield stages. The decreasing magma supply was accompanied by changing lava composition, from tholeiitic basalt that dominated the shield stage, through transitional and alkali basalt that dominated the postshield basaltic substage, to hawaiitic lava of the postshield hawaiitic substage. The transition from the shield to the postshield stage was also accompanied by a change in eruptive style: from fissure eruptions that recurred at the summit and along the conspicuous east rift zone, to isolated eruptions from numerous individual point-source vents, many of which are now marked by cinder cones scattered over much of the subaerial part of the volcano.

COMPOSITIONAL DATA SET

This study has generated a new major-oxide data set representing 444 analyzed samples (table 1). Samples from approximately 85 percent of the individually mapped flows have been analyzed; most (354) samples were analyzed for major elements by X-ray-fluorescence methods at the U.S. Geological Survey's laboratory in Denver, Colo. In addition, samples were analyzed from three gulches along the northeast coast (Frey and others, 1991; K.J. Murata, unpub. data, 1961–66), from Waikahalulu Gulch on the upper south slope, from surface flows on the lower northwest slope (Frey and others, 1990), and from shield-stage rocks dredged from Hilo Ridge (D.L. Peck, unpub. data, 1965).

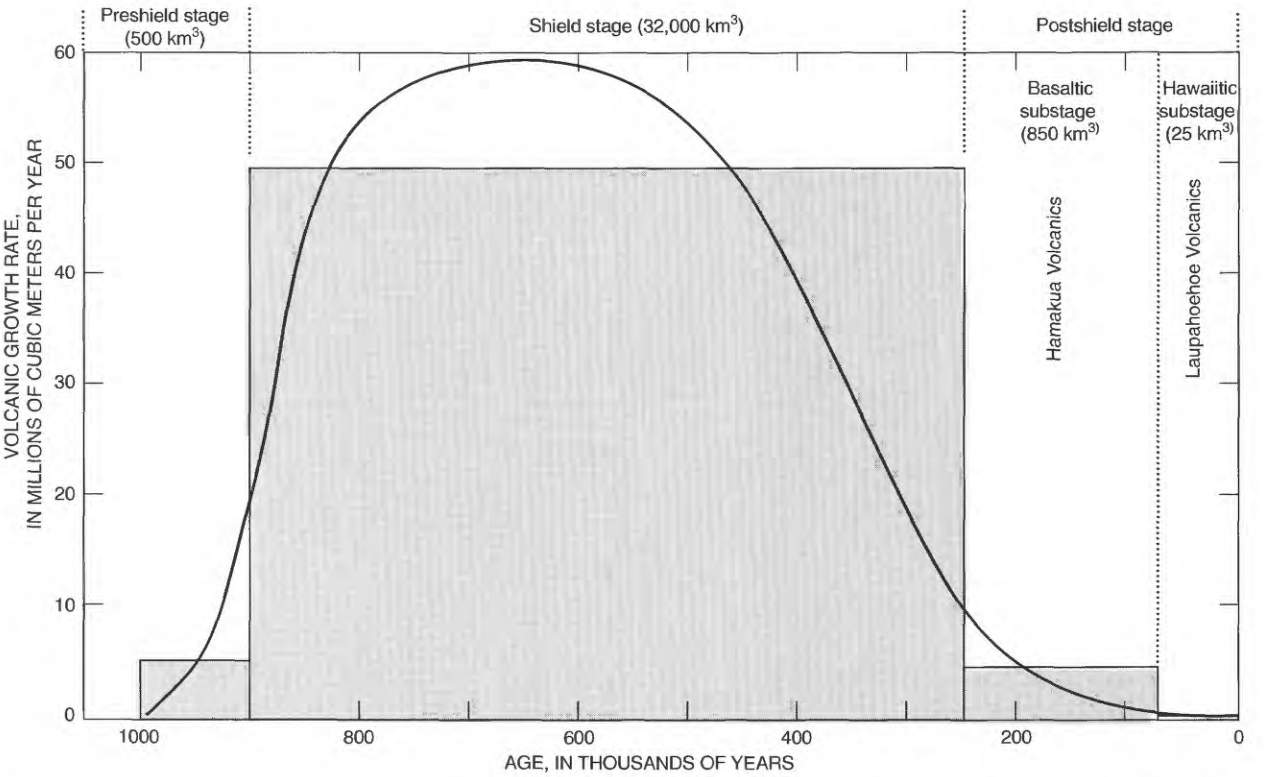

Figure 4. Volume versus time for lavas of Mauna Kea, illustrating three stages of growth (modified from Wise, 1982, and Frey and others, 1990). Shaded areas are proportional to estimated rock volumes for each stage. Curve shows inferred variation in growth rate over time. Growth rate for preshield and shield stages equals magma-supply rate, but because volume of postshield stage includes only extruded lava (intruded volume is unaccounted for), growth rate for postshield stage equals lava-supply rate.

MAJOR ROCK CLASSES AND PETROGRAPHIC GROUPS

For consistency with usage elsewhere, we generally follow the recently accepted International Union of Geodesy and Geophysics' (IUGG) compositional classification (Le Bas and others, 1986). The entire data set, on a plot of total alkali versus silica contents[2] according to the IUGG scheme, is shown in figure 5; a clear separation of the Hamakua and Laupahoehoe lavas is evident. In this scheme, all but four of the Hamakua lavas, including most of the evolved basalts, fall within the basalt field. The three Hamakua hawaiites are compositionally and petrographically akin to other evolved Hamakua basalts but not to Laupahoehoe hawaiites. For simplicity, we refer to the Hamakua lavas generally as basalt or designate them by petrographic type, such as plagioclase basalt or ankaramite, on the basis of phenocryst type and abundance, as defined in table 2. Additional compositionally based basalt groups are discussed below in the section entitled "Petrology."

Early uses of the terms "hawaiite," "mugearite," and "benmoreite" largely depended on petrographic determination of the plagioclase composition. Later, Coombs and Wilkinson (1969) proposed a set of criteria based on differ-

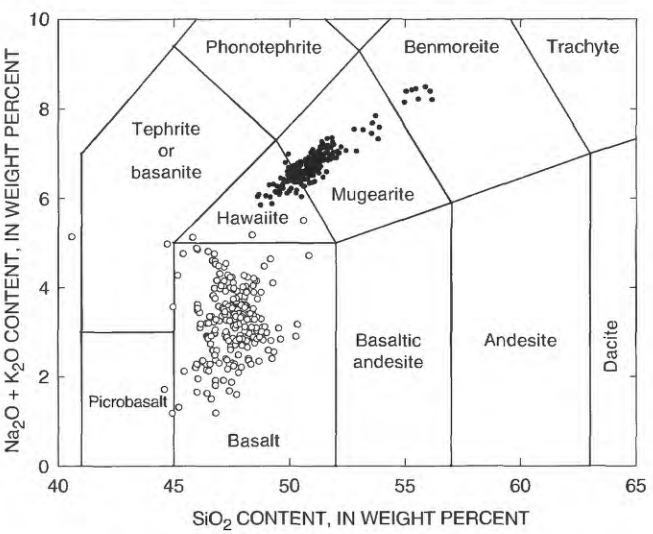

Figure 5. Na_2O+K_2O versus SiO_2 contents for all analyzed Mauna Kea lavas, showing field boundaries of lava types from Le Bas and others (1986). Circles, Hamakua Volcanics; dots, Laupahoehoe Volcanics.

[2] Data of table 1 have been adjusted by removal of normative calcite, partitioning of Fe to FeO and Fe_2O_3 in the ratio of 88:12, and recalculation to 100 percent dry weight for plotting in all diagrams showing major oxides or their calculated derivatives.

Table 2. Petrographic nomenclature for lavas of the Hamakua Volcanics

Rock name	Criterion	Relative phenocryst abundances
Olivine basalt	Olivine phenocrysts >5 volume percent	Olivine > augite or plagioclase
Plagioclase basalt	Plagioclase phenocrysts >5 volume percent	Plagioclase > olivine or augite
Porphyritic basalt	Phenocrysts >5 volume percent	Olivine ~ augite ~ plagioclase
Basalt	Phenocrysts <5 volume percent	
Ankaramite	Olivine+augite phenocrysts ~25 volume percent	Olivine ~ augite
Picrite	Olivine phenocrysts ~25 volume percent	Augite ~ 0 volume percent

entiation index and the anorthite (an) content of normative plagioclase. By these criteria, again a clear separation of the Hamakua and Laupahoehoe lavas is evident (fig. 6). However, a significant number of evolved Hamakua lavas fall within the hawaiite field, as do nearly all the Laupahoehoe lavas. Even though the nomenclature of Coombs and Wilkinson was used by West and others (1988) in describing Mauna Kea rocks, in this report we use the terminology of Le Bas and others (1986) because we expect that it will become the more widely used standard. Furthermore, Le Bas and others' scheme provides a compositional grouping of basalt versus hawaiite and mugearite that coincides nearly perfectly with clear lithologic distinctions which we recognize and use in the field. In contrast, we cannot distinguish a Hamakua basalt in Coombs and Wilkinson's scheme from a Hamakua hawaiite.

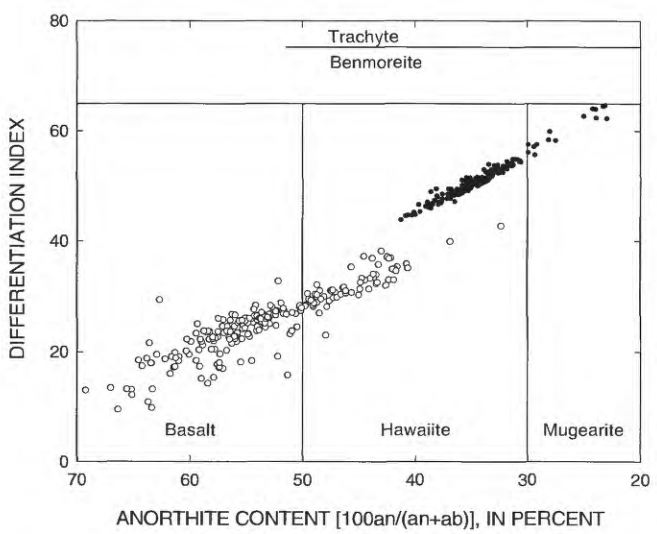

Figure 6. Differentiation index versus anorthite content in normative plagioclase for all analyzed Mauna Kea lavas, showing field boundaries of lava types from Coombs and Wilkinson (1969). Circles, Hamakua Volcanics; dots, Laupahoehoe Volcanics.

The Laupahoehoe lavas are largely represented in figure 5 by such a tight cluster across the hawaiite-mugearite boundary that the distinction seems meaningless for lavas of the Laupahoehoe Volcanics. Therefore, we generally refer to the lavas represented in that cluster as hawaiite-mugearite, to the most evolved lavas as benmoreite, and to the entire Laupahoehoe suite as hawaiitic.

STRATIGRAPHIC OVERVIEW

PREVIOUS STRATIGRAPHIC NOMENCLATURE

Surface exposures on Mauna Kea Volcano consist largely of lava flows and cinder cones, as well as several types of sedimentary deposits. Macdonald (1945, 1949) and Stearns and Macdonald (1946) divided the lavas into two units, the Laupahoehoe and Hamakua Volcanic Series (fig. 7), and recognized, but did not map, two sedimentary units, fluvial and glacial conglomerates and the Pahala Ash. They divided the Hamakua Volcanic Series into a lower member (Stearns and Macdonald, 1946, p. 154) composed "very largely of olivine basalt with less abundant primitive picrite-basalt," and an upper member "largely of olivine basalt" but with associated "andesites and picrites of the augite-rich type" (ankaramites). The overlying Laupahoehoe Volcanic Series was thought to consist of "andesite" and basalt that in some localities lay above an erosional unconformity. Where an obvious unconformity could not be recognized, relative age distinction was based on the thickness of ash or soil

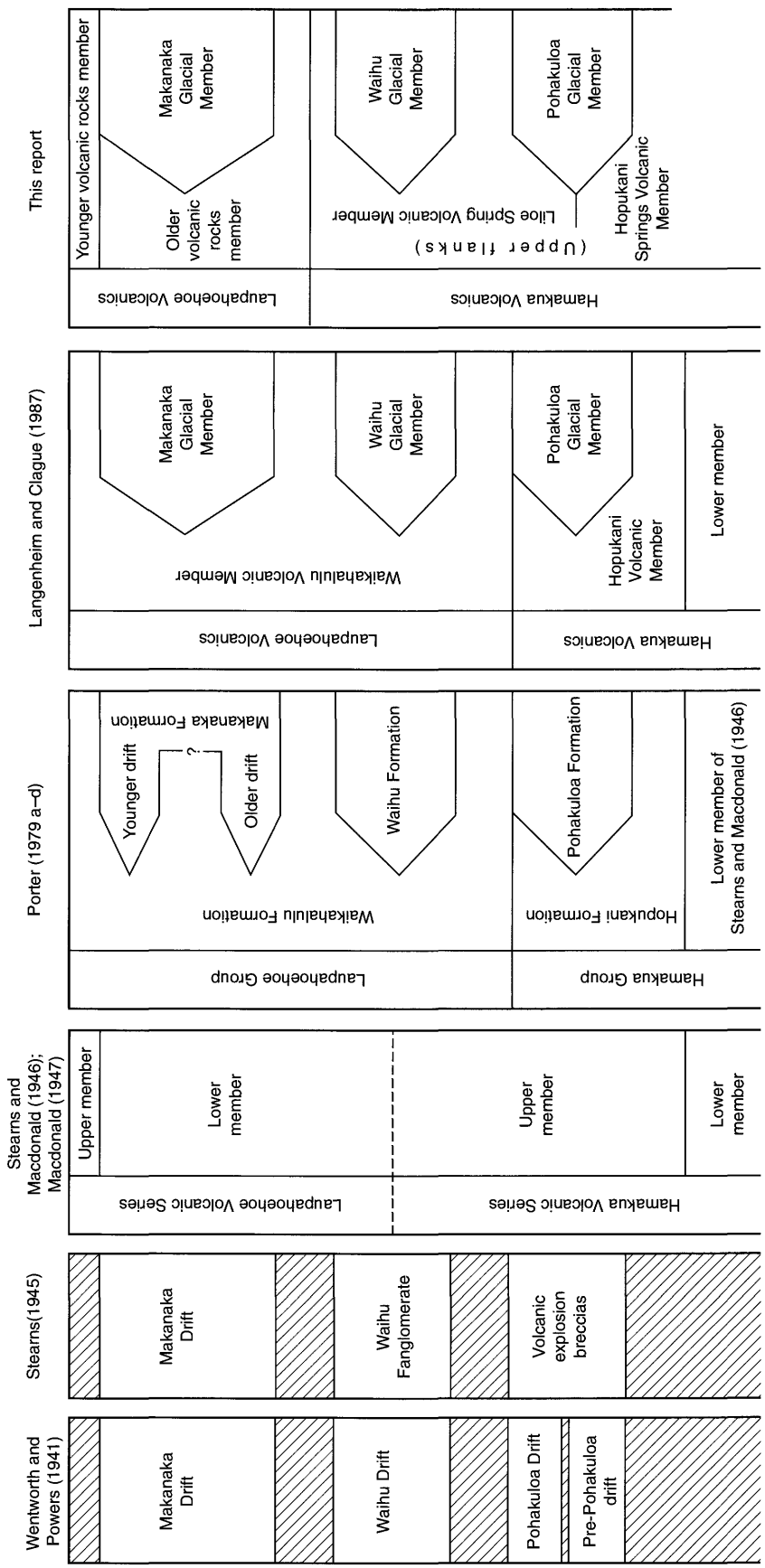

Figure 7. Correlation diagram comparing stratigraphic terminology for Mauna Kea used by previous workers with that used in this report. Diagonal-line pattern indicates unnamed lavas. Dashed line separating Hamakua and Laupahoehoe Series of Stearns and Macdonald (1946) reflects vague distinction between these two series (see text)

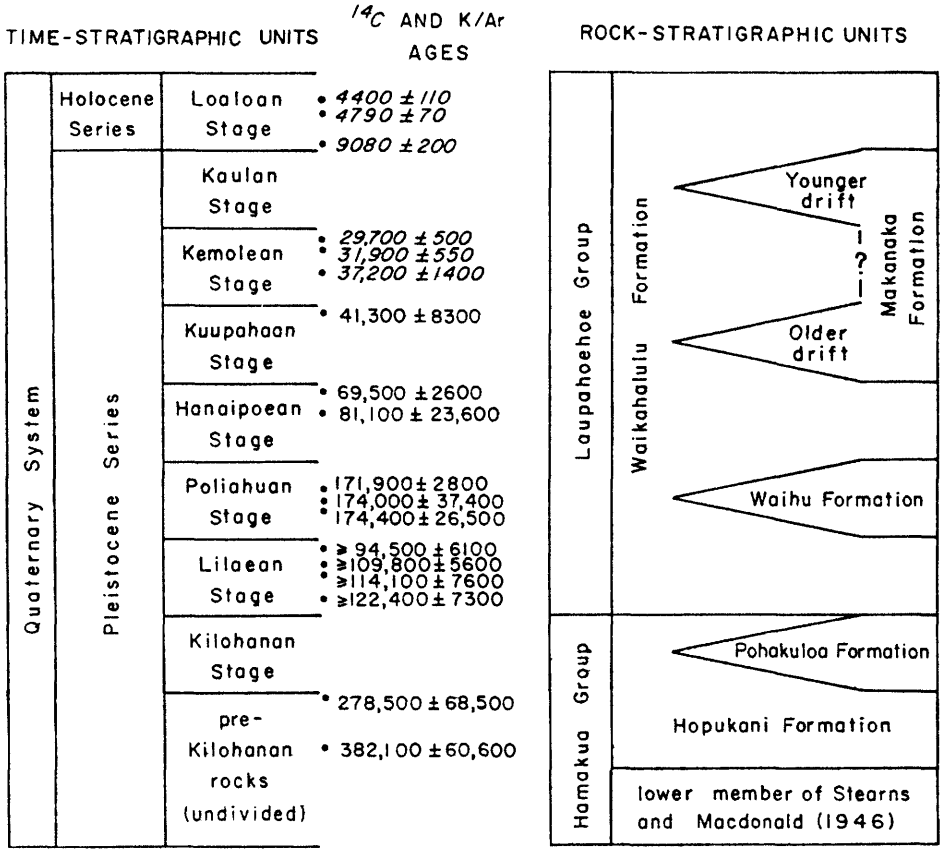

Figure 8. Correlation diagram showing time-stratigraphic and rock-stratigraphic units and isotopic ages as reported by Porter (1979a–d) for Mauna Kea. See figure 7 for comparison of Porter's stratigraphic units with those used in this report.

mantling a given lava flow. Thus, except that picritic basalts were mapped with the Hamakua Volcanic Series, the distinction between the two volcanic series is vague: "Locally, the criteria of ash cover and picrite-basalts fail, and the assignment of the flow to one series or the other depends entirely on the judgment of the field geologist" (Stearns and Macdonald, 1946, p. 169). The Laupahoehoe Volcanic Series was also divided into two members, an upper member of postglacial (Holocene) age and a lower member of Pleistocene age.

Figure 7 shows that several sedimentary units, interbedded with volcanic rocks, were recognized in the summit region of Mauna Kea. Porter (1979c) redefined the stratigraphic nomenclature to include these units as formations. He renamed the upper member of Stearns and Macdonald's (1946) Hamakua Volcanic Series, calling it the Hopukani Formation, and assigned its sedimentary interbeds to the Pohakuloa Formation, which he determined to represent glacial drift. These particular sedimentary deposits were first recognized as glacial drift by Wentworth and Powers (1941) but were later reinterpreted as explosion breccias by Stearns (1945) and included in the upper member of the Hamakua Volcanic Series by Stearns and Macdonald (1946). Porter (1979c) raised the Laupahoehoe Volcanic Series to group status, so that it could be divided into a volcanic unit, the Waikahalulu Formation, and two sedimentary units of glacial origin, the Waihu and Makanaka Formations. The latter two names had also been introduced by Wentworth and Powers (1941), but the Waihu Drift was reinterpreted by Stearns (1945) as a fanglomerate.

Porter (1979a–d) described and mapped two separate glacial-drift deposits within his Makanaka Formation; thus, he indicated that the Mauna Kea sequence recorded four glacial episodes. He correlated these sequences with marine oxygen-isotope stages 2, 4, 6, and 8 (Porter, 1979d). Porter assigned the lavas of Mauna Kea to chronostratigraphic stages on the basis of his interpretation of the relations of the lavas to the glacial deposits (fig. 8).

CHANGES IN STRATIGRAPHIC DEFINITIONS AND NOMENCLATURE

A major result of our mapping of the summit region of Mauna Kea is the recognition that basaltic lavas continued to be erupted after the Pohakuloa glacial episode and until shortly after the Waihu glacial episode. No hawaiitic lavas appeared throughout this interval; in fact, no intertonguing

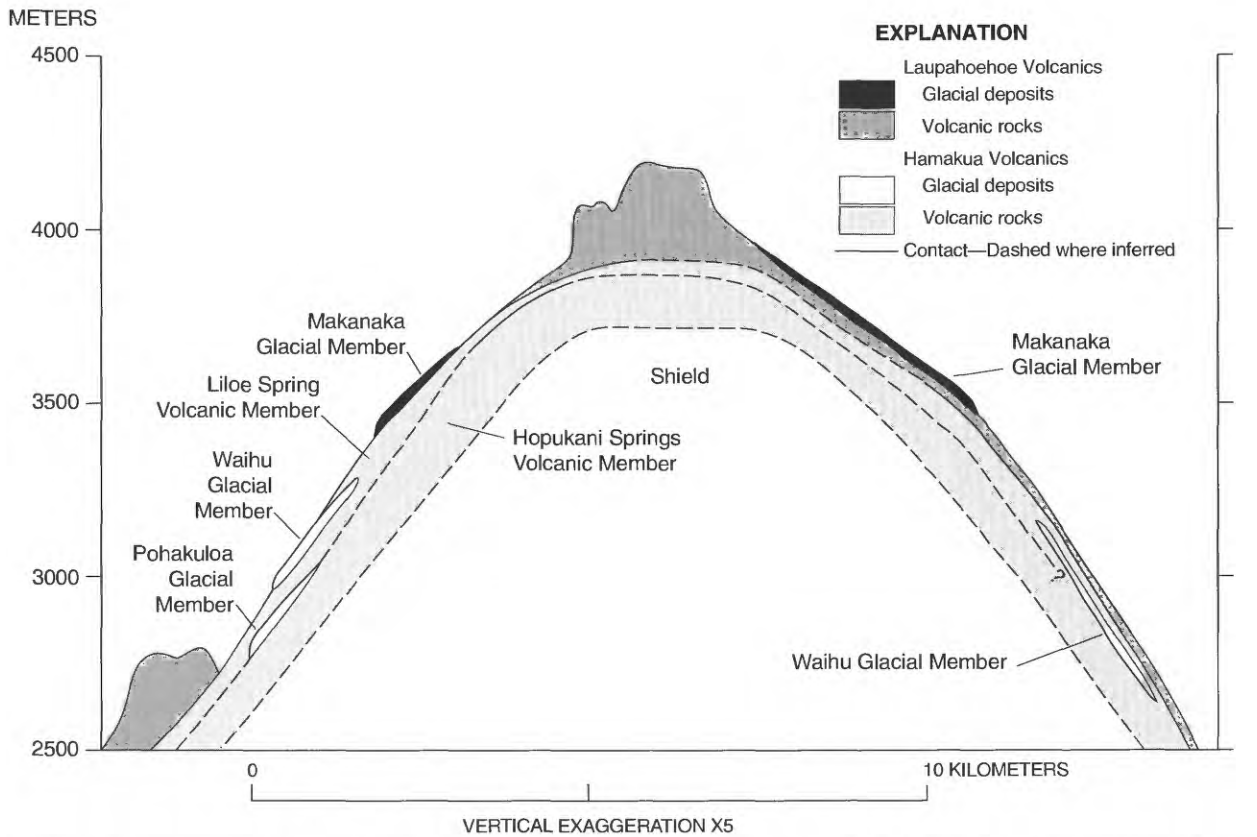

Figure 9. Diagrammatic cross section through summit and upper north and south flanks of Mauna Kea, illustrating spatial relations among stratigraphic units. Cross section runs approximately south to north (left to right). See plate 2 for description of units.

of basalt and hawaiitic lava has been observed anywhere on the volcano. In this report, the Hamakua and Laupahoehoe Volcanics are redefined to reflect these newly recognized compositional distinctions (figs. 7, 9; table 3). We assign all of the basaltic lavas to the Hamakua Volcanics and all of the hawaiitic lavas to the Laupahoehoe Volcanics. Modifying the stratigraphic format of Langenheim and Clague (1987), we have identified two new units, the Liloe Spring and Hopukani Springs Volcanic Members of the Hamakua Volcanics, to distinguish, respectively, olivine-poor basalts above the Pohakuloa Glacial Member from olivine-rich basalts below.

Porter's (1979a–d) major focus in his fieldwork was on the glacial chronology; in contrast, ours has been on volcanic and magmatic history. Building on Porter's published work, we have been able to devote greater attention to the lithologic and spatial relations of the volcanic units; therefore, we have significantly revised Porter's stratigraphic assignments of the lavas. We believe that field evidence does not justify Porter's detailed chronostratigraphic subdivision of the lavas (fig. 8), and so we have not perpetuated it. Part of Porter's detailed chronostratigraphic scheme hinges on his interpretation of two distinct Makanaka glacial episodes separated by an interglacial interval. Field relations (see subsection below entitled "Makanaka Glacial Member") and new K-Ar ages provide no evidence of a major interglacial hiatus, indicating to us only one Makanaka glacial episode, which included some retreat and readvance of the icecap.

GEOCHRONOLOGY

We report 30 new K-Ar ages (table 4) that significantly enlarge the previous data base of K-Ar ages (table 5) and provide important new constraints on the Pleistocene geochronology of Mauna Kea. Likewise, six new ^{14}C ages (table 6) determined by Meyer Rubin (written commun., 1987) on charcoal collected from directly beneath lava flows appreciably amplify the Holocene geochronology. Additional geochronologic evidence derived from the exposure ages determined by Dorn and others (1991) is discussed below in the section entitled "Stratigraphy."

Samples for K-Ar analysis (table 4) were selected on the basis of thin-section examination; those selected were generally free of alteration products and interstitial glass. In some samples, there was minor alteration of olivine to iddingsite, but this alteration is thought to be deuteric and, because both olivine and iddingsite contain negligible K_2O, has no effect on the K-Ar age. A few samples contained minor (less than 1 volume percent) interstitial glass, but

Table 3. Summary of postshield stratigraphic units of Mauna Kea

Unit	Description
Laupahoehoe Volcanics, undivided.	Hawaiitic lava flows, cinder cones, tephra-fall deposits, and associated glacial deposits. Forms much of the subaerial surface of Mauna Kea. Typical exposed thickness: more than 50 m. Type locality: Laupahoehoe Gulch. Reference locality: along road from Hale Pohaku to summit of Mauna Kea. Contains the Makanaka Glacial Member. Age: younger volcanic rocks member (postglacial), about 13 to 4 ka; older volcanic rocks member about 65 to 13 ka.
Makanaka Glacial Member.	Diamict and gravel. Exposed on upper slopes of volcano. Exposed thickness: 0 to 30-40 m. Type locality: Puu Makanaka. Reference localities: in Waikahalulu and Kemole Gulches. Age: about 40 to 13 ka, equivalent to late Wisconsin glaciation and marine oxygen-isotope stages 2 and 3 (part).
Hamakua Volcanics, undivided.	Basaltic lava flows and cinder cones and associated glacial deposits. Maximum exposed thickness: 170 m. Divided into four formally named members on upper slopes, where glacial deposits are intercalated with the lavas; elsewhere, the formation is undivided. Type locality: south wall of Laupahoehoe Gulch and adjacent seacliff. Reference localities: Maulua and Kaawalii Gulches and lower northwest flank of Mauna Kea. Base not exposed. Age: from about 200-250 ka to 65-70 ka.
Waihu Glacial Member.	Diamict and gravel. Exposed thickness: generally less than 30 m. Type locality: near Waihu Spring. Reference localities: Waikahalulu and Pohakuloa Gulches. Age: poorly constrained by K-Ar dating to between about 150 and 70 ka; exposure age of about 70 to 60 ka (Dorn and others, 1991) suggests approximate equivalence to marine oxygen-isotope stage 4.
Liloe Spring Volcanic Member.	Basaltic lava flows and cinder cones, composed largely of aphyric to weakly porphyritic basalt. Maximum exposed thickness: approximately 50 m. Overlies the Pohakuloa Glacial Member; underlies and locally overlies the Waihu Glacial Member. Type locality: Waikahalulu Gulch. Reference locality: Pohakaloa Gulch, near Liloe Spring. Age: poorly constrained, within interval from about 150 to 70-65 ka.
Pohakuloa Glacial Member.	Diamict and gravel. Exposed in Pohakuloa and Waikahalulu Gulches and in upper part of Wailuku River drainage. Maximum thickness: about 40 m. Type locality: west wall of Pohakuloa Gulch. Reference locality: Waikahalulu Gulch. Overlies lavas of the Hopukani Springs Volcanic Member. Age: equivalent to part of marine oxygen-isotope stage 6. Dorn and others (1991) report exposure ages of 156 to 140 ka.
Hopukani Springs Volcanic Member.	Basaltic lava flows and cinder cones, composed largely of porphyritic olivine basalt, plagioclase-olivine basalt, and ankaramite. Exposed mainly in gulches on upper slopes of south side of volcano. Maximum exposed thickness: approximately 30 m. Base not exposed. Type locality: Waikahalulu Gulch. Reference locality: Pohakuloa Gulch near Hopukani Springs. Age of exposed part: within interval from about 200 to 150 ka.

most were holocrystalline. Samples from flows that contained abundant ultramafic xenoliths, common in some hawaiite flows, were avoided.

For each whole-rock K-Ar analysis, a block of rock was crushed and sized to 0.5 to 1.0 mm. One aliquant was used for Ar analysis, and another was crushed to a fine powder for K_2O analysis. Four K_2O measurements were done on each sample by flame photometry, using the lithium metaborate fusion technique (Ingamells, 1970). Ar analyses were done by isotope dilution, using a multiple-collector rare-gas mass spectrometer (Dalrymple and Lanphere, 1969; Stacey and others, 1981).

Because the sampled lava flows are young, radiogenic ^{40}Ar contents are low, ranging from 0.3 to 10.2 percent, in most samples less than 6 percent (table 4). Thus, the precisions of the calculated ages, particularly those containing less than 3 percent radiogenic ^{40}Ar, are also low. Nevertheless, the K-Ar ages provide reasonable constraints on the ages of the mapped units.

Our new K-Ar ages and the analytical data on which they are based are listed in table 4. Previously determined K-Ar ages (Porter, 1979c; B.D. Turrin, written commun., 1986) are listed in table 5. Using precise map locations provided by B.D. Turrin and the approximate locations and stratigraphic descriptions of Porter, we have fitted these samples to our mapped rock units. The entire data set of K-Ar and ^{14}C ages for the volcanic units is graphically summarized in figure 10; the locations of the dated samples are

Table 4. Analytical data for newly reported whole-rock K-Ar ages on Mauna Kea lavas

[Map localities are listed by plate number and quadrangle identifier; see plates 3 and 4 for locations of samples and explanation of locality-numbering system. K_2O content is listed as mean and standard deviation of four analyses. Ages calculated using International Union of Geological Sciences constants for 1976 (Steiger and Jäger, 1977): $\lambda_B=4.962\times10^{-10}$/yr, $\lambda_E=0.581\times10^{-10}$/yr, and $^{40}K/K_{total}=1.167\times10^{-4}$ mol/mol. Error limits are estimates of analytical precision at the 68-percent-confidence level; mean ages for multiple analyses are weighted by the inverse of the variances. do., ditto]

Field sample No.	Map locality (pl., quad)	Rock type	K_2O (weight pct.)	Argon			Calculated Age
				Aliquant weight (g)	$^{40}Ar_{rad}$ (10^{-13} mol/g)	$^{40}Ar_{rad}$ (pct)	(ka)
Laupahoehoe Volcanics							
85G034	4,IP	Benmoreite	2.579±0.009	14.325	2.488	5.3	66±8
				14.853	2.271	1.7	
85G038	[1]3,GR	Hawaiite/ mugearite.	1.812±0.001	15.414	.646	.8	18±10
				15.292	.274	.3	
85G039	3,GR	do-------	1.831±0.049	12.581	1.067	1.8	40±13
85G044	3,HR	do-------	1.875±0.011	15.409	.845	1.8	31±9
85G045	3,HR	do-------	1.868±0.005	15.030	.689	2.0	39±7
				14.997	1.918	3.0	
W86G6-29	3,GR	do-------	2.006±0.006	10.221	1.140	4.6	39±20
W86G6-30	3,GR	do-------	1.852±0.003	10.502	1.307	2.6	49±21
W87H6-310	3,HR	do-------	2.203±0.006	11.586	1.678	1.7	53±14
W87H6-311	3,HR	do-------	2.192±0.003	10.691	3.384	4.4	107±13
W87H6-312	3,HR	do-------	2.027±0.007	10.371	.968	2.5	33±12
Liloe Spring Volcanic Member of the Hamakua Volcanics							
57-4	3,HQ	Basalt	1.057±0.002	10.438	1.981	7.1	130±33
85G040	3,HR	do-------	.711±0.004	15.995	1.601	4.3	157±23
85G042	3,HR	do-------	.951±0.002	14.544	1.181	1.8	86±22
85G043	3,HR	do-------	.871±0.004	15.482	1.252	2.1	100±22
W86I6-218	4,IR	do-------	.833±0.002	10.055	2.179	4.5	167±32
				10.109	1.823	4.7	
W86I6-219	4,IR	do-------	1.131±0.005	10.283	2.359	6.3	145±29
W87H6-288	3,HR	do-------	.732±0.009	10.305	1.569	3.0	136±29
				10.815	1.172	1.9	
W87H5-298	3,HQ	do-------	.892±0.000	11.078	3.206	5.0	218±25
				9.843	1.994	3.7	
W87H5-300	3,HQ	do-------	1.022±0.002	10.843	1.705	1.9	116±30
W87H5-304	3,HQ	do-------	.852±0.003	10.364	1.395	1.8	114±34
Hopukani Springs Volcanic Member of the Hamakua Volcanics							
85G041	3,HR	Basalt	0.657±0.005	14.744	1.447	1.7	153±38
Hamakua Volcanics (undivided)							
85G027	4,JO	Basalt	1.200±0.011	16.250	2.072	0.8	81±36
				16.216	1.017	.5	
85G036	[2]4,HP	do-------	.885±0.004	14.377	1.493	.9	117±50
85G033	[2]4,IP	do-------	.880±0.004	17.371	1.886	2.7	149±23
85G037	4,IO	do-------	1.453±0.005	15.164	2.151	10.2	103±10
La-7	4,IT	do-------	1.081±0.002	10.299	3.698	5.4	237±31
La-11	4,IT	do-------	.590±0.003	10.378	3.522	1.9	415±208
P86-2	[2]4,JP	do-------	.538±0.006	9.195	1.982	.3	256±389
P86-2A	[2]4,JP	do-------	.654±0.002	10.340	2.563	1.7	2,720±1,360
P86-21A	[2]4,JQ	do-------	.581±0.004	10.601	1.567	5.1	187±40

[1]Sample is from small unmapped lava-flow outcrop.
[2]See also plate 1, which shows lava flow from which sample was collected on diagram entitled "Correlation of Lavas of the Hamakua Volcanics."

Table 5. Other K-Ar ages on Mauna Kea lavas

[Map localities are listed by plate number and quadrangle identifier; see plates 3 and 4 for locations of samples and explanation of locality-numbering system. All samples are from lava flows except sample QLA–10a, which is from a bomb on Puu Waiau. Samples are correlated with mapped rock units by using map locations provided by B.D. Turrin (written commun., 1986) and approximate locations and stratigraphic descriptions of Porter (1979c). Sources of data: 1, Porter (1979c); 2, B.D. Turrin (written commun., 1986)]

Field sample No.	Map locality (pl., quad)	Source	Age and Standard Deviation (ka)
Laupahoehoe Volcanics			
MKL-1	4,HP	2	24±22
MKL-2	4,HP	2	50±14
MKL-3	4,HP	2	60±20
QLA-6d	3,HR	1	41±8
QLA-10a	3,HR	1	174±37
Liloe Spring Volcanic Member of the Hamakua Volcanics			
QLA-3c	3,HR	1	70±3
QLA-4a	4,IQ	1	81±24
QLA-5c	4,IQ	1	101±15
QLA-7f	3,HQ	1	174±27
QLA-9c, QLA-9d, QLA-9e	3,HR	1	110±6
QLA-15	3,HR	1	172±3
QLA-17b, QLA-17c	3,HQ	1	114±8
QLA-18	3,HQ	1	95±6
QLA-19	3,HR	1	121±4
QLA-20	3,HR	1	122±7
Hopukani Springs Volcanic Member of the Hamakua Volcanics			
QLA-8b	3,HR	1	279±69
Hamakua Volcanics (undivided)			
MKH-4	4,IO	2	153±22
QLA-11c	4,JP	1	382±61

shown on plates 3 and 4. K-Ar ages of several individual flows of the Hamakua Volcanics from the northwest flank of Mauna Kea are shown on the correlation diagram of plate 1.

Relative stratigraphic positions are known from field relations for many of the samples, especially those from the upper flanks of the volcano. This information is useful in assessing the errors and reliability of the K-Ar ages. Generally, K-Ar and ^{14}C ages for the Laupahoehoe Volcanics are closely grouped between approximately 65 and 4 ka (fig. 10), a range that is consistently younger than that determined for the underlying Hamakua Volcanics. Only the ages for Puu Waiau [our age of 107±13 ka (sample W87H6–311, table 4) for the flow from Puu Waiau (flow PW, pl. 2) and an age of 174±37 ka (sample QLA–10a, table 5) reported by Porter, 1979c, for a bomb from the Puu Waiau cinder cone] overlap the age range of the Hamakua Volcanics, including ages determined for flows of the Liloe Spring Volcanic Member that are stratigraphically below the Waihu Glacial Member. These data indicate that the age range of the Laupahoehoe Volcanics is approximately 65 to 4 ka and possibly as old as 100 ka. However, an exposure age of approximately 70 to 60 ka (Dorn and others, 1991) for the Waihu Glacial Member, which is older than the lava flow from Puu Waiau, supports 65 ka as the approximate older limit for the age of the Laupahoehoe Volcanics.

The ages of samples from the Hamakua Volcanics are poorer in quality than those from the hawaiitic Laupahoehoe Volcanics because of the substantially lower K_2O contents in Hamakua basalts. Stratigraphic control is excellent for the Hamakua Volcanics on the upper flanks of Mauna Kea because the Pohakuloa and Waihu Glacial Members provide excellent mappable stratigraphic markers and the sequence is well exposed in continuous canyon-wall sections in Pohakuloa and Waikahalulu Gulches (pl. 2). Our ages on samples from the Liloe Spring Volcanic Member range from 218 to 86 ka. In spite of apparent internal strati-

Table 6. Radiocarbon ages on charcoal from beneath Mauna Kea lava flows

[Map localities are listed by plate number and quadrangle identifier; see plates 3 and 4 for locations of samples and explanation of locality-numbering system. Age of sample I5292 from Porter (1971) and of sample W5541 from Rubin and others (1987); age of AA6795 determined by accelerator mass spectrometry at the University of Arizona (Meyer Rubin, written commun., 1991); all other ages from Meyer Rubin (written commun., 1987). Do., ditto]

Laboratory No.	Map locality (pl., quad)	Collector	^{14}C Age (yrs BP)	Description
I5292	[1]3,GR	S.C. Porter	4,400±110	Flow from Puu Kole (south flank).
W5825	4,IR	M.A. Kuntz	4,410±150	Flow from Puu Lehu.
W5776	3,GR	E.W. Wolfe	4,510±150	Flow from Puu Kole (south flank).
W5779	3,GR	do	4,550±150	Do.
W5823	4,HS	W.S. Wise	4,850±150	Flow from Puu Kanakaleonui.
AA6795	4,IS	P.M. Vitousek	5,085±97	Do.
W5773	3,GR	E.W. Wolfe	5,320±150	Flow originating 1 km southeast of Hale Pohaku.
W5541	3,GR	J.P. Lockwood	5,630±200	Flow from Kalaieha.
W5821	4,IR	M.A. Kuntz	7,100±150	Flow from Puu Kole (north flank).

[1]Location not shown on plate 3; Porter (1971) describes location as "2195 m in gully 1.8 km northeast of Puu Loaloa on north side of Keanakolu Road."

graphic inconsistency (fig. 11), none of these ages differs significantly at the 95-percent-confidence level except for sample W87H5–298, which has an apparent age of 218±25 ka. Our remaining ages are consistent with an age of from about 150 to 100 ka for the Liloe Spring Volcanic Member, and one age of 70±3 ka (Porter, 1979c; sample QLA–3c, table 5) suggests that the Liloe Spring Volcanic Member could be as young as 70 ka. An exposure age of approximately 70 to 60 ka, determined by Dorn and others (1991) for the Waihu Glacial Member of the Hamakua Volcanics, supports an age of 70 ka or slightly younger for the upper part of the Liloe Spring Volcanic Member, because the youngest lava flows of the Liloe Spring Volcanic Member overlie the Waihu Glacial Member.

We dated only one sample from the Hopukani Springs Volcanic Member. It has an apparent age of 153±38 ka, which does not differ at the 95-percent-confidence level from Porter's (1979c) previously reported age of 279±69 ka (table 5). Considered together with the range in ages for the Liloe Spring Volcanic Member, these results suggest that the age of the upper part of the Hopukani Springs Volcanic Member is approximately 200 to 150 ka.

Ages of samples of the Hamakua Volcanics from the lower flanks of Mauna Kea are generally consistent with those of samples from the upper flanks. Three samples (La–11, P86–2, P86–2A) are of such poor quality and have such large error limits that they provide no useful age information and so are omitted in figure 10. The remaining ages, which range from 237±31 to 81±36 ka, suggest that the shield-building stage of Mauna Kea, lavas of which are not exposed on the subaerial part of the volcano, ended before about 250–200 ka.

STRATIGRAPHY

HAMAKUA VOLCANICS

GENERAL STATEMENT

The Hamakua Volcanic Series was named for exposures of basalt in the seacliffs and gulches along the Hamakua coast from Hilo to Honokaa (Macdonald, 1945; Stearns and Macdonald, 1946). The type section is along the old coastal highway south of Laupahoehoe Gulch. The road has been abandoned since 1953 and now is so completely overgrown that the original section is no longer accessible (see Stearns and Macdonald, 1946, p. 195, pl. 46B, for a view and detailed description of this section).

As noted above in the subsection entitled "Previous Stratigraphic Nomenclature," Stearns and Macdonald's definition of the Hamakua Volcanic Series is vague; the Hamakua contains both basalt and "andesite." Our mapping shows that all of the hawaiitic lavas of Mauna Kea overlie all of the basaltic lavas and that there is no interlayering of these two compositional types. Accordingly, we here redefine the Hamakua Volcanics to include all the exposed

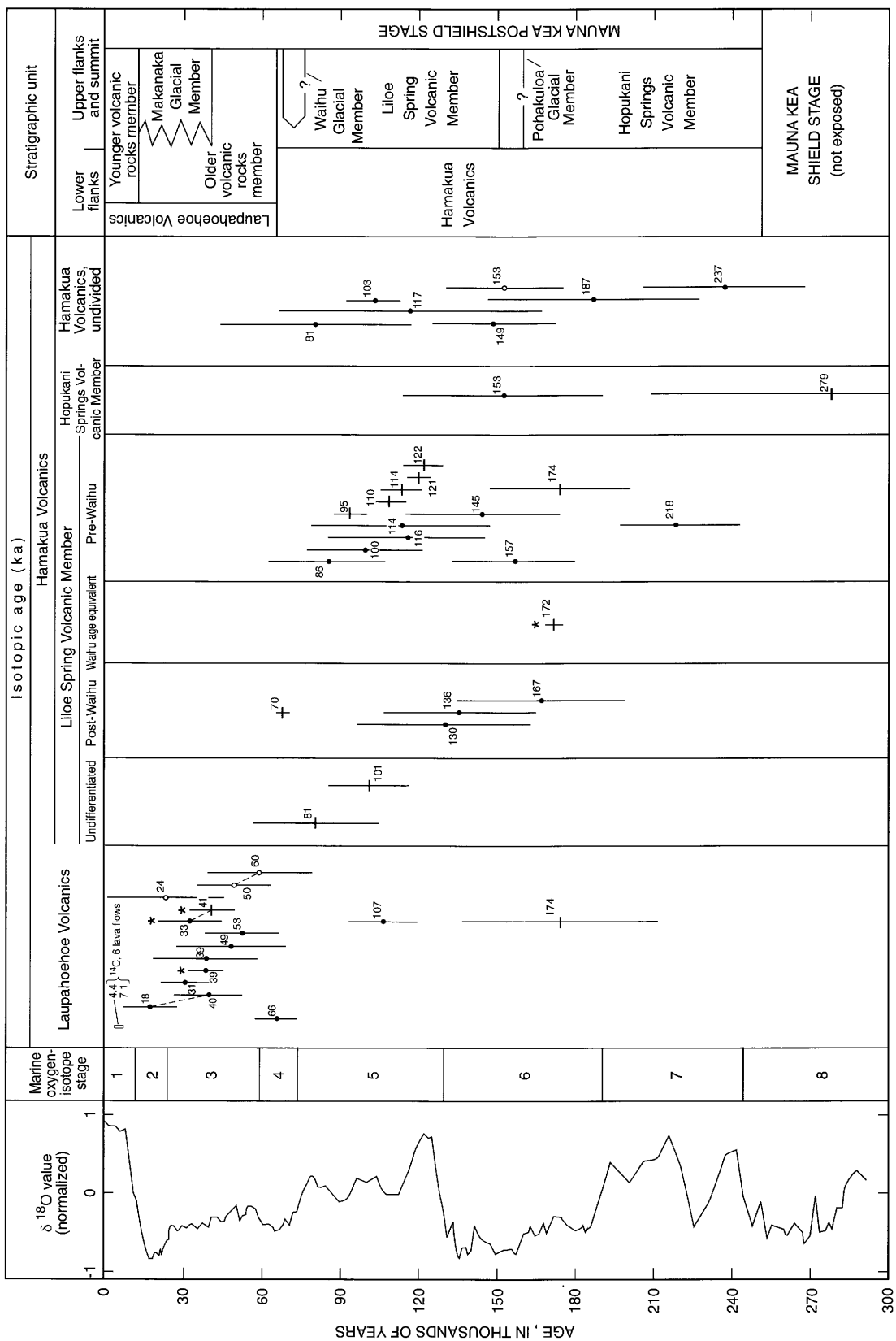

Figure 10. Correlation diagram of stratigraphic units and summary of isotopic ages of Mauna Kea lavas, showing $\delta^{18}O$ curve and boundaries of marine oxygen-isotope stages from Martinson and others (1987). Box, range of ^{14}C ages between 4.4 and 7.1 ka from six flows (see table 6); dots, newly reported K-Ar ages (see table 4); circles, K-Ar ages of B.D. Turrin (written commun., 1986) (see table 5); crossbars, K-Ar ages of Porter (1979c) (see table 5). Dashed lines connect ages from same flow. Vertical bars, standard deviations of K-Ar ages; asterisks, K-Ar ages determined for flows that display ice-contact fabric. Queries indicate uncertainty of older age limits of the Waihu and Pohakuloa Glacial Members of the Hamakua Volcanics. Samples La–11, P86–2, and P86–2A (table 4) are of such poor quality and have such large error limits that they provide no useful age information and so are omitted; sample QLA–11c (382±61 ka, table 5) is considered anomalous and also is omitted from this diagram. See plate 2 for description of units.

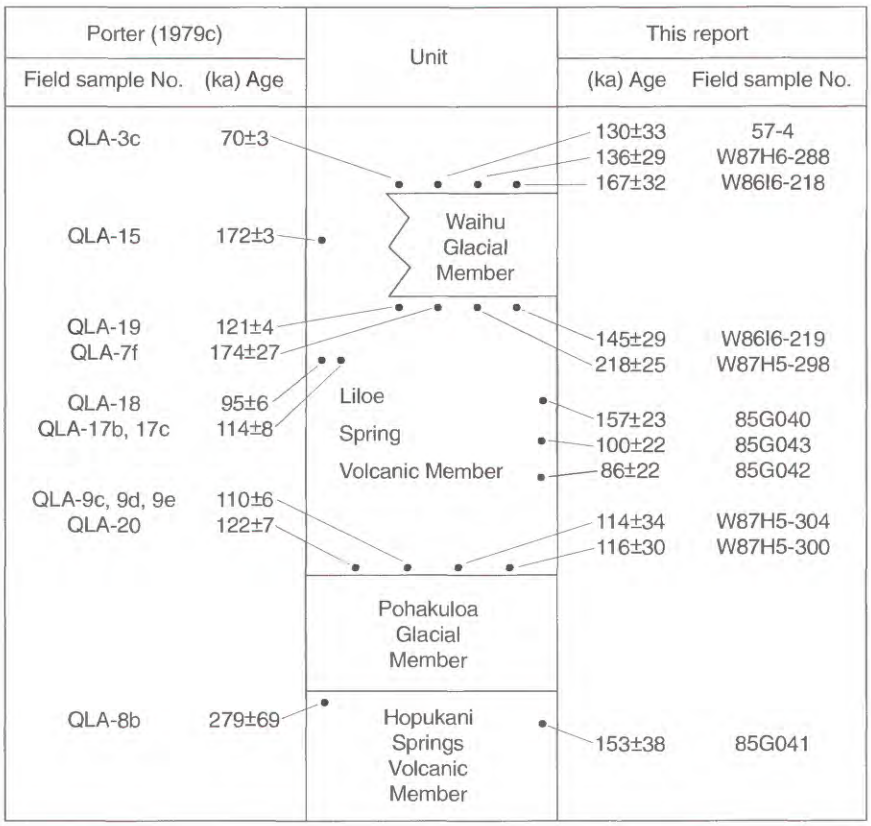

Figure 11. Summary of K-Ar ages for lavas of the Liloe Spring and Hopukani Springs Volcanic Members of the Hamakua Volcanics, showing relative stratigraphic positions of samples with respect to the Waihu and Pohakuloa Glacial Members of the Hamakua Volcanics. At left, ages from Porter (1979c) (see table 5); at right, newly reported ages (see table 4). Ages for samples QLA–4a and QLA–5c (table 5) are omitted because stratigraphic relation of these samples to the Waihu Glacial Member is unknown. See plate 2 for description of units.

basaltic flows and pyroclastic deposits of Mauna Kea Volcano, as well as the sedimentary units interlayered with them. Generally, the formation is exposed in two major areas of the volcano: (1) on the lower slopes, a belt around the volcano that is largely between sea level and about 1,000-m elevation but extends locally to higher elevations; and (2) the upper slopes, extensive but discontinuous exposures within kipukas above approximately 2,000-m elevation (fig. 12).

No consistent criteria exist for stratigraphic subdivision of the Hamakua lavas exposed on the lower slopes of the volcano. However, the glacial interbeds allow the upper-flank exposures to be subdivided into four formally named members, two volcanic and two glacial (fig. 7; table 3). Therefore, we describe first the undivided Hamakua Volcanics of the lower flanks and then the members of the upper flanks.

HAMAKUA VOLCANICS (UNDIVIDED)

DEFINITION AND OCCURRENCE

On the lower slopes of Mauna Kea, the Hamakua Volcanics consists of all the basaltic flows, cinder cones, and minor pyroclastic deposits that lie stratigraphically below the Laupahoehoe Volcanics. Typical sequences are well exposed in the seacliffs and gulches along the Hamakua Coast between Hilo and Honokaa, and surfaces of individual flows are best exposed on the north and northwest flanks of the volcano between Honokaa and Kawaihae.

The type section of Stearns and Macdonald (1946) in the walls of Laupahoehoe Gulch is appropriate for the undivided Hamakua Volcanics of the lower flanks. It is supplemented by additional measured reference sections in Laupahoehoe Gulch and in nearby Kaawalii and Maulua Gulches (figs. 12, 13). Because these gulches are distant

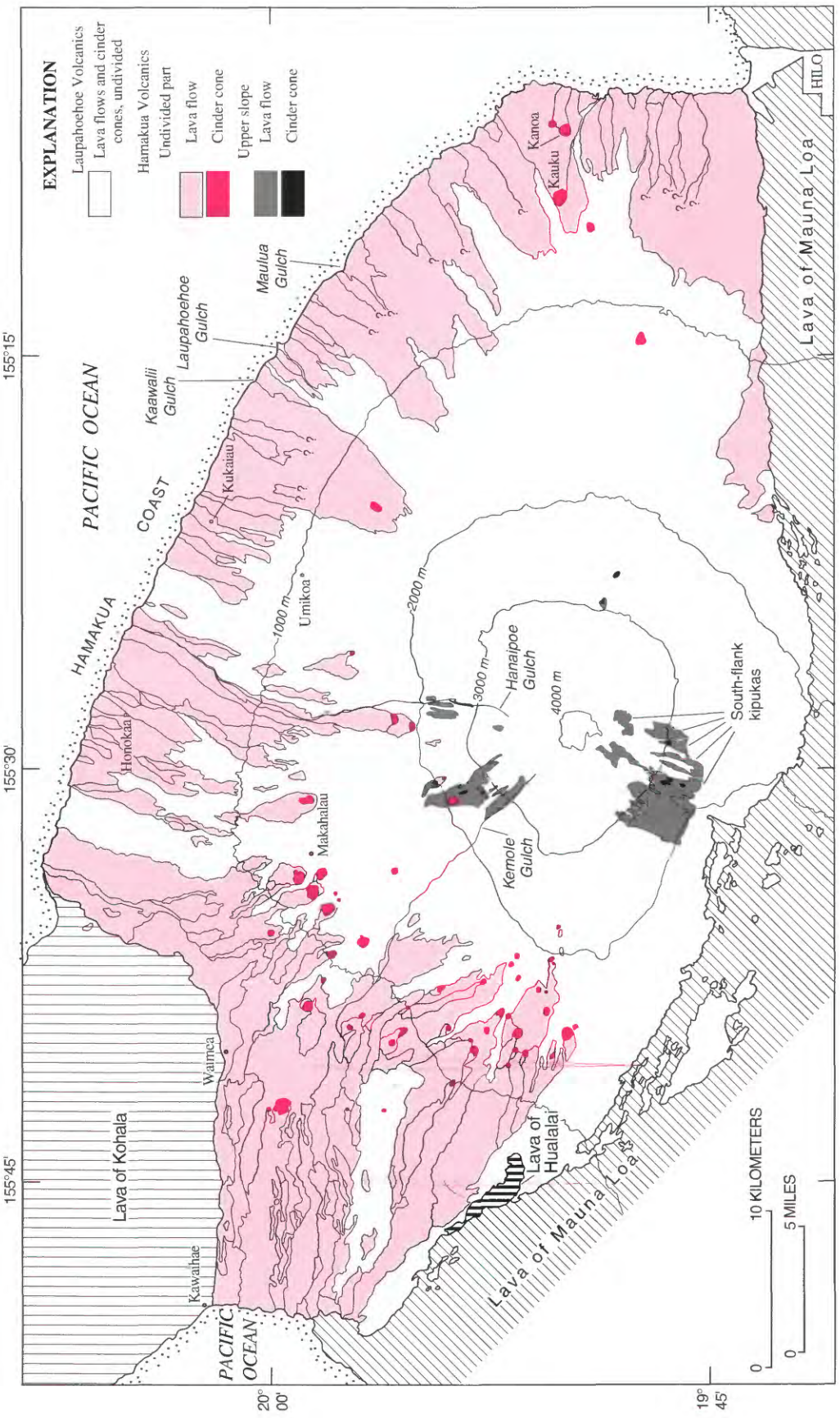

Figure 12. Geologic map of Mauna Kea, showing generalized distribution of the Hamakua Volcanics. Internal contacts distinguish individual lava flows and cinder cones. Queries mark limits of mapping at edge of dense rain forest. The Hamakua Volcanics on upper slopes consists of the Liloe Spring and Hopukani Springs Volcanic Members and the Waihu and Pohakuloa Glacial Members (see pl. 2 for distribution of all mappable outcrops on Mauna Kea of these four members). Local porphyritic basalt flows above 2,000-m (6,560 ft) elevation on upper part of north flank are assigned to the undivided Hamakua Volcanics because their stratigraphic relation to the Pohakuloa Glacial Member is unknown. Geology simplified from plates 1 and 2 and Wolfe and Morris (1996).

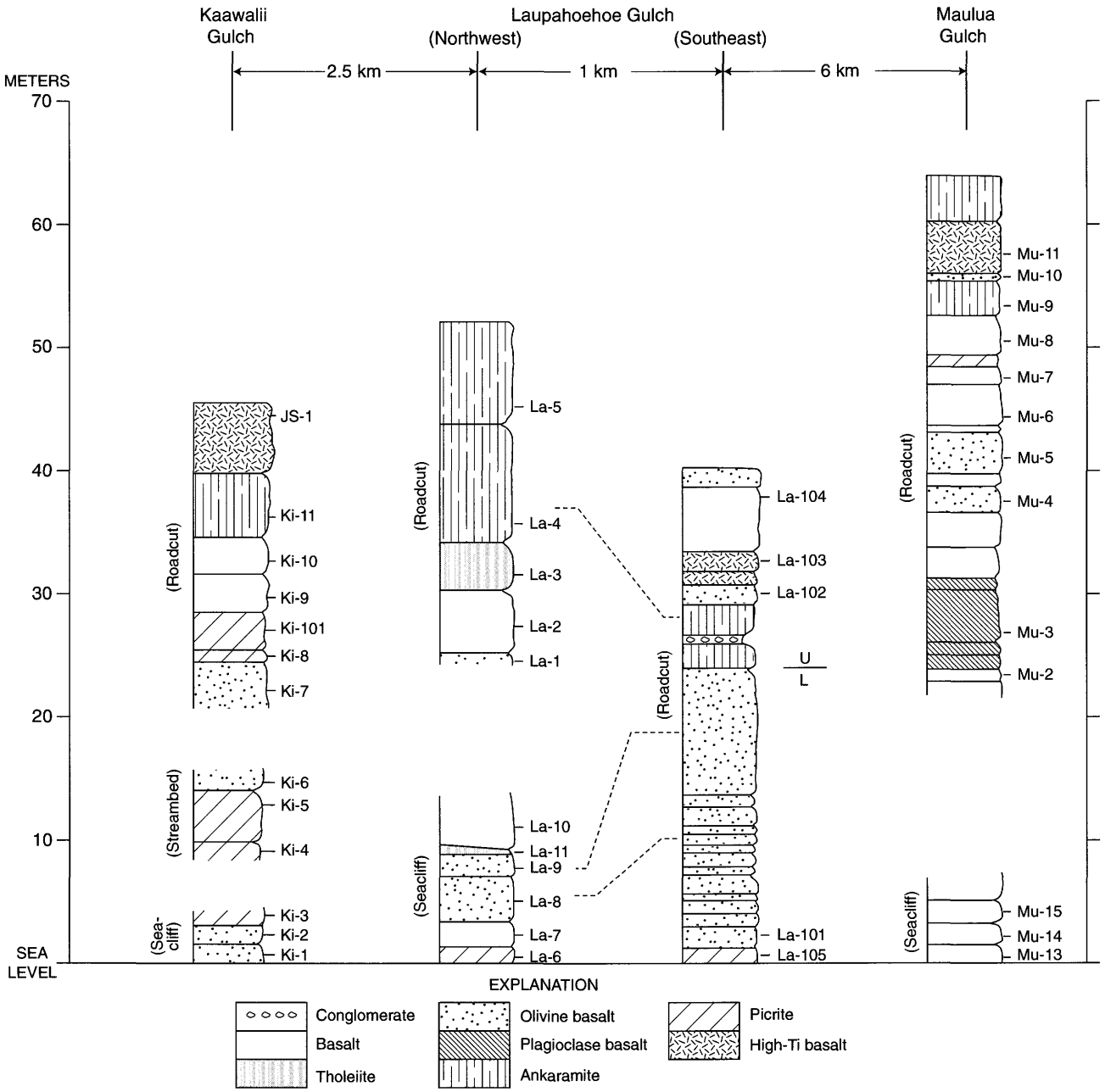

Figure 13. Stratigraphic sections of the Hamakua Volcanics exposed in Kaawalii, Laupahoehoe, and Maulua Gulches, showing stratigraphic positions of sampled units. Sections from Kaawalii, Maulua, and northwestern part of Laupahoehoe Gulches from Frey and others (1991); section from southeastern part of Laupahoehoe Gulch from Stearns and Macdonald (1946). Type of outcrop is shown in parentheses to left of column; gap in column indicates break in outcrop exposure. Dashed line, correlated lava flows; short horizontal line to right of southeast Laupahoehoe Gulch column, position of boundary between Stearns and Macdonald's (1946) upper (U) and lower (L) members of the Hamakua Volcanic Series. Horizontal axis not to scale; approximate distance between gulches shown for reference. See plate 4 for locations of traverses associated with sample-locality numbers. Chemical analyses are listed in table 1; see table 2 for description of basalt types.

from the Hamakua vents, as well as from the east rift zone of the volcano, the measured sections represent typical lower-flank lava-flow sequences. The maximum exposed thickness of the Hamakua Volcanics on the entire volcano is 170 m, in the Maulua Gulch section.

Many individual flows and their cinder cones are exposed on the north and northwest slopes of Mauna Kea (fig. 12). These cones, which are 10 to 30 km from the present summit, represent vents that were not covered by later Hamakua and Laupahoehoe flows. Exposures on the

lower northwest flank constitute a reference locality for these flows and cinder cones (pl. 1). K-Ar analyses indicate that these northwest-flank flows are generally younger than 200 ka; thus, they postdate the flows exposed deepest in the gulch sections along the Hamakua Coast.

PREVIOUS WORK

Stearns and Macdonald (1946) and Macdonald (1949) recognized petrologic differences between the stratigraphically lowest basalts exposed along the Hamakua Coast and those higher in the sequence. On this basis, they separated the Hamakua Volcanic Series into two members: a lower member containing abundant olivine basalt and some picrite, and an upper member containing abundant olivine basalt and some hawaiite ("andesite") and ankaramite ("picrite-basalts of the augite-rich type"). In a few gulches, red soil zones between certain lava flows were mapped as the boundary between these members (see Macdonald, 1949, pl. 12). During recent sampling and description of sections in the major gulches of the Hamakua Coast (Frey and others, 1991) and in our geologic mapping, the distribution of rock types was verified (fig. 13), but it proved impossible to map a consistent boundary.

Porter (1979c) retained the lower member of Stearns and Macdonald (1946) and assigned lavas of the upper member, on the lower flanks of the volcano, to his Hopukani Formation.

GEOLOGIC OBSERVATIONS

The Hamakua basalts vary widely in lithology, primarily because of variations in abundance and size of phenocrysts—olivine, augite, and plagioclase. These phenocrysts range most commonly from 1 to 4 mm in diameter but in rare flows may reach 2 cm. The most common abundances are less than 10 volume percent; in only a few flows does phenocryst content exceed 30 volume percent. Completely aphyric basalts are few. Although local variations in the phenocryst assemblage occur in some lavas, generally each flow and its vent deposits have a persistent phenocryst assemblage, which, in most flows, differs recognizably from that of its neighbors. These differences provide the primary basis for recognizing and mapping individual flows.

In the seacliff and roadcut exposures on the Hamakua Coast, individual flows range in thickness from 0.3 to 20 m. Most flows appear to have a wide lateral extent, at least across the width of any exposure. Judging from the lateral extent of flows mantling the surface immediately above these cliffs, most flows are from 0.5 to 2.5 km wide. Although Laupahoehoe and Kaawalii Gulches are only 2.4 km apart, no single flow can be correlated between the sections measured in these two gulches (fig. 13).

Most of the lavas exposed in the coastal sections are dense, thick (more than 3 m) aa flows with rubble at the tops and bases. Several thick (max 20 m) accumulations of olivine basalt pahoehoe are composed of individual flows less than 1 m thick. The lavas on the northwest flank also are predominantly aa flows with rare pahoehoe sequences. The basaltic lavas flowing off the northwest flank of the volcano spread out, building a gently sloping saddle and turning seaward as they approached the flank of Kohala Volcano. Some of these flows were more than 20 km long and averaged 2 km in width; one late olivine basalt pahoehoe flow spread out over an area of 20 km^2 south of Waimea (flow 33, pl. 1).

Cinder cones formed at all the Hamakua vents exposed on the lower slope. Most are single, crescentic cones in which part of the wall was rafted away as lava welled out of the conduit. A few vents are represented by cone complexes; for example, Puu Pa, near Waimea (pl. 1), was built by a sequence of eruptions from the same conduit system. Because most of the cones are older than 100 ka, their shapes have been degraded by erosion and mass wasting. These remnants range in width from 120 to 925 m and in height from 25 to 140 m.

Exposed Hamakua cinder cones are mainly concentrated on the north and northwest slopes (fig. 12). A few additional cinder cones, which overlie the landward extension of the shield-stage Hilo Ridge rift zone (fig. 1), are exposed on the lower east flank north of Hilo. The distribution of cinder cones is partly due to burial by later Laupahoehoe lavas and, probably, by Mauna Loa lavas, in the saddle between Mauna Kea and Mauna Loa. However, much of the Laupahoehoe Volcanics on the lower flanks is only a single flow thick, insufficient for burial of many Hamakua cones. Therefore, Hamakua flows of the northeast slope were derived from vents high on the volcano, whereas those of the lower northwest slope largely were locally derived.

Mildly porphyritic lava types are distributed throughout the gulch sections and over all the slopes. The strongly porphyritic lava types, however, are restricted in occurrence. As Stearns and Macdonald (1946) noted, picrites and olivine-rich basalts generally are restricted to the lowest exposures along the Hamakua Coast. No picrites are exposed in surface flows anywhere on the lower slopes. Conversely, ankaramite, plagioclase-rich basalt, and flows of highly evolved basalt are exposed only in the upper parts of coastal exposures and form surface flows on all the flanks of the volcano.

AGE

New K-Ar ages on samples of Hamakua basalt flows from the lower flanks of Mauna Kea range from 237±31 ka to 81±36 ka (tables 4, 5). An age of 382±61 ka (sample QLA–11c, table 5) previously reported by Porter (1979c) is

Figure 14. Members of the Hamakua Volcanics exposed in west wall of Waikahalulu Gulch. Contacts dashed where approximately located. Hawaiian Volcano Observatory photograph 88.3.10EW135A#20.

stratigraphically inconsistent; field relations (pl. 1) show that the sample is from a flow stratigraphically above the one with an age of 81±36 ka.

HOPUKANI SPRINGS VOLCANIC MEMBER

DEFINITION AND OCCURRENCE

The herein-named Hopukani Springs Volcanic Member consists of basalt flows and rare cinder-cone deposits that lie stratigraphically below the Pohakuloa Glacial Member. We assign lavas to the Hopukani Springs Volcanic Member only on the upper flanks of Mauna Kea, where the Pohakuloa Glacial Member is present and serves as a stratigraphic marker. The unit is extended locally beyond the outcrop of the Pohakuloa Glacial Member by lithologic correlation. Elsewhere on the volcano, well beyond the limit of the Pohakuloa Glacial Member, similar basalt is assigned to the undivided Hamakua Volcanics (fig. 7).

Hopukani Springs lavas are the oldest exposed rocks on the upper flanks of Mauna Kea. Exposures occur in and near Pohakuloa and Waikahalulu Gulches on the south flank and Waipahoehoe Gulch on the upper east flank of the volcano (pl. 2). Their maximum exposed thickness in these gulches is about 30 m.

Owing to their good exposure and relative ease of access, we designate the outcrops along Waikahalulu Gulch, between approximately 2,775-m (9,100 ft) and 3,095-m (10,160 ft) elevation, as the type section of the Hopukani Springs Volcanic Member (fig. 14). The unit is named for exposures in Pohakuloa Gulch, near the Hopukani Springs, which are just west of Pohakuloa Gulch, at 3,175-m (10,420 ft) elevation.

PREVIOUS WORK

Stearns and Macdonald (1946) and Macdonald (1949) mapped the south-flank exposures of the Hopukani Springs Volcanic Member as part of the upper member of their Hamakua Volcanic Series. Their upper member included basalts of the lower flanks of Mauna Kea except for those in a narrow band of outcrops near sea level on the northeast flank.

Porter (1979a–c) applied the name "Hopukani Formation" to most of the lavas that Stearns and Macdonald (1946) had referred to the upper member of their Hamakua Volcanic Series. Porter's Hopukani Formation included lavas exposed below the Pohakuloa Glacial Member in Pohakuloa and Waikahalulu Gulches and excluded lavas above the Pohakuloa Member. Our usage of the name "Hopukani Springs Volcanic Member" applies, on the upper flanks, to the same lavas as does Porter's usage of the name "Hopukani Formation" but differs in excluding basalts of the lower flanks.

GEOLOGIC OBSERVATIONS

Hopukani Springs basalt is predominantly porphyritic, vesicular pahoehoe and, locally, aa, in which phenocrysts of olivine, plagioclase, and clinopyroxene compose about 10 to 20 volume percent of the rock. Olivine phenocrysts are normally conspicuous, and where plagioclase phenocrysts are abundant, the laths commonly radiate from cumulophyric plagioclase-clinopyroxene-olivine clots, giving an appearance on the outcrop of plagioclase rosettes. Weakly porphyritic basalt, aphyric basalt, and picrite are subordinate rock types.

Vent deposits are represented by two eroded cinder cones along Waipahoehoe Gulch and by a third cone (not mapped) exposed in the steep west wall of Waikahalulu Gulch, where it is overlain by diamict of the Pohakuloa Glacial Member (fig. 15). The bulk of exposed Hopukani Springs flows must have been erupted from vents that are

Figure 15. West wall of Waikahalulu Gulch, showing members of the Hamakua Volcanics—basalt cinder cone of the Hopukani Springs Volcanic Member, overlain by approximately 40 m of diamict and gravel of the Pohakuloa Glacial Member, in turn overlain by flows of the Liloe Spring Volcanic Member. Contacts dashed where approximately located. Hawaiian Volcano Observatory photograph 88.2.23EW135A#16.

now buried by younger volcanic and glacial deposits high on the upper slopes or summit of Mauna Kea.

AGE

The K-Ar age of a lava flow sampled 26 m below the top of the Hopukani Springs Volcanic Member in Waikahalulu Gulch is 153±38 ka (table 4). An additional sample collected from the Hopukani Springs Volcanic Member immediately below the Pohakuloa Glacial Member in Waikahalulu Gulch gave a K-Ar age of 279±69 ka (table 5; Porter, 1979c), comparable to our age at the 95-percent-confidence level. These results, along with the range in K-Ar ages for the overlying Liloe Spring Volcanic Member (fig. 11), suggest that the age of the upper part of the Hopukani Springs Volcanic Member is approximately 150 to 200 ka.

POHAKULOA GLACIAL MEMBER

DEFINITION AND OCCURRENCE

The Pohakuloa Glacial Member consists of till between the underlying Hopukani Springs and the overlying Liloe Spring Volcanic Members. The Pohakuloa Glacial Member is exposed on the south and upper east flanks of Mauna Kea. Exposures on the south flank occur only in the most deeply incised sections of Pohakuloa and Waikahalulu Gulches and in a small gulch 400 m southeast of Pohakuloa Gulch (pl. 2; figs. 14, 15). On the upper east flank, the unit is exposed in the headwaters of the Wailuku River and in a kipuka along Waipahoehoe Gulch. There, the Liloe Spring Volcanic Member is absent, and the Pohakuloa Glacial Member is directly overlain by flows of the Laupahoehoe Volcanics. The type section was defined by Porter (1979c) as an exposure deep in Pohakuloa Gulch at approximately 2,935-m (9,630 ft) elevation.

PREVIOUS WORK

Wentworth and Powers (1941) described three glacial drifts of pre-Makanaka age on the south flank of Mauna Kea. They named them, in ascending order, "pre-Pohakuloa drift," the "Pohakuloa Drift," and the "Waihu Drift." They assigned the deep canyon-wall exposures of Pohakuloa Gulch and of the neighboring small gulch to their pre-Pohakuloa drift. The drift outcrops between Pohakuloa and Waikahalulu Gulches, here all considered parts of the Waihu Glacial Member, were divided into two units, the Pohakuloa Drift and the Waihu Drift, and the deep canyon-wall exposure in Waikahalulu Gulch was assigned to their Pohakuloa Drift.

Stearns (1945) greatly clarified the map distribution of Waihu and pre-Waihu sedimentary units, assigning the Pohakuloa Drift (of Wentworth and Powers, 1941) on the slopes between Pohakuloa and Waikahalulu Gulches to the Waihu. Stearns, however, challenged the interpretation of Wentworth and Powers that the pre-Makanaka sedimentary units are glacial-drift deposits and referred the pre-Pohakuloa drift of Pohakuloa Gulch and the Pohakuloa Drift of Waikahalulu Gulch to a unit of "explosion deposits."

Porter (1979c) assigned the deep canyon-wall outcrops of gravel and diamict in Pohakuloa and Waikahalulu Gulches to his Pohakuloa Formation and designated an exposure in Pohakuloa Gulch as the type section. Thus, the present type section of the Pohakuloa Glacial Member is an outcrop that Wentworth and Powers (1941) had assigned to their pre-Pohakuloa drift. Applying the terminology of Langenheim and Clague (1987), we assign these same out-

crops in Pohakuloa and Waikahalulu Gulches to the Pohakuloa Glacial Member.

GEOLOGIC OBSERVATIONS

The Pohakuloa Glacial Member is exposed in discontinuous outcrops along 1.5 km of Pohakuloa Gulch between approximately 2,740- and 3,170-m (9,000 and 10,400 ft) elevation. It forms a continuous exposure, nearly 800 m long, in the west wall of Waikahalulu Gulch (talus buries the unit in the east wall), between approximately 2,800- and 3,110-m (9,200 and 10,200 ft) elevation. The Pohakuloa Glacial Member is essentially concordant with lava flows in the underlying and overlying volcanic members, and all the layers dip approximately parallel to the mountain flank, which slopes about 15°–25°. In the excellent Waikahalulu Gulch exposure, the unit gradually thickens southward from approximately 12 m near the north (uphill) end of the exposure to nearly 40 m before abruptly wedging out, thinning to the south, so that overlying Liloe Spring flows descend steeply to rest directly on underlying Hopukani Springs flows (fig. 9).

In the south-flank exposures, the Pohakuloa Glacial Member consists of matrix-supported diamict (till), with some interlayered gravel that is distinctly bedded and sorted. The unit is light gray except where oxidized red by the overlying basalt flows. In the diamict, subangular to subrounded cobbles and boulders, as large as about 1 m in diameter, occur in a moderately indurated, massive, unsorted, silty to pebbly matrix. The boulders are of vesicular porphyritic basalt lithologically identical to flows of the underlying Hopukani Springs Volcanic Member. The gravel facies is particularly well developed near the south end of the Waikahalulu Gulch exposure (fig. 16), where it consists of framework-supported, bedded gravel containing pebbles, cobbles, and boulders lithologically similar to those of the interlayered diamict. Steep dips and coarse fabric suggest that these particular beds were formed by energetic runoff over the downhill face of the Pohakuloa deposit. Porter (1979c) identified these diamict and gravel facies, which he examined and described in detail and interpreted, respectively, as glacial till and outwash.

Exposures on the upper east flank of the volcano display about 10 m of bouldery till and minor bedded sandy gravel overlying porphyritic basalt of the Hopukani Springs Volcanic Member. The till consists of subangular to subrounded cobbles and boulders of basalt in a massive, unsorted, moderately indurated, light- to medium-gray matrix. The boulders include porphyritic basalt similar to exposed underlying Hopukani Springs flows, as well as an unusual basalt containing abundant, coarse-grained plagioclase phenocrysts, as large as 1 cm across. Near its upper contact, the unit has been oxidized red by the overlying lava flows. Where the surface of the drift deposit is exposed in a kipuka just southwest of Waipahoehoe Gulch—the only surface exposure of the Pohakuloa Glacial Member—the boulders are weathered dark brown. The Liloe Spring Volcanic Member is absent in these upper-east-flank exposures, and the drift is directly overlain by the Laupahoehoe Volcanics. Porter (1979a) included the underlying basalts in his Laupahoehoe Group and mapped this drift as his Waihu Formation. We assign this drift to the Pohakuloa Glacial Member because its porphyritic-basalt clasts indicate that the source rocks included only lavas of the Hopukani Springs Volcanic Member.

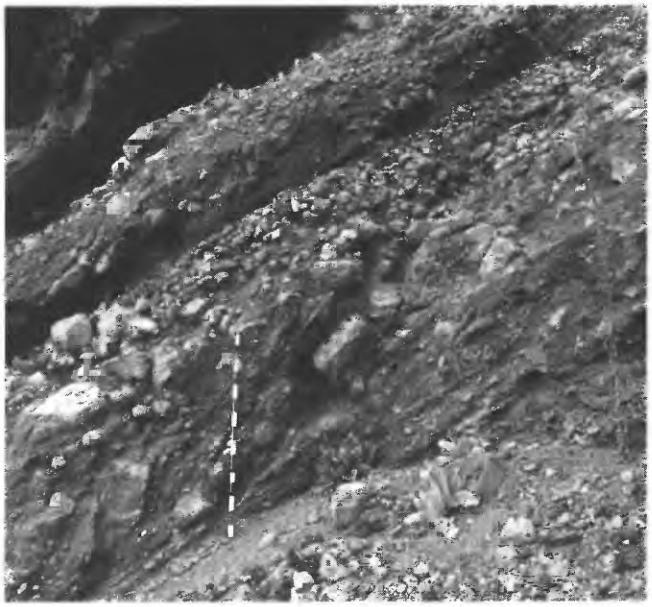

Figure 16. Beds of diamict and gravel of the Pohakuloa Glacial Member of the Hamakua Volcanics exposed in west wall of Waikahalulu Gulch (see fig. 15 for location). Gravel beds dip 30°–35° SW., slightly more steeply than overlying flows of the Liloe Spring Volcanic Member of the Hamakua Volcanics (upper left corner). Pole is 1.5 m long. Hawaiian Volcano Observatory photograph 88.2.23EW135A#18.

To assess the origin of the Pohakuloa sedimentary deposits, which was controversial because of the conflicting glacial-drift (Wentworth and Powers, 1941) and explosion-breccia (Stearns, 1945) hypotheses, Porter (1979c) exhaustively studied the outcrops, analyzed their size distribution and fabric, and compared the results with similar studies of historical and prehistoric explosion breccias in unspecified outcrops at Kilauea Volcano. Porter found a striking dissimilarity between the Pohakuloa sedimentary deposits and the Kilauea explosion breccias. However, he demonstrated a strong similarity between the Pohakuloa deposits and the younger Waihu and Makanaka deposits, which, as discussed below, are definitely glacial-drift deposits. Thus, Porter showed that the Pohakuloa is a glacial-drift deposit. His evidence included the following: (1) Though rare, polished and striated fragments are present; (2) though difficult to find

because of limited exposure, grooves and striations occur on abraded or polished underlying bedrock surfaces; (3) the Pohakuloa deposit is similar in thickness to the Waihu and Makanaka deposits and has similar gravel and diamict facies; (4) size and fabric analyses show a similar size distribution and poor sorting of the matrices of the Pohakuloa, Waihu, and Makanaka diamicts, a similar degree of rounding of the clasts (predominantly subrounded to subangular), and development of a strong unidirectional clast fabric in diamicts of each of the three deposits.

By analogy with the younger, well-exposed Makanaka Glacial Member, the Pohakuloa till and associated gravel exposed in south-flank gulches represent terminal- or lateral-moraine deposits that formed an annulus surrounding the glacially eroded summit of the volcano. Thus, uphill from these morainal deposits, in exposures along the upper parts of Pohakuloa and Waikahalulu Gulches, Pohakuloa glacial deposits are absent, and basalt of the Liloe Spring Volcanic Member rests directly on that of the Hopukani Springs Volcanic Member (fig. 9).

AGE

The age of the Pohakuloa Glacial Member is bracketed by basalt of the underlying Hopukani Springs Volcanic Member, with a K-Ar age of approximately 150 to 200 ka, and the overlying Liloe Spring Volcanic Member, which includes flows with an age within the range 100–150 ka, and possibly younger (fig. 11). Dorn and others (1991) reported exposure ages of 140 to 156 ka based on varnish cation ratios from weathered boulder surfaces in the Waipahoehoe Gulch exposure. Thus, the age of the Pohakuloa Glacial Member corresponds approximately to some part of marine oxygen-isotope stage 6 (fig. 10).

LILOE SPRING VOLCANIC MEMBER

DEFINITION AND OCCURRENCE

The herein-named Liloe Spring Volcanic Member of the Hamakua Volcanics consists of the basaltic lava flows and vent deposits that lie between the underlying Pohakuloa Glacial Member and the overlying hawaiitic rocks and sedimentary deposits of the Laupahoehoe Volcanics. Till and gravel of the Waihu Glacial Member form a lens enclosed, at least in part, by the Liloe Spring Volcanic Member. Although Porter (1979a, c) assigned these rocks to his Laupahoehoe Group, we assign them to the Hamakua Volcanics because, like all the other Hamakua lavas, they are basalts.

Lavas of the Liloe Spring Volcanic Member are exposed in kipukas surrounded by flows of the Laupahoehoe Volcanics on the south, northwest, and north flanks of Mauna Kea. The most extensive exposures, covering an area of more than 20 km^2, are on the south flank (pl. 2). There basaltic lavas of the Liloe Spring Volcanic Member are exposed from the mountain base, in the saddle between Mauna Kea and Mauna Loa at approximately 1,930-m (6,320 ft) elevation, to within about 300 m of the summit, in the upper reaches of Pohakuloa Gulch at approximately 3,900-m (12,790 ft) elevation. An additional nearly 10 km^2 of exposure is on the upper north and northwest flanks (fig. 12). Deep, steep-walled Waikahalulu and Pohakuloa Gulches on the south flank provide excellent exposures of the Liloe Spring Volcanic Member and of its relations to underlying and overlying stratigraphic units.

The type section of the Liloe Spring Volcanic Member is in a near-vertical exposure in the west wall of Waikahalulu Gulch, at approximately 3,100-m (10,170 ft) elevation (fig. 17). A supplementary section, exposing part of the Waihu Glacial Member and, overlying the Waihu, the uppermost part of the Liloe Spring Volcanic Member (fig. 18), is in the west wall of Waikahalulu Gulch, approximately 800 m farther upstream, at 3,270-m (10,720 ft) elevation. The name is derived from Liloe Spring, about 0.5 km west of Pohakuloa Gulch, at 2,720-m (8,921 ft) elevation.

PREVIOUS WORK

Stearns and Macdonald (1946) mapped the pre-Waihu lavas, including lavas of the Liloe Spring Volcanic Member, as part of their Hamakua Volcanic Series in and near the upper parts of Waikahalulu and Pohakuloa Gulches. They showed much of the Liloe Spring outcrop area of the south-flank kipukas—including outcrops of the Waihu Glacial Member and all the slopes below—as alluvium and talus of Quaternary age. Macdonald's (1949) more generalized map, however, includes most of these kipukas in the Hamakua Volcanic Series. Stearns and Macdonald also included exposures of Liloe Spring basalt in the upper parts of the north and northwest flanks (pl. 2; fig. 12) in their Laupahoehoe Volcanic Series.

Porter (1979c) defined his Laupahoehoe Group to include all strata younger than the Pohakuloa glacial deposits. Accordingly, he (1979a) assigned most of the basaltic lavas exposed in south-flank kipukas to his Waikahalulu Formation, the volcanic facies of his Laupahoehoe Group. He also included most Liloe Spring basalt exposed in the upper parts of the north and northwest flanks of Mauna Kea in his Waikahalulu Formation.

Porter (1979c) designated exposures, which include Liloe Spring lavas, along Pohakuloa and Waikahalulu Gulches as reference sections for his Waikahalulu Formation and Laupahoehoe Group. In addition, he designated exposures of the stratigraphic interval between the Pohakuloa and Waihu glacial deposits in Pohakuloa Gulch as the type section for his Liloean Stage, the oldest age division

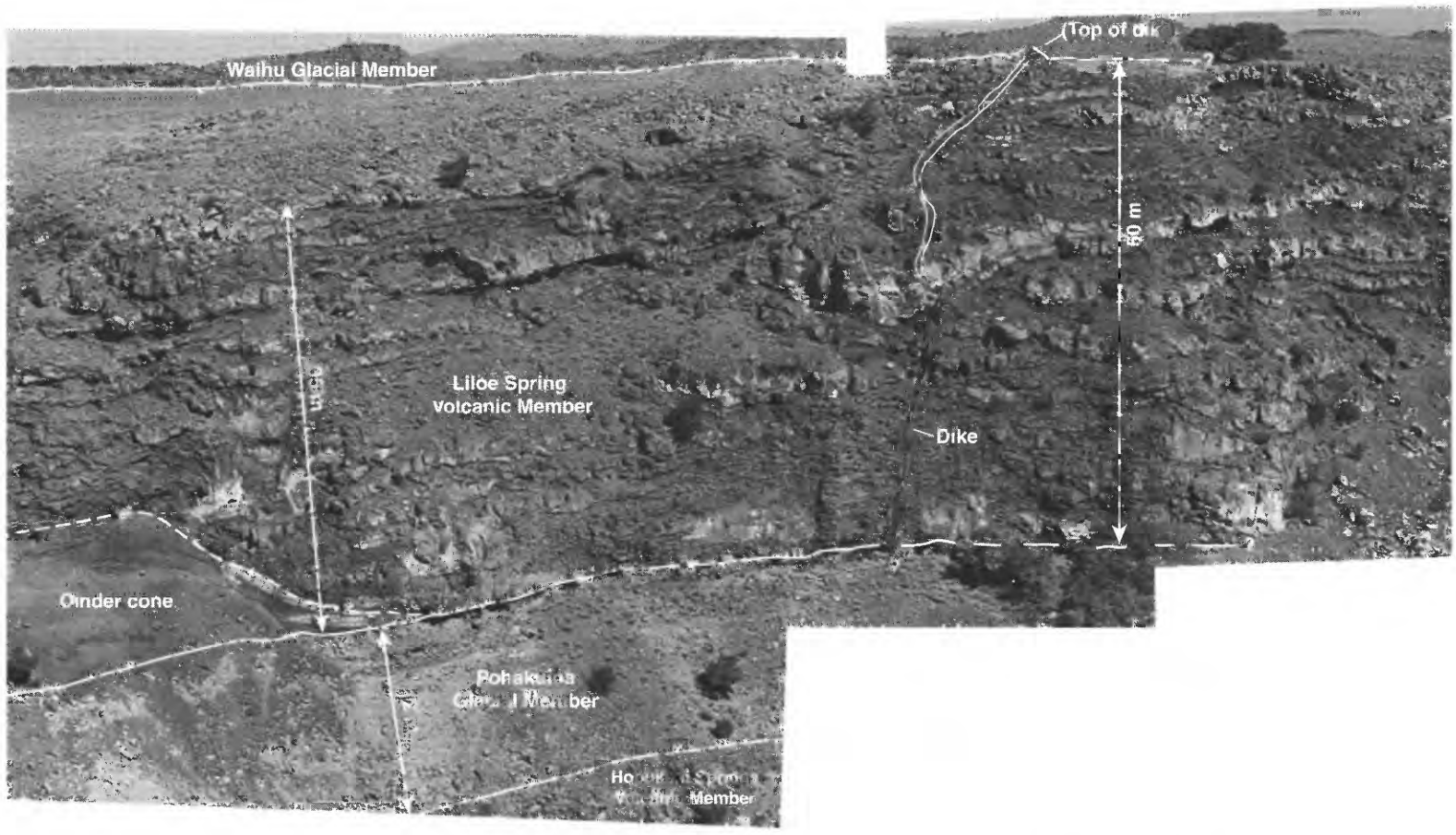

Figure 17. Type section of the Liloe Spring Volcanic Member of the Hamakua Volcanics in west wall of Waikahalulu Gulch at approximately 3,100-m (10,170 ft) elevation. Contacts dashed where approximately located, queried where uncertain. Cinder-cone deposits, formed during an early Liloe Spring eruption, overlie the Pohakuloa Glacial Member of the Hamakua Volcanics. Light-colored lenses on north (right) flank of cinder cone consist of palagonitized hyaloclastite. Cone is overlapped and buried by sequence of aa flows exposed in walls of gulch. Three dikes, one of which is discernible in photograph, intrude sequence. Surface outcrop of dike, along with its enveloping scoria, forms small knob on canyon rim (top center). Lower extent of dike is queried because it is not evident through rubble on outcrop surface. Terminal moraine of the Waihu Glacial Member of the Hamakua Volcanics, which overlies the Liloe Spring Volcanic Member in this area, forms low ridge on skyline (upper left and center). Hawaiian Volcano Observatory photographs 88.2.24EW135B#20, 88.2.24EW135B#22, and 88.2.24EW135B#23.

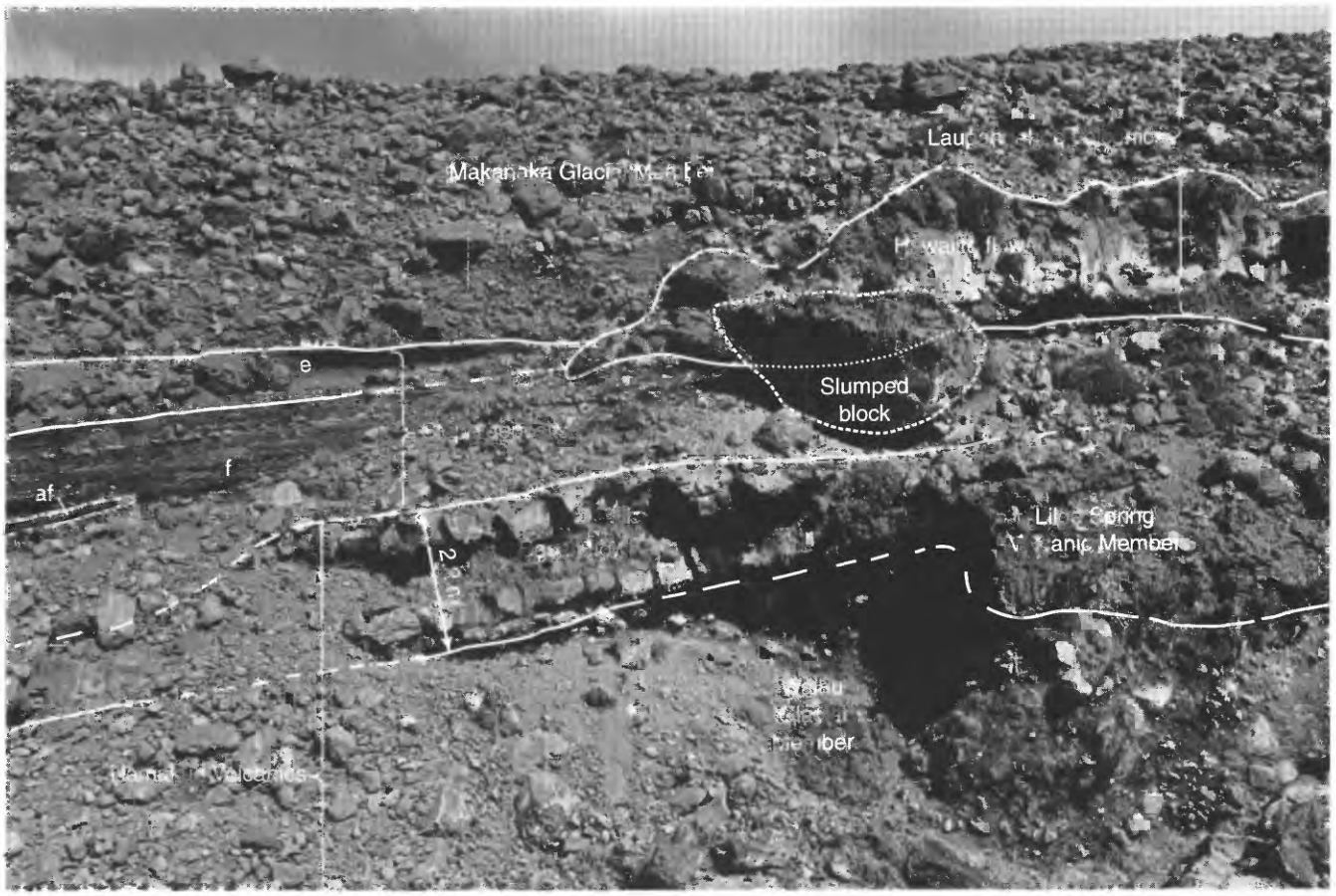

Figure 18. Supplementary type section of the Liloe Spring Volcanic Member of the Hamakua Volcanics in west wall of Waikahalulu Gulch at 3,270-m (10,720 ft) elevation. Contacts dashed where approximately located, dotted where concealed by slumped block, queried where not discernible through rubble on outcrop surface. The Hamakua Volcanics is represented by till of its Waihu Glacial Member and a single overlying basalt flow of the Liloe Spring Volcanic Member. Poorly consolidated slope deposits, which overlie Liloe Spring basalt flow, are both overlain by and intercalated with a hawaiitic flow of the Laupahoehoe Volcanics. Slope deposits include bedded ashy fluvial deposits (f) that contain pebbles and pebble layers, air-fall lapilli (af), and ashy eolian deposits (e) that envelop colluvial boulders derived from nearby Laupahoehoe flow. Weakly consolidated, bouldery till of the Makanaka Glacial Member of the Laupahoehoe Volcanics caps sequence. Hawaiian Volcano Observatory photograph 88.3.9EW135A#13.

within his Laupahoehoe Group (fig. 8), named for nearby Liloe Spring. As mapped, Porter's (1979a) Liloean Stage includes some basaltic lavas that we assign to our Liloe Spring Volcanic Member, among which is the basalt sequence of our type section along Waikahalulu Gulch. Thus, our Liloe Spring Volcanic Member corresponds in part to the lavas of Porter's Liloean Stage. However, significant errors in stratigraphic interpretation are reflected in Porter's mapping. He mapped extensive outcrops of our Liloe Spring basalt as Laupahoehoe lava of his Poliahuan and Hanaipoean Stages, both of which he interpreted as younger than his Liloean Stage. Furthermore, Porter's Liloean-, Poliahuan-, and Hanaipoean-Stage rocks all include hawaiitic cinder cones and flows of our Laupahoehoe Volcanics, as well as basaltic lavas of our Hamakua Volcanics. As noted above, our mapping shows that the hawaiitic lavas (our Laupahoehoe Volcanics) are distinct from and younger than the basaltic lavas (our Hamakua Volcanics). We observed no interlayering of basaltic and hawaiitic lavas.

GEOLOGIC OBSERVATIONS

LITHOLOGY

Most basalt of the Liloe Spring Volcanic Member is aphyric to weakly porphyritic. Plagioclase is the dominant phenocryst phase; its abundance normally ranges as high as about 2 volume percent, and it occurs as randomly oriented, subequant crystals, 1 to 2 mm in diameter. Scattered, small (generally less than 2 mm diam) olivine and clinopyroxene phenocrysts are common; together, olivine and clinopyrox-

ene phenocrysts generally compose less than 1 volume percent of the rock. Scattered, small (generally less than 2 cm diam) gabbroic xenoliths occur locally.

A few flows and related vent deposits are slightly more porphyritic. In these rocks, plagioclase phenocrysts compose as much as about 5 volume percent, and olivine phenocrysts as much as about 2 volume percent. Because of their more porphyritic texture, these lavas are easily distinguished from the more common, less porphyritic Liloe Spring basalts and so are here mapped separately (pl. 2).

The relative paucity of phenocrysts and predominance of plagioclase among the phenocryst phases distinguishes Liloe Spring basalt from stratigraphically lower Hopukani Springs basalt. Almost all the Hopukani Springs lavas are much more porphyritic and, in particular, much richer in olivine phenocrysts. Except in a few aphyric or more porphyritic lavas, the scattered, small, randomly oriented, subequant plagioclase phenocrysts are a hallmark of the Liloe Spring Volcanic Member. Along with scattered olivine phenocrysts, they distinguish Liloe Spring lavas from stratigraphically higher Laupahoehoe lavas, which are aphyric or, if plagioclase phyric, contain thin, tabular plagioclase phenocrysts in a well-developed preferred orientation.

The groundmass of Liloe Spring basalt is normally dense, fine grained, and dark gray. In contrast, Laupahoehoe flows normally have lighter gray groundmasses that commonly are conspicuously plagioclase rich and trachytic.

LAVA-FLOW CHARACTERISTICS

The Liloe Spring Volcanic Member consists predominantly of aa flows stacked one above another in alternating layers of dense, massive basalt and breccia (figs. 14, 15, 17); thin-layered pahoehoe is rare but occurs locally. Exposed sequences of these flows give the impression that the member consists of many thin flows that are commonly from about 0.5 to 2 m thick. Gully-wall exposures of the Liloe Spring Volcanic Member differ in their thin layering from most gully-wall exposures of thick, massive hawaiitic flows of the overlying Laupahoehoe Volcanics. The flow layering dips downslope approximately parallel to the surface of the volcano, commonly 15°–25°. Pyroclastic deposits or other sedimentary materials are rare between flows except near the top of the Liloe Spring Volcanic Member, where diamict or gravel of the Waihu Glacial Member and lenses of hyaloclastite tuff are present. The maximum exposed thickness of the Liloe Spring Volcanic Member is about 50 m.

Although some thin flow layers may represent individual eruptions, at least some of the layering is caused by alternation of scoriaceous basalt breccia (aa) and dense, massive basalt within a single flow (for example, the Liloe Spring flow shown in fig. 18) or within a group of related flows generated in a single prolonged eruption. A good example of such a group is exposed in the west wall of Pohakuloa Gulch, at about 2,680-m (8,800 ft) elevation. There, a thick sequence of thin aa flows, represented by alternating massive and brecciated layers, extends downslope from a cinder cone. The cinder cone and the lava layers are all composed of the same distinctive plagioclase-phyric basalt and are products of the same eruption. Downslope from the cone, thin-layered, plagioclase-phyric basalt composes the entire canyon-wall sequence, which is as much as about 30 m thick.

The Liloe Spring Volcanic Member on the northwest slope is only one to three flows thick. Along Kemole Gulch, one weakly porphyritic basalt flow overlies strongly porphyritic basalt (unmapped, resembling basalt of the Hopukani Springs Volcanic Member) and underlies two Laupahoehoe hawaiite-mugearite flows. About 2 km northeast of Kemole Gulch, thin Liloe Spring flows surround kipukas of more porphyritic Hamakua basalt; one of these kipukas includes a Hamakua cinder cone that was partly buried by a Liloe Spring basalt flow. Along Hanaipoe Gulch, several Liloe Spring flows, totaling about 25 m in thickness, are exposed above Hamakua basalt flows.

Broad flow-surface outcrops of Liloe Spring basalt have commonly been eroded, either by ice or running water, and so little original aa fabric remains; such surfaces, as seen in aerial photographs, are relatively smooth.

HYALOCLASTITE TUFF

The best exposures of hyaloclastite tuff are high on the walls of Waikahalulu Gulch. Although most tuff lenses are separated from the overlying Waihu Glacial Member by a basalt flow, locally Waihu sedimentary deposits rest directly on hyaloclastite. The tuff lenses are 0 to 2 m thick and consist of yellowish- to reddish-orange, palagonitic lapilli. In some outcrops, these lapilli are accompanied by scattered, coarser grained, darker scoria fragments. The lapilli are highly vesicular, with thin vesicle walls, so that hand-lens examination reveals a delicate honeycomb or foamlike texture. Thin sections show that the lapilli consist of yellowish-orange isotropic glass; their yellowish-orange color presumably reflects palagonitization of normally light-brown basalt glass.

Additional hyaloclastite lenses are associated with Liloe Spring lava in exposures near Keanakakoi, in rare exposures along Pohakuloa Gulch, and on the north flank of a small cinder cone exposed at the base of the Liloe Spring Volcanic Member in Waikahalulu Gulch (fig. 17). Proximity of much of the palagonitic hyaloclastite tuff to deposits of Waihu drift, as well as to flows with ice-contact fabric (described below), suggests that the tuff records interaction between lava and meltwater which resulted in quenching and fragmentation of the lava and subsequent hydration of the glass.

ICE-CONTACT FABRIC

Fabrics suggestive of rapid quenching at the time of eruption of the Liloe Spring lavas are pervasive in the broad outcrop areas immediately south and east of Puu Kookoolau and in the upper reaches of the Pohakuloa Gulch drainage west and southwest of Puu Waiau. Similar fabrics are also found in the top two flows on the west rim of Waikahalulu Gulch in the locality illustrated in figure 17 and, across the gulch on the east wall, on the uppermost Liloe Spring flow, which rests on thin, unmapped Waihu till. The dominant feature of this fabric is mosaic jointing, a network of fractures bounding polygonal fragments and blocks with flat to gently curved faces that intersect in sharp, straight boundaries. Mosaic-jointed lava commonly is very fine grained or glassy. Oxidized, brecciated spiracles extend upward in places into these flows, bounding more massive, mosaic-jointed zones with curving, glassy, orange to reddish-brown, palagonitic margins reminiscent of pillow structure. Scattered cavelike voids, from tens of centimeters to several meters across, also are common in these flows, particularly at the flow bases. Porter (1979a, c, 1987) ascribed the development of such features to emplacement of flows in contact with glacial ice; we agree with his interpretation. In addition, well-developed subhorizontal sheeting occurs locally in association with these ice-contact fabrics in Liloe Spring basalt flows. The ice-contact fabric was handsomely illustrated for a Laupahoehoe flow near the summit of Mauna Kea by Porter (1987, figs. 21.11, 21.12).

VENTS

Four cinder and spatter cones are exposed in the south-flank kipukas (pl. 2), all in the lower part of the south flank, below 3,000-m (9,840 ft) elevation. One of these cones is beautifully exposed in cross section in the west wall of Pohakuloa Gulch, at approximately 2,700-m (8,860 ft) elevation. As noted above, another cone, which is unmapped, is exposed within the basal part of the Liloe Spring Volcanic Member in the Waikahalulu Gulch exposure (fig. 17). Three additional cones are exposed on the upper northwest flank (fig. 12).

Prominent, south-facing, sharp-crested scarps of dense, dark-gray basalt and red agglutinated scoria, along with minor yellowish-orange hyaloclastite tuff, project westward and northeastward from beneath Puu Kookoolau (fig. 19), which is a hawaiitic Laupahoehoe cinder cone. Dense basalt of these scarps was extensively quarried by prehistoric Hawaiians for adzheads; thus, the northeast scarp has the geographic designation "Keanakakoi" (adz-making cave). Cruikshank (1986) provided an informative discussion of prehistoric human activity in this area.

Ice-contact fabric is well developed in the scarps, as well as in the flows that extend southward from them. Porter (1979a, c, 1987) also recognized the ice-contact fabric of these scarps and interpreted them as the terminus of a subglacial flow from Puu Waiau. However, the flow from Puu Waiau (flow PW, pl. 2) is a Laupahoehoe hawaiite, lithologically and compositionally distinct from the basalt that composes the scarps. The flow from Puu Waiau overlies basalt of the scarps and locally terminates immediately uphill from the scarps (pl. 2), a relation suggesting that the scarp crests were actually ridge crests against which the flow from Puu Waiau ponded. The occurrence of agglutinated scoria and the linearity of the scarp crests suggest that these crests mark the trace of a fissure-vent system which supplied some of the Liloe Spring basalt flows to the south. The ice-contact fabric and occurrence of hyaloclastite tuff imply that the fissure ridge formed in a subglacial setting, and the stratigraphy indicates that this eruption occurred during the Waihu glacial episode. Later, Makanaka ice vigorously eroded both the scarps and the superjacent flow from Puu Waiau.

Three topographic prominences in the upper part of Pohakuloa Gulch contain deposits of cinders or agglutinated scoria, as well as mosaic-jointed and strongly sheeted basalt. The assemblage of fabrics resembles that of the Keanakakoi scarp, and we interpret them as indicative of additional vents (pl. 2) formed beneath Waihu ice. Like the Keanakakoi scarp, they underwent significant later erosion during the Makanaka glacial episode.

DIKES

Dikes of aphyric or weakly porphyritic basalt, interpreted as local feeders for Liloe Spring lavas, are exposed at several localities along Pohakuloa and Waikahalulu Gulches (pl. 2). Most of these dikes range in thickness from about 0.3 to 2 m and are generally similar in texture to the dense, massive parts of the flows; they probably chilled fairly rapidly against the shallow country rocks.

An unusually wide (8 m) dike occurs in Pohakuloa Gulch at approximately 3,750-m (12,300 ft) elevation. It apparently crystallized more slowly than most. Except for 10-cm-wide, fine-grained, chilled margins, the dike consists of megascopically crystalline, aphyric, diktytaxitic basalt. Vesicles are confined to a 20-cm-wide zone just inside the chilled margin and to scattered, vertical vesicle pipes, about 10 cm in diameter; otherwise, the dike is massive.

One dike, exposed where Waikahalulu Gulch transects segments of the Keanakakoi scarp (pl. 2), is compositionally and mineralogically zoned. Porphyritic basalt at the center, containing plagioclase and olivine phenocrysts, grades to aphyric basalt at the margins. The dike, about 30 cm wide, cuts scoria and hyaloclastite tuff at the base of a Liloe Spring basalt flow. At this same locality, the Liloe Spring Volcanic Member overlies porphyritic pahoehoe flows of the Hopukani Springs Volcanic Member. Although this dike is somewhat off the trend of the nearby Keanaka-

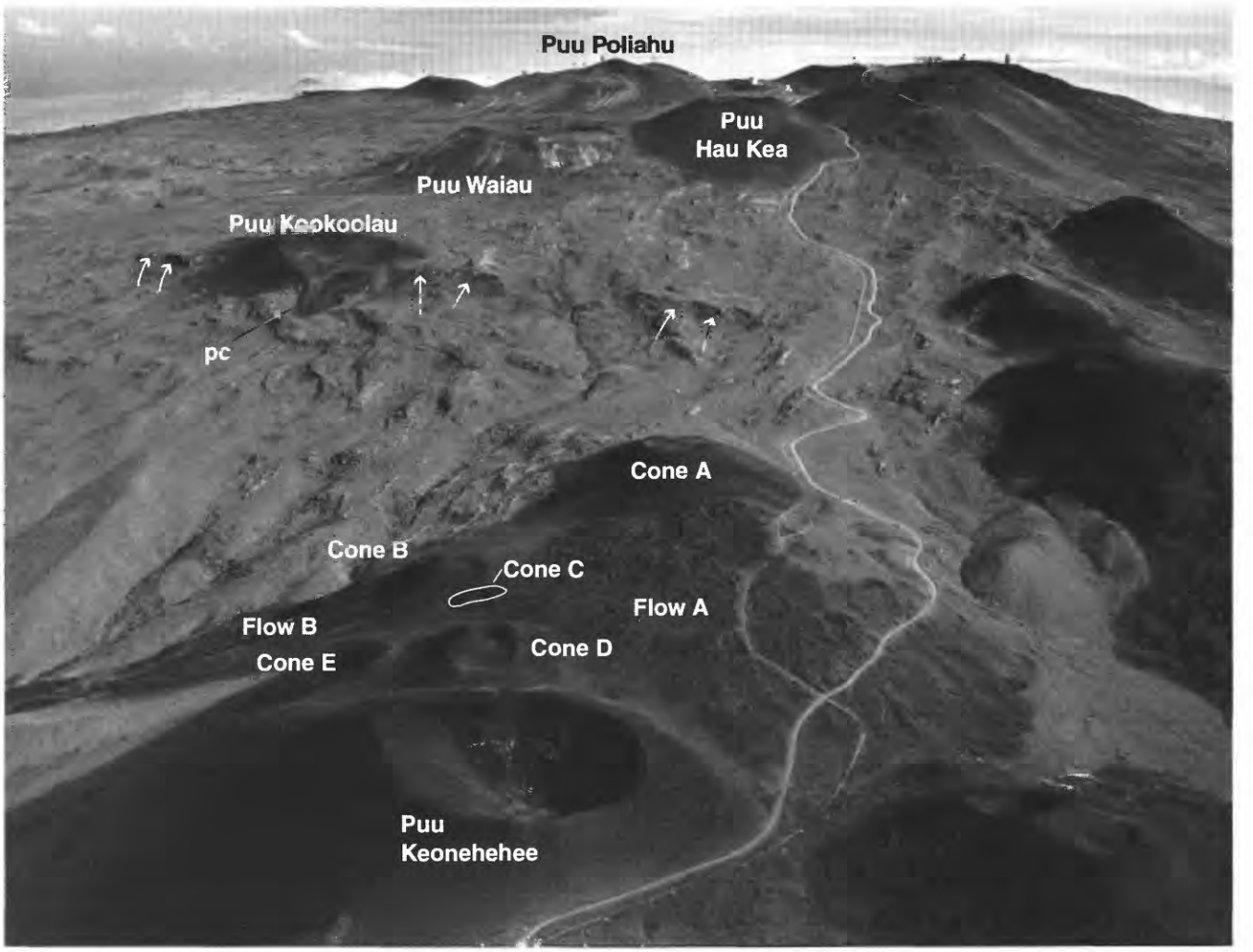

Figure 19. South-summit region of Mauna Kea. Prominent scarps (arrows, center), which consist of basalt of the Liloe Spring Volcanic Member of the Hamakua Volcanics, are interpreted as remnants of possible subglacial fissure ridge. Scarps extend westward (to left) and northeastward (to right) from beneath Puu Kookoolau, cinder cone of older volcanic rocks member of the Laupahoehoe Volcanics. Note pit crater (pc) in front of Puu Kookoolau. Field relations among cones and flows in foreground determine probable stratigraphic sequence of flows of younger volcanic rocks member of the Laupahoehoe Volcanics (see subsection of text entitled "Younger Volcanic Rocks Member"; see pl. 2). Sharp-rimmed cinder cone that has large bowl-shaped crater (bottom center) is Puu Keonehehee, cinder cone of younger volcanic rocks member of the Laupahoehoe Volcanics. Ledges inside north crater wall are outcrops of broad, dark lava flow A exposed uphill from Puu Keonehehee. Low knob filling crater bottom is hawaiitic lava extruded after explosive enlargement of crater. Flow A and cones A (source of flow A), D, and E are mapped as older volcanic rocks member of the Laupahoehoe Volcanics; flow B and cones B (source of flow B) and C are mapped as younger volcanic rocks member of the Laupahoehoe Volcanics (see pl. 2). View northwestward; Hawaiian Volcano Observatory photograph 88.7.11EW135A#21.

koi scarp segments, its proximity to the scarps supports our interpretation that the scarp crests record the trace of a Liloe Spring vent.

Three closely spaced dikes cut the Liloe Spring sequence exposed in the deeply incised part of Waikahalulu Gulch (because of limited space, only two dikes are shown on pl. 2). One of these dikes penetrates the capping flow of the canyon-wall sequence and forms a low knob on the west canyon rim (fig. 17). An envelope of red agglutinated scoria between the uppermost part of this dike and the enclosing flows that it intruded records vesiculation and fragmentation as the dike neared the ground surface. Even though this dike apparently reached the ground surface, we recognize no associated lava flow that it fed.

The positions and strikes of five mapped dikes and the segments of the inferred fissure ridge (pl. 2) define a narrow, 3-km-long arc between 3,730- and 3,790-m (12,240 and 12,440 ft) elevation. The angular width of this arc is

about 120°; its radius is about 1.5 to 2 km, and its center of curvature is approximately 1 to 1.5 km southwest of the summit of Mauna Kea in the vicinity of Puu Waiau. Exposed tops of these dikes are now at a level that was no more than a few meters below the mountain surface when the dikes were emplaced; we presume that they were feeders for some Liloe Spring flows. These dikes and the fissure ridge were apparently emplaced along a set of circumferential fractures—possibly related to buried, preexisting caldera-bounding faults or to a shallow, contemporaneous magma reservoir that fed ring dikes.

INFERRED NEAR-SUMMIT VENTS

Liloe Spring basalt flows are exposed uphill from the topographically highest vents and dikes in the Pohakuloa Gulch drainage, and no exposed vents are related to the topographically highest Liloe Spring flows on the north flank of Mauna Kea. Therefore, we infer that near-summit vents, now buried by the overlying Laupahoehoe Volcanics, supplied a significant volume of the Liloe Spring flows.

AGE

The age of the Liloe Spring Volcanic Member is not well determined by K-Ar dating (fig. 11); 10 new K-Ar ages range from about 85 to 218 ka. All but the oldest determination, which is stratigraphically inconsistent, suggest an age of approximately 100 to 150 ka, and a K-Ar age (sample QLA–3c, table 5) previously reported by Porter (1979c) indicates that the upper part may be as young as 70 ka. Dorn and others (1991) reported an exposure age of approximately 60 to 70 ka for the Waihu Glacial Member, which is overlain by the youngest lava flows of the Liloe Spring Volcanic Member.

WAIHU GLACIAL MEMBER

DEFINITION AND OCCURRENCE

The Waihu Glacial Member is a lens of till and gravel enclosed, at least in part, by the upper part of the Liloe Spring Volcanic Member (fig. 9). Because overlying flows of the Liloe Spring Volcanic Member are discontinuous, most Waihu outcrops occur as kipukas (pl. 2; fig. 20) surrounded by either Liloe Spring basalt or the still-younger Laupahoehoe Volcanics. Wentworth and Powers (1941) designated as the type locality conspicuous outcrops of the Waihu Glacial Member west of Pohakuloa Gulch near Waihu Spring, at about 2,960-m (9,700 ft) elevation.

Discontinuous outcrops of Waihu drift form an arcuate pattern across the upper south flank of the volcano (pl. 2; fig. 20). This arc is approximately concentric to the summit of Mauna Kea; its lower topographic limit is at about 2,740-m (9,000 ft) elevation. The exposure is limited eastward and westward by large flows of the Laupahoehoe Volcanics. Additional, thin (0–3 m thick), discontinuous, unmapped exposures of the Waihu Glacial Member occur locally between lava flows of the upper part of the Liloe Spring Volcanic Member in the steep canyon walls of Waikahalulu Gulch and along Hanaipoe Gulch, on the north flank of Mauna Kea. In addition, outwash deposits are locally exposed in a small gulch west of Pohakuloa Gulch.

PREVIOUS WORK

Wentworth and Powers (1941) interpreted the belt of south-flank outcrops as representing two separate glacial-drift deposits: the Pohakuloa Drift, which they considered to be older, and the Waihu Drift, which they considered to be younger. They showed the distribution of these units in a schematic map that is difficult to relate precisely to the geology as now mapped.

Stearns (1945) recognized that the Pohakuloa and Waihu Drifts of Wentworth and Powers (1941), where exposed on the interfluves and in the shallow drainages between Pohakuloa and Waikahalulu Gulches, belong to a single unit. He clarified their map distribution and assigned all of these outcrops to the Waihu. However, he disputed the interpretation of Wentworth and Powers that these sedimentary rocks were deposited as glacial drift. Instead, he interpreted the Waihu as fanglomerate that could have been deposited by floods resulting from eruptions which melted an icecap during early Wisconsin time.

Porter (1979c), in his thorough study of Mauna Kea glacial deposits, conclusively showed that this south-flank belt of Waihu sedimentary rocks represents a lobate end moraine, modified by erosion and partly buried by younger lava. He assigned the end-moraine deposits, as well as sedimentary deposits farther downhill that he interpreted as outwash, to his Waihu Formation.

GEOLOGIC OBSERVATIONS

Numerous gulch-wall exposures show that the Waihu Glacial Member consists predominantly of massive to crudely layered till (fig. 21) in which subangular to subrounded cobbles and boulders of Liloe Spring basalt are enclosed in a moderately indurated, gray through yellowish-brown to reddish-brown, unsorted matrix. Locally, on the west rim of Waikahalulu Gulch, this matrix contains abundant hyaloclastite fragments, which impart a yellow color to the lower part of the deposit. The boulders range in size to as large as about 2 m across. The maximum thickness of the unit is about 30 m.

More distinctly sorted and layered gravel occurs locally, particularly near the downslope end of the south-flank outcrop belt. One especially conspicuous exposure of

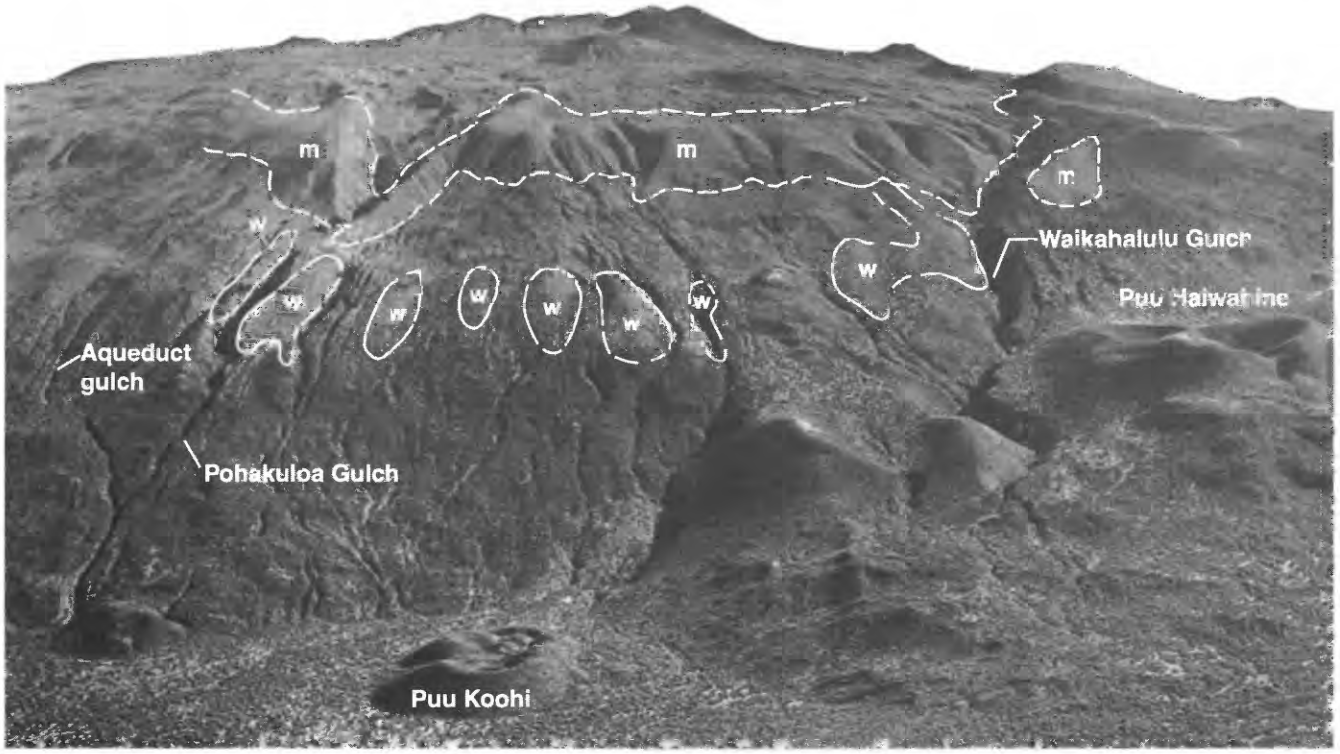

Figure 20. Part of south flank of Mauna Kea, showing approximate extent of end moraine of the Makanaka Glacial Member (m) of the Laupahoehoe Volcanics and conspicuous exposures of end moraine of the Waihu Glacial Member (w) of the Hamakua Volcanics. Contacts dashed where approximately located. Aqueduct gulch is an informally named feature. Hawaiian Volcano Observatory photograph 88.7.11EW120A#4.

the gravel facies is on the west rim of Pohakuloa Gulch, at approximately 2,740- to 2,800-m (9,000 to 9,200 ft) elevation. There, the gravel, which is not mapped separately from the till, buries a cinder cone of the Liloe Spring Volcanic Member exposed in the west wall of the gulch (pl. 2). Coarse, bedded, indurated gravel interpreted as Waihu outwash is also exposed in a small gulch about 0.7 km northwest of Pohakuloa Gulch (see fig. 33).

Boulders and cobbles are concentrated as a lag deposit in surface exposures, where they form a rough pavement. The boulder surfaces are dark gray to brown or, locally, reddish brown. Spalled boulders are common. The dark, spalled boulder surfaces contrast markedly with the fresher, light-gray to yellowish-brown boulder surfaces on Makanaka glacial deposits.

In surface exposures, Waihu moraine segments form low, smooth, gently convex hills—like the bowls of inverted spoons—that are elongate downslope (fig. 20). They are easily recognized on aerial photographs because of their gentle convexity and smoothness and because they are virtually devoid of the scrub trees that grow on parts of the nearby lava flows and slope deposits. Porter (1979c) concluded that these segments represent lateral moraines formed at the margins of small ice lobes and that younger lava flows commonly had buried the terminal loops.

Our map pattern (pl. 2) for Waihu morainal deposits is generally similar to that shown by Porter (1979a) but differs greatly in detail. In particular, he showed a significant part of each of the spoonlike morainal hills as composed of outwash. Except for local gravel, such as that described above on the west rim on Pohakuloa Gulch, we find that the hills composed of Waihu drift are monotonously uniform, and we are unable to identify and map Porter's separate till and outwash facies on these surfaces. Furthermore, the long streams of Waihu outwash that Porter showed extending far downslope include various younger air-fall and sedimentary slope deposits (see subsection below entitled "Slope Deposits").

The map pattern also differs because Porter (1979a) purposely mapped only the morainal deposits that he interpreted as end moraines. However, we have included areas of more or less continuous ground moraine, such as the elongate outcrop of Waihu drift just west of Waikahalulu Gulch, above 3,140-m (10,300 ft) elevation (pl. 2; fig. 20). A post-Waihu flow of Liloe Spring basalt apparently buried this ground moraine near Waikahalulu Gulch. Thin (1–3 m

Figure 21. Consolidated diamict (till) of the Waihu Glacial Member of the Hamakua Volcanics exposed in northwest wall of unnamed gulch about 3.3 km northwest of Pohakuloa Gulch, at about 3,020-m (9,900 ft) elevation. Diamict fabric, largely expressed by orientation of long axes of boulders, dips downslope (to left), parallel to volcano surface and to contact between the Waihu Glacial Member and overlying flows (outside of photograph) of the Liloe Spring Volcanic Member of the Hamakua Volcanics. Pole is 1.5 m long and approximately vertical. Hawaiian Volcano Observatory photograph 88.3.2EW135A#29.

thick) unmapped diamict occurs below the uppermost Liloe Spring basalt flow in the west wall of Waikahalulu Gulch (fig. 18), just east of the mapped ground moraine. Locally, the underlying basalt surface is abraded and striated. Similar thin diamict, overlain and baked by the uppermost Liloe Spring flow, is exposed farther downstream in the east wall, where the gulch is deeply incised.

Like Makanaka drift, which is younger, Waihu drift formed an annulus surrounding glacially eroded rocks nearer the volcano summit. Thus, uphill from the mapped Waihu drift deposits, between them and the Makanaka moraine, we have mapped kipukas of glacially eroded Liloe Spring basalt that was scoured by the Waihu icecap. Downslope from the outcrops of Waihu drift, we are unable to distinguish post-Waihu Liloe Spring basalt from older Liloe Spring flows. The virtual absence in Waihu drift of boulders derived from the distinctive porphyritic basalt of the Hopukani Springs Volcanic Member indicates that the summit of Mauna Kea was extensively capped by Liloe Spring basalt at the time of the Waihu glacial episode.

AGE

The age of the Waihu Glacial Member is not well constrained by K-Ar dating, but it must be in the range 100–150 ka, possibly as young as 70 ka (fig. 11). This age corresponds to some part of marine oxygen-isotope stages 4 through 6 (fig. 10). Dorn and others (1991) report varnish cation-ratio exposure ages of approximately 65 ka for striated Liloe Spring basalt eroded by Waihu ice and for a basalt boulder in Waihu drift. This boulder also gave a ^{36}Cl exposure age of approximately 68 ka. Both the boulder and the striated lava-flow surface are from exposures 200 to 300 m west of Waikahalulu Gulch. These results suggest that the Waihu glacial episode corresponds approximately to marine oxygen-isotope stage 4.

LAUPAHOEHOE VOLCANICS

GENERAL STATEMENT

The Laupahoehoe Volcanics form the magmatically evolved cap of Mauna Kea Volcano; the lavas consist exclusively of hawaiite, mugearite, and benmoreite that overlie the basaltic Hamakua Volcanics. We estimate the volume of Laupahoehoe flows and pyroclastic deposits at approximately 25 km^3. About 90 percent of the lavas is hawaiite and mugearite, and 10 percent is benmoreite. As noted above in the subsection entitled "Major Rock Classes and Petrographic Groups," we refer to the range of Laupahoehoe compositions collectively as hawaiitic. Furthermore, we refer to the hawaiite and mugearite lavas collectively as hawaiite-mugearite. We divide the unit into three members: older volcanic rocks (lavas and pyroclastic deposits of late Pleistocene age), younger volcanic rocks (postglacial lavas and pyroclastic deposits of latest Pleistocene? and Holocene age), and the Makanaka Glacial Member (till and outwash of late Pleistocene age). In addition, we have also mapped (pl. 2) air-fall deposits (ash and lapilli of late Pleistocene and Holocene age) within the Laupahoehoe Volcanics.

Macdonald (1945) and Stearns and Macdonald (1946) applied the term "Laupahoehoe Volcanic Series" to the younger volcanic rocks of Mauna Kea. They designated Laupahoehoe Point as the type locality. There, a hawaiite-mugearite flow, occupying a canyon eroded in basaltic

rocks of the Hamakua Volcanics, had built a lava delta at the coast.

As reviewed above in the subsection entitled "Stratigraphic Overview," definition of the Laupahoehoe Volcanic Series was vague. Stearns and Macdonald (1946) believed that there was a gradation between the predominantly basaltic lavas of the Hamakua Volcanic Series and the predominantly andesitic (hawaiitic in our terminology) lavas of the Laupahoehoe Volcanic Series. Thus, they indicated that each series contained both basaltic and andesitic rocks.

In their mapping, Stearns and Macdonald (1946; see Macdonald, 1949) included most south-flank exposures of our Liloe Spring Volcanic Member in their Hamakua Volcanic Series. In remapping this area, Porter (1979a) included the basalts of our Liloe Spring Volcanic Member and the intercalated tongue of Waihu drift in his Laupahoehoe Group.

Our mapping shows that hawaiitic flows and pyroclastic deposits overlie basaltic lavas of the Hamakua Volcanics. No interleaving or gradation occurs between the older basaltic lavas and the younger hawaiitic lavas. Therefore, we redefine the Laupahoehoe Volcanics to correspond to the cap of hawaiitic lavas, including the intercalated Makanaka Glacial Member; all the underlying basaltic lavas, as well as the Waihu Glacial Member, are excluded (figs. 5, 7; table 3). Exposures along the road from Humuula Saddle to the summit of Mauna Kea constitute a useful and readily accessible reference locality for the Laupahoehoe Volcanics.

Laupahoehoe volcanism continued throughout the period of growth and disappearance of the Makanaka icecap and into Holocene time. The presence of Makanaka glacial deposits and the glacially and periglacially enhanced erosion and weathering of the volcano surface during latest Pleistocene time provide a means for us to distinguish the postglacial Laupahoehoe lavas. Because the style of volcanism, as well as the composition and lithology of Laupahoehoe lavas, was constant from Pleistocene to Holocene time, we describe the general characteristics of the older and younger volcanic rocks members together and, thereafter, discuss the characteristics and relations that pertain to each member individually.

BENMOREITE FLOWS AND CINDER CONES

All the benmoreite occurs in the northwest sector of the volcano (fig. 22). The vent cinder cones (Kaluamakani and Puu Pueo) for two of the flows are exposed, but the vents and proximal ends of the other flows have been buried by younger hawaiite-mugearite flows. Interestingly, the benmoreite flows are among the oldest of the Laupahoehoe lavas; however, the flows from Kaluamakani and Puu Pueo overlie earlier hawaiite-mugearite flows.

Except for one flow containing abundant plagioclase microphenocrysts, the benmoreite is aphyric. It is all light gray and commonly displays a megascopic trachytic texture, as well as platy jointing. Euhedral, reddish-brown biotite crystals are common on vug walls. Two of the flows contain scattered to common gabbroic and ultramafic xenoliths. Because none of these characteristics is sufficient to distinguish the benmoreite from flows of hawaiite-mugearite, we base the distinction on chemical analyses.

The benmoreite flows are mostly extensive. The flow from Kaluamakani is 20 km long, and that from Puu Pueo extended 20 km to the present coastline. The flows are of aa, with remnants of branching and rejoining channels preserved on their surfaces. These channels are bounded by prominent levees, spaced 400 to 500 m apart, and contain conspicuous transverse pressure ridges. The ridges have a local relief of 5 to 10 m and commonly are bowed, ogive-like, so as to be convex downslope as seen in plan view. Average flow thicknesses range from about 20 to 25 m. Each of the two larger flows has a volume of about 0.8 km^3.

HAWAIITE-MUGEARITE

LITHOLOGY

Hawaiite-mugearite is dark gray to light gray and most commonly aphyric. In hand specimen, the trachytic texture of the groundmass gives the rock a sheen that is not seen in the basalts. Some flows (possibly 20 percent) contain plagioclase microphenocrysts (less than 1 mm diam), and a very few flows contain plagioclase phenocrysts (1–3 mm diam). The microphenocrysts and phenocrysts normally have the same crystallographic orientation as plagioclase of the trachytic groundmass, and so they participate in the trachytic sheen. These phenocrysts and microphenocrysts form conspicuous reflecting plates in the plane of trachytic layering, but because the plates are thin, these crystals are indistinct in hand-specimen surfaces oblique to the trachytic layering. In contrast, the subequant plagioclase phenocrysts common in basalt of the Liloe Spring Volcanic Member are randomly oriented and equally conspicuous on all fresh rock surfaces. Gabbroic and ultramafic xenoliths and xenocrysts are common in about 20 to 30 percent of the flows and cinder cones.

LAVA FLOWS

Exposed surfaces of the hawaiite-mugearite flows consist mostly of clinkery to blocky aa. These flows are commonly about 5 to 10 m thick; aa as thick as 25 m or more occurs locally. Pahoehoe occurs locally, particularly in the proximal areas of some flows, where branching pahoehoe lava-tube structures are evident. Such pahoehoe is thick and relatively massive and dense, unlike the thinner layered, vesicular, basaltic pahoehoe of the Hamakua Volcanics or of the active tholeiitic shield volcanoes, Mauna Loa and

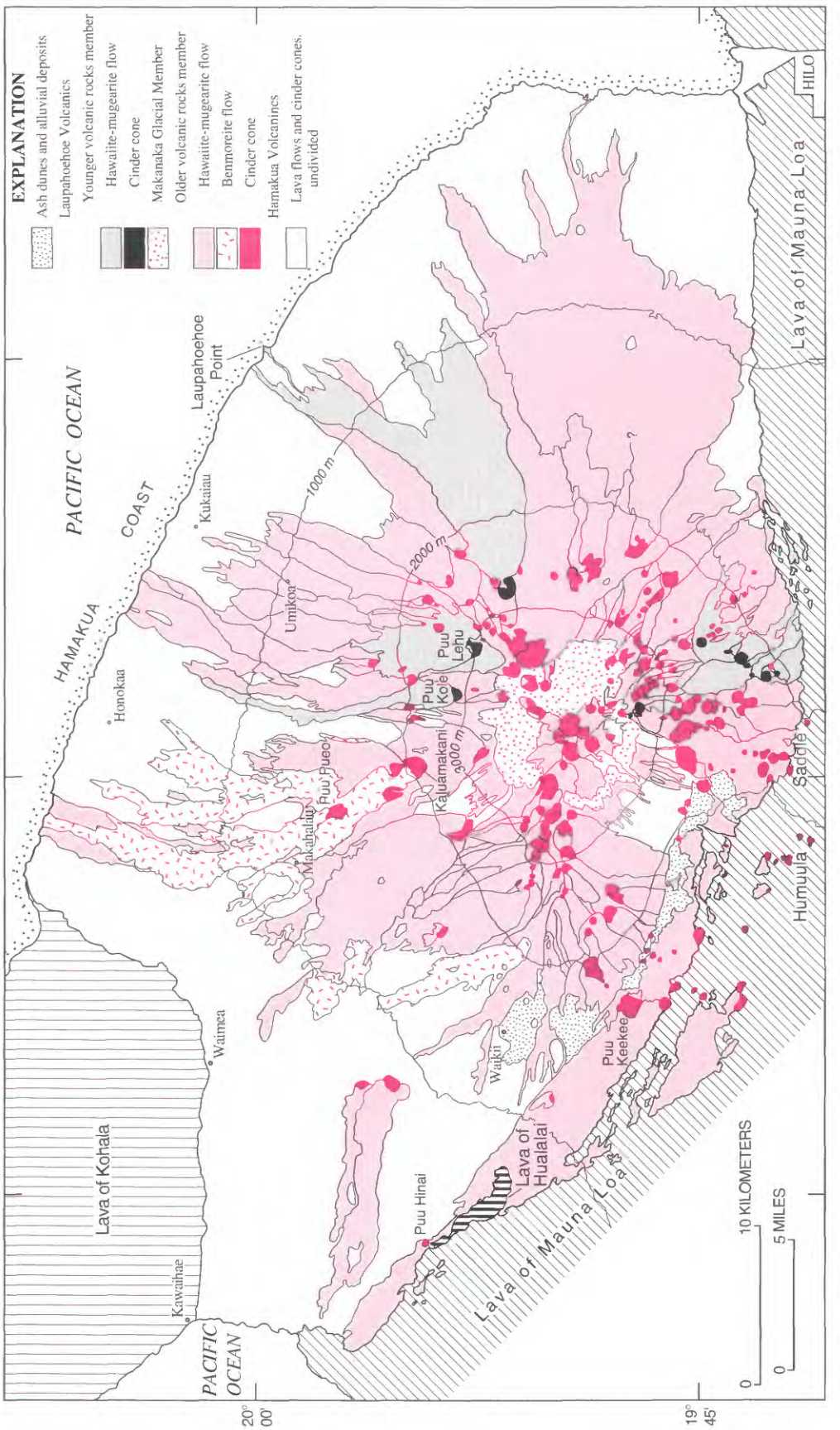

Figure 22. Geologic map of Mauna Kea, showing generalized distribution of flows, cinder cones, and glacial deposits of the Laupahoehoe Volcanics. Queries mark limits of mapping at edge of dense rain forest. Internal contacts distinguish individual lava flows and cinder cones. Contour showing 4,000-m (13,120 ft) elevation is omitted for simplicity. Geology simplified from plate 2 and Wolfe and Morris (1996).

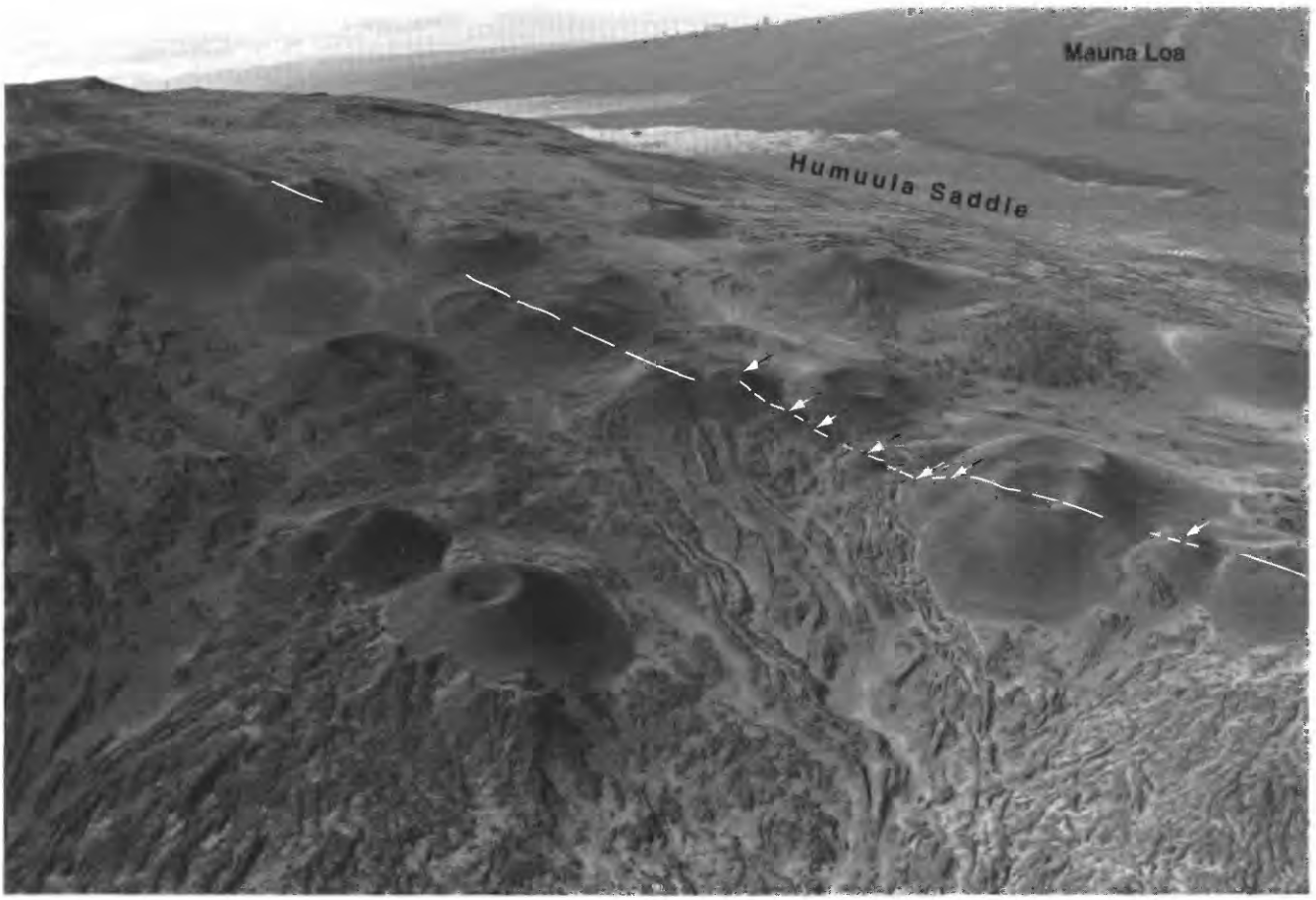

Figure 23. Cinder cones and lava flows of older volcanic rocks member of the Laupahoehoe Volcanics on upper west flank of Mauna Kea. Flows that display conspicuous ridge-and-trough fabric emanate from lower flanks or bases of cones; some flows breached their source cones. Seven small, aligned cones (arrows) of cinder or spatter that vented lithologically similar lavas probably formed during one fissure eruption. Short-dashed line, inferred trace of fissure; long-dashed line, crest of prominent ridge formed by several larger, similarly aligned cones. Lava from these larger cones flowed both northwestward and southwestward, down flanks of ridge. Late-stage explosive activity deposited excavated basalt blocks on rim of large breached cone at upper left. View southeastward; Hawaiian Volcano Observatory photograph 88.7.11EW135A#5.

Kilauea. Broad, subhorizontal pahoehoe surfaces, interspersed with aa, occur in the Pohakuloa Training Area on the gently sloping Laupahoehoe flow (flow PTA, pl. 2) that extends northwestward parallel to the sharp base of Mauna Kea's south flank.

Gully walls commonly expose thick, dense, massive flow interiors overlying and capped by aa rubble. In some outcrops, the massive facies and the aa breccia facies are complexly interlayered within single flows. Locally, flows rest on deposits of air-fall lapilli.

The longest flows extend 15 to 25 km from their sources, but their thicknesses increase only moderately from their proximal to their distal ends; the flow from Puu Hinai, for example, is approximately 7 m thick near its source and 12 m thick at its terminus. Flow widths range from about 0.5 to 7 km, but elongate lobes as narrow as 50 m extend hundreds of meters down steep slopes from some flows. Volumes of individual flows range from very small (much less than 1 million m^3) to very large; for example, the volume of the flow from Puu Keekee is approximately 0.4 km^3.

The surfaces of flows that descended slopes steeper than about 5° are typically marked by networks of subparallel, discontinuous, linear to gently curving, locally anastomosing, longitudinal ridges. In aerial photographs (figs. 23, 24), these flow surfaces appear corrugated to braided. The ridges and the intervening troughs are generally hundreds of meters to several kilometers long, with a crossflow spacing of about 30 to 200 m. The ridges are as much as about 15 m high, although most are appreciably lower. Troughs on the older flows are partly filled by air-fall and eolian deposits and, particularly on the upper slopes, by colluvium.

Some of the ridges branch; some truncate earlier-formed neighbors. The trends of the ridge segments parallel the flow directions, and, at some flow boundaries, the ridge-and-trough networks display crosscutting contacts from which interflow age relations can be interpreted (fig. 24).

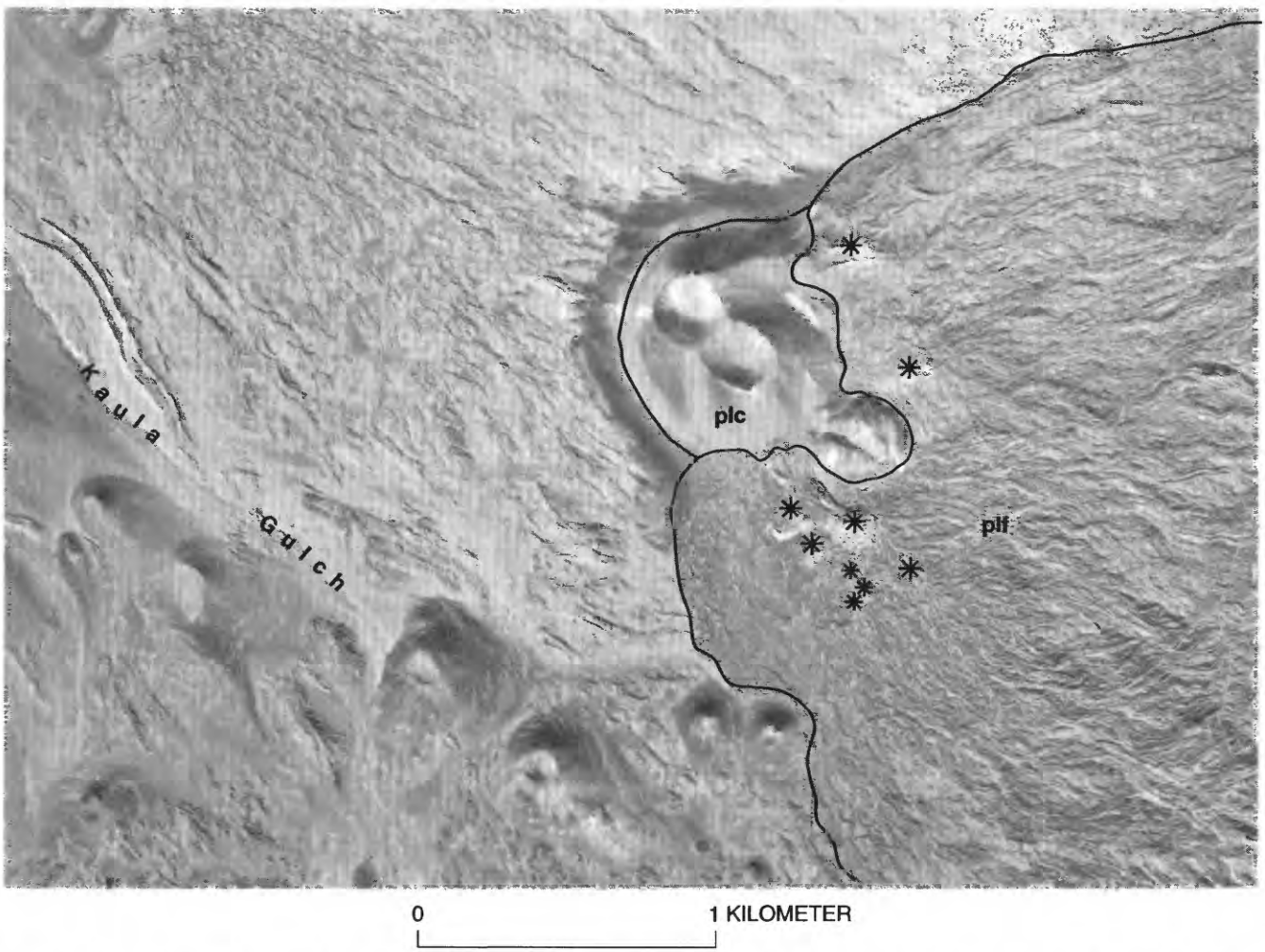

Figure 24. Puu Lehu (Holocene), showing nearby lava flows and cinder cones of the Laupahoehoe Volcanics on upper northeast flank of Mauna Kea. North is to right; illumination is from east-southeast. Cones and craters of Puu Lehu (plc) are aligned northeastward; asterisks mark secondary vents on flow-field surface north and northeast of Puu Lehu. Edge of dark, fresh flow from Puu Lehu (plf), which is virtually devoid of ash or colluvium, crosscuts partly debris-filled ridge-and-trough fabrics of older flows to south and west. Dark annulus adjacent to south and west flanks of Puu Lehu is deposit of air-fall cinders and bombs. Sharply defined, prominent ridges that bound narrow channel northwest of Kaula Gulch represent coherent cores of aa flow levees that have been stripped of loose rubble by torrential meltwater. Part of U.S. Department of Agriculture, Agricultural Stabilization and Conservation Service aerial photograph EKL–14CC–126, taken March 7, 1965.

Some of the ridges are levees that bounded lava-channel segments; others are narrow, steep-sided flow lobes, some of which have narrow channels along their axes. Foshag and González R. (1956) observed the development of similar channel-and-levee morphology on parts of the complex flow field that was emplaced during the first 2½ years of the Parícutin eruption. They described (p. 467) a narrow (6 m wide) lava stream approximately paralleled by "irregular low ridges of clinkers, apparently old levees formed on preceding days when the lava had flowed by a somewhat different course." They also illustrated (Foshag and González R., 1956, pl. 50) narrow, steep-sided, elongate flow lobes composed of aa levees bounding a central channel and a complex network of such flow lobes, with conspicuous channel-and-levee segments, that developed over a period of several months.

By analogy with the Parícutin eruption, we suppose that typical Laupahoehoe flows were emplaced during eruptions that lasted for months or years. The corrugated or braided Laupahoehoe flow surfaces are largely composites of narrow, elongate, steep-sided flow lobes, most of which were created by relatively short-lived lava channels encased in their own levees. The discontinuity of channel segments suggests that the surface channels originated not only at the eruptive vent but also on the flow-field surface, as channeled lava broke through the confining levee walls or as lava from the molten flow interior (represented by the dense outcrops seen in stream exposures) leaked through the capping aa rubble.

On lower slopes, particularly in the terminal parts of flows, Laupahoehoe aa tended to advance more nearly as broad sheets, as in the zone of dispersed flow recognized by

Lipman and Banks (1987) near the toes of Mauna Loa aa lobes. In these areas, channels tend to be broader, with levees less well defined than on the steeper slopes or even absent; and hummocks and ogivelike transverse pressure ridges abound. These features record buckling of the lava-flow carapace in response to compressive forces from the downslope movement of the more fluid flow interior.

VENT DEPOSITS

Most of the hawaiite-mugearite flows were erupted from single, point-source vents. In most places, pyroclastic deposits accumulating at such a vent built a large cinder cone. Wentworth (1938) included all of these cinder cones in the "central cone phase" of his Waiau Formation. Flows commonly issued from the bases or lower flanks of the associated cinder cones (fig. 23) or from tube-fed vents that built small shields or small, steep lava domes in the proximal part of the flow field (fig. 24). Some flows carried away part of the cone, leaving a crescentic remnant. Observations at Parícutin (Foshag and González R., 1956), where the main cone closely resembles many Laupahoehoe cones, show that continued pyroclastic activity may repeatedly "heal" the flanks of a cone that has failed or been breached by a lava flow. Local shifts of the vent during the course of some Mauna Kea eruptions built overlapping cones and complex flow fields (fig. 24). Porter (1972b) fully described the morphology and size frequency of the cinder cones. His observations are summarized as follows. The cones consist of ejecta of strombolian-type eruptions, cinders 1 to 10 cm in diameter, and ubiquitous spindle bombs that mostly are as much as about 0.5 m long but may be as much as 3 m long. Cone diameters range from less than 100 m at the base to as much as 1,250 m. Their maximum height is about 200 m. Most cones, however, are 200 to 600 m in basal diameter and 30 to 100 m high, with a nearly constant height/width ratio of 0.18. Many cones have craters; the ratio of crater-rim diameter to basal cone diameter is generally about 0.4. Craters are commonly from a third to a half filled by colluvium and air-fall tephra. Maximum slopes on most cones are 25°–27°. Steep slopes occur where cones are capped by consolidated spatter or where the flanks have been steepened by eroding glacial ice. Most cones are asymmetric, probably because of accumulation of ejecta during persistent winds.

Parícutin Volcano provides a useful modern example of the growth of a cinder cone similar to those of the Laupahoehoe Volcanics. The main cone at Parícutin grew quickly from a rapid accumulation of bombs, ash, and lapilli ejected by closely spaced explosions that generated a varying, pyroclast-laden eruption column which was sometimes as much as 5 or 6 km high (Foshag and González, R., 1956).

Some Laupahoehoe vents produced little or no pyroclastic ejecta; eruption at such a vent produced a flow with a low lava dome at its source. One good example is the flow of the younger volcanic rocks member that issued approximately 1 km southeast of Hale Pohaku (pl. 2).

A few fissure vents with low spatter ramparts, as much as about 10 m high, have been found. In addition, local occurrences of aligned cones of cinders or spatter (figs. 23, 24) at the sources of lithologically similar flows may record fissure eruptions.

Late, explosive eruptive activity at several Laupahoehoe cinder cones excavated blocks of older, subsurface lava flows, depositing the blocks on the crater rims, cone flanks, and beyond. These explosive eruptions also deposited local blankets of air-fall tephra and probably enlarged the cinder-cone craters. Good examples are Puu Kookoolau, Puu Keonehehee, Puu Kanakaleonui, and a broad unnamed cinder cone that crests at 3,900-m (12,800 ft) elevation, 3.4 km northwest of the summit of Mauna Kea (pl. 2; fig. 23).

Glacial erratics, as well as ejecta blocks, occur on both Puu Kookoolau and the unnamed cinder cone mentioned above. In both places, however, the ejecta includes porphyritic basalt that is absent in the nearby glacial deposits and can have originated only from eruptive excavation of the substrate. The rim and flanks of Puu Keonehehee are littered by light-gray ejecta blocks of hawaiite-mugearite; a quarried hawaiite-mugearite flow is exposed in steep outcrops in the lower part of the crater wall (fig. 19).

The most extraordinary example of quarrying by explosive eruption and the most extensive ejecta blanket clearly related to such an explosive eruption are at Puu Kanakaleonui (fig. 25). Black air-fall tephra mantles part of the cinder cone and extends as a thick, continuous blanket for approximately 0.5 to 1 km beyond the buried base of the cone (pl. 2). Only part of the flow that exited through the breached crater rim is mantled, an observation suggesting that the explosive phase of the eruption occurred after part of this flow had been extruded. The air-fall-tephra blanket is littered by basalt blocks that are mostly 10 to 50 cm in diameter but that may be as much as 3 m long. The eruption quarried a large variety of porphyritic basalt types from flows of the Hamakua Volcanics; some of these rock types are unknown in surface exposures anywhere else on the volcano. The nearest outcrops of Hamakua basalt are 9 km away, downslope to the northeast.

Distribution of Cinder Cones

Laupahoehoe cinder cones are scattered over the upper flanks of Mauna Kea and in the western part of Humuula Saddle (fig. 22). All but four cones, low on the west flank, are above 1,400-m (4,920 ft) elevation and within 20 km of the summit. Thus, the upper flanks of the volcano are peppered with Laupahoehoe cones, whereas the lower flanks are essentially devoid of them.

A weak preferred concentration of Laupahoehoe cinder cones in sectors west, northeast, and south to southeast of

Figure 25. Blanket of dark air-fall tephra partly surrounding and mantling Puu Kanakaleonui (foreground). Maximum width of crater is approximately 700 m, and air-fall blanket is about 3.5 km wide. Bright surface in lower part of photograph is unmantled lava flow from Puu Kanakaleonui. View southwestward, toward summit of Mauna Kea (top center); Hawaiian Volcano Observatory photograph 88.7.11EW120B#10.

the volcano summit is shown in figure 22. Macdonald (1945) and Porter (1972b) previously pointed out these zones of more closely spaced cinder cones and referred to them as having erupted along rift zones radial to the summit.

The best defined of the three areas of more closely spaced vents is the western cluster, which extends about 11 km westward of the summit and has a maximum width, north-south, of 2.5 km. Eruptions in this zone built a prominent west-trending ridge; Laupahoehoe flows extend northwestward and southwestward down its flanks from the vents on the ridge crest (pl. 2). Some cone alignments along the ridge crest (fig. 23) may reflect fissure eruptions and strongly enhance the sense of linearity and east-west elongation of the cone cluster. Furthermore, a topographic bulge in this sector of the volcano extends westward of the Laupahoehoe lavas that cap and flank this western ridge. Cinder cones and lava flows of Hamakua basalt form this more westerly bulge, a relation suggesting that this sector of the volcano was a preferred locus of Hamakua as well as Laupahoehoe eruptions.

The northeastern cluster extends about 9 to 12 km from the summit, depending on which cones are selected for inclusion in it. Its width, from Puu Lehu to Puu Kanakaleonui, is about 5 km; thus, the zone is not strikingly elongate. However, a concentration of about a dozen cinder cones in a 6-km-long by 1-km-wide zone extending northeastward through Puu Makanaka and Red Hill (pl. 2) gives a sense of elongation and alignment radial to the summit. Predominance of the same alignment through the overlapping cinder cones of Puu Lehu (fig. 24) suggests that the Puu Lehu eruption occurred along a short radial fissure.

The cluster of more closely spaced cinder cones south to southeast of the summit is broad, and its boundaries are indistinct, with no suggestion of radial elongation. Local alignments of cinder cones radial to the summit of the volcano summit are identifiable within this cluster, but they are insufficient to indicate the existence of a convincing preferred radial fabric. Furthermore, several Holocene cinder cones in this sector of the volcano, from Kalaieha through Puu Kole, are aligned north-northeast, oblique to any radial structure. The lava flows related to these aligned cones are all chemically identical.

The distribution of Laupahoehoe cinder cones scarcely resembles the well-defined vent alignments of other Hawaiian volcanoes, such as Kilauea, with active rift zones. Furthermore, no preferred concentration or alignment of Laupahoehoe cinder cones is evident on the east flank, where we would most expect it, coincident with the landward extension of Hilo Ridge (fig. 1). Thus, we conclude that Laupahoehoe cinder-cone distribution is not significantly controlled by preexisting rift-zone structure but records only varying radial-stress anisotropies, possibly related to gravitationally induced deformation of the volcano.

Macdonald (1945) and Porter (1972b) recognized arcuate alignments of Mauna Kea cinder cones concentric to the summit of the volcano. Both workers suggested that these alignments might reflect the presence of arcuate, concentric fissures along which magma had intruded. We doubt the reality of significant concentric cone alignments and suggest that the arcuate patterns discerned among the cones by previous workers are unlikely to have any structural significance.

Scattered Laupahoehoe cinder cones occur between approximately 1,600- and 2,000-m (5,250 and 6,560 ft) elevation, in the western part of the broad saddle (Humuula Saddle) between Mauna Loa and Mauna Kea. This part of the saddle apparently formed where relatively fluid lava flows of Mauna Loa Volcano ponded and were diverted westward by the steep opposing front of Mauna Kea Volcano. Laupahoehoe cinder cones of the saddle, which are found as far as 8 km southwest of the steep Mauna Kea mountain front, must have erupted through the gently sloping north flank of Mauna Loa; many of these cones and their related flows were subsequently surrounded, and some evidently completely buried, by younger Mauna Loa lavas. Thus, the Laupahoehoe cinder cones exposed in the saddle record intertonguing between the lavas of Mauna Loa and Mauna Kea.

Several Laupahoehoe flows in the saddle extend north-northwestward, parallel to the steep mountain front of Mauna Kea. The terminus of the flow from Puu Keekee underlies a cinder cone (Puu Iwaiwa) and flow compositionally related to Hualalai Volcano. Thus, the far-western part of the saddle is a zone of interlayering of lavas from all three volcanoes, Mauna Kea, Mauna Loa, and Hualalai.

PIT CRATERS

Two small, shallow pit craters occur on the upper south flank of Mauna Kea. They most probably formed during eruptive activity at the nearest Laupahoehoe vent and record collapse of the roof above a shallow part of the local magmatic plumbing system then active. The first pit crater, an oval about 150 by 250 m across at the rim and 15 to 25 m deep, cuts Liloe Spring basalt adjacent to the southeast base of Puu Kookoolau (fig. 19). A few glacial erratics occur within this crater, and loose scoria from Puu Kookoolau spills into its northwest end; it is unclear from field evidence whether Puu Kookoolau predates or postdates the pit crater. However, the crater formed before or during the Makanaka glacial episode and is most likely related in origin to the Puu Kookoolau eruption.

The second pit crater, 1.5 km north of Hale Pohaku at about 3,300-m (10,840 ft) elevation, is nearly circular, about 150 m in diameter, and 15 to 20 m deep. Its east rim cuts the edge of a flow of the younger volcanic rocks member of the Laupahoehoe Volcanics. This crater apparently records collapse related to the eruption of the young Laupahoehoe vent centered about 300 m to the north-northeast.

OLDER VOLCANIC ROCKS MEMBER

DEFINITION AND OCCURRENCE

We map the hawaiitic lava flows and vent deposits that are older than or coeval with the Makanaka Glacial Member as the older volcanic rocks member of the Laupahoehoe Volcanics. They overlie basaltic rocks of the Hamakua Volcanics. The older volcanic rocks member covers the summit and most of the upper flanks of Mauna Kea. Individual flows extend locally onto the lower flanks (fig. 22), and several flows reach the present coastline.

PREVIOUS WORK

Stearns and Macdonald (1946) included many of the same flows and cinder cones in the lower member of their Laupahoehoe Volcanic Series that we include in our older volcanic rocks member. Their map differs in detail, however, because they included some basaltic cones and flows of our Hamakua Volcanics in their Laupahoehoe Volcanic Series and some hawaiitic cones and flows of our Laupahoehoe Volcanics in their Hamakua Volcanic Series. Furthermore, Stearns and Macdonald (1946) recognized fewer Holocene cones and flows, and so their lower member includes several cones and flows that we map with the younger volcanic rocks member of the Laupahoehoe Volcanics.

Porter (1979a) reassigned some of the basaltic cones and flows of the Laupahoehoe Volcanic Series of Stearns and Macdonald (1946) to his Hamakua Group and reas-

signed some of the hawaiitic cones and flows from the Hamakua Volcanic Series of Stearns and Macdonald (1946) to his Laupahoehoe Group. Furthermore, Porter recognized some additional Holocene cinder cones and lava flows, which he mapped accordingly. Thus, Porter's (1979a) map agrees better in some respects with ours than does that of Stearns and Macdonald. However, Porter included rocks of our Liloe Spring Volcanic Member and the intercalated lens of our Waihu Glacial Member (Porter's Waihu Formation) in his Laupahoehoe Group.

Detailed chronostratigraphy was a major emphasis of Porter's (1979a) study. On the basis of his interpretations of the relations between groups of lava flows and the intercalated glacial deposits, he recognized seven chronostratigraphic stages represented among the lavas of his Laupahoehoe Group. Porter's (1979a) stratigraphic scheme and the K-Ar and ^{14}C ages that were then available are summarized in figure 8.

GEOLOGIC OBSERVATIONS

MODIFICATION OF FLOW AND CINDER-CONE SURFACES

Within the annular Makanaka morainal belt (pl. 2), the surfaces of flows of the older volcanic rocks member, whether preglacial or synglacial, were extensively modified by glacial erosion that generally stripped away the aa breccia and rubble, exposing the massive, dense flow interiors. On parts of some lava flows, however, such as the flows from Puu Wekiu, Puu Mahoe, and Puu Pohaku (flow PPH), that are in the "lee" of their source cinder cones, erosion was minimal or absent. As pointed out by Porter (1979c), many of the Laupahoehoe cinder cones within the Makanaka glacial limit also were glacially eroded. Some of these cones have oversteepened slopes, and many have glacial erratics on their flanks or summits. However, some of the oversteepening, as well as some occurrences of erratics, has probably been obscured by more recent mass wasting of unconsolidated cinders on the flanks of the cones.

Surfaces of lava flows of the older volcanic rocks member beyond the Makanaka glacial limit have been modified by weathering and erosion that reflect periglacial conditions, as well as the greater age of these flows than of flows of the younger volcanic rocks member. Particularly, on the steeper flanks of the volcano, colluvium fills longitudinal troughs on the flow surfaces (fig. 26). This colluvium consists primarily of aa fragments and ash but locally includes glacial erratics as well.

Locally, within a few kilometers of the glacial boundary, some flow surfaces were eroded by glacial meltwater. In the most extreme cases, meltwater torrents stripped all unconsolidated aa rubble from the flow surface, exposing the underlying welded aa breccia as delicate ridges and spines (fig. 26) and leaving rounded erratic boulders wedged into the stripped flow surface. The welded cores of aa flow levees have been etched into sharp relief by such meltwater erosion on some flow surfaces; an excellent example is just northwest of Kaula Gulch (fig. 24).

With decreasing elevation on the volcano, erosion of the flow surfaces, as well as transport and deposition of colluvium, diminished, but flows of the older volcanic rocks member are extensively mantled by air-fall and reworked deposits of ash and lapilli derived from the eruption columns that built the numerous Laupahoehoe cinder cones. Commonly, this mantle fills only depressions on the flow surfaces, but, locally, extensive areas of flow surface are completely buried by ash and lapilli (see subsection below entitled "Laupahoehoe Air-Fall Deposits").

On the east flank of the volcano, below approximately 1,950-m (6,400 ft) elevation, relatively thick, deeply weathered ash deposits form a nearly continuous mantle on some flows and cinder cones; these deposits now consist largely of yellow to orange-brown clay. Such a deposit, estimated at about 3 to 10 m thick, mantles a flow(s) immediately south of the Puu Oo Ranch, as well as the cinder cones 0.5 km southwest and 1.2 km southeast of the ranch (pl. 2). The thickness and intense weathering of this ash deposit imply that these thickly mantled Laupahoehoe cones and flows are older than their thinly and discontinuously mantled neighbors. Wentworth (1938) included this thick, weathered ash deposit in the "yellow tuff phase" of his Waiau Formation.

PUU WAIAU, PUU POLIAHU, AND RELATED FLOWS

Because glacial erosion and periglacial processes affected both pre- and syn-Makanaka flows, the distinction between pre- and syn-Makanaka flows and cinder cones is generally difficult, if not impossible, on the basis of field evidence. The best pre-Makanaka candidates in the summit region are Puu Waiau and Puu Poliahu and their related flows. The flows from these two cones (PW and PPL flows, respectively, pl. 2), both of hawaiite-mugearite typical of the Laupahoehoe Volcanics, extend southward and westward over Liloe Spring basalt of the south-flank kipukas. Both flows disappear beneath Makanaka morainal deposits and reappear to the south and southwest beyond the Makanaka glacial limit (pl. 2); locally, they rest directly on Waihu drift. We interpret the thin, unmapped diamict or gravel between the flow from Puu Waiau (PW flow, pl. 2) and underlying Liloe Spring basalt at and below approximately 3,500-m (11,000 ft) elevation in Pohakuloa Gulch as Waihu drift. Otherwise, we found no sedimentary deposits beneath these two Laupahoehoe flows within the Makanaka glacial limit. No ice-contact features are evident on these flows. Upslope from the Makanaka moraine, the two flows have been deeply eroded; they are unusual in that local erosional outliers have been isolated by Makanaka glacial erosion (pl. 2).

The vent cinder cones for these flows, Puu Waiau and Puu Poliahu (fig. 19), are the most conspicuously gullied

Figure 26. Eroded surface of lava flow (flow A, pl. 2; see fig. 19) of older volcanic rocks member of the Laupahoehoe Volcanics, 200 m east of Waikahalulu Gulch at 3,100-m (10,200 ft) elevation. Torrential meltwater runoff stripped away loose aa carapace, exposing delicate ridges and spines of welded aa and depositing large rounded hawaiite-mugearite boulders directly on eroded flow surface (center, near pole). Flow surface, which extends beyond skyline at center and left, is partly mantled by ash (lower right); colluvium forms surficial deposit in foreground and in trough between lava spines (at pole) and more distant low ridge. Part of Mauna Loa's slope is visible at upper right. Pole is 1.5 m long. View east-southeastward; Hawaiian Volcano Observatory photograph 88.3.10EW135A#36.

and otherwise-eroded cones of the Laupahoehoe Volcanics. Their flanks appear to have retreated back from the proximal parts of their flows, particularly along the southeast and south flanks of Puu Waiau, where the uphill edge of the flow parallels the base of the cone but is locally separated from the cone by an alluvium-filled moat. Furthermore, a medial moraine composed of cinders extends nearly 1 km southward from the present base of Puu Waiau. This moraine apparently was formed from cinders eroded from Puu Waiau by tongues of Makanaka ice that split around the cinder cone and rejoined at its south base.

The relatively intense gullying of Puu Waiau and Puu Poliahu is at least partly related to their mineralogy. The materials of these cones are ash, lapilli, and bombs. The ash and lapilli were once glassy and commonly are highly vesicular; some fragments are palagonitic. The internal structure of the cones, as expressed by layering and the distribution of bombs, resembles that of other cinder cones. Unaltered deposits of red or black cinders are exposed in each cone, but parts of the cones have been pervasively altered. Glass and phenocrysts in a sample from Puu Poliahu are nearly completely altered to the sulfate mineral alunite, which presumably formed as hot, sulfur-bearing magmatic gas percolated upward through the cone. The glassy components of a sample from Puu Waiau are largely altered to smectite, and voids are encrusted with the zeolites phillipsite and gismondine(?). These minerals record percolation of warm water or steam through the cone during or soon after its eruption. In both cones, the alteration products weakly cemented the pyroclasts and reduced the permeability of the deposits. Because of reduced permeability, such cones are more susceptible to gullying; water runs off instead of percolating downward. The reduced permeability also apparently accounts for retention of water to form a small permanent lake (Lake Waiau) within the crater of Puu Waiau.

Similarly altered deposits occur locally in a few other Laupahoehoe cones, for example, on the north flank of Puu Hauoki and near the summit of Puu Wekiu. Such alteration, however, is unknown in most Laupahoehoe cones, including those that have been deeply quarried for cinders. One significant exception is a large Laupahoehoe cone incised by Waikahalulu Gulch west of Puu Haiwahine. There, stream erosion has exposed altered cinders much like those of Puu Waiau or Puu Poliahu, suggesting that such alteration has no necessary connection to the presence of glacial ice. Indeed, similarly altered cones occur in the San Francisco volcanic field of northern Arizona (Wolfe and others, 1987a, b), where they are far removed from glacial effects. In those cones, hydrothermally altered sectors are profoundly gullied; unaltered sectors are undissected and resemble typical, relatively smooth-surfaced Laupahoehoe cinder cones.

Puu Waiau and Puu Poliahu and their flows are pivotal to a major difference in mapping and stratigraphic interpretation between our work and the earlier work of Porter (1979a, c, 1987), who concluded that these two cones are the oldest within the Makanaka glacial limit. He interpreted the altered pyroclastic deposits as hyaloclastite tuff formed in standing water as these cones grew beneath the Waihu icecap. He assigned the cones and their flows, as he mapped them, to his Poliahuan Stage, equivalent in age to the Waihu glacial deposits and overlain to the south by lavas of his Hanaipoean Stage. His subglacial interpretation derived additional support because he mapped the scarp east and west of Puu Kookoolau as the terminus of the flow from Puu Waiau. As described above in the subsection entitled "Liloe Spring Volcanic Member," ice-contact features abound in that scarp.

The critical relations that underlie our revised interpretation are as follows: (1) The scarp exposures consist of basalt (Liloe Spring Volcanic Member of the Hamakua Volcanics); (2) the flows from Puu Waiau and Puu Poliahu consist of hawaiite-mugearite (older volcanic rocks member of the Laupahoehoe Volcanics) overlying basalt (Liloe Spring Volcanic Member) with a pervasive ice-contact fabric related to the Waihu icecap; (3) and no ice-contact fabrics are exposed in the hawaiite-mugearite flows from Puu Waiau and Puu Poliahu.

A subaerial origin for these two cones seems more probable than a subglacial one. Previously described stratigraphic relations indicate that the Puu Waiau and Puu Poliahu eruptions occurred not during a glacial episode but between the Waihu and Makanaka glacial episodes. The structure of the cones, the presence of normal red or black cinder deposits in parts of them, and the occurrence of typical blocks and spindle-shaped bombs suggests that normal, subaerial, Strombolian eruptive processes formed the cones. Beds containing some delicately vesicular, palagonitic fragments may record short-lived phreatomagmatic events during the eruptive activity.

ICE-CONTACT FEATURES

Some, at least, of the other cones and flows of the older volcanic rocks member of the Laupahoehoe Volcanics exposed within the Makanaka glacial limit erupted while the Makanaka icecap was present. Four flows, from vents at or near the summit, have distinct ice-contact margins (pl. 2); and a fifth, erupted from the south flank of Puu Wekiu, has local mosaic-jointed zones on its surface. (For a discussion of ice-contact fabrics, see the subsection above entitled "Liloe Spring Volcanic Member"; for illustrations of Laupahoehoe ice-contact fabrics, see Porter, 1987, figs. 21.11, 21.12.) The surfaces of all five of these flows were eroded by Makanaka ice that reformed over them, and all but one flow are partly buried by Makanaka till. Porter (1979a, c, 1987) recognized the same ice-contact features and assigned these flows to his Kuupahaan Stage (fig. 8), equivalent in age to his older Makanaka drift.

The ice-contact flow that originates at the base of Puu Hau Kea buried the north rim of Puu Waiau. A small lobe of this flow extended into the crater, where an isolated remnant now occurs, along with Makanaka drift, on the south side of Lake Waiau. The relative freshness of the flow surface between Puu Waiau and Puu Hau Kea suggests that thick, strongly eroding ice did not reform in the lee of Puu Hau Kea. Thus, the small, intracrater flow remnant probably was not isolated by deep glacial erosion. The flow may have extended into the crater on a bridge of glacial ice or through a narrow channel in the ice; as the ice melted, the missing flow connection collapsed into the crater, where it was buried by talus and other crater-filling sedimentary deposits.

Most of the vent deposits for these ice-contact flows are cinder cones that resemble the numerous Laupahoehoe cones which formed beyond the Makanaka glacial limit. These ice-contact cones (for example, Puu Hau Kea, fig. 19) display no special features indicative of subglacial eruption. One distinctive vent deposit, adjacent to the northeast flank of Puu Poliahu, consists of a low mound of spatter and bombs, rather than the normal steep-sided cinder cone; this vent deposit, too, shows no features that we recognize as indicative of subglacial eruption. Steep slopes may have facilitated drainage instead of ponding of meltwater around subglacial vents on Mauna Kea, or insufficient ice thickness may have prevented formation of deep englacial ponds. Thus, conditions suitable for subaqueous eruption and production of hyaloclastite cones probably were not sustained. An alternative suggestion by Porter (1987) is that some of these cones may have hidden cores of hyaloclastite which was buried by subaerially erupted pyroclasts as the cones grew.

FLOW FROM PUU POEPOE

A short flow that extends 1 km eastward from the base of Puu Poepoe apparently was erupted as the Makanaka ice

was retreating. Gregory and Wentworth (1937) and Stearns and Macdonald (1946) mapped this flow as postglacial, and Porter (1979a) interpreted it as older than his "Younger Makanaka drift." Puu Poepoe and the flow that issued from its northeast flank have been glacially eroded and are overlain by till. A later eruption constructed a small satellitic cone low on the southeast flank of Puu Poepoe and emplaced the aforementioned small flow to the east. That flow overlies Makanaka drift and has not been glacially eroded. However, the presence of a few erratic boulders resting on the flow near its edges suggests that the flow was erupted against stagnant ice as the Makanaka glacial episode was waning.

AGE

Most K-Ar ages for lava flows of the older volcanic rocks member of the Laupahoehoe Volcanics range from approximately 18 to 66 ka (fig. 10). Two K-Ar ages are older, both related to Puu Waiau. Porter (1979c) reported an age of 174±37 ka (sample QLA–10a, table 5) on a bomb collected from the rim of Puu Waiau. Our new K-Ar age for the lava flow from Puu Waiau (PW flow, pl. 2) is 107±13 ka (sample W87H6–311, table 4), which does not differ significantly from Porter's at the 95-percent-confidence level. Although these ages for Puu Waiau and its lava flow overlap many of those for basalts of the Liloe Spring Volcanic Member of the Hamakua Volcanics that are stratigraphically beneath the Waihu Glacial Member of the Hamakua Volcanics (fig. 10), the flow from Puu Waiau is stratigraphically above the Waihu Glacial Member (pl. 2). On the basis of physiographic similarity, we would expect Puu Waiau and its flow to be comparable in age to Puu Poliahu and its lava flow (PPL flow, pl. 2), which has a K-Ar age of 53±14 ka (sample W87H6–310, table 4). Furthermore, Dorn and others (1991) reported an exposure age of approximately 60 to 70 ka for the Waihu Glacial Member of the Hamakua Volcanics, which predates the lava flow from Puu Waiau.

Considered alone, the K-Ar data suggest an older age limit for the Laupahoehoe Volcanics of at least 65 ka, possibly as much as 100 ka. However, the exposure-age results indicate that 65 ka is a more likely older limit. As noted below in the subsection entitled "Makanaka Glacial Member," the Makanaka glacial episode apparently ended about 13 ka. Thus, the probable age of the older volcanic rocks member of the Laupahoehoe Volcanics is approximately 13 to 65 ka.

MAKANAKA GLACIAL MEMBER

DEFINITION AND OCCURRENCE

The Makanaka Glacial Member consists primarily of till that forms ground- and end-moraine deposits encircling the summit of Mauna Kea. Local gravel deposits interpreted as glacial outwash extend beyond the morainal limits. The Makanaka Glacial Member postdates the oldest flows of the older volcanic rocks member, is coeval with much of the older volcanic rocks member, and predates the younger volcanic rocks member of the Laupahoehoe Volcanics. Most of the Makanaka Glacial Member overlies flows and cones of the older volcanic rocks member. Locally, adjacent to or within south-flank kipukas, it rests on basalt of the Liloe Spring Volcanic Member or on the Waihu Glacial Member of the Hamakua Volcanics (pl. 2).

Wentworth and Powers (1941) named the Makanaka Drift for Puu Makanaka, against which is banked conspicuous blocky till. Porter (1979c) designated Puu Makanaka as the type locality. He identified additional reference localities along Kemole Gulch between 3,350- and 3,600-m (11,000 and 11,800 ft) elevation, along Waikahalulu Gulch at about 3,260-m (11,700 ft) elevation, on the west rim of Pohakuloa Gulch between 2,865- and 3,500-m (9,400 and 11,500 ft) elevation, and near the head of Hanaipoe Gulch.

PREVIOUS WORK

The glacial features of Mauna Kea have long attracted geologic interest. Early observations that the upper slopes of Mauna Kea had been glaciated were based on brief visits to the area. R.A. Daly was the first geologist to publish a report (Daly, 1910) that the uppermost slopes of Mauna Kea had been glaciated. W.A. Bryan of the College of Hawaii visited the summit briefly in 1916. Apparently unaware of Daly's observation, he recognized and examined the glacial features. His "discovery" was described in a Honolulu newspaper, the *Pacific Commercial Advertiser* (Bryan, 1916), and he later published a scientific notice (Bryan, 1918). T.A. Jaggar visited the upper slopes, amplified the descriptive record (Jaggar, 1925), and recognized the presence of postglacial as well as preglacial lavas. He also described the extensive alluvial deposits in the western part of Humuula Saddle and interpreted them as glacial outwash.

Gregory and Wentworth (1937) published the first comprehensive study of glacial effects on Mauna Kea, focusing on the latest (Makanaka) glacial episode. They mapped the reconstructed distribution and thickness of the ice and described many important geologic features and relations.

Wentworth and Powers (1941) documented the record of repeated, episodic glaciation of Mauna Kea. They formalized the glacial stratigraphy, applying the name "Makanaka" to the latest glacial episode and its products. They correlated the Makanaka glacial episode with the Wisconsin glaciation of North America.

Porter (1979a, c) mapped and described the Makanaka deposits in detail. He investigated the stratigraphic relations between the lavas of his Laupahoehoe Group and the glacial

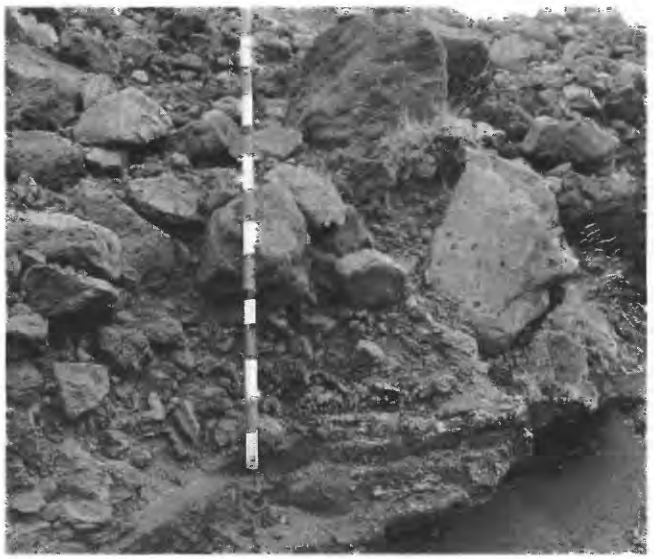

Figure 27. Detail of poorly consolidated till in lateral moraine of the Makanaka Glacial Member of the Laupahoehoe Volcanics in west wall of Waikahalulu Gulch, at 3,270-m (10,720 ft) elevation (same locality as in fig. 18). More friable eolian slope deposits underlie till at base of pole. Larger divisions on pole are 10 cm wide. Hawaiian Volcano Observatory photograph 88.3.9EW135A#19.

deposits and recognized specific lava flows that had been extruded within the Makanaka icecap. Porter identified and mapped separate older and younger drift units within his Makanaka Formation; he interpreted these units as representing two distinct glacial episodes, which he correlated (Porter, 1979d) with marine oxygen-isotope stages 2 and 4.

GEOLOGIC OBSERVATIONS

The Makanaka morainal deposits are primarily massive, poorly consolidated till (figs. 18, 27) composed of angular to subrounded cobbles and boulders, as much as 2 m or more in diameter, in an unsorted, finer grained, gray to light-yellowish-brown matrix. The cobbles and boulders are mostly dense, light- to medium-gray hawaiitic rock, although admixed basalt occurs locally. Boulders are concentrated as a lag over much the surface of the deposit; matrix exposures are rare. The surface boulders are much less weathered than those on Waihu drift. The surfaces of Makanaka boulders are mostly light gray to tan or yellowish brown and highly reflective. As seen from a distance, these boulders give the surface of Makanaka till a distinctly bright, light-gray, or pale-tan hue. Porter (1979c) reported many additional details, including the results of fabric and size analyses.

As mapped in this report (pl. 2), Makanaka till forms a thin ground moraine and, near the downslope limit of the deposit, thicker end moraines. Lateral moraines occur where ice lobes extended downslope between cinder cones or along preexisting topographic lows. The thickness of the till ranges from 0 to 30–40 m; maximum thicknesses occur in prominent lateral moraines near Pohakuloa and Hanaipoe Gulches.

The downslope map boundary of Makanaka till is distinct and agrees well with the outer boundary of Makanaka drift as mapped by Porter (1979a). The position of our inner boundary is somewhat arbitrary because of a gradation downslope from well-exposed, deeply eroded, glacially striated lava flows, through lava flows with discontinuous till, to more or less continuous till. Our inner boundary differs from that shown by Porter (1979a) because he chose to portray only the till that forms end moraines; his map shows many additional details of end-moraine crests.

Thin deposits of subrounded to rounded bouldery gravel extend locally downslope from the lower limit of the Makanaka moraine. The more extensive and continuous of these deposits are mapped as Makanaka outwash deposits. The boulders are similar in composition, degree of weathering, and color to those of the till.

A topographically distinct morainal front, within Makanaka till north of the summit, extends 3 km northeastward from Kemole Gulch (pl. 2). Two Laupahoehoe lava flows extend from beneath this inner morainal front and overlie the till downslope from it (fig. 28); thus, these flows separate older and younger tills. In addition, a prominent pair of parallel lateral moraines occurs about 0.5 km east of Hanaipoe Gulch; the inner moraine of the pair overlaps the outer one, extending farther downslope.

Porter (1979c) concluded that these two till units represented separate glacial episodes, which he referred to as the older and younger drifts of his Makanaka Formation. Distinguishing the two tills on the basis of subtle weathering and morphologic characteristics, he identified and mapped discontinuous outcrops of the older (outer) till in many localities at the perimeter of the younger till. The differences between the two Makanaka till units, however, are so subtle that we could not distinguish them except on the north flank, where they have distinct morphologic expressions and the intervening intercalation of the two lava flows is unmistakable. Therefore, we have mapped a single unit of Makanaka till everywhere except on the north flank (pl. 2).

The similarities in degree of weathering and general surface characteristics between the older and younger Makanaka tills suggest that their age difference is slight. Evidently, the Makanaka glacial episode was complex, with alternating advance and retreat of the glacier front. We cannot determine whether the Makanaka icecap actually disappeared and reformed. Evidence from the two intertill lava flows (fig. 28) neither supports nor refutes Porter's (1979c) hypothesis of an ice-free interval within the Makanaka glacial episode.

The more northwesterly intertill lava flow (flow 2, fig. 28) displays no ice-contact fabric, nor is its exposed surface

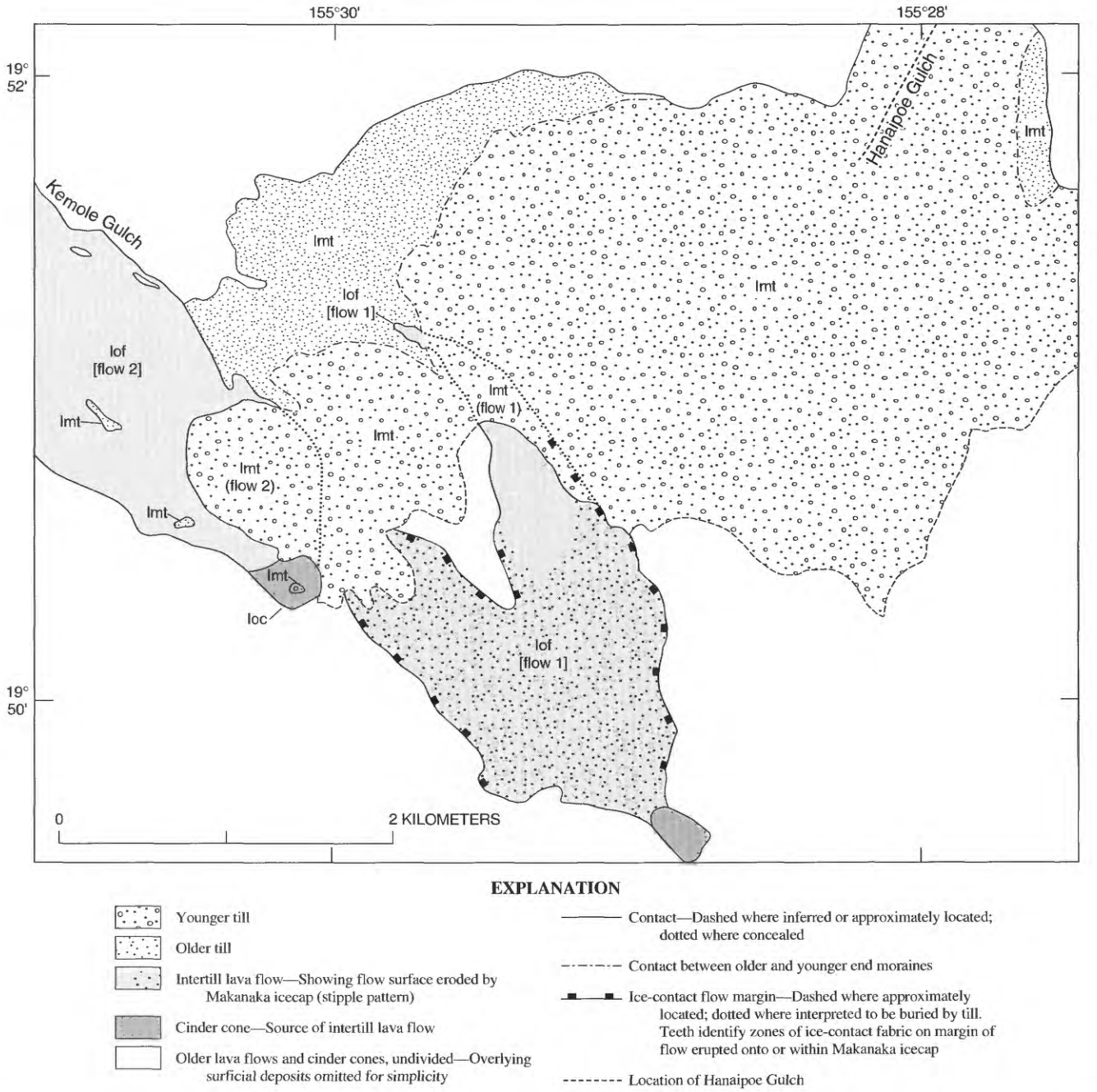

Figure 28. Geologic map of part of upper north flank of Mauna Kea, showing relations among intertill lava flows and older and younger tills of the Laupahoehoe Volcanics. Geology from plate 2; alluvial and colluvial deposits are omitted for simplicity. Bracketed numbers denote intertill lava flows discussed in text; parenthetic numbers denote intertill lava flows where buried by younger till. Units of the Laupahoehoe Volcanics: lmt, till of the Makanaka Glacial Member; loc, cinder cones of older volcanic rocks member; lof, lava flows of the older volcanic rocks member. See plate 2 for description of units.

glacially eroded. It locally buried the older till, which is exposed in small kipukas within the flow, and subsequently was partly buried by the younger till. Field evidence indicates only that after deposition of the older till, the ice retreated sufficiently for the lava flow to be emplaced beyond the ice front; thereafter, the ice readvanced to deposit the younger till.

The more southerly intertill lava flow (flow 1, fig. 28) has an ice-contact margin. Its surface has been glacially eroded except for the northern part of its more easterly lobe, including the small lava-flow tip exposed between outcrops of the older and younger tills. That flow tip is within a deep reentrant in the outer margin of the younger till. Apparently, the lava flow was erupted within glacial ice. The ice front

had retreated from the limit represented by the outer margin of the older till and, when flow 1 was erupted, was no higher than approximately 3,730-m (12,240 ft) elevation, which is the lowest elevation at which we recognize ice-contact fabric in flow 1 (see pl. 2). After the eruption of flow 1, glacier movement was reestablished over much of the surface of the new lava flow. However, the flowing ice split around the prominent eastern lobe of the lava flow, forming a reentrant in the younger moraine front.

An additional lava flow, from an unnamed cinder cone (cone A, pl. 2; see fig. 19) on the upper south flank of the volcano, is known to separate Makanaka glacial deposits. This flow (flow A, pl. 2; see fig. 19), which forms the east rim of Waikahalulu Gulch, overlies an unmapped gravel deposit that contains large hawaiite-mugearite boulders and probably represents Makanaka outwash. The flow is, in turn, locally overlain by Makanaka till and outwash (pl. 2; fig. 26). Like flow 2 on the north flank of Mauna Kea, flow A displays no ice-contact fabric, a feature suggesting that the ice front was upslope from the vent when the lava flow was emplaced.

AGE

Field relations suggest that Puu Poliahu and its lava flow (flow PPL, pl. 2), dated at 53±14 ka, predate the Makanaka Glacial Member. K-Ar ages on two different ice-contact lava flows (fig. 10) suggest that the Makanaka glacial episode was underway by about 40 ka. K-Ar ages for two lava flows, flow 1 (fig. 28) and flow A (pl. 2; see fig. 19), that are bracketed by deposits of the Makanaka Glacial Member are 33±12 and 31±9 ka, respectively.

Dorn and others (1991) reported exposure ages, based on varnish radiocarbon dating and ^{36}Cl dating, of approximately 16 to 21 ka for the younger till on the north flank of Mauna Kea and for glacially eroded lava near the summit. Varnish radiocarbon ages for the older till range from about 20 ka to greater than 37 ka.

Study of cores of the sediment that accumulated beneath the floor of Lake Waiau, in Puu Waiau, indicate that lakebeds began accumulating in the crater between 14 and 13 ka (J.W. King, oral commun., 1990); the Makanaka glacial episode must have terminated at about that time.

The Makanaka glacial episode apparently began during marine oxygen-isotope stage 3 and continued into stage 2. It coincided, at least in part, with the late Wisconsin glaciation of North America.

YOUNGER VOLCANIC ROCKS MEMBER

DEFINITION AND OCCURRENCE

The younger volcanic rocks member of the Laupahoehoe Volcanics consists of hawaiitic cinder cones and lava flows of post-Makanaka age. Interpretation of its stratigraphic position is based on various criteria, including demonstrable superposition, relative freshness of lava-flow surfaces, paucity of mantling ash or colluvium, and ^{14}C ages. The unit is exposed on the upper north and northeast flanks and on the southeast flank of Mauna Kea (fig. 22).

PREVIOUS WORK

Jaggar (1925) alluded to volcanic rocks that partly bury glacial deposits, and Gregory and Wentworth (1937) described and mapped flows east of Puu Poepoe and along Waikahalulu Gulch that they interpreted as postglacial. Wentworth and Powers (1941) also recognized these flows as post-Makanaka. Stearns and Macdonald (1946) identified several additional postglacial flows: from Puu Lehu, from Puu Kole (south flank), and from 1 km southeast of Hale Pohaku. They mapped the group of post-Makanaka flows and their vent deposits as the upper member of their Laupahoehoe Volcanic Series.

Porter (1973) recognized an additional group of post-Makanaka cones, flows, and air-fall deposits northeast of Humuula Sheep Station on the south flank of Mauna Kea. He indicated that these units overlie his Humuula soil, having buried it about 4.5 ka. Subsequently, Porter (1979a, c) assigned the post-Makanaka lavas to his Loaloan stage, named for Loaloa, a large cinder cone in the group of cones northeast of Humuula Sheep Station.

GEOLOGIC OBSERVATIONS

Lava flows of the younger volcanic rocks member are mostly rubbly to blocky aa; pahoehoe occurs locally, for example, in the proximal part of the flow from Puu Kole (south flank). The flow surfaces generally appear distinctly fresher than those of nearby flows of the older volcanic rocks member. The more distinct freshness reflects not only less weathering and erosion of surface detail but also, in most places, the absence or near-absence of mantling eolian or air-fall deposits.

Cinder cones of the younger volcanic rocks member have been less modified by erosion and mass wasting than those of the older volcanic rocks member. Although the visual differences are subtle, a morphometric reconnaissance by J.C. Dohrenwend (written commun., 1986) shows that cones of the younger volcanic rocks member have greater mean maximum slope angles (31°–34°; average of steepest 50 percent of each of four to six representative slope profiles of the unbreached periphery of the cone) than nearly all cones of the older volcanic rocks member. With rare exceptions, cones of the older volcanic rocks member with comparably steep flanks are glacially eroded cones within the Makanaka glacial limit. Furthermore, Dohrenwend found that cones of the younger volcanic rocks mem-

ber have sharply defined crests and essentially unmodified craters. In comparison, cones of the older volcanic rocks member show rounding of their crests, lower crater-wall slope angles, and crater infilling by colluvial, air-fall, or eolian deposits.

A probable stratigraphic sequence of flows of the younger volcanic rocks member on the south flank can be determined from field relations (pl. 2). The northwesternmost flow (flow B, pl. 2; see fig. 19) is tentatively considered the oldest in the sequence. This flow issued as two lobes from a small cinder cone and an adjacent mound of spatter (cones B and C, respectively, pl. 2; see fig. 19) near the east rim of Waikahalulu Gulch, at about 3,540-m (11,600 ft) elevation. Colluvium buries the proximal end of the eastern lobe, and so it cannot be traced to its source. Lava of the two lobes flowed over a thin Makanaka moraine and then spilled over the east rim of Waikahalulu Gulch. The two lobes merged within the gulch and flowed approximately 2 km along the gulch floor, which had already been incised to its present level by runoff from the melting Makanaka icecap. The occurrence on the eastern lobe of rare hawaiitic blocks that resemble those ejected from Puu Keonehehee suggests that this Waikahalulu Gulch flow predates Puu Keonehehee.

We consider Puu Keonehehee (fig. 19) to be postglacial because both the cone and its crater have been virtually unmodified by mass wasting and because the short lava flow from its west flank overlies a small, isolated outcrop of Makanaka drift. Late, explosive eruptive activity exposed the underlying lava in the crater wall; subsequently, a small hawaiitic flow filled the crater floor. These features are not mantled by younger deposits.

Stearns and Macdonald (1946) and Porter (1979a) mapped Puu Keonehehee as Pleistocene in age and a small red cinder cone (cone D, pl. 2; see fig. 19) adjacent to its northwest flank as postglacial. However, we map them in reverse sequence because Puu Keonehehee ejecta overlaps the small red cinder cone. The stratigraphic relation is ambiguous, however, between the small red cinder cone and a small black cone (cone E, pl. 2; see fig. 19) immediately to the southwest that is partly overlain by Makanaka drift. Nevertheless, we interpret the small red cone as Pleistocene because several 1-m-diameter glacial boulders rest against the northeast flank of the cone. In the present postglacial setting, no mechanism for the transport of these boulders onto the cone is apparent, although they may have been transported by colluvial processes from the nearby Makanaka glacial front across snow and ice that formerly buried the surface upslope from the cone. We note that the ice was thick enough less than 1 km upslope from cone D to deposit till on the crest of cone A (fig. 19).

The Puu Keonehehee eruption produced black air-fall tephra deposits that partly mantle the flow from Puu Keonehehee. Similar tephra is overlain by an aa flow that originated from a vent less than 1 km southeast of Puu Keonehehee, at approximately 3,400-m (11,150 ft) elevation. The relation between the younger flow and the underlying ash is well exposed in a roadcut in a switchback at approximately 2,900-m (9,500 ft) elevation. There, the hot lava flow oxidized the weathered upper surface of the underlying ash deposit. No ash overlies the aa flow surface in this area, and, in comparison with nearby flows of the older volcanic rocks member, the surface has been very little modified by erosion or mass wasting. These relations indicate that the aa flow is postglacial and younger than Puu Keonehehee.

Approximately 1 km east of Hale Pohaku, the abovementioned aa flow is overlain by two small cinder cones; 1 km southeast of Hale Pohaku, it is overlain by a thick, blocky flow of the younger volcanic rocks member that built a low lava dome at the vent but no cinder cone. This blocky flow, which originated southeast of Hale Pohaku, extended downslope at least as far as the line of cones and flows of the younger volcanic rocks member northeast of Humuula Sheep Station.

The west edge of the lava flow from Puu Kole (south flank) truncates flow structure of the flow that originated southeast of Hale Pohaku; thus, the flow from Puu Kole is younger. Distinct superposition relations indicate a decrease in the age of the flows and related cinder cones from Puu Kole through Loaloa. Except for the flow from Huikau, which differs only because its surface is mantled by scoria and bombs, the flows of the younger volcanic rocks member, from the flow from Loaloa (flow L, pl. 2) southwestward through the flow from Kalaieha, are lithologically and chemically indistinguishable. The contacts separating these flows (pl. 2) are largely based on photointerpretation of morphology, much of which is subtle; thus, significant parts of these contacts are conjectural. The distal part of the flow from Loaloa is marked by rugged relief, expressed as steep-sided knobs and longitudinal ridges. Such positive features form Puu Kahiliku and numerous other exposures of the flow from Loaloa within kipukas to the south and southeast that are surrounded by lava from Mauna Loa (pl. 2).

Flows from the Puu Kole-Kalaieha cone alignment are not only lithologically similar but also virtually identical in composition. In combination with the general alignment of the cinder cones, this similarity suggests that this group of cones and flows represents a magma batch delivered to the surface along a single intruding dike.

Relatively fresh, youthful-appearing flows issued from vents on the north and northeast flanks of Mauna Kea at Puu Kole (north flank), Puu Lehu, and Puu Kanakaleonui. ^{14}C data indicate middle Holocene ages for all three of these flows (see next subsection).

Puu Lehu overlies a lava flow with its source at a low lava dome northeast of Puu Hoaka. This flow, in turn, overlies a still-older flow that originates at Puu Hoaka. North of Kaula Gulch, the flow from Puu Hoaka has been strikingly eroded by glacial meltwater and has erratic boulders scat-

tered on its surface. Flow levees etched into sharp relief by meltwater stripping of the flow from Puu Hoaka are shown in figure 24. The flow from the low lava dome northeast of Puu Hoaka is much fresher; its surface shows no sign of glacial-meltwater scouring, and no erratics rest on it. Because it was not scoured by meltwater, we tentatively interpret it as postglacial.

AGE

Porter (1971) reported six ^{14}C ages of approximately 4,400 to 4,800 yr B.P. on charcoal collected from his Humuula soil. One age (4,400±110 yr B.P., table 6) was determined on charcoal from beneath the flow from Puu Kole (south flank); the other ages were determined on charcoal from beneath tephra layers interpreted as derived from the eruptions of Puu Kole (south flank) and Loaloa. Porter (1973) concluded that the Humuula soil was buried and wood fragments within the soil carbonized at about 4,500 yr B.P., during the eruptions that formed the line of cinder cones northeast of Humuula Sheep Station.

New ^{14}C ages (table 6) confirm Porter's (1973) estimate of a middle Holocene age for the Puu Kole (south flank)-Kalaieha group of vents and flows and extend the chronology to the northeast and north flanks of Mauna Kea. These data suggest a striking concentration of eruptive activity from about 5.6 to 4.4 ka: Lava was vented southeast of Hale Pohaku, along the group of cinder cones of the younger volcanic rocks member northeast of Humuula Sheep Station, and at Puu Kanakaloenui and Puu Lehu during that brief period. The only other dated lava flow of the younger volcanic rocks member is the flow from Puu Kole (north flank), which has a ^{14}C age of approximately 7.1 ka.

Evidence from the sediment that accumulated in Lake Waiau indicate that the Makanaka glacial episode was over by about 13 ka (see subsection above entitled "Makanaka Glacial Member"). Thus, the potential age range for the younger volcanic rocks member of the Laupahoehoe Volcanics is approximately 4 to 13 ka.

LAUPAHOEHOE AIR-FALL DEPOSITS

DEFINITION AND OCCURRENCE

Deposits of bedded, black air-fall lapilli and ash are mapped (pl. 2) where they are thick enough to form a locally continuous blanket on the underlying lava flows and cinder cones. Local sheets and dunes of reworked black ash occur within and near some of these deposits; conspicuous deposits of such reworked ash occur north and northeast of Puu Kanakaleonui and on the steep south-facing slopes northwest of Puu Haiwahine and east of Waikahalulu Gulch. The air-fall deposits are scattered over the upper flanks of the volcano. Deeply weathered ash, now represented by 3 to 10 m of clay mantling apparently older lava flows and cinder cones south and east of the Puu Oo Ranch (see subsection above entitled "Older Volcanic Rocks Member"), is not mapped with these relatively fresh deposits of ash and lapilli.

PREVIOUS WORK

Wentworth (1938) assigned all the pyroclastic deposits on Mauna Kea Volcano to his Waiau Formation. These air-fall deposits, though not specifically addressed by Wentworth, would have been included within the "central cone phase" of his Waiau Formation.

Porter (1973) interpreted the tephra stratigraphy and the sequence of eruptions that it represents on the lower south flank of Mauna Kea in an area approximately bounded by Puu Haiwahine, Puu Kole, and Humuula Sheep Station. He identified the late Pleistocene and Holocene Humuula soil, which he used as a marker in distinguishing between Pleistocene and Holocene tephra deposits.

GEOLOGIC OBSERVATIONS

Continuous deposits of air-fall tephra occur only close to the source vents. Many of the mapped deposits are adjacent to single, isolated cinder cones that mark individual source vents. In some places—for example, at Puu Lehu, Puu Kanakaleonui, and Puu Keonehehee—the air-fall tephra deposit forms a collar partly surrounding its related cinder cone (pl. 2; figs. 24, 25). At Puu Kanakaleonui, the dark-gray air-fall tephra is also distinguished and mapped where it overlies the redder scoria of the cinder cone. As at Puu Kanakaleonui, some of these tephra deposits were vented by late-stage explosive activity that enlarged the cinder-cone crater and excavated blocks from underlying, older lava flows (see subsection above entitled "Vent Deposits").

An extensive blanket of air-fall tephra, as much as 15 m thick, extends about 3 km westward and southward of Hale Pohaku (pl. 2). Locally, this deposit is intricately gullied. It is situated among a cluster of cinder cones of the older volcanic rocks member of the Laupahoehoe Volcanics. Several individual late Pleistocene eruptions probably contributed to the deposit; Porter (1973) identified the Puu Haiwahine eruption as a major source. This tephra deposit is continuous with air-fall tephra surrounding Puu Keonehehee, a cinder cone of the younger volcanic rocks member, and overlying the lava flow from Puu Keonehehee. Thus, the Holocene Puu Keonehehee eruption also contributed to the deposit.

A black air-fall tephra deposit mantles the northwest slopes of Puu Makanaka and Red Hill. Its position suggests that it may represent a late eruptive episode at Puu Makanaka. The black tephra deposit locally overlies Makanaka till and buries the upper reaches of Makanaka

outwash deposited along Kaula Gulch. Therefore, the tephra is apparently postglacial. A Makanaka moraine, however, is banked against Puu Makanaka, and the lava flow from Puu Makanaka is overlain locally by Makanaka till and outwash. Thus, the tephra deposit may reflect renewed eruption during latest Pleistocene or Holocene time from a late Pleistocene vent.

Renewed pyroclastic activity at Puu Makanaka may have been related to eruption of the lava flow of the younger volcanic rocks member 2 km north of Puu Makanaka (pl. 2). A low lava dome but no cinder cone was built at the vent for that flow. The nearly universal occurrence of prominent cinder cones at the vents for Laupahoehoe lava flows indicates that large volumes of exsolved gas and vesiculating magma normally escaped through the eruptive vent, forming a tephra-laden eruption column. Where no cinder cone formed, the exsolved gas must have found a vent separate from the one that supplied the lava flow. Thus, exsolved gas and tephra may have been erupted at Puu Makanaka while degassed lava issued quietly 2 km to the north.

Similarly, the flow of the younger volcanic rocks member that was erupted southeast of Hale Pohaku has no cinder cone at its vent. One or more cinder cones of the younger volcanic rocks member uphill (to the north) from the source of that flow may mark the vent through which magma supplying that flow degassed.

Modern analogs of lava emission from one vent with simultaneous degassing through another are found in the recent eruptive activity of Mauna Loa and Kilauea. During the 1984 Mauna Loa eruption, magmatic fume continued to be emitted profusely throughout the 3-week-long eruption from vents at 3,400-m (11,150 ft) elevation, even though after the first day all the lava was emitted from vents approximately 7 km to the northeast at 2,800-m (9,190 ft) elevation. Greenland (1987) concluded that the gases emitted at the noneruptive 3,400-m (11,150 ft)-elevation vents originated from magma in transit through the conduit system to the active vents at 2,800-m (9,190 ft) elevation. From July 1986 to February 1992, relatively degassed lava issued nearly continuously from a new lava shield, Kupaianaha, in the middle east rift zone of Kilauea (Clague and Heliker, 1992). During this period, copious magmatic gas issued through the orifice of Puu Oo[3], a spatter cone built 3 km uprift at the previously active vent for the same Kilauea eruption, which began in 1983. Although these examples differ from the Puu Makanaka occurrence on Mauna Kea in their absence of significant tephra ejection, they effectively document degassing of magma at one vent and extrusion of lava partly depleted in gas at a topographically lower vent.

[3]Two cones on the Island of Hawaii are named Puu Oo: One is on the southeast flank of Mauna Kea, about 13 km from the summit (pl.2); the other, to which we here are referring, is on the east flank of Kilauea, about 20 km from the summit caldera.

AGE

To avoid unnecessary proliferation of map units on plate 2, we have assigned all of the Laupahoehoe air-fall deposits to a single unit of Pleistocene and Holocene age. However, a mapped air-fall tephra deposit is coeval with its source vent(s). Thus, air-fall deposits specifically associated with cinder cones of the younger volcanic rocks member (for example, Puu Kanakaleonui) are of Holocene age, and those specifically associated with cinder cones of the older volcanic rocks member (for example, Puu Kookoolau) are of late Pleistocene age. As noted above, an apparent exception to this age equivalence occurs at Puu Makanaka, where the air-fall deposit postdates till that is banked against the cinder cone. Air-fall tephra near Hale Pohaku issued from vents of both late Pleistocene and Holocene age. Because we are unable to differentiate and map separately the late Pleistocene and Holocene components, we interpret this tephra deposit as Pleistocene and Holocene in age.

ALLUVIAL, COLLUVIAL, AND EOLIAN DEPOSITS

SLOPE DEPOSITS

DEFINITION AND OCCURRENCE

The slope deposits are a complexly interlayered assemblage of ash-rich sedimentary materials that include air-fall lapilli and ash, eolian sand, fluvial sand and sandy gravel, colluvial gravel, and diamict deposited as debris flows. All are weakly consolidated or unconsolidated except for the diamicts, which are locally moderately to well consolidated and form ledges. The slope deposits are distributed across much of the surface of the south-flank kipukas below approximately 3,050-m (10,000 ft) elevation. Much of the unit occurs on brushy slopes. Its mapped boundaries are largely approximate; further fieldwork would probably reveal additional scattered outcrops.

Instructive exposures occur in a small steep gully about 0.7 km northwest of Pohakuloa Gulch. Because this gully is near the aqueduct from Hopukani Springs, we refer to it as the aqueduct gulch (see fig. 20). A useful reference section for the slope deposits is in the west wall of the aqueduct gulch, at 2,720-m (8,920 ft) elevation (see subsection below entitled "Geologic Observations").

PREVIOUS WORK

Wentworth and Powers (1941) reported indurated deposits that they referred to as till at several localities on the lower slopes of the south-flank kipukas. One particular deposit, which they described and sketched as being as low as at 2,100-m (6,900 ft) elevation, is probably an indurated diamict exposed near Puu Koohi.

Stearns (1945) referred to deposits of the Waihu Fanglomerate as low as at 2,100-m (6,900 ft) elevation; pre-

sumably, these deposits were the same outcrops described by Wentworth and Powers (1941) as till. Stearns (1945) also reported "ashy hillwash deposits" characterized by "thin bedding, abundant vitric ash commonly containing cinders, poor sorting, weak consolidation, and boulders that show little diversity in rock types." Although he indicated that these deposits occur as "lenses exposed between lavas of all ages in the southwestern slope of the mountain," his description seems to apply to our slope deposits. With a few exceptions, we have not found such deposits exposed in vertical section between lavas.

Stearns and Macdonald (1946) mapped most of the surface of the south-flank kipukas as unconsolidated and consolidated alluvium and talus. This unit includes (1) their Waihu Fanglomerate, which incorporated the Waihu moraines and included indurated sedimentary deposits on the lower slopes; and (2) younger gravels, formed in part by reworking of the older deposits. The younger gravels were deposited before the present major canyons were incised and, Stearns and Macdonald (1946) believed, were largely deposited by glacial meltwater.

Porter (1979a) mapped elongate trains of Waihu outwash extending downslope from the Waihu moraines. He showed additional outcrops of Waihu outwash on the gently sloping alluviated surface from Puu Koohi to the mouth of Waikahalulu Gulch. Porter's Waihu outwash coincides in part with our slope deposits.

GEOLOGIC OBSERVATIONS

The slope deposits are well exposed across the south-flank kipukas from Waikahalulu Gulch westward to the long narrow lobe of the flow from Puu Poliahu that extends downslope to 2,680-m (8,800 ft) elevation, 0.7 to 0.8 km northwest of Pohakuloa Gulch. The following detailed observations are on these exposures.

All facies of the slope deposits are exposed along the aqueduct gulch between approximately 2,560- and 2,740-m (8,400 and 9,000 ft) elevation. Most of these facies are well exposed in a reference section (fig. 29; table 7) in the west wall of the gulch at 2,740-m (8,920 ft) elevation. There, the slope deposits consist of approximately 9 m of bedded, pebbly fluvial sand (fig. 30) and sandy gravel, plane-laminated and crosslaminated, well-sorted eolian sand (fig. 31), and sandy diamict (fig. 31). An additional facies, black air-fall lapilli and ash, occurs within the sequence elsewhere along the aqueduct gulch.

Except for the air-fall deposits, in which lapilli dominate, the matrices of all of these sedimentary facies consist chiefly of very fine to fine volcanic sand; silt- and clay-size fragments are virtually absent. Winnowed volcanic ash was apparently the major source of sediment. Pebbles and cobbles within the fluvial units and those locally incorporated into the basal parts of diamicts are fragments of aa rubble from the surfaces of nearby lava flows; these fragments represent colluvial materials reworked into the ashy fluvial deposits or thin sheets of colluvium formed between other depositional events.

The diamicts in the reference section are less than 1 m thick; however, throughout the slope deposits, they are as much as about 2 m thick. Like unit 4 in the reference section, all are massive, yellowish brown to brown, and well enough indurated to form resistant ledges; they contain subangular to rounded cobbles and boulders enclosed in a pebbly-sand matrix. Thin sections show that the matrix consists predominantly of highly angular, very fine to fine sand, with a continuum of grain sizes through granules to pebbles. The fragments are yellowish orange to black, glassy, and vesicular; like the hawaiitic lavas of the Laupahoehoe Volcanics, many of these fragments contain abundant plagioclase microlites. Some grain boundaries of sand-size fragments are vesicle-wall segments, a feature that, in addition to the angularity of these fragments, suggests that they originated as pyroclasts.

Boulders in the diamicts of the slope deposits are as large as about 1 m in diameter. Lithologically, they are similar to either lava flows or boulders in glacial drift exposed upslope. Thus, the diamicts exposed along the aqueduct gulch include abundant boulders of Liloe Spring basalt derived either from Liloe Spring basalt flows or from boulders of the Waihu Glacial Member. The diamict exposed along the lower reaches of Waikahalulu Gulch contains both basaltic and hawaiitic boulders, including boulders of the distinctive xenolith-rich flow of Puu Haiwahine (older volcanic rocks member of the Laupahoehoe Volcanics), on which the Waikahalulu Gulch diamict rests.

The larger boulders in the slope-deposit diamicts are fairly well rounded and smooth. Although spalled fragments are absent, the fresh surfaces seem to have been exposed by exfoliation, apparently before the boulders were incorporated into the diamict. Thus, because of their size, shape, and apparent exfoliation, the boulders on the surfaces of the diamicts resemble the spalled boulders on the surface of Waihu drift. Evidently, the appearance of these boulders, occurring within an indurated, massive diamict largely exposed at elevations lower than that of the Waihu moraine, was responsible for the previous reports of till, Waihu fanglomerate, or Waihu outwash on the lower slopes of the south-flank kipukas. However, as discussed below, the slope deposits, including the diamicts, are stratigraphically above the Waihu Glacial Member and in many places clearly postdate some flows of the older volcanic rocks member of the Laupahoehoe Volcanics.

The slope deposits of the reference section in the aqueduct gulch overlie a Liloe Spring basalt flow, which, in turn, overlies Waihu drift (pl. 2). Thus, these particular slope deposits postdate the Waihu and cannot be Waihu outwash. The reference section occurs within a 100-m-wide band of slope deposits that filled a topographic trough

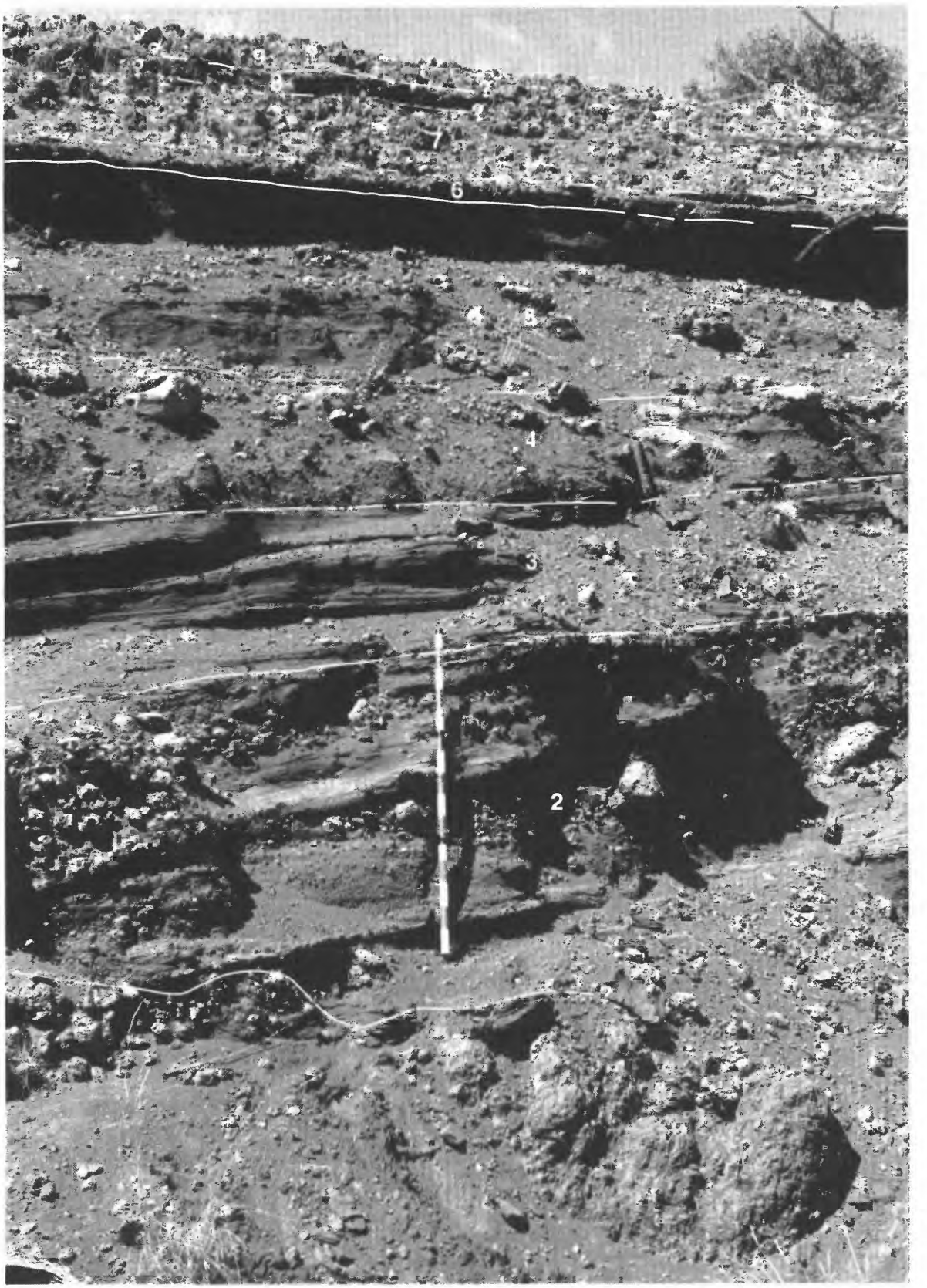

Figure 29. Reference section of slope deposits exposed in west wall of the aqueduct gulch 0.7 km northwest of Pohakuloa Gulch, at 2,720-m (8,920 ft) elevation (see figs. 1*C* and 20 for location). Numbers 1 through 9 denote units listed in table 7. Contacts dashed where approximately located, queried where not discernible through debris on outcrop surface. Pole is 1.5 m long. Hawaiian Volcano Observatory photograph 88.2.17EW135A#20.

Table 7. Reference section of slope deposits

[Section located in aqueduct gulch at 2,720-m (8,920 ft) elevation (see fig. 29)]

Unit	Description	Thickness (m)
9	Weathered bouldery rubble ----------	2.0
8	Diamict, indurated, yellowish-brown to brown, massive, consisting of unsorted, very fine sand to granules; basal part incorporates a layer of angular pebbles and cobbles derived from aa.	.4
7	Poorly exposed, brown pebbly sand, 0.5 m thick, overlying a covered interval, 0.9 m thick.	1.4
6	Diamict, thin, resistant ledge similar to unit 8; basal part incorporates angular pebbles and cobbles derived from aa (see fig. 30).	.1
5	Sand, dark-brown to brownish-gray, weakly consolidated, sorted, with scattered pebbles and layers of pebbles, bedded (see fig. 30).	2.1
4	Diamict, yellowish-brown to dark-yellowish-brown, moderately indurated, massive, containing subangular to subrounded cobbles and boulders, as large as 0.5 m in diameter, in a matrix of unsorted, very fine sand to pebbles, as large as 1 cm; boulders are concentrated in upper part of unit (see fig. 31).	.7
3	Sand, eolian, dark-gray, laminated, partly crossbedded, fine-grained, well-sorted, unconsolidated to weakly consolidated.	.8
2	Pebbly sand and sandy gravel, brown, weakly consolidated; angular pebbles and cobbles derived from aa rubble occur as layers and lenses, as much as 0.6 m thick; fragments are matrix supported, angular, 1 to 25 cm in diameter, mostly 2 to 5 cm in diameter.	1.5
1	Basalt, aa, plagioclase-phyric ----------	1.2

aligned downslope between a lobe to the west of the flow from Puu Poliahu (older volcanic rocks member of the Laupahoehoe Volcanics; flow PPL, pl. 2) and a low ridge to the east composed of Waihu drift and an overlying flow of Liloe Spring basalt.

The west edge of the aqueduct gulch group of slope deposits is exposed in a small gulch eroded along the east edge of the narrow lobe of the flow from Puu Poliahu, at 2,700-m (8,800 ft) elevation. Two sedimentary units in the west wall of this gulch separate Liloe Spring basalt from the overlying flow from Puu Poliahu (fig. 32). The sedimentary units are a lower yellowish-gray deposit, 20–50 cm thick, of angular boulders of Liloe Spring basalt in a silty to sandy matrix and an upper discontinuous deposit, as much as 40 cm thick, of crudely layered, pebbly sand and laminated, black eolian sand. The yellowish-gray rubble is a pre-Laupahoehoe colluvial deposit, possibly derived from Waihu till that was exposed upslope; the overlying sandy deposits resemble the fluvial pebbly sands and well-sorted eolian sands seen elsewhere in the slope deposits.

A few meters to the east, in the east wall of this small gulch, the Laupahoehoe flow is missing. In its place, eolian sand, fluvial pebbly sand, and diamict of the slope deposits overlie the yellowish-gray rubble and the Liloe Spring basalt flow on which the rubble rests. Boulders in diamict exposed in the east gully wall include hawaiite-mugearite derived from one or more Laupahoehoe lava flows. Because the flow from Puu Poliahu is the oldest known Laupahoehoe flow in this sector of the volcano, we infer that most of the slope-deposit sequence in the east gully wall was deposited after the Puu Poliahu lobe was in place.

At approximately 2,560-m (8,400 ft) elevation along the aqueduct gulch, slope deposits consisting of bedded and crossbedded sand and pebbly sand and a 1-m-thick diamict (fig. 33) overlie indurated gravel containing basalt boulders with light-gray surfaces. We believe that this small outcrop of indurated gravel represents Waihu outwash overlain by the slope deposits. Upgulch, at about 2,650-m (8,700 ft) elevation, approximately 10 m of slope deposits overlies similar coarse, indurated gravel capped by yellowish- to light-

Figure 30. Bedded, dark pebbly sand in unit 5 in slope deposits and 10-cm-thick diamict of unit 6, which incorporates angular fragments derived from aa rubble, exposed in west wall of the aqueduct gulch (see fig. 29; table 7). Unit 6 is overlain by covered part of unit 7. Larger divisions of pole are 10 cm wide. Hawaiian Volcano Observatory photograph 88.2.17EW135A#24.

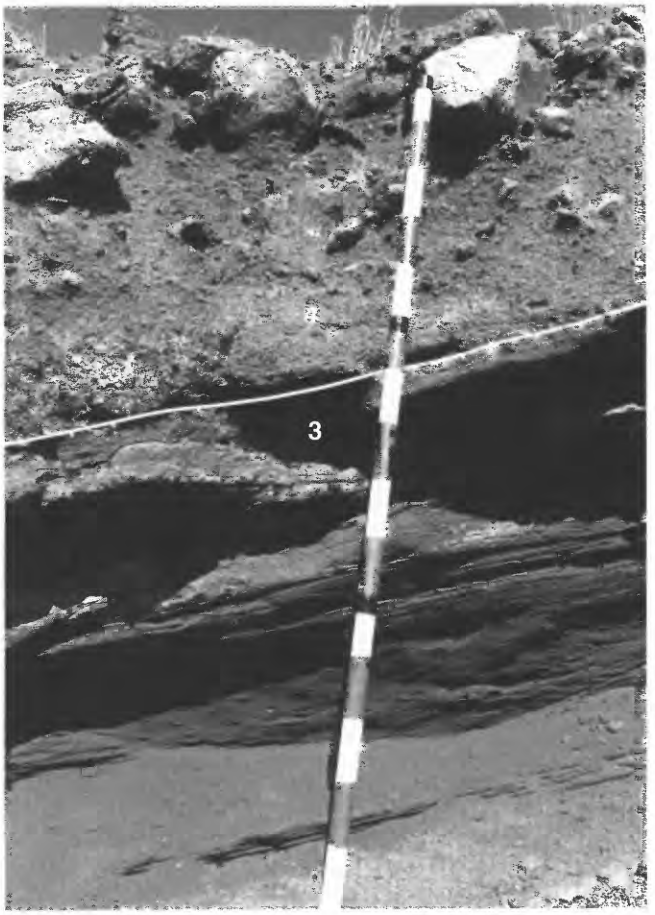

Figure 31. Diamict of unit 4 in slope deposits (see fig. 29; table 7), showing boulders in upper part of layer. Diamict overlies laminated and crosslaminated eolian sand of unit 3. Pole is 1.5 m long. Hawaiian Volcano Observatory photograph 88.2.17EW135A#22.

gray bouldery rubble (fig. 34). At the upstream end of this outcrop, a lens of Liloe Spring basalt separates the lower coarse gravel and the light-gray rubble from the overlying slope deposits. We interpret the coarse gravel and the light-gray bouldery rubble as Waihu outwash and colluvium locally separated by a Liloe Spring basalt flow from the overlying sand and diamict of the slope deposits.

Clear stratigraphic relations are exposed farther east. Near Waikahalulu Gulch, the slope deposits consist of scattered outcrops of a single diamict that formed a thin sheet extending downhill from about 2,440-m (8,000 ft) elevation onto the gentle slope below the mouth of Waikahalulu Gulch at about 2,070-m (6,800 ft) elevation (pl. 2). This diamict was lobate; it widened downslope to about 1 km. The diamict overlies the lava flow from Puu Haiwahine (older volcanic rocks member of the Laupahoehoe Volcanics; flow PH, pl. 2). Much of this diamict caps the rims of Waikahalulu Gulch; apparently, its deposition preceded incision of the gulch.

Another diamict, which impinged against the northeast flank of Puu Koohi (older volcanic rocks member of the Laupahoehoe Volcanics), overlies a small lava flow from Puu Koohi (pl. 2). This flow from Puu Koohi overlies a deposit of air-fall ash and lapilli east of Puu Koohi that was most likely derived from the Puu Koohi vent. The air-fall deposit, in turn, overlies the flow from Puu Haiwahine. The Puu Koohi diamict emerges downslope from a thick deposit of reworked lapilli and ash and scattered large lava boulders that forms the slope-deposit outcrop northeast of Puu Koohi, above 2,130-m (7,000 ft) elevation. This sedimentary deposit, apparently derived in part from the nearby Laupahoehoe air-fall deposit, extends up the steep south flank of Mauna Kea to about 2,350-m (7,700 ft) elevation and locally overlies a lobe of the lava flow from Puu Waiau (older volcanic rocks member of the Laupahoehoe Volcanics; flow PW, pl. 2). Subsequent canyon cutting has incised the deposit.

Farther west, slope deposits overlap the cinder cone (of the older volcanic rocks member of the Laupahoehoe Volcanics) immediately east of the mouth of Pohakuloa Gulch. At this locality, the slope deposits consist of a sequence of two diamicts interlayered with air-fall lapilli and ash. Like their counterparts to the east, these deposits postdate part of the older volcanic rocks member and predate the erosional event that incised Pohakuloa Gulch.

Additional ashy slope deposits occur upslope along the east rim of Pohakuloa Gulch, as high as at approximately

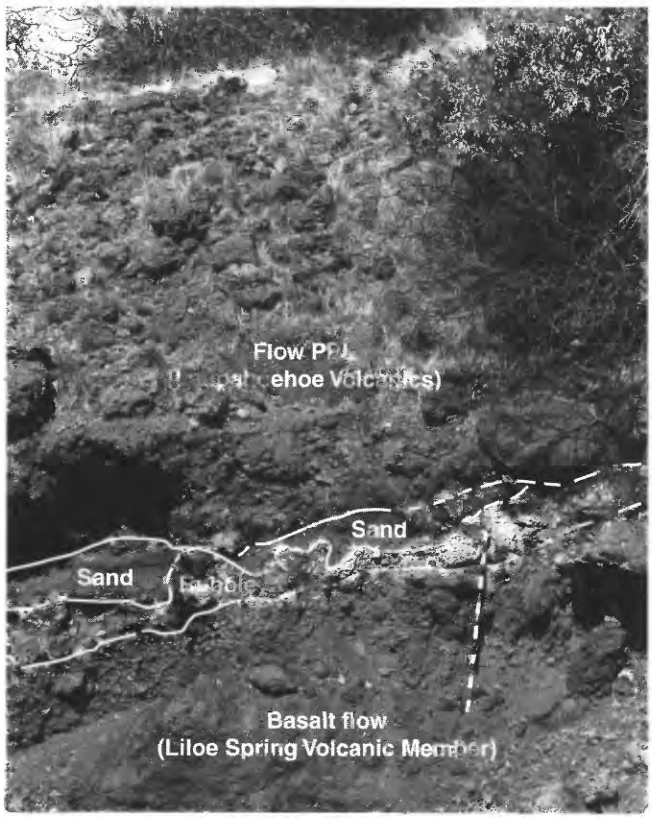

Figure 32. West wall of small gulch about 0.7 km northwest of Pohakuloa Gulch at 2,700-m (8,800 ft) elevation. Yellowish-gray rubble (at top of pole) consists of angular boulders of Liloe Spring basalt; rubble overlies plagioclase-phyric basalt flow of the Liloe Spring Volcanic Member of the Hamakua Volcanics. Discontinuous sand and pebbly-sand deposits, which resemble ashy sand beds exposed elsewhere in slope deposits, are present between rubble and overlying aphyric lava flow (PPL, pl. 2) of older volcanic rocks member of the Laupahoehoe Volcanics. Contacts dashed where approximate. Pole is 1.5 m long. Hawaiian Volcano Observatory photograph 88.2.17EW135A#3.

2,800-m (9,200 ft) elevation. At their upper limit, these slope deposits contact the bouldery Waihu Glacial Member. This contact is indistinct; apparently, colluvium from the Waihu Glacial Member supplied this part of the slope deposits. The effect, right at the contact, is that the slope deposits appear to be a downslope facies of the Waihu Glacial Member. Within a short distance downslope, however, their less consolidated, ash-rich characteristics become apparent; unlike broad, undissected surfaces of Waihu morainal deposits, broad outcrops of these slope deposits are cut by closely spaced gullies. As previously noted, stratigraphic relations downslope indicate that the slope deposits are much younger than the Waihu Glacial Member.

The westernmost slope deposits, west of the aqueduct gulch, have the same, apparently gradational relation to the Waihu outcrops immediately upslope, and the mapped contacts (pl. 2) are approximate. Broad surfaces of these westernmost slope deposits are gullied like those of their counterparts east of Pohakuloa Gulch, and these exposures indicate that the unit consists of similar, essentially unconsolidated, ash-rich sand and gravel. We have not seen a definitive stratigraphic relation between these westernmost slope deposits and lobes of the Laupahoehoe lava flow from Puu Poliahu (flow PPL, pl. 2). We surmise that, like their counterparts farther east, which flanked preexisting topographic ridges, the westernmost slope deposits may also have flanked a preexisting topographic ridge capped by the lava flow from Puu Poliahu.

The slope deposits described thus far are local surficial units that are mostly, if not entirely, stratigraphically equivalent to some part of the older volcanic rocks member of the Laupahoehoe Volcanics. Unmapped slope deposits interlayered with lava flows of the older volcanic rocks member are exposed along Waikahalulu Gulch. In a steep, gully-wall outcrop (fig. 18) at 3,270-m (10,720 ft) elevation, air-fall tephra and bedded pebbly sand overlie a post-Waihu basalt flow of the Liloe Spring Volcanic Member and are overlain by a hawaiitic lava flow of the older volcanic rocks member. Eolian sand postdates this Laupahoehoe flow, and all the rocks are overlain by Makanaka drift.

Outcrops farther downstream, below approximately 3,100-m (10,200 ft) elevation, show that an identical, most likely the same, lava flow of the older volcanic rocks member is the second flow below the east rim of Waikahalulu Gulch. Bedded ashy, pebbly sand occurs beneath this second flow, and ashy gravel containing large hawaiitic boulders separates this flow from the top flow (flow A, pl. 2). Map relations still farther downstream show that flow A predates Puu Haiwahine, which, in turn, predates the Waikahalulu Gulch and Puu Koohi diamicts. We conclude that the slope deposits accumulated over an extended time period during which recurring eruptions formed numerous flows and cinder cones of the older volcanic rocks member of the Laupahoehoe Volcanics.

AGE AND ORIGIN

We interpret the slope deposits exposed in the aqueduct gulch as younger than the Laupahoehoe lava flow from Puu Poliahu (flow PPL, pl. 2). The K-Ar age of that flow is 53±14 ka. Slope deposits occur beneath lava flows of the older volcanic rocks member of the Laupahoehoe Volcanics along Waikahalulu Gulch upslope from Puu Haiwahine; the K-Ar age of the youngest of these lava flows, flow A, which caps the east rim above Puu Haiwahine, is 31±9 ka. In addition, slope deposits overlie two additional flows, from Puu Haiwahine and Puu Koohi, that we know are younger than flow A. Thus, the slope deposits near the lower part of Waikahalulu Gulch and near Puu Koohi are younger than 31±9 ka.

Apparently, the south-flank gulches were deeply incised after at least some of the slope deposits were

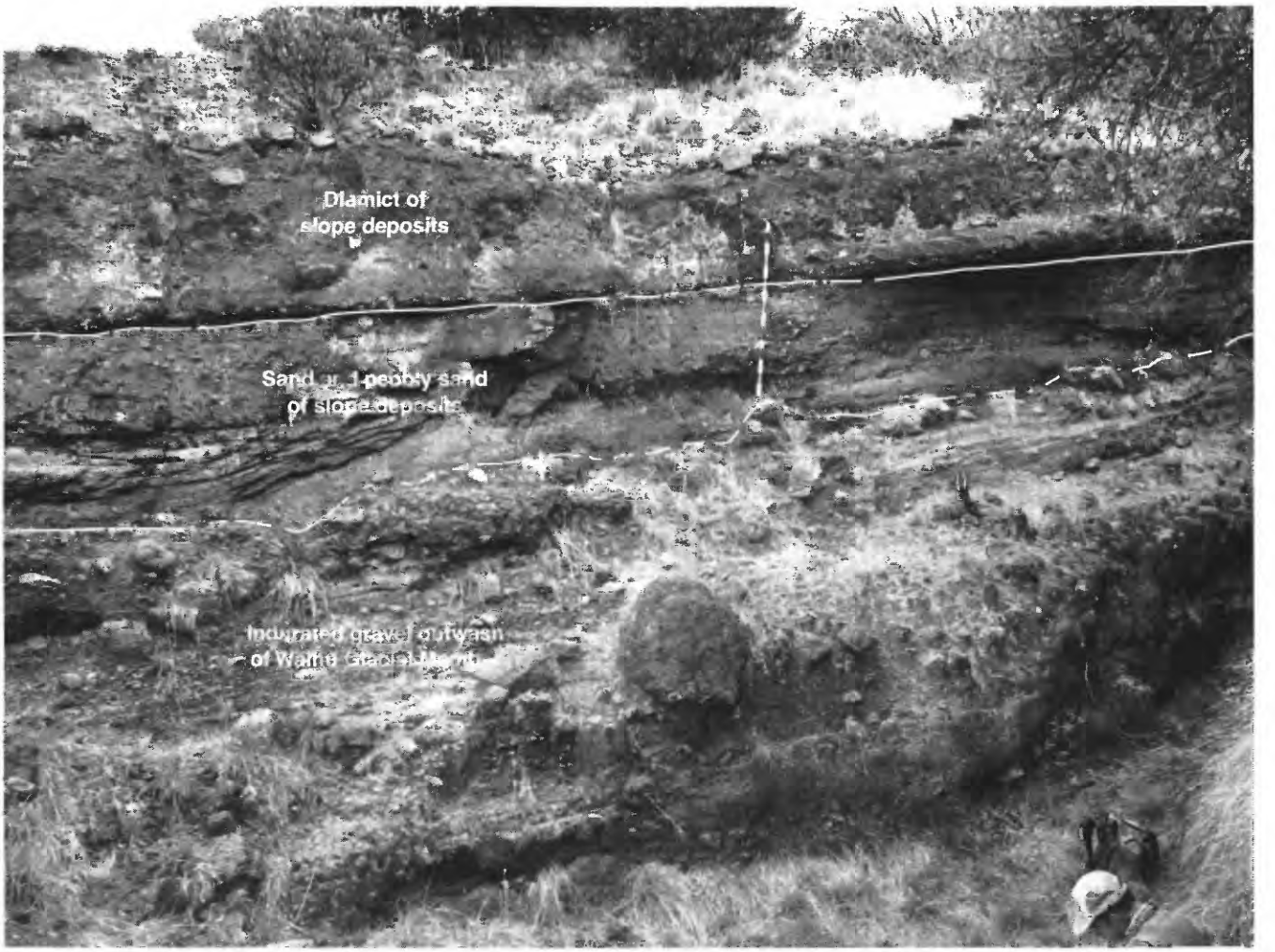

Figure 33. Slope deposits overlying indurated coarse gravel and sandy gravel, which are interpreted as outwash of the Waihu Glacial Member of the Hamakua Volcanics, in west wall of aqueduct gulch at approximately 2,560-m (8,400 ft) elevation (see figs. 1*C* and 20 for location). Slope deposits consist of about 1 m (near pole) of bedded and crossbedded sand and pebbly sand, and an overlying 1-m-thick diamict. Contacts dashed where approximate. Pole is 1.5 m long. Hawaiian Volcano Observatory photograph 88.2.18EW135A#7.

emplaced. In Waikahalulu Gulch, the occurrence as remnants on the canyon rims of slope deposits representing a single debris flow indicates that canyon cutting occurred after the approximately 31,000-yr-old lava flow A, the Puu Haiwahine lava flow (flow PH, pl. 2), and the slope deposits were in place. Along Pohakuloa Gulch, the slope deposits also form remnants capping the canyon rims. The stratigraphic evidence, therefore, is that the slope deposits are of late Pleistocene age and accumulated mostly, if not entirely, during the Makanaka glacial episode.

The occurrence of air-fall tephra interstratified with other facies of the slope deposits and the abundance of reworked ash throughout the slope deposits imply that air-fall tephra was the ultimate source of the bulk of the slope deposits. Although we have mapped a few Liloe Spring cinder cones within the south-flank kipukas (pl. 2), we found virtually no air-fall deposits in the canyon-wall exposures of Liloe Spring basalt flows. However, we know that abundant tephra was erupted during formation of the many large Laupahoehoe cinder cones. Furthermore, superposition relations show that at least some of the slope deposits formed during an interval of Laupahoehoe volcanism. On the basis of these observations, we believe that the slope deposits are equivalent in age to the older volcanic rocks member of the Laupahoehoe Volcanics. The ash that dominates these deposits was reworked from air-fall tephra derived from eruptions that formed the numerous nearby cinder cones of the older volcanic rocks member.

Thick deposits of tephra reworked by wind have accumulated locally on and beyond the air-fall lapilli and ash sheets. Such ash deposits fill gullies and bury much of the lava-flow surface on the steep slope east of Waikahalulu

Figure 34. Outwash of the Waihu Glacial Member of the Hamakua Volcanics, overlain, in turn, by bouldery rubble and overlying slope deposits, exposed in west wall of aqueduct gulch at approximately 2,650-m (8,700 ft) elevation (see figs. 1*C* and 20 for location). Slope deposits are approximately 10 m thick and consist of fluvial pebbly sand, laminated eolian sand, and diamict. Waihu outwash consists of coarse, indurated basaltic gravel that is capped by conspicuous light-gray layer of bouldery rubble. At far right, basalt flow of the Liloe Spring Member of the Hamakua Volcanics separates slope deposits from Waihu outwash and light-gray rubble. Slope deposits dip southwest (to left), downhill and away from gulch. Thick air-fall deposits occur within these slope deposits just downstream (to left) from this exposure. Contacts dashed where approximately located. Pole (circled) is 1.5 m long. Hawaiian Volcano Observatory photographs 88.2.18EW135A3 through 88.2.18EW135A5.

Gulch and northwest of Puu Haiwahine. They are obvious analogs of the eolian facies of the slope deposits, as well as of the source of the ashy sand that dominates all facies of the slope deposits.

The pebbly sands record reworking of the windblown ash and of pebbles and cobbles from the rubbly surfaces of nearby aa flows. These sands are apparently products of fluvial processes on broad slope surfaces. We are unaware of significant redistribution of ash by such fluvial processes at present on the slopes of Mauna Kea. Thus, the fluvial slope deposits may have accumulated during periods of heavier rainfall or vigorous snowmelt—probably under periglacial conditions in either case.

The massiveness and widely varying grain size of the diamicts (very fine sand to boulders) indicate that they were deposited by debris flows. The debris flows were sufficiently competent to entrain the abundant large boulders that are enclosed in the sandy matrices of the diamicts. The map pattern of the Waikahalulu Gulch diamict suggests that it was emplaced as a broad, but thin, sandy slurry that spread downslope and laterally, seeking topographic lows in the surface of the lava flow from Puu Haiwahine (flow PH, pl. 2).

Because of the evidence that eruptions occurred within the Makanaka icecap, we were intrigued by the possibility that these debris flows were generated by eruptions within the ice. However, the abundance of ash, the scarcity of silt- and clay-size components, and our inability to trace any debris-flow deposit upslope to a source lava flow or even to the Makanaka moraine all militate against an origin by eruption within the icecap. More likely, thick, rapidly formed, wind-winnowed ash deposits blocked drainageways at times. Saturation of such an ash accumulation by heavy rainfall, by water from snowmelt, or by meltwater discharged from the icecap would have led to gravitational instability, which was relieved by failure of the saturated ash and generation of a debris flow. Because the debris flows formed only during late Pleistocene time, they were probably a consequence of periglacial climate, in combination with voluminous Laupahoehoe ash production.

EOLIAN DEPOSITS

Sand-dune deposits blanket part of the lower west flank of Mauna Kea. They overlie lavas of both the Hamakua and Laupahoehoe Volcanics and are locally overlain by Laupahoehoe lavas. Local outcrops near the east limit of these dunes are shown near the west boundary of plate 2. Porter (1975) noted that the dune crests strike east-west and the beds dip north or northwest. He concluded that these dunes, as well as loess deposits mantling the lower northwest flank, originated from deflation during Pleistocene time of alluvial deposits, now buried by younger lava flows, along the southwest base of Mauna Kea. Charcoal from beneath cinder layers interleaved with the dune sand gives ^{14}C ages ranging from approximately 30 to 37 ka (Porter, 1975, 1979c).

The dunes are formed of unconsolidated, bedded, very fine to fine, angular to subangular sand. The grains are of black to yellowish-orange, glassy, vesicular ash. Because black grains dominate, overall the sand is dark gray. The yellowish-orange grains, however, which commonly are extremely vesicular, give the deposit a salt-and-pepper aspect at hand-specimen scale. North-dipping foreset beds of these sand-dune deposits are well exposed in a roadcut approximately 3 km south of Waikii.

The major body of dune-sand deposits is bounded on the south by the Laupahoehoe lava flow of Puu Keekee (fig. 22). K-Ar ages on that flow are 50±14 and 60±20 ka. Thus, there is no alluvial source immediately south of the dune sands, nor has there been one for at least the past 50,000 yr. An alternative to Porter's (1975) suggested origin for these sands—deflation of alluvial deposits—seems more plausible: The dune sands are deposits of reworked ash derived from tephra related to Laupahoehoe eruptions along the lower southwest flank of Mauna Kea. Such cinder cones as Ahumoa or Puu Keekee are possible sources. The delicate glassy fragments are pyroclasts, unlike the diverse lithic and mineral fragments that compose the very fine to fine sand component of alluvium from Pohakuloa Gulch. The angularity and delicacy of the sand-dune pyroclasts imply that they have undergone only minimal transport since their initial deposition from an eruption-related ash cloud. Good analogs for these western dune deposits are the ash dunes near the north edge of the Puu Kanakaleonui tephra blanket or near the west edge of the complex tephra deposit between Hale Pohaku and Waikahalulu Gulch.

LOESS

Loess, consisting of soft, yellowish-orange, massive, flourlike silt, mantles much of the lower southwest, west, and northwest flanks of Mauna Kea. Although the deposit is widespread and as much as about 2 m thick, we have not mapped it separately on plates 1 and 2. A good exposure occurs in a roadcut approximately 3 km south of Waikii. There, 0.5 to 2 m of loess overlies the ash-dune deposits described above. The loess in this outcrop contains thin interbeds of ashy eolian sand and air-fall lapilli and ash. This loess is composed of yellowish-brown particles that are isotropic to slightly birefringent and, as shown by X-ray diffraction, amorphous. There is no X-ray evidence of the presence of clay minerals. We interpret this material to be largely hydrated volcanic glass, probably derived from hawaiitic ash.

The occurrence of loess mantling cinder cones and flows of the older volcanic rocks member of the Laupahoehoe Volcanics, as well as ash dunes apparently derived from

tephra of the older volcanic rocks member, implies that at least some of the loess could be as young as latest Pleistocene or Holocene. It could have been winnowed directly from ash-rich eruptive columns during Laupahoehoe eruptions or stripped by wind from the surfaces of Laupahoehoe air-fall deposits. Transport by wind is easy for us to imagine; we have witnessed dense clouds of yellowish-orange silt transported many kilometers by wind blowing across the western part of Humuula Saddle, where human activities have disturbed the vegetation and the ground surface.

ALLUVIUM AND COLLUVIUM

Unconsolidated alluvium and colluvium are mapped on plates 1 and 2 only where the deposits are areally extensive or where they conceal map units or contact relations that we would otherwise map. In other words, we have ignored small outcrops of alluvium or colluvium wherever possible.

Jaggar (1925) recognized that the broad alluvial deposits at the south base of Mauna Kea were largely deposited by glacial meltwater. Porter (1979a) mapped the alluvial-fan surfaces near the mouths of Waikahalulu and Pohakuloa Gulches and near the gulch mouth 0.7 km northwest of Puu Pohakuloa as coalesced deposits of Makanaka outwash.

We agree that the bouldery sand and gravel of these fan deposits were largely deposited as meltwater from the Makanaka icecap incised the deep gulches. An exposure age of 12 to 13 ka (Dorn and others, 1991) for boulders on the alluvial-fan surface just below the mouth of Pohakuloa Gulch (approx 1 km northeast of Mauna Kea State Park) supports this view. However, we cannot confidently distinguish the margins of the youngest fan and channel deposits, which are graded to the floors of the deep gulches and have been recently active. The topographically recognizable fan deposits grade westward into a nearly flat alluvial plain. The alluvial-fan deposits, as well as the deposits of this flat alluvial plain, overlap the relatively young flow PTA (older volcanic rocks member of the Laupahoehoe Volcanics, pl. 2). Thus, the surfaces of these alluvial deposits are of latest Pleistocene or Holocene age.

Kemole Gulch is the only one of the several gulches that fed meltwater off the north side of Mauna Kea to contain extensive alluvial deposits (pl. 1). This alluvium, formed during late Pleistocene time, has since been incised down to the preexisting bedrock surface. Meltwater draining down Hanaipoe Gulch apparently emptied directly into the ocean, leaving only minor deposits along its streamcourse.

Less extensive deposits of alluvium or colluvium have been mapped at numerous localities (pl. 2), mostly on the upper slopes. In particular, trains of scoria fragments burying adjacent flow surfaces extend downslope from some cinder cones. Stone stripes and solifluction lobes abound on the upper slopes, attesting to the vigor of frost-related processes in redistributing the surface debris.

PETROLOGY

INTRODUCTION

CHARACTERISTICS OF POSTSHIELD LAVAS

Even though the first petrologists to visit Mauna Kea (Daly, 1911; Washington, 1923) recognized that the capping lavas are distinctly "andesitic," not until most of the Hawaiian Islands had been mapped at least on a broad scale was it realized that each volcano has evolved through approximately the same stages (Stearns, 1946). From many new analyses of lavas from the major volcanoes, Macdonald and Katsura (1962, 1964) were able to recognize two different types of Hawaiian volcanoes on the basis of the characteristics of the postshield stage: the Haleakala and Kohala types. Wright and Clague (1989), with further study, increased the number of types to four:

(1) Haleakala type—characterized by a thick, transitional zone of interbedded tholeiitic basalt, transitional basalt, and ankaramite. These are overlain by hawaiite and mugearite. Most analyzed "alkalic basalt" in this type is close to saturation and may be either slightly hypersthene- or slightly nepheline-normative. Other volcanoes of this type are Mauna Kea (Macdonald and Katsura, 1964) and East Molokai (Beeson, 1976).

(2) Kohala type—mafic alkalic rocks are subordinate. The dominant rock types are hawaiite and mugearite, which form a thin cap of lava that was erupted from vents scattered on the tholeiitic shield. Trachyte may be present, although in Kohala itself, the most differentiated rocks are benmoreite. As in the first type, "alkalic basalt" in these alkalic series is close to saturation. Other examples, are Waianae and West Maui (Macdonald and Katsura, 1964).

(3) Hualalai type—characterized by a bimodal suite of alkalic basalt and trachyte (Macdonald, 1968; Clague and others, 1980). There are no other representatives this type.

(4) Koolau type—alkalic postshield series is either absent or occurs only as a few flows at the top of the tholeiitic sequence. Other examples are Lanai (Bonhommet and others, 1977), Niihau, Kahoolawe, Kauai (Macdonald and others, 1983), and West Molokai (D.A. Clague, unpub. data).

In our investigation of the geology and petrology of Mauna Kea, we have defined the transitional zone of basaltic lavas of Wright and Clague (1989) as the basaltic substage and have found that these lavas consist of rare tholeiite, abundant transitional basalt, and some alkali basalt. These rocks include many lavas that have evolved from the latter two types either by crystal accumulation or by crystal removal. Overlying these basalts are hawaiite, mugearite, and benmoreite lavas of the Laupahoehoe Volcanics, which we refer to the hawaiitic substage.

DEVELOPMENT OF PETROGENETIC CONCEPTS

The recognition that the Hawaiian volcanoes were built largely from primary tholeiitic magma and capped

with alkalic basalt (Tilley, 1950; Powers, 1955) was a major turning point in basalt petrology. Previously, tholeiites were thought to have originated from alkalic basalts through crustal contamination (Kennedy, 1933). This reversal drew much attention to the origin of the alkalic basalts, and early attempts to relate the two types through crystal fractionation were unsuccessful.

Because each of the Hawaiian volcanoes evolved through the same sequence of basalt types, petrologists sought a parent common to both series. For example, Macdonald (1968) found olivine-control lines for each series converging with high MgO contents, and he hypothesized that such picrites might be the common parent.

Recent geochemical studies of the tholeiitic and alkalic lavas of Kohala (Feigenson and others, 1983; Lanphere and Frey, 1987; Hofmann and others, 1987), Kauai (Feigenson, 1984), and Haleakala (Chen and Frey, 1985) have resulted in the consideration of partial-melting models. Isotopic compositions, trace- and major-element data, and inversion techniques relate the magma type to the degree of partial melting in the mantle source (Frey and others, 1991). Wise (1982) suggested that the shield-building stage, with its high rate of magma production, resulted from high degrees of partial melting. As the production rate diminished by an order of magnitude, the degree of partial melting also decreased, and the magma type changed toward alkalic compositions of the postshield stage.

ISOTOPIC COMPOSITIONS

Frey and others (1990) analyzed a range of basalts and hawaiites for Nd-, Sr-, and Pb-isotopic compositions; their results are summarized in figure 35. These plots show that in terms of $^{143}Nd/^{144}Nd$ versus $^{87}Sr/^{86}Sr$ ratios (fig. 35*A*), there is no isotopic distinction among Hamakua lavas or between Hamakua and Laupahoehoe lavas. However, Laupahoehoe lavas and several Hamakua lavas have slightly lower $^{206}Pb/^{204}Pb$ ratios (fig. 35*B*) than Hamakua basalts generally (Frey and others, 1990). These isotopic compositions are similar to those of the postshield Kula Volcanic Series of Stearns and Macdonald (1942) of Haleakala (fig. 35*A*; Chen and Frey, 1985). Variations in Sr- and Nd-isotopic ratios from the shield stage through the postshield and rejuvenated stages of Haleakala are evidence for differing amounts of at least two source components in each stage (Chen and Frey, 1985). Within any single stage, however, the spread of isotopic ratios is almost within experimental error and is similar to the field of points for the Mauna Kea postshield stage.

Frey and others (1990) interpreted the isotopic ratios in Mauna Kea lavas as indicating that the source region was largely homogeneous with respect to Sr, Nd, and Pb. Possible contamination of some magmas with other source material may account for the slight differences in Pb-isotopic compositions.

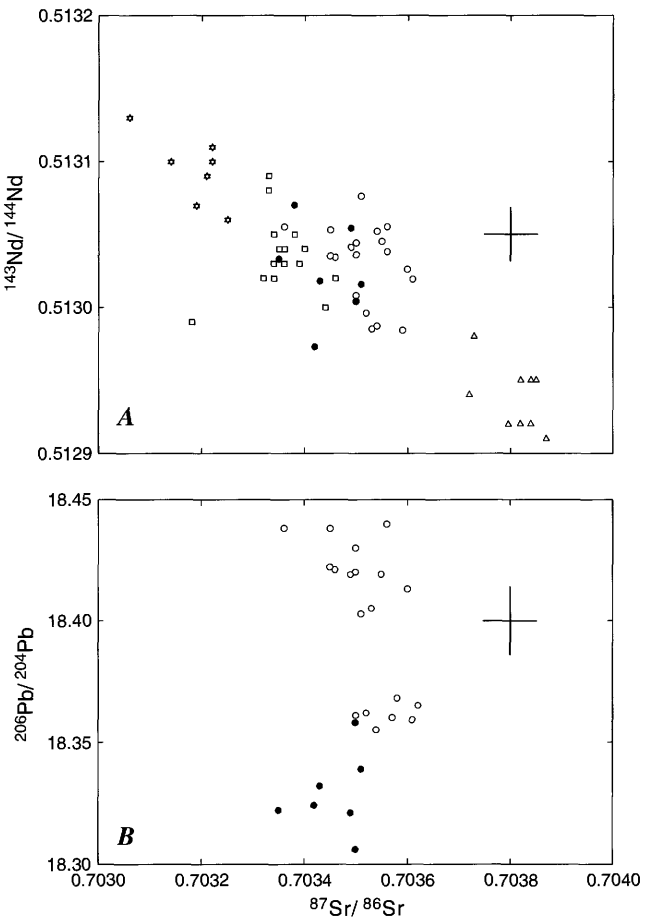

Figure 35. Isotopic compositions of Mauna Kea postshield lavas (Frey and others, 1990). *A*, $^{143}Nd/^{144}Nd$ versus $^{87}Sr/^{86}Sr$ ratios in Mauna Kea lavas in comparison with Haleakala lavas (Chen and Frey, 1985). *B*, $^{206}Pb/^{204}Pb$ versus $^{87}Sr/^{86}Sr$ ratios in Mauna Kea lavas. Circles, Hamakua Volcanics; dots, Laupahoehoe Volcanics; triangles, Haleakala shield stage; squares, Haleakala postshield stage; stars, Haleakala rejuvenated stage. Horizontal and vertical bars, 2σ error limits.

SCOPE OF THIS PETROLOGIC STUDY

The following sections contain descriptions of critical petrographic features and the chemical compositions of groups of Hamakua and Laupahoehoe lavas. Our goal is to assess the evolution of postshield magmas. We describe and interpret the wide compositional variation within the basaltic lavas and the origin of and compositional variation within the hawaiitic lavas. Because the geochemistry, including trace-element and isotopic compositions, was fully discussed by Frey and others (1990, 1991), we do not attempt here to repeat that approach to the study of Mauna

Kea lavas. Our investigation is based on extensive field observations and a large data set of major-element chemical analyses of samples from mapped lava flows and measured stratigraphic sections (table 1).

HAMAKUA VOLCANICS

COMPOSITIONAL GROUPS

Hamakua lavas consist almost entirely of alkali basalt (ne normative) and transitional basalt (ol and hy normative) that occupies the compositional space between tholeiitic and alkali basalt in a plot of alkalis versus SiO_2 contents (fig. 36*A*). Figure 36 also shows evolved alkali and transitional basalt (containing less than 7.2 weight percent MgO), as well as ankaramite and picrite, which we identify on lithologic grounds (table 2).

The Hamakua sample suite includes two samples (La–3, La–11, table 1) of tholeiitic basalt from Laupahoehoe Gulch (fig. 13) that represent the only two tholeiitic basalt flows known from the subaerial part of Mauna Kea. Except for an unusual plagioclase basalt (sample IP–2, table 1) and one basalt (sample Wa–11, table 1) from the Hopukani Springs Volcanic Member that contains a trace of normative quartz, the two Laupahoehoe Gulch tholeiites are the only q-normative basalts in the sample set.

The distinction between olivine-rich tholeiites, which have low SiO_2 contents, and alkali-poor Hamakua basalts is unclear in the plot of alkalis versus SiO_2 contents (fig. 36*A*). The problem is easily resolved, however, in a plot of CaO versus SiO_2 contents (fig. 36*B*), where olivine-rich tholeiites define a field, with less CaO at any SiO_2 content, that excludes most transitional or alkali basalts. The few evolved Hamakua basalts that plot within this field have high Na_2O+K_2O contents that clearly distinguish them from tholeiitic basalts in the plot of alkalis versus SiO_2 contents.

ALTERATION OF BASALTS

Feigenson and others (1983), Chen and Frey (1985), and Frey and others (1990) noted that samples of some of the lavas of Haleakala, Kohala, and Mauna Kea have lost K and Rb, probably through reaction of ground water with the glassy parts of the rocks. The apparent depletion of K is evident when K_2O content is compared with P_2O_5 content. Both K and P exhibit incompatible behavior over the full range of basaltic compositions and so might be expected to occur in an approximately constant ratio. The K_2O/P_2O_5 ratio for most samples of Hamakua flows from the north and northwest slopes (the dry side), where rainfall is about 10 percent of that on the windward slopes, ranges from 1.75 to 2.25 (fig. 37*A*). For all of the remaining Hamakua samples, collected over an area receiving a widely varying rainfall, the K_2O/P_2O_5 ratio ranges from 0.5 to 2.2. For many of these samples, this ratio is appreciably less than the minimum for the dry-side samples, suggesting that many Hamakua basalts have lost part of their original K_2O through posteruptive leaching (Frey and others, 1990).

Although preferential leaching of K_2O is evidently reflected in the wide variation in K_2O/P_2O_5 ratios, weathering is apparently not the sole cause of this variation; thus, the assumption of a limited initial K_2O/P_2O_5 ratio of about 2 may be an oversimplification. Comparison of figures 36*A* and 37*B* shows that low (less than 1.75) K_2O/P_2O_5 ratios occur among Hamakua flows only in transitional and evolved transitional basalts, ankaramites, and picrites; alkali basalts and evolved alkali basalts are unaffected, an unlikely consequence of weathering alone. Furthermore, K_2O/P_2O_5 ratios for the three samples dredged from Hilo Ridge, which have been uniformly exposed to seawater but never exposed to subaerial weathering, range from 1.63 (sample Er–20) to 2.70 (sample Er–22). Because no basalt exposed on the dry side has a low K_2O/P_2O_5 ratio, we conclude that K_2O has probably been leached in areas of high rainfall, although we have no certain means for distinguishing between K_2O leaching and initially low K_2O/P_2O_5 ratios.

MINERAL COMPOSITIONS

Most Mauna Kea lavas contain only three crystalline silicate phases—olivine, augite, and plagioclase—in association with magnetite and, less commonly, ilmenite. Mineral compositions were determined by electron-microprobe analysis, using the ARL–EMX microanalyzer at the University of California, Santa Barbara. This microprobe is equipped with both wavelength- and energy-dispersive detectors; the beam is typically 15 kV, with a sample current of 10 nA, and the spot size is 5 to 10 μm. Reference materials are analyzed silicates, such as albite, anorthite, microcline, augite, hypersthene, olivine, and rhodonite, and the oxides hematite, rutile, spinel, and chromite. Output from the two detector systems is combined and corrected for interelement effects.

Typical analyses of phenocryst and groundmass crystals from various rock types are listed in table 8. Although limited variation in mineral compositions occurs between rock types, several generalities are worth noting. The maximum Fo content of olivine is near 87 percent, and this value occurs in phenocryst cores of several different basalt types. All clinopyroxenes are augitic, with high Ca contents and low Ti, Al, and Na contents. As is typical of Hawaiian clinopyroxenes, these augites contain iron in both oxidation states (avg Fe_2O_3/FeO ratio, 0.12; Basaltic Volcanism Study Project, 1981, p. 345). The compositional variation of augites through even the most evolved basalts is slight.

Compositions of plagioclase phenocryst cores generally vary only slightly throughout a thin section. However, compositions in some basalts range from An_{75} to An_{85}, suggesting two periods of crystallization or mixing of

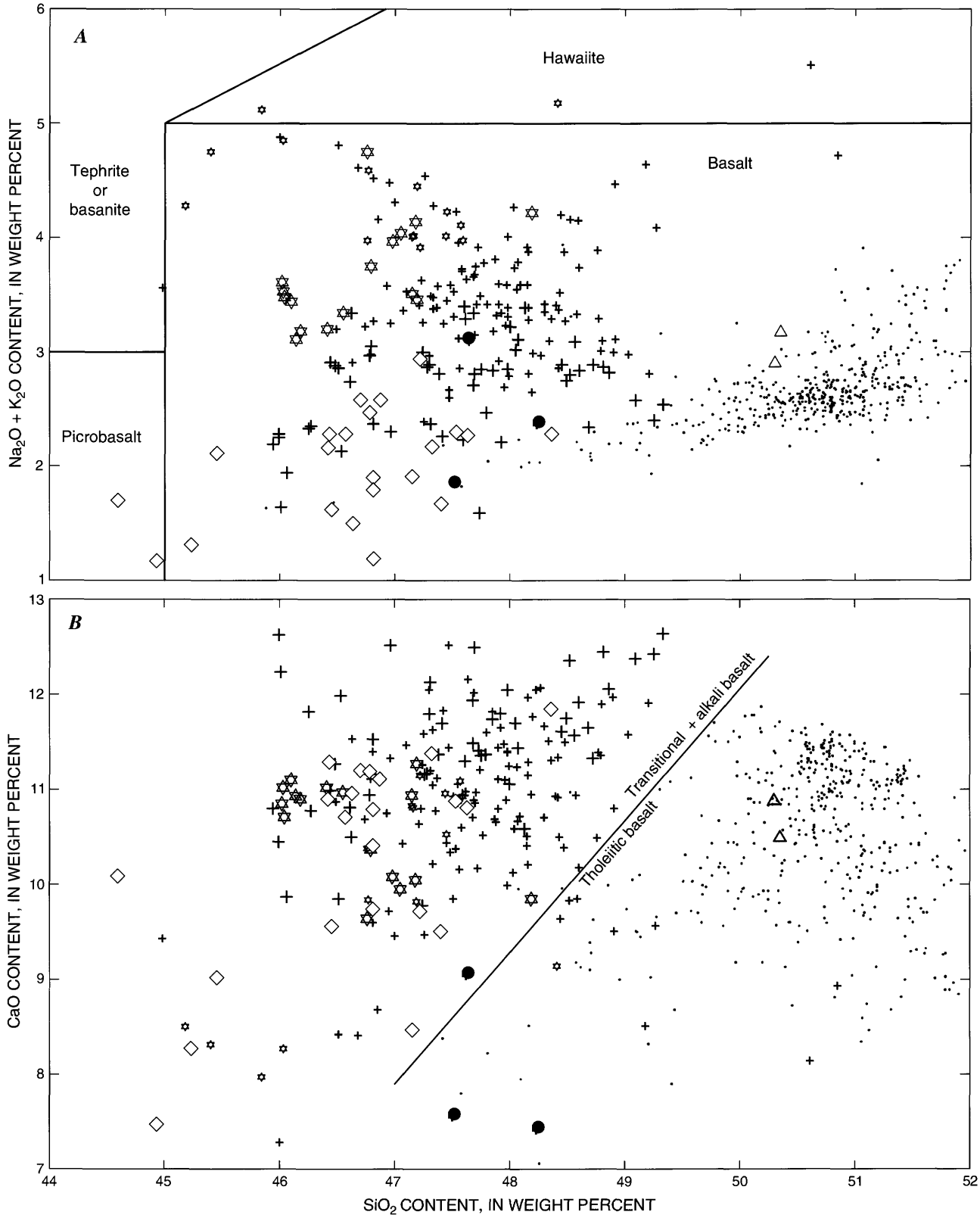

Figure 36. SiO_2-variation diagrams for lavas of the Hamakua Volcanics and Hilo Ridge in comparison with Kilauea lavas. *A*, Na_2O+K_2O versus SiO_2 contents, showing compositional fields of Le Bas and others (1986). *B*, CaO versus SiO_2 contents, showing approximate boundary between fields of tholeiitic basalt and transitional and alkali basalt. Lavas of the Hamakua Volcanics: large stars, alkali basalt; small stars, evolved alkali basalt; large crosses, transitional basalt; small crosses, evolved transitional basalt; triangles, tholeiitic basalt; diamonds, ankaramite and picrite. Other lavas: large dots, picrite and basalt dredged from Hilo Ridge (samples Er–20, Er–21, Er–22, table 1); small dots, basalt from Kilauea (from Wolfe and Morris, 1996).

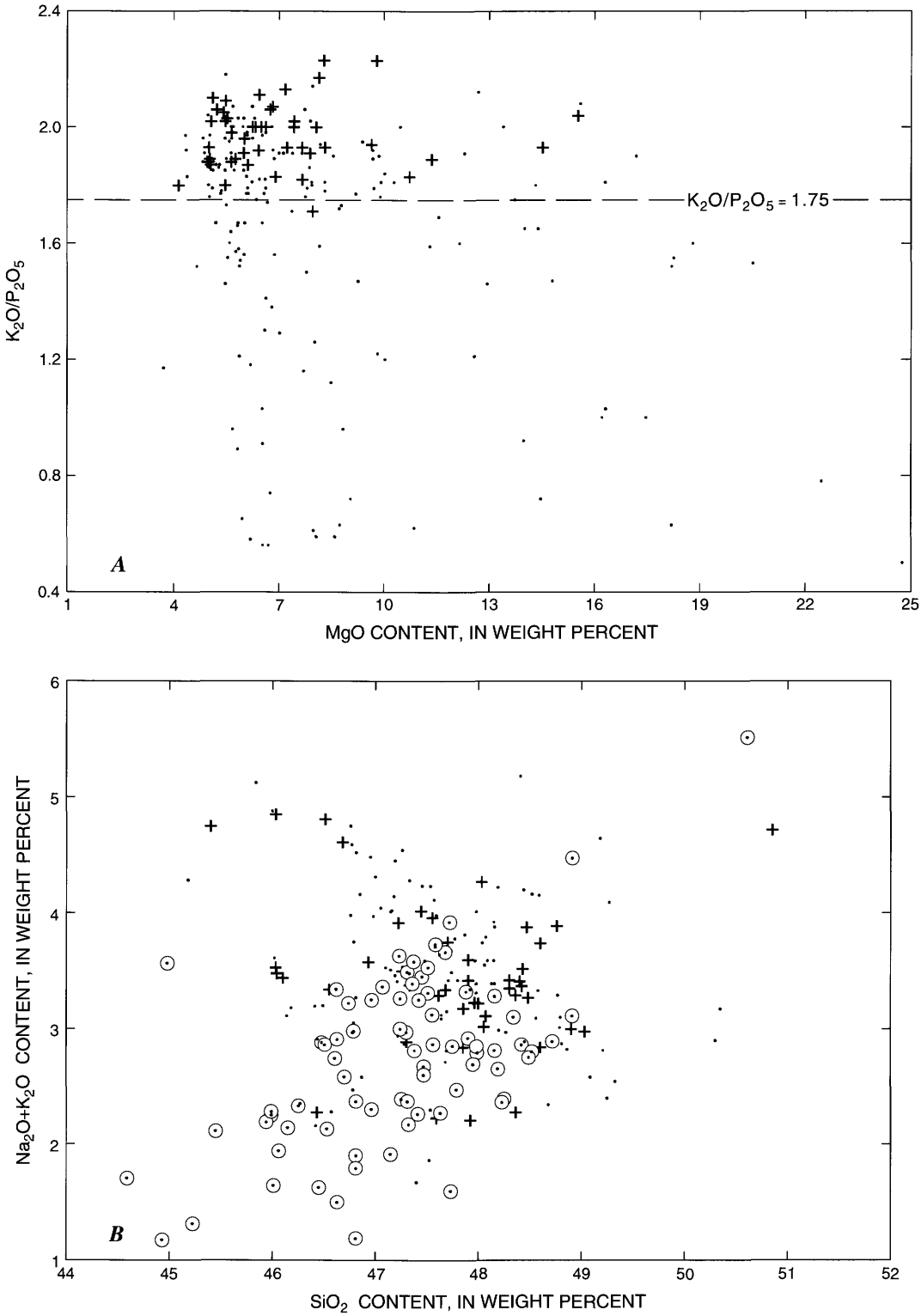

Figure 37. Variation diagrams for lavas of the Hamakua Volcanics and Hilo Ridge. *A*, K_2O/P_2O_5 ratio versus MgO contents. *B*, Na_2O+K_2O versus SiO_2 contents. Plotted lava compositions: crosses, samples of the Hamakua Volcanics from dry (west) side of Mauna Kea (Kamuela, Kawaihae, Keamuku, Nohonaohae, and Puu Hinai quadrangles; see fig. 2); dots, samples of the Hamakua Volcanics from elsewhere on Mauna Kea and samples from Hilo Ridge; circles, samples for which K_2O/P_2O_5 ratio is <1.75.

Table 8. Representative electron-microprobe analyses of minerals in basalts of the Hamakua Volcanics

[All values in weight percent. ctl, crystal; grd, groundmass; mph, microphenocryst; phn, phenocryst. Fe_2O_3/FeO ratio calculated by charge balance in formula unit]

Plagioclase:

Host	Olivine basalt	High-Ti basalt	Ankara-mite	Olivine basalt		Olivine basalt	Picrite	Xeno-lith
Occur-rence.	phn	grd	phn	mph	grd	phn	mph	ctl
SiO_2	48.21	52.90	47.82	49.01	50.96	47.61	50.61	52.77
Al_2O_3	32.97	29.55	33.03	32.40	31.49	33.80	31.26	29.81
CaO	16.47	11.67	16.41	15.31	13.82	17.07	15.12	12.74
Na_2O	2.33	5.01	2.35	3.04	3.57	2.01	3.30	4.25
K_2O	.12	.48	.07	.12	.20	.09	.15	.28
Total	100.10	99.61	99.68	99.88	100.04	100.58	100.44	99.85
An	79.1	54.7	79.0	72.9	67.3	81.9	71.0	61.5
Ab	20.2	42.6	20.5	26.3	31.5	17.5	28.1	37.0
Or	.7	2.7	.5	.8	1.2	.6	.9	1.5

Clinopyroxene:

Host	Olivine basalt	High-Ti basalt	Ankaramite		Olivine basalt	Olivine basalt	Xeno-lith
Occur-rence.	phn	grd	phn[1]	mph	mph	phn	ctl[2]
SiO_2	52.57	46.03	50.24	50.36	45.91	48.48	50.66
TiO_2	.67	4.02	1.61	0.91	2.91	1.85	1.25
Al_2O_3	2.35	4.46	3.62	3.94	6.44	4.78	3.00
Cr_2O_3	.20	.10	.10	.26	.22	.19	.13
Fe_2O_3	1.11	4.08	2.33	3.16	4.49	3.57	.13
FeO	4.68	7.19	6.10	3.56	4.43	5.28	7.88
MnO	.02	.15	.06	.18	.13	.16	.03
MgO	17.04	11.72	15.20	16.27	13.34	14.59	16.52
CaO	21.18	21.50	20.09	20.96	21.43	20.48	20.01
Na_2O	.27	.62	.56	.31	.37	.37	.39
Total	100.09	99.87	99.91	99.91	99.67	99.75	99.30
Wo	41.8	44.2	40.2	41.0	42.1	40.2	40.8
En	50.8	39.1	48.4	52.1	47.6	48.5	45.1
Fs	7.4	16.6	11.5	6.9	10.3	11.3	14.1

[1]Compositions used in mass-balance calculations: clinopyroxene, tables 10, 13, 17, and 22; magnetite and ilmenite, tables 10, 13, 15, and 17.
[2]Augite composition used in mass-balance calculations (see table 15).

Olivine:

Host	Olivine basalt	High-Ti basalt	Ankara-mite	Olivine basalt		Olivine basalt	Picrite	Xeno-lith
occur-rence	phn	grd	phn	mph	grd	phn	mph	ctl
SiO_2	40.52	38.11	40.59	40.05	38.06	40.35	40.24	37.37
FeO	11.64	24.65	13.60	13.73	24.13	13.88	13.54	24.95
MnO	.15	.25	.16	.40	.31	.29	.17	.49
NiO	.27	.10	.22	.22	.20	.18	.26	--
MgO	46.12	36.12	44.88	44.87	36.61	45.32	44.81	36.52
CaO	.34	.40	.32	.28	.33	.51	.37	.23
Total	99.04	99.63	99.77	99.55	99.64	100.53	99.39	99.56
Fo	87.6	72.3	85.5	85.3	73.0	85.3	85.5	72.3

Magnetite:

Host	Olivine basalt	High-Ti basalt	Ankara-mite	Olivine basalt	Olivine basalt	Picrite
Occur-rence.	grd[1]	grd	grd	grd	grd	grd
TiO_2	19.06	24.58	19.42	23.30	21.05	19.86
Al_2O_3	1.47	2.10	1.59	0.98	1.93	1.87
Fe_2O_3	31.27	20.03	30.11	23.79	27.13	27.92
FeO	45.71	50.14	46.95	48.85	48.31	47.35
MnO	.43	.73	.56	.54	.58	.42
MgO	1.81	2.14	1.17	2.19	1.41	1.02
Total	99.75	99.73	99.80	99.65	100.41	98.44

Ilmenite:

Host	Olivine basalt	High-Ti basalt	Ankara-mite	Olivine basalt	Picrite
Occur-rence.	grd	grd	grd[1]	grd	grd
TiO_2	48.69	49.47	49.24	48.59	47.74
Al_2O_3	.36	.17	.09	.33	.32
Fe_2O_3	9.84	7.61	9.09	9.26	10.02
FeO	37.09	39.63	38.67	38.08	39.15
MnO	.56	.62	.56	.65	.55
MgO	3.43	2.37	2.83	2.78	1.81
Total	99.97	99.87	100.48	99.69	99.59

magmas. The most sodic plagioclases, groundmass crystals in the most evolved basalts, are approximately An_{55} in composition.

PRIMARY MAGMAS AND PICRITES

Considerable progress has been made in the understanding of basalt magma genesis during the past few decades. Particularly important is the composition of the primary magma generated in the mantle under each volcano. Several lines of reasoning suggest that such melts are MgO rich (15–18 weight percent), which, if crystallized, would be olivine rich, like picrites. There has been some disagreement, however, over the interpretation of picrites as primary basaltic magmas. Field observations by early petrologists, such as Macdonald (1949) and Powers (1955), suggested that picrites are olivine accumulations in basaltic magma. However, when high-pressure-melting studies of peridotite and eclogite (for example, Green and Ringwood, 1967; O'Hara and Yoder, 1967) showed that primary melts forming in the mantle must contain 16 to 18 weight percent MgO, Hawaiian picrites were reexamined.

Two other lines of evidence support the early conclusions of Macdonald (1949) and Power (1955) that picrites are not primary magmas. First, in a recent study of picrites from Kilauea and Mauna Loa, Wilkinson and Hensel (1988) showed that the olivine phenocrysts are not in equilibrium with their host magma. The Mg-Fe olivine phenocryst-"liquid" partition coefficient K_D $[=(FeO/MgO)_{olivine}\times(MgO/FeO)_{liquid}]$ between olivine and whole rock is greater than 0.30 (Roeder and Emslie, 1970), implying that the olivine crystals are too iron rich to be in equilibrium with a magma of the whole-rock composition and thus would not have crystallized from such a magma. Second, the compositions of suites of closely associated olivine-rich rocks from Kilauea and Mauna Loa define linear trends (olivine-control lines) on MgO diagrams (Wright, 1973; Maaloe and others, 1988). These trends are consistent with the addition or subtraction of olivine of nearly constant composition from a basaltic magma, indicating that these phenocrysts generally are not in equilibrium with the "bulk rock.

If picrites are not primary magmas, do these picritic rocks or any other basalt retain enough of the characteristics of the original melt to allow us to infer the composition of the primary magma? If olivine and minor chrome-rich spinel inclusions are the only phases removed during the ascent of basaltic magma, these phases can be added in sufficient quantities to return the "liquid" to equilibrium with an assumed crystal composition (Wright, 1984).

The most magnesian olivine in any Mauna Kea lava, whether a basalt or picrite, is Fo_{87} (table 8). None of these phenocrysts appear to be in equilibrium with their host magmas. The K_D values for Hamakua picrites and this olivine range from 0.50 to 0.60, indicating that the olivine is too iron rich. The Fo_{85} olivine phenocrysts in olivine-bearing basalts, for which the K_D values range from 0.21 to 0.24, are too magnesian. The MgO content of the magma that crystallized these Fo_{85} olivine phenocrysts can be approximated by adding (or subtracting, in the case of picrites) this olivine to the basalt until K_D=0.30. For example, sample IP–20 is an olivine-bearing basalt containing about 8.0 weight percent MgO. For magma with the composition of sample IP–20 to be in equilibrium with its $Fo_{85.3}$ olivine phenocrysts, olivine must be added sufficiently to increase the MgO content to 10.7 weight percent (table 9). For the magma to be in equilibrium with mantle olivine (Fo_{91}) (Kuno, 1969), assuming 0.33 as an average K_D value between the mantle and surface (Takahashi and Kushiro, 1983), sufficient olivine must be added to increase the MgO content to 18.3 weight percent (table 9).

These relations between olivine phenocryst and basalt whole-rock compositions suggest that each primary Hamakua magma had an MgO content near 18 weight percent. As these magmas ascended from the mantle, high-Mg olivine crystallized and was removed. By the time the magma reached a level of neutral buoyancy somewhere within the volcano, its MgO content was between 10 and 12 weight percent, and the crystallizing olivine had a composition of about Fo_{85} (fig. 38). Further olivine fractionation changed the magma composition only along the olivine-control line until the MgO content reached about 7 weight percent. Lavas erupted from shallow magma chambers at this stage of fractionation contain varying amounts of olivine, all of about Fo_{86} composition. Many magmas resided in such chambers sufficiently long to begin fractionation of olivine+augite or olivine+augite+plagioclase, causing compositions to depart markedly from olivine control. As long as a magma remains olivine controlled, its composition is a function only of original melt composition and the proportion of olivine fractionated.

ALKALI, TRANSITIONAL, AND THOLEIITIC BASALTS

We refer olivine-controlled lavas of the Hamakua Volcanics to the alkali (ne normative) and transitional (ol plus hy normative) basalt groups. Their compositions differ from primary compositions only by the addition or removal of olivine. These basalts have undergone neither extensive low-pressure fractionation nor extreme accumulation of crystals. Thus, they provide the closest representatives of possible parental magmas for the varieties of accumulative basalts, such as the ankaramites and picrites, or for the evolved basalts, which differentiated beyond olivine control in shallow reservoirs. We use 7.2 weight percent MgO as a convenient boundary between these olivine-controlled basalts and the less magnesian, evolved basalts, which record fractionation of other silicate crystalline phases in addition to olivine. Although the two Hamakua tholeiites

Table 9. Chemical compositions of basaltic magma, adjusted by addition of olivine to be in equilibrium with olivine phenocrysts ($Fo_{85.3}$; see table 8) and mantle olivine (Fo_{91}; Kuno, 1969)

[All values in weight percent. Analysis of sample IP–20 recalculated from data of table 1 to 100 percent dry weight after partitioning of Fe to FeO and Fe_2O_3 in the ratio 88:12.]

	IP-20	IP-20, in equilibrium with $Fo_{85.3}$ phenocrysts	IP-20, in equilibrium with Fo_{91} mantle olivine
SiO_2	47.60	47.05	45.76
Al_2O_3	13.90	12.84	10.42
Fe_2O_3	1.61	1.63	1.56
FeO	10.66	10.79	10.30
MgO	7.87	10.68	18.25
CaO	11.03	10.23	8.28
Na_2O	2.56	2.37	1.92
K_2O	.84	.78	.63
TiO_2	3.30	3.05	2.47
P_2O_5	.44	.41	.33
MnO	.18	.20	.18

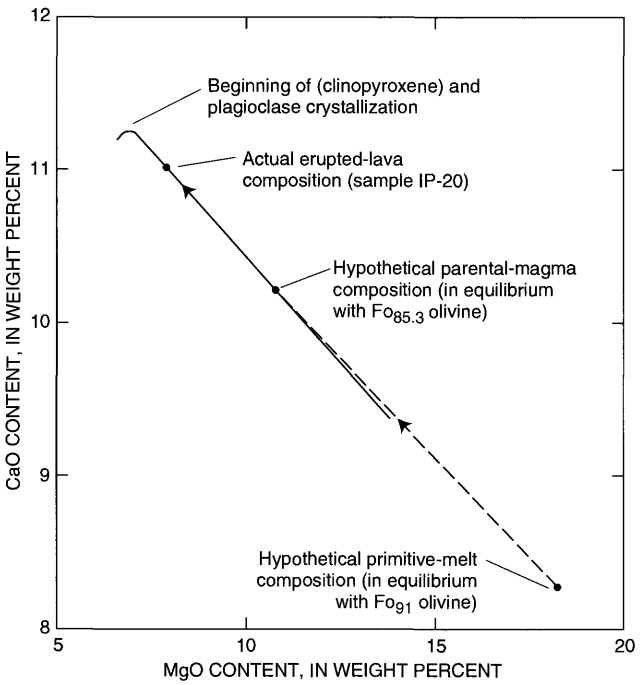

Figure 38. CaO versus MgO contents for sample IP–20 (table 9), with olivine contents adjusted to illustrate relations among erupted basalt composition, parental-magma composition, and primary composition. Olivine-controlled fractionation paths: dashed line, as magma ascends to shallow magma chamber; solid line, while magma is contained in shallow magma chamber.

(samples La–3, La–11) are evolved, as indicated by an MgO content less than 7.2 weight percent, we include them in this discussion, which deals largely with the genesis of parental magmas.

The petrographic features of the alkali, transitional, and tholeiitic basalts are similar. Each type has varying amounts (0–10 volume percent) of olivine, augite, and plagioclase phenocrysts (see table 8 for mineral compositions). The groundmass of most samples is nearly completely crystalline and is composed predominantly of brown augite and plagioclase, with lesser amounts of olivine, magnetite, and ilmenite.

The olivine-controlled basalts form broad bands on MgO-variation diagrams (fig. 39). The breadth of these bands suggests that they represent a whole family of olivine-control lines, one for each different composition of basalt.

To compare this suite of lavas without the effect of variations in olivine content, their compositions are projected in figure 40 onto the CS–MS–A plane of the C–M–S–A tetrahedron of O'Hara (1968). To have the plotted points represent magmas close to melt compositions, samples from lavas containing few phenocrysts, or containing only olivine phenocrysts, and having MgO contents greater than 7.2 weight percent were used. Tholeiite sample La–3, containing 6.6 weight percent MgO, is the single exception to these requirements. All of the points form an array near the 30-kbar liquidus phase boundaries of O'Hara (1968). This univariant boundary representing liquids in equilibrium with olivine+garnet+clinopyroxene was extended, using data on alkaline compositions determined by Takahashi and Kushiro (1983); it almost exactly bisects the array of Hamakua basalt compositions. Furthermore, the points are essentially sequenced with respect to the degree of silica saturation, that is, normative ne decreasing or hy increasing from left to right. Before interpreting this array as representing a series of melts controlled by univariant mantle phase equilibria, we first discuss this sequence with respect to the low-pressure cotectic.

A peculiarity of the olivine projection in the C–M–S–A tetrahedron is the near-coincidence of the position of the 30-kbar univariant curve representing liquids in equilibrium with clinopyroxene, garnet, and olivine with the 1-bar curve representing liquids in equilibrium with plagioclase, clinopyroxene, and olivine (fig. 41). Because most of

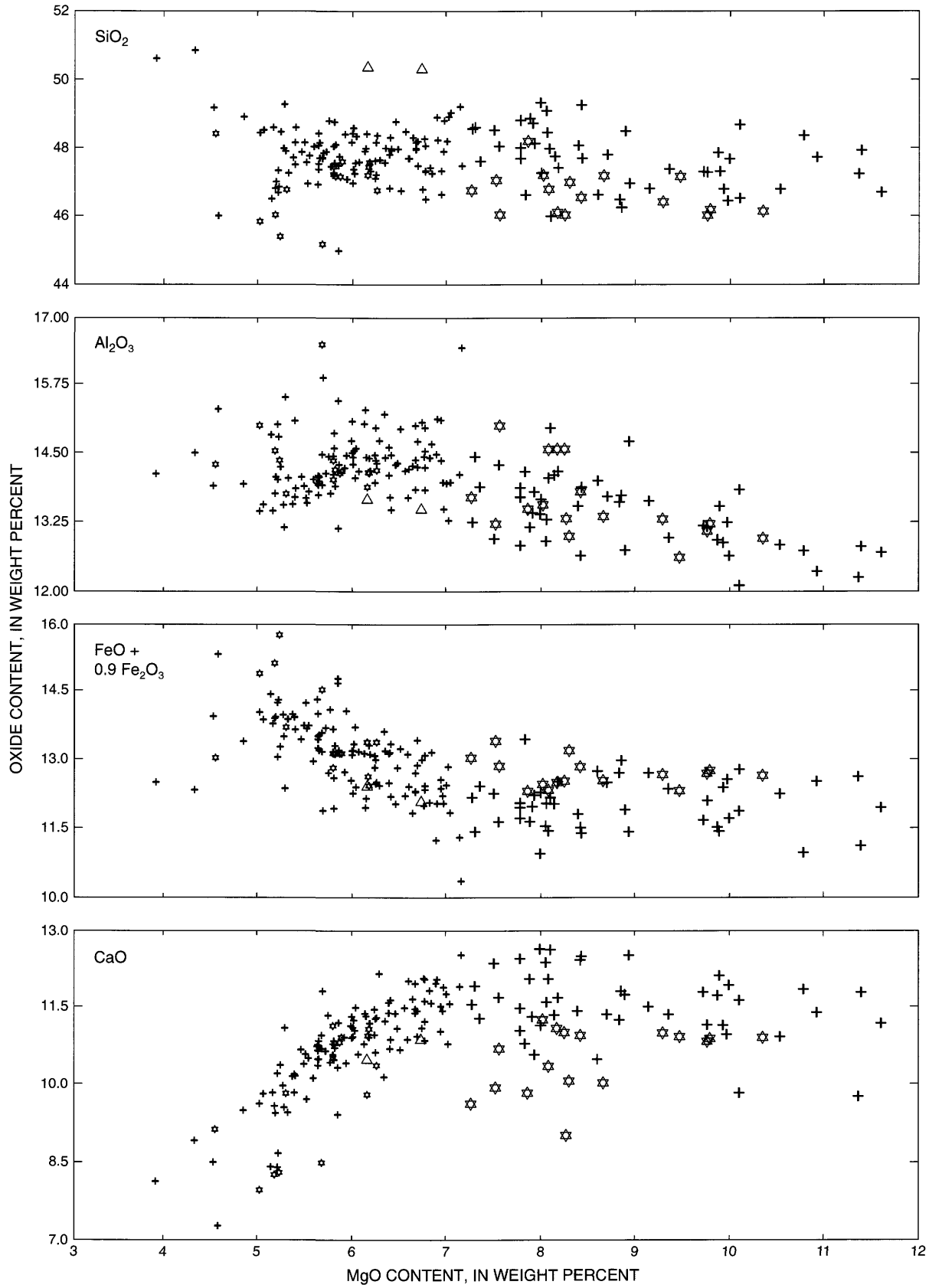

Figure 39. MgO-variation diagrams for basaltic rocks of the Hamakua Volcanics, exclusive of picrites and ankaramites. Large stars, alkali basalt; small stars, evolved alkali basalt; large crosses, transitional basalt; small crosses, evolved transitional basalt; triangles, tholeiitic basalt.

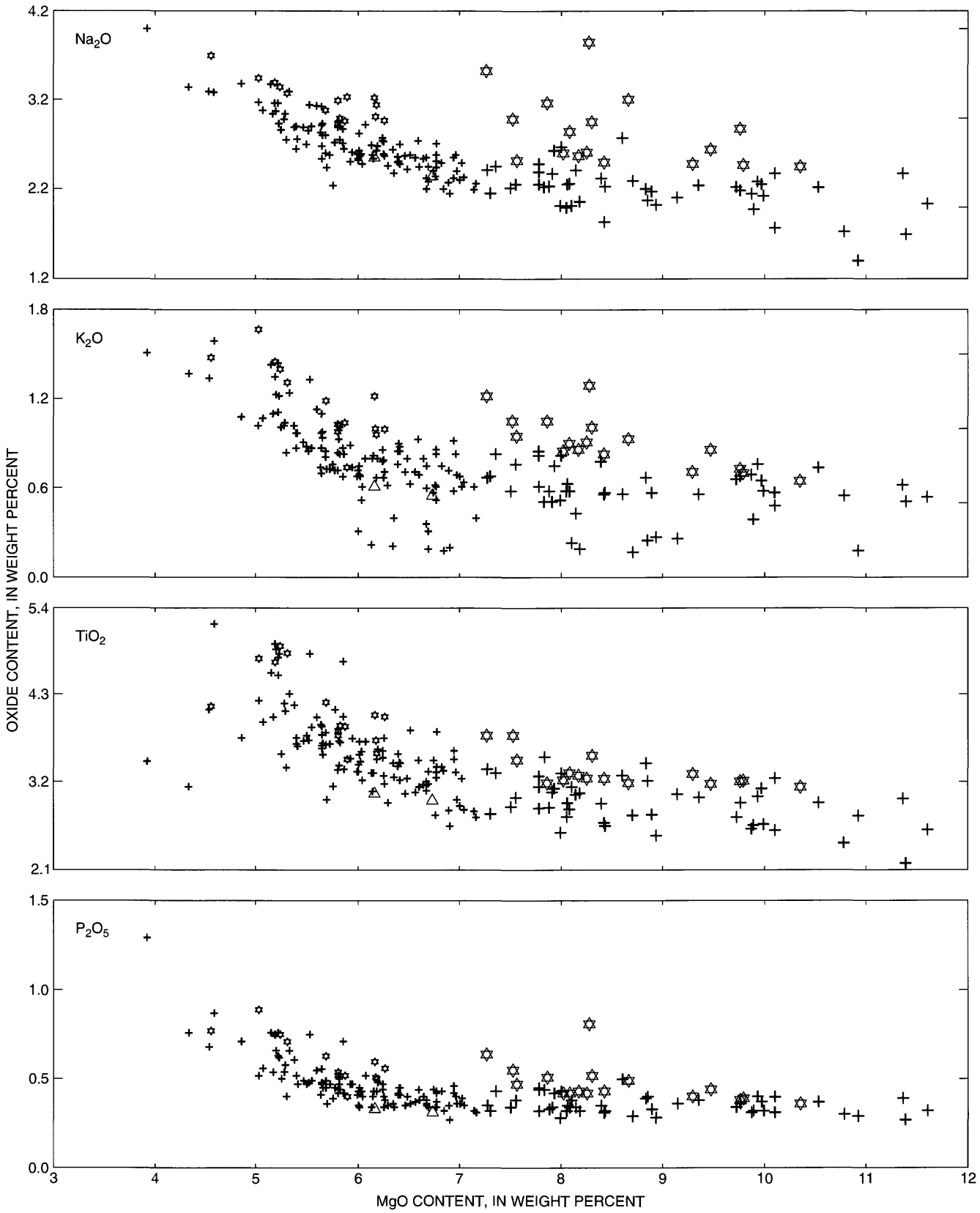

Figure 39. Continued.

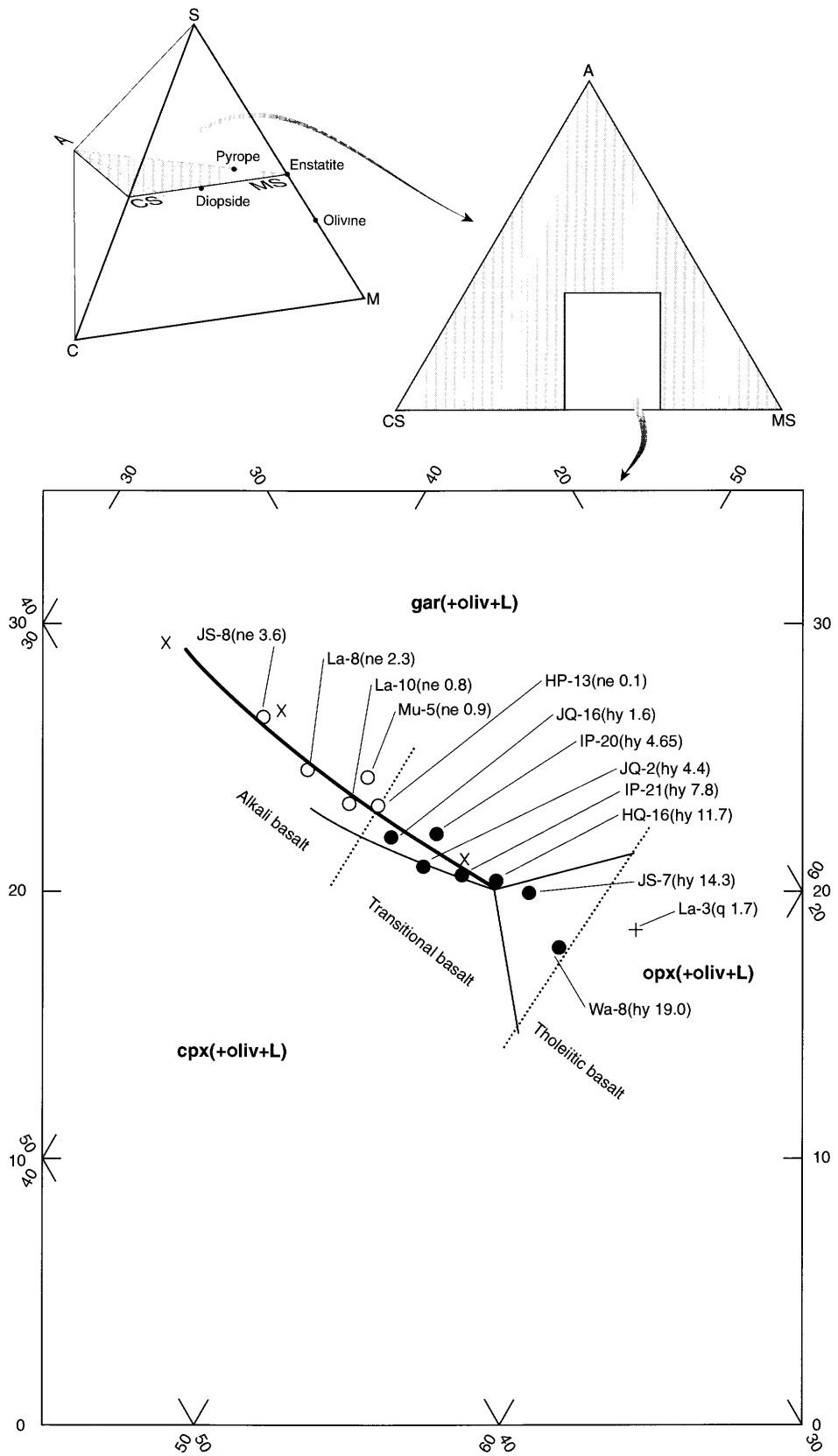
S
A
Pyrope
Enstatite
CS
MS
Diopside
Olivine
M
C
A
CS
MS
gar(+oliv+L)
JS-8(ne 3.6)
La-8(ne 2.3)
La-10(ne 0.8)
Mu-5(ne 0.9)
HP-13(ne 0.1)
JQ-16(hy 1.6)
IP-20(hy 4.65)
JQ-2(hy 4.4)
IP-21(hy 7.8)
HQ-16(hy 11.7)
JS-7(hy 14.3)
La-3(q 1.7)
Alkali basalt
Transitional basalt
Tholeiitic basalt
opx(+oliv+L)
Wa-8(hy 19.0)
cpx(+oliv+L)

← **Figure 40.** Selected compositions of basalt of the Hamakua Volcanics projected from olivine onto CS–MS–A plane of C–M–S–A tetrahedron of O'Hara (1968). Components of tetrahedron (see O'Hara, 1968, for full discussion of projection): A, (molecular proportion $Al_2O_3+Cr_2O_3+Fe_2O_3+Na_2O+K_2O+TiO_2)\times 101.96$; C, (molecular proportion, $CaO\cdot 3\,1/3P_2O_5+2Na_2O+2K_2O)\times 56.08$; M, (molecular proportion, $FeO+MnO+NiO+MgO-TiO_2)\times 40.31$; S, (molecular proportion, $SiO_2-2Na_2O-K_2O)\times 60.09$. Plotted lava compositions, showing sample numbers and normative-mineral-component contents (in weight percent; see table 1): circles, nepheline (ne) normative; dots, hypersthene (hy) normative; plus, quartz (q) normative. Light lines, 30-kbar phase boundaries of O'Hara (1968); heavy line, phase boundary (cpx, clinopyroxene; gar, garnet) as indicated by liquid compositions (x's) determined by Takahashi and Kushiro (1983); dotted lines, boundaries between fields of alkali basalt (ne normative), transitional basalt (hy normative), and tholeiitic basalt (q normative). opx(+oliv+L) [orthopyroxene(+olivine+liquid)], cpx(+oliv+L), and gar(+oliv+L) fields are separated by experimentally determined phase boundaries, which represent liquid compositions from partially melted mantle peridotite.

the plotted Hamakua basalt compositions lie very near the 1-bar cotectic, we consider that the plotted compositions may either be related by low-pressure fractionation processes or have at least been modified by low-pressure crystal removal.

Several lines of evidence support the conclusion that low-pressure fractionation has not affected the magma compositions plotted in figure 41. (1) All of the compositions could be derived from a single parent, because the points plot on both sides of a thermal divide, near sample HP–13 if based on normative minerals or near sample IP–21 if based on the dry-melting experiments of O'Hara and Yoder (1967). (2) A test of crystal fractionation may be made by using mass-balance calculations with the crystal compositions of phenocryst or microphenocryst phases in the tested daughter rock (table 10). Such an attempt, using samples IP–21 and HP–13, gives a fairly close fit for the derivation of the daughter product. However, a subtle, but important, mismatch for SiO_2 and alkalis indicates that the chosen parental magma is somewhat more alkaline than the daughter, and so the two magmas cannot be related by crystal fractionation. Other pairs of basalts along the sequence in figure 41 give similar results.

The array of points in figure 40 from samples JS–8 to HQ–16 can be interpreted as a succession of melts formed along a univariant curve controlled by garnet+clinopyroxene+olivine. Progression along this univariant curve from the most alkaline composition toward higher degrees of silica saturation represents melting with increasing temperature and, therefore, with increasing degrees of partial melting in the peridotite assemblage (fig. 42). Sample Wa–8 represents magma from a part of the source region in which garnet was depleted before clinopyroxene, whereas sample JS–7 represents magma generated by melting in which the clinopyroxene was depleted slightly before garnet. The tholeiitic sample, La–3, followed a path similar to that of sample JS–7, but much more orthopyroxene was melted.

We note that the above model assumes that the mantle source is a garnet peridotite, and the curves of figure 42 are for dry melting. The melting in this model in the range between transitional and tholeiitic compositions is not controlled by univariant mantle phase equilibria; olivine and orthopyroxene are the only remaining liquidus phases within this interval. This polyvariant melting agrees somewhat with the melting model of Wright (1984); however, the model of Hofmann and others (1984), which is based on trace-element abundances, requires that both garnet and clinopyroxene remain in the source.

PICRITES AND ANKARAMITES

On Mauna Kea, picrite flows are generally exposed only in the deeper part of the Hamakua Volcanics along the Hamakua Coast (fig. 13), whereas ankaramite flows are near the tops of gulch sections and locally form the present ground surface (figs. 13, 43). However, picrite is included in the uppermost part of the exposure of the Hopukani Springs Volcanic Member in Waikahalulu Gulch, at 3,785-m (12,420 ft) elevation, and forms an additional extensive exposure of the Hopukani Springs Volcanic Member above Mauna Kea State Park (see pl. 2). Ankaramite flows, though sparse, are evenly distributed on the surface of the lower flanks of the volcano (fig. 43); an additional small exposure, not individually mapped, occurs in the uppermost part of Pohakuloa Gulch, at 3,735-m (12,260 ft) elevation (pl. 2).

Picrites and ankaramites are visually striking both in outcrop and in thin section (figs. 44*A*, 44*B*) because of their abundant large crystals. The petrographic features of Mauna Kea picrites are similar to those of picrites from other Hawaiian volcanoes (Wilkinson and Hensel, 1988) in that the size distribution of olivine is bimodal or trimodal. The largest crystals are blocky, 4 to 5 mm across, and range in composition from Fo_{84} to Fo_{86}. Microphenocrysts 0.5 to 1 mm across have compositions near Fo_{82}, and groundmass olivine ranges in composition from Fo_{75} to Fo_{80}. The groundmass of the picrites typically consists of small grains of olivine, augite, plagioclase, titanomagnetite, and ilmenite with a pilotaxitic to intergranular texture.

Ankaramites, like the picrites, also exhibit several sizes of phenocrysts. Olivine is similar in size and composition to that in the picrites described above, and clinopyroxene phenocrysts are diopsidic augites, 5 to 10 mm long, whereas microphenocrysts are slightly more iron rich and 1 to 2 mm long (fig. 44*B*; see table 8 for representative crystal compositions). Some ankaramites contain as much as 8 volume percent plagioclase phenocrysts (An_{80}). For example, Puu Pa (fig. 43) was the source for at least two

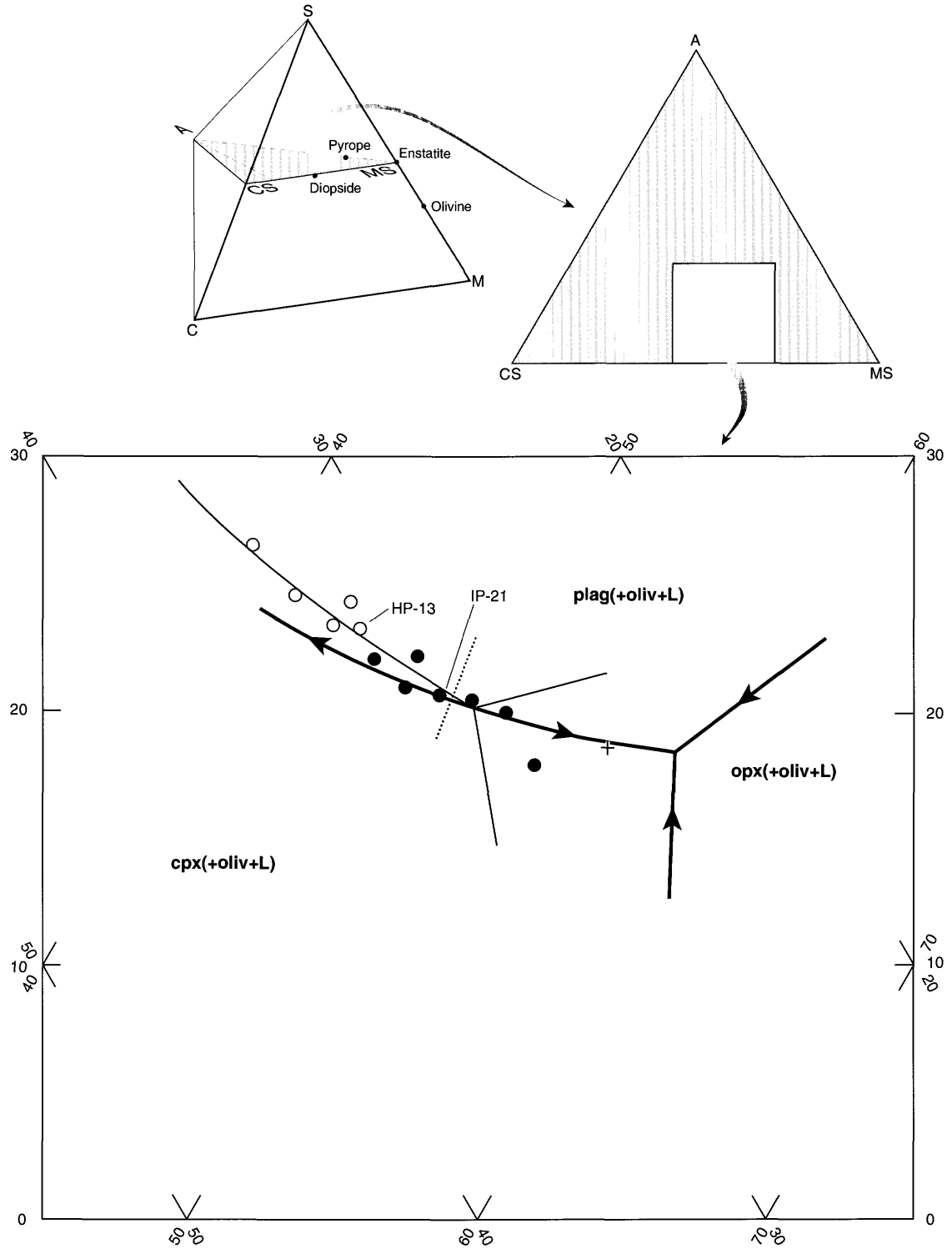

Figure 41. Selected compositions of basalt of the Hamakua Volcanics, projected from olivine onto CS–MS–A plane of C–M–S–A tetrahedron of O'Hara (1968). See figure 40 for algorithm used to derive components of tetrahedron. Heavy lines, 1-bar phase boundaries (cpx, clinopyroxene; plag, plagioclase; opx, orthopyroxene) of O'Hara (1968), showing thermal divide (dotted line) and arrows that indicate direction of liquid path with falling temperature; light lines, 30-kbar phase boundaries of O'Hara (1968), adjusted for consistency with data of Takahashi and Kushiro (1983) (see fig. 40). Plotted lava compositions: circles, nepheline normative; dots, hypersthene normative; plus, quartz normative. Sample HP–13 is modeled as parental magma of sample IP–21 (see table 10 for mass-balance calculations); oliv, olivine; L, liquid.

Table 10. Mass-balance calculations testing the relation by crystal fractionation among the basalts plotted in figure 40

[All values in weight percent, calculated to 100 percent dry weight; modeled composition (b) determined using the matrix-inversion method of Bryan and others (1969)]

	Parental magma (sample HP-13)	Daughter (sample IP-21)		
		observed (a)	modeled (b)	residual (a-b)
SiO_2	46.01	47.68	47.60	[1]0.08
Al_2O_3	13.83	13.92	13.88	.05
Fe (as FeO)	12.90	12.14	12.09	.04
MgO	8.43	7.88	7.86	.02
CaO	10.99	11.05	11.04	.01
Na_2O	2.51	2.56	2.68	[1]-.12
K_2O	.83	.84	.92	[1]-.08
TiO_2	3.27	3.31	3.26	.05
P_2O_5	.43	.44	.47	-.03
MnO	.20	.18	.20	-.02
Sum of the squares of residuals				.034

Phases removed from parental magma in calculating modeled composition:

Olivine-------Fo_{74}	-2.80
Plagioclase---An_{79}	-4.07
Clinopyroxene[2]	-2.22
Magnetite[2]----	-1.86
Ilmenite[2]-----	.21

[1]In general, a sum of the squares of residuals less than 0.10 is a close match. In this case, the mismatch in these oxides shows that the hypothetical daughter has too much SiO_2 and insufficient alkalis to be derived by crystal fractionation from this parent.

[2]See table 8 for compositions of these phases; clinopyroxene is ankaramite phenocryst of table 8.

ankaramite flows, the second of which contains about 3 volume percent plagioclase phenocrysts. The groundmass in ankaramites is pilotaxitic and consists of the same five minerals as in the picrites.

Analyses of several typical Mauna Kea picrites and ankaramites are listed in table 11, and the compositions of all the samples of these rocks in our data set are plotted in figures 45 and 46. A few picritic samples, such as HR–46, contain moderate amounts of augite and thus have compositions between those of picrite and ankaramite.

One of the most notable features of Mauna Kea picrites and olivine basalts is the absence of a single olivine-control line on a plot of CaO versus MgO contents (fig. 45). For a given MgO content—for example, 18 weight percent—the CaO content varies by 3 weight percent. This variation is related to the type of parental magma, which is better illustrated in a CS–MS–A projection (fig. 46), where the spread of points ranges from tholeiite nearly to alkalic basalt.

One demonstration that picrites with varying CaO contents are crystal cumulates in basaltic magma is provided by the analyses obtained by K.J. Murata (see table 1). Murata collected picrite samples from two gulch sections on the Hamakua Coast (fig. 13) and analyzed the whole rock and groundmass (by mechanical removal of the phenocryst phases). Two pairs of these analyses are indicated in figure 45, in which the connecting lines are approximately Fo_{86} olivine-control lines.

Similarly, Murata analyzed the whole rock and groundmass for two ankaramite flows from the gulch sections on the Hamakua Coast. The line connecting the compositions of one pair, shown in figure 45, has a slope equivalent to a control line of Fo_{86} olivine and clinopyroxene in approximately a 1:1 ratio, whereas the line connecting the other pair has a slope indicative of a 3:2 ratio. The addition of clinopyroxene to basaltic magma displaces points toward the ankaramitic augite composition in a CS–MS–A projection (fig. 46).

These results show that the picritic lavas have developed through the accumulation of olivine, in magmas of not only tholeiitic composition but also varying transitional-basalt compositions (fig. 46). Any of these picrites could have formed by emplacement of a basaltic magma in the superstructure of the volcano, where only the crystallization of olivine takes place before eruption. Basaltic lava, somewhat depleted in olivine, and picrite could be erupted from such a magma chamber.

Ankaramitic lavas, cumulates of both olivine and clinopyroxene, develop primarily in magmas of transitional-basalt composition (fig. 46) and require somewhat-different crystallization conditions. Their parental magmas are emplaced at levels deeper in the volcano than those developing picrites. These parental magmas crystallize much smaller amounts of olivine before augite begins to form, because pressure tends to enlarge the clinopyroxene field at the expense of olivine (Mahood and Baker, 1987). This observation suggests that with approximately the same degree of cooling, a moderately deeply emplaced basaltic magma can crystallize and accumulate both olivine and augite, whereas a shallow magma can crystallize and accumulate only olivine.

EVOLVED ALKALI AND TRANSITIONAL BASALTS

INTRODUCTION

Evolved basalts, which we define as those containing less than 7.2 weight percent MgO, occur in the upper parts of the gulch sections on the Hamakua Coast (fig. 13) and are widely distributed over the flanks of Mauna Kea. On MgO-variation diagrams (fig. 39), the broad bands of points representing MgO contents greater than approximately 7.2 weight percent reflect the variety of parental magmas. The sharp inflection in trends on a plot of CaO versus MgO contents at approximately 7.2 weight percent MgO indicates the end of olivine control and the beginning of clinopyroxene

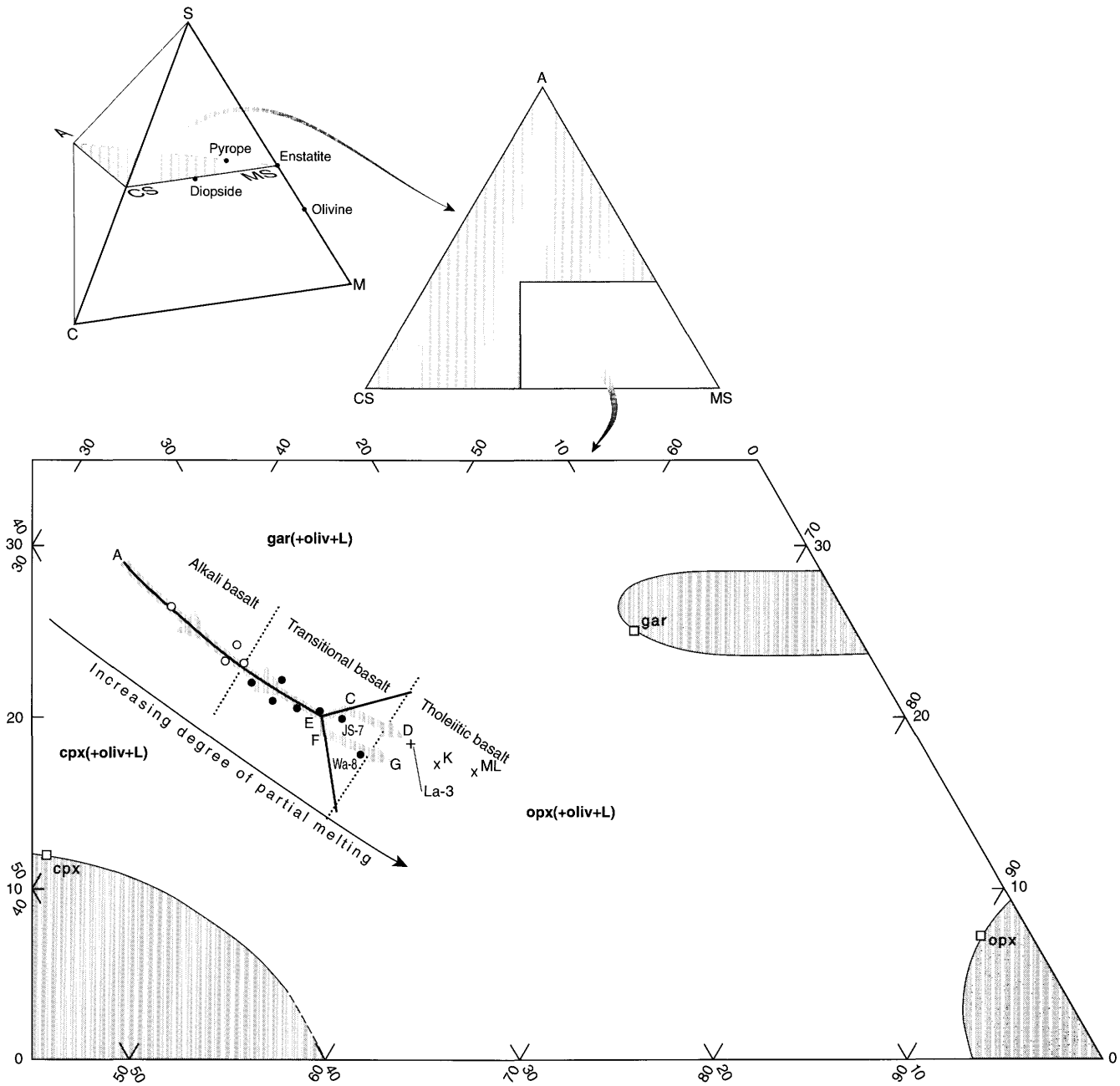

and (or) plagioclase crystallization. However, the exact MgO content at the inflection point depends on the CaO content of the parental magma. Distinct compositional similarities, stratigraphically and spatially related occurrences, and distinct petrographic similarities serve in varying combination to suggest significant grouping among the evolved basalts. Therefore, we describe and discuss the origins of four major groups of evolved basalts: (1) high-Ti basalts, (2) basalts of the Liloe Spring Volcanic Member, (3) plagioclase-rich basalts, and (4) basalts of the Hopukani Springs Volcanic Member.

HIGH-Ti BASALTS

High-Ti basalts are defined on the basis of their distinctly large TiO_2 contents (greater than 4.5 weight percent);

← **Figure 42.** Selected compositions of basalt of the Hamakua Volcanics, projected from olivine onto CS–MS–A plane of C–M–S–A tetrahedron of O'Hara (1968). See figure 40 for algorithm used to derive components of tetrahedron. Plotted lava compositions: circles, nepheline normative; dots, hypersthene normative; plus, quartz normative; x's, average compositions of tholeiites from Kilauea (K) and Mauna Loa (ML) (Macdonald and Katsura, 1964, table 9); squares, coexisting mineral compositions of three mantle silicate phases (cpx, clinopyroxene; opx, orthopyroxene; gar, garnet) as determined from Hawaiian olivine eclogite xenolith (Kuno, 1969). Shaded areas, solid-solution range of phases (boundary dashed where extrapolated); heavy black lines, 30-kbar phase boundaries of O'Hara (1968), adjusted for consistency with data of Takahashi and Kushiro (1983) (see fig. 40); dotted lines, boundaries between fields of alkali basalt (nepheline normative), transitional basalt (hypersthene normative), and tholeiitic basalt (quartz normative). Thick gray lines show inferred melting paths of garnet peridotite, based largely on dry-melting experiments of O'Hara (1968); arrows indicate direction of increasing degree of partial melting. Path from point A to point E is controlled by assemblage garnet+clinopyroxene(+olivine, oliv). If clinopyroxene is depleted before garnet (for example, sample JS–7), liquid (L) trends toward point C; from point E to point C, controlling assemblage is garnet+orthopyroxene(+olivine). After all garnet is melted, liquid trends toward orthopyroxene apex (from point C to point D). If garnet is depleted before clinopyroxene (for example, sample Wa–8), liquid trends toward point F; path from point E to point F is controlled by clinopyroxene+orthopyroxene(+olivine). After all clinopyroxene is melted, liquid again moves toward orthopyroxene apex (from point F to point G). With increasing degree of melting of orthopyroxene (for example, sample La–3), liquid approaches compositions seen in tholeiites of Kilauea and Mauna Loa.

all of these basalts have evolved to MgO contents of less than 6.0 weight percent. These lavas are aphyric to very weakly porphyritic and contain microphenocrysts of plagioclase, augite, and olivine. Where these microphenocrysts occur, they are typically skeletal, less than 0.5 mm long, and make up about 10 volume percent of the rock. In samples from well-crystallized flow interiors, the groundmass minerals, olivine, augite, plagioclase, titanomagnetite, and ilmenite (see table 8), form intergranular to diktytaxitic textures (fig. 44*F*). Biotite is a rare but persistent constituent of well-crystallized high-Ti basalts.

The distribution of high-Ti basalts on the surface of Mauna Kea is shown in figure 47 (see also, pl. 1). These basalts are among the latest Hamakua lavas. In gulch sections (fig. 13), they occur either at the top or within a flow or two of the top. High-Ti basalts show no obvious preferential association with any other particular basalt type.

Chemical analyses and normative compositions of several representative high-Ti basalts are listed in table 12. On the basis of Al_2O_3/CaO ratios, these basalts can be divided into two groups, those with a ratio above 1.6 and those with a ratio below 1.6. These groups occupy mutually exclusive fields on such plots as CaO versus MgO contents and Al_2O_3 versus SiO_2 contents (fig. 48), as well as in the CS–MS–A plane of the C–M–S–A tetrahedron (fig. 49).

The positions of points representing the high (greater than 1.6)- and low (less than 1.6)-Al_2O_3/CaO-ratio groups of high-Ti basalts in figure 48*A*, at the ends of parallel liquid-descent lines, suggests that these two compositional types reflect fractionation of olivine, augite, and plagioclase in approximately the same proportions. Such an interpretation, however, is not supported by the scatter representing the same compositions in figure 48*B*. Because the two groups project into different fields on the CS–MS–A plane (fig. 49) and on the DI–OL–NEPH plane of Sack and others (1987) (fig. 50), fractionation probably occurred under different pressures. To evaluate this interpretation, the proportions of fractionating phases were determined through mass-balance calculations, assuming that all the high-Ti basalts came from the same general parental magma.

The results of mass-balance calculations, using a weakly alkaline basalt (sample HP–13) as parental magma to derive a representative high-Ti basalt (samples La–103, JS–2) from each group, are listed in table 13. The same mineral compositions were used for each daughter magma, and the resulting proportions reveal two important differences. Even though sample La–103 is richer in MgO than sample JS–2, derivation of its composition requires less olivine removal, compensated by greater augite removal. The different ratios of olivine to augite and of augite to plagioclase can be explained by enlargement of the clinopyroxene field, as illustrated in the system diopside-anorthite-forsterite (Presnall and others, 1978), as pressure increases (fig. 51).

The different ratios of olivine to augite and of augite to plagioclase in the fractionating assemblages are caused by a reversal of the appearance of augite and plagioclase on the liquidus. This reversal can be illustrated by comparing the liquid-descent lines on variation diagrams (LP, HP, fig. 48). The two paths coincide as long as only olivine is being removed. With the onset of augite crystallization on the higher-pressure trend and of plagioclase on the lower-pressure trend, the paths diverge, as is especially evident on a plot of Al_2O_3 versus SiO_2 contents (fig. 48*B*).

Although we cannot calibrate the separation of the two groups of high-Ti basalts in figures 49 and 50 in terms of pressure, the group with higher Al_2O_3 and lower CaO contents probably fractionated in magma chambers much deeper within the volcanic system than did those with higher CaO contents.

The arbitrary selection of 4.5 weight percent TiO_2 as the lower limit for high-Ti basalts eliminates several intermediate compositions. Four such compositions are plotted in figure 48. Mass-balance calculations demonstrate that these compositions require removal of crystals amounting to 25 to 40 weight percent of the parental magma.

In summary, this group of basalts with the characteristic compositional signature of high TiO_2 content represents

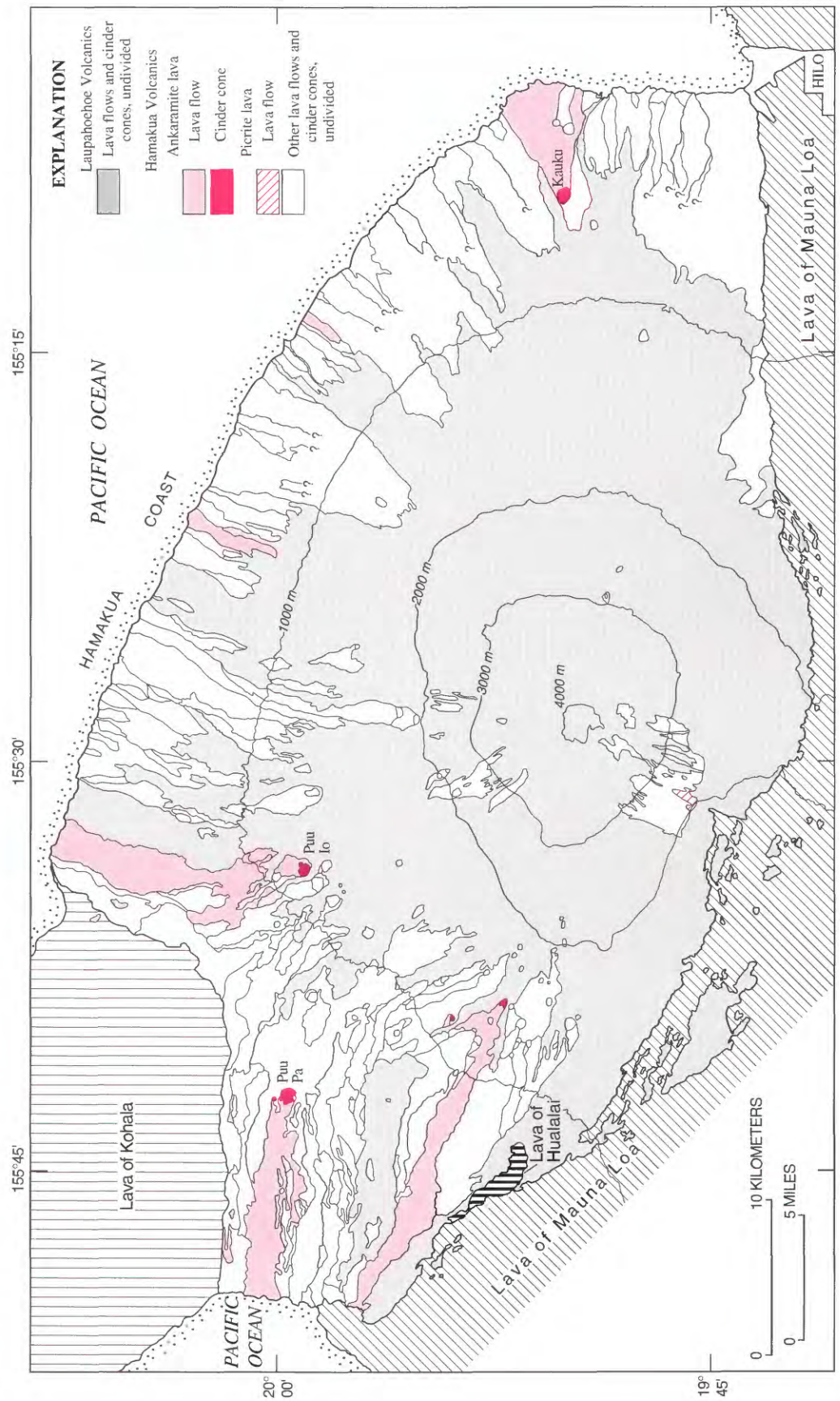

Figure 43. Geologic map of Mauna Kea, showing generalized distribution of all extensively exposed ankaramite and picrite lava flows of the Hamakua Volcanics. Internal contacts distinguish individual lava flows and cinder cones. Queries mark limits of mapping at edge of dense rain forest. Geology simplified from plates 1 and 2 and Wolfe and Morris (1996).

Table 11. Major-oxide and normative-mineral compositions of typical ankaramites and picrites of the Hamakua Volcanics and Hilo Ridge

[Major-oxide compositions and Cross, Iddings, Pirsson, and Washington (CIPW) norms in weight percent; major oxides adjusted to 100 percent dry weight after partitioning of Fe to FeO and Fe_2O_3 in the ratio 88:12. See table 1 for original analyses and analysts]

	Picrites			Ankaramites		
Sample ----	Er-20	La-6	La-105	IO-9	JQ-13	La-5
			Major oxides			
SiO_2 ------	48.23	45.44	45.22	46.42	46.56	47.21
Al_2O_3 ------	10.49	10.71	8.52	10.48	10.81	10.77
Fe_2O_3 ------	1.52	1.76	1.61	1.53	1.52	1.74
FeO -------	10.06	11.60	10.61	10.11	10.07	11.51
MgO -------	17.45	16.26	22.29	15.48	15.55	12.70
CaO -------	7.44	9.02	8.26	11.28	10.71	9.72
Na_2O ------	2.00	1.78	1.18	1.71	1.76	2.22
K_2O -------	[1].39	[1].33	[1].14	.57	.52	.72
TiO_2 ------	1.99	2.59	1.81	1.96	2.08	2.86
P_2O_5 ------	.24	.32	.18	.28	.25	.34
MnO -------	.17	.19	.18	.19	.17	.20
			CIPW norms			
q ---------	0.00	0.00	0.00	0.00	0.00	0.00
or --------	2.30	1.95	.83	3.37	3.07	4.25
ab --------	16.92	15.06	9.98	14.17	14.89	18.79
an --------	18.49	20.26	17.54	19.24	20.06	17.30
ne --------	.00	.00	.00	0.16	.00	.00
di --------	13.50	18.02	17.77	28.04	25.25	23.22
hy --------	19.20	7.43	10.20	.00	2.43	6.57
ol --------	23.02	29.07	37.50	28.44	27.57	21.12
mt --------	2.20	2.55	2.33	2.22	2.20	2.52
il --------	3.78	4.92	3.44	3.72	3.95	5.43
ap --------	.57	.76	.43	.66	.59	.81

[1]Low K_2O/P_2O_5 suggests that posteruptive depletion of K_2O may have occurred.

Samples:

Er-20. Tholeiitic picrite dredged from Hilo Ridge.
IO-9. Ankaramite flow from Puu Pa (see fig. 43).
JQ-13. Ankaramite flow from Puu Io (see fig. 43).
La-5. Ankaramite in Laupahoehoe Gulch (see fig. 13).
La-6. High-Ca picrite in Laupahoehoe Gulch (see fig. 13).
La-105. High-Ca picrite in basal part of measured section at Laupahoehoe Gulch (see fig. 13).

a type of late-stage process in Hamakua magmatic activity. Slightly alkalic parental magma emplaced at moderate to deep levels within the volcano had sufficiently long periods of time to crystallize as much as about 50 percent of the starting volume before the remaining magma was erupted. We note that the erupted lavas carry very few, if any, fractionated phenocrysts and no xenoliths. Furthermore, no preferential spatial relations are evident between these lavas and those with accumulated phenocryst phases, such as ankaramite, that might be expected to be complementary accumulative products.

BASALTS OF THE LILOE SPRING VOLCANIC MEMBER

A distinctive group of nearly aphyric basalts constitutes the Liloe Spring Volcanic Member of the Hamakua Volcanics. As previously described, these basalts crop out in kipukas on the upper flanks of the volcano (pl. 2; fig. 12). These lavas represent the latest Hamakua magmatic activity in the summit region. The analyses listed in table 14 span the compositional range of basalts of the Liloe Spring Volcanic Member. Some flows (for example, sample IO–13, table 14) on the lower slopes of Mauna Kea are similar in composition and petrography to those of the upper flanks. Mapped exposures of Liloe Spring basalt, as well as of those lower-flank flows that are petrographically and chemically similar, are shown in figure 52. Because these lower-flank flows may represent voluminous eruptions from the same summit vents as the Liloe Spring flows, they are included in the following descriptions and interpretations.

The more mafic basalts of the Liloe Springs Volcanic Member (for example, sample HR–8, table 14) are moderately porphyritic, containing 1- to 2-mm-diameter phenocrysts of olivine, plagioclase, and augite in approximately equal proportions and totaling 5 to 6 volume percent in abundance. The groundmass consists of rare olivine and abundant plagioclase, augite, magnetite, and ilmenite in a pilotaxitic texture. Basalts with more evolved compositions contain few phenocrysts; they have similar groundmass

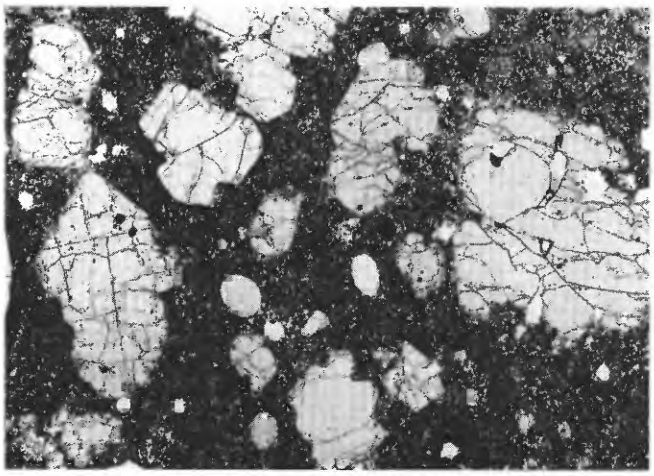

A 0 1 MILLIMETER

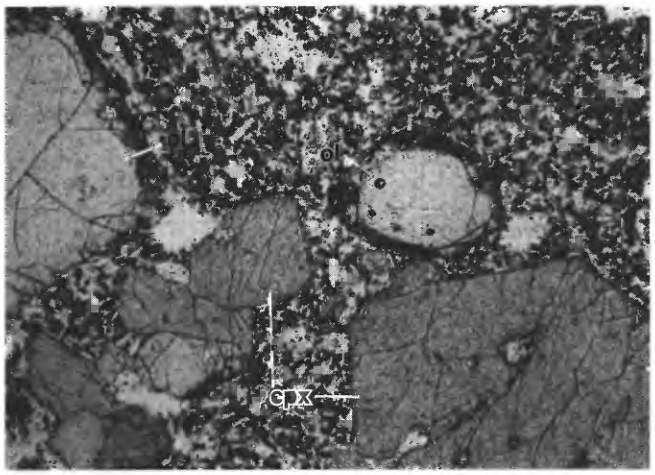

B 0 1 MILLIMETER

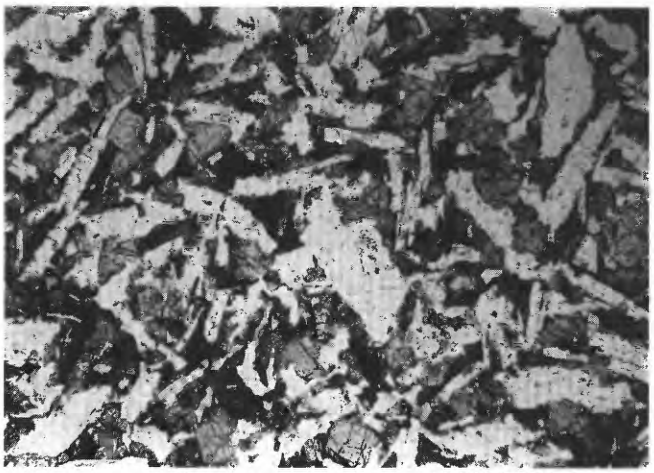

C 0 1 MILLIMETER

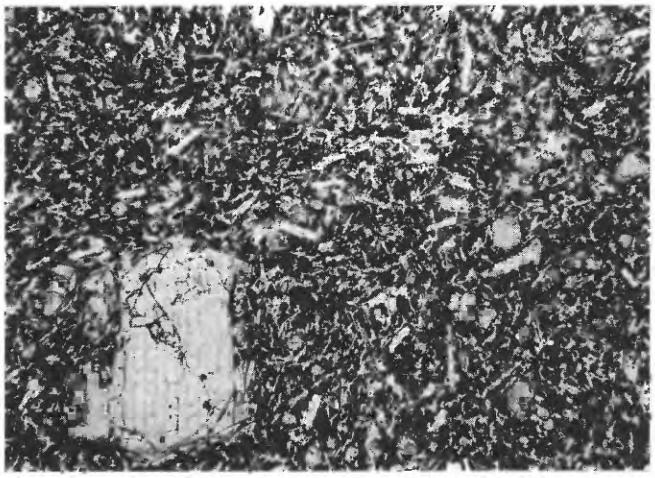

D 0 1 MILLIMETER

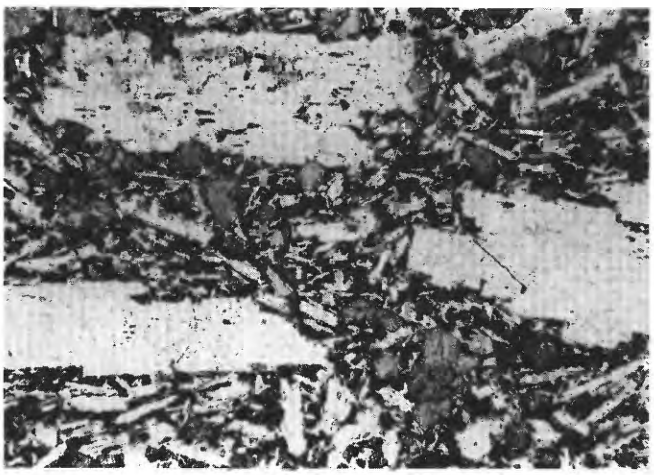

E 0 1 MILLIMETER

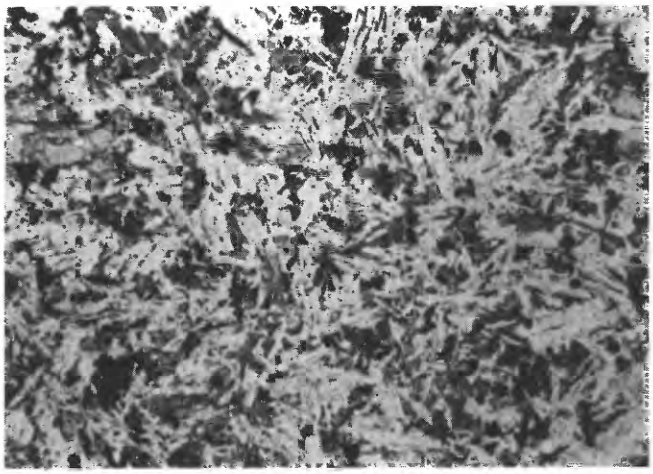

F 0 1 MILLIMETER

← **Figure 44.** Photomicrographs of Mauna Kea lavas and xenoliths. Plane-polarized light. *A*, Picrite (sample Ki–5), containing abundant olivine phenocrysts, as much as 3 mm long. *B*, Ankaramite (sample JQ–13), containing augite (cpx) and olivine (ol) phenocrysts, as much as 1 mm or more in diameter. Groundmass texture is intergranular. *C*, Tholeiitic basalt (sample La–3), containing intergranular groundmass of augite, plagioclase, rare olivine, ilmenite, and magnetite. *D*, Transitional olivine-bearing basalt (sample HP–13), containing olivine phenocryst embedded in fine-grained, intergranular groundmass. *E*, Plagioclase basalt (sample IP–6), containing plagioclase phenocrysts, as much as 2 mm long. Intergranular groundmass contains plagioclase, augite, rare olivine, and magnetite. *F*, High-Ti basalt (sample IO–6), containing groundmass of plagioclase, augite, olivine, ilmenite, and magnetite. Texture is intergranular to diktytaxitic. *G*, Hawaiite (sample IO–2), containing coarse-grained groundmass of plagioclase, olivine (ol), augite, magnetite, and ilmenite. Texture is trachytic. *H*, Benmoreite (sample JQ–6), containing trachytic to intergranular groundmass that includes larger crystals of apatite (ap), biotite (bio), and olivine (ol). *I*, Gabbroic xenolith in evolved basalt exposed near sample locality HR–41 (pl. 3). Augite and plagioclase exhibit equilibrium crystal boundaries with host basalt. *J*, Gabbroic xenolith in hawaiite-mugearite (sample HQ–61). Olivine crystal (ol) projects into host rock, unlike augite (cpx), which is preferentially embayed, indicating that part of augite dissolved into hawaiitic magma. This relation represents best petrographic evidence that augite is not in equilibrium with hawaiitic magma at lower pressures.

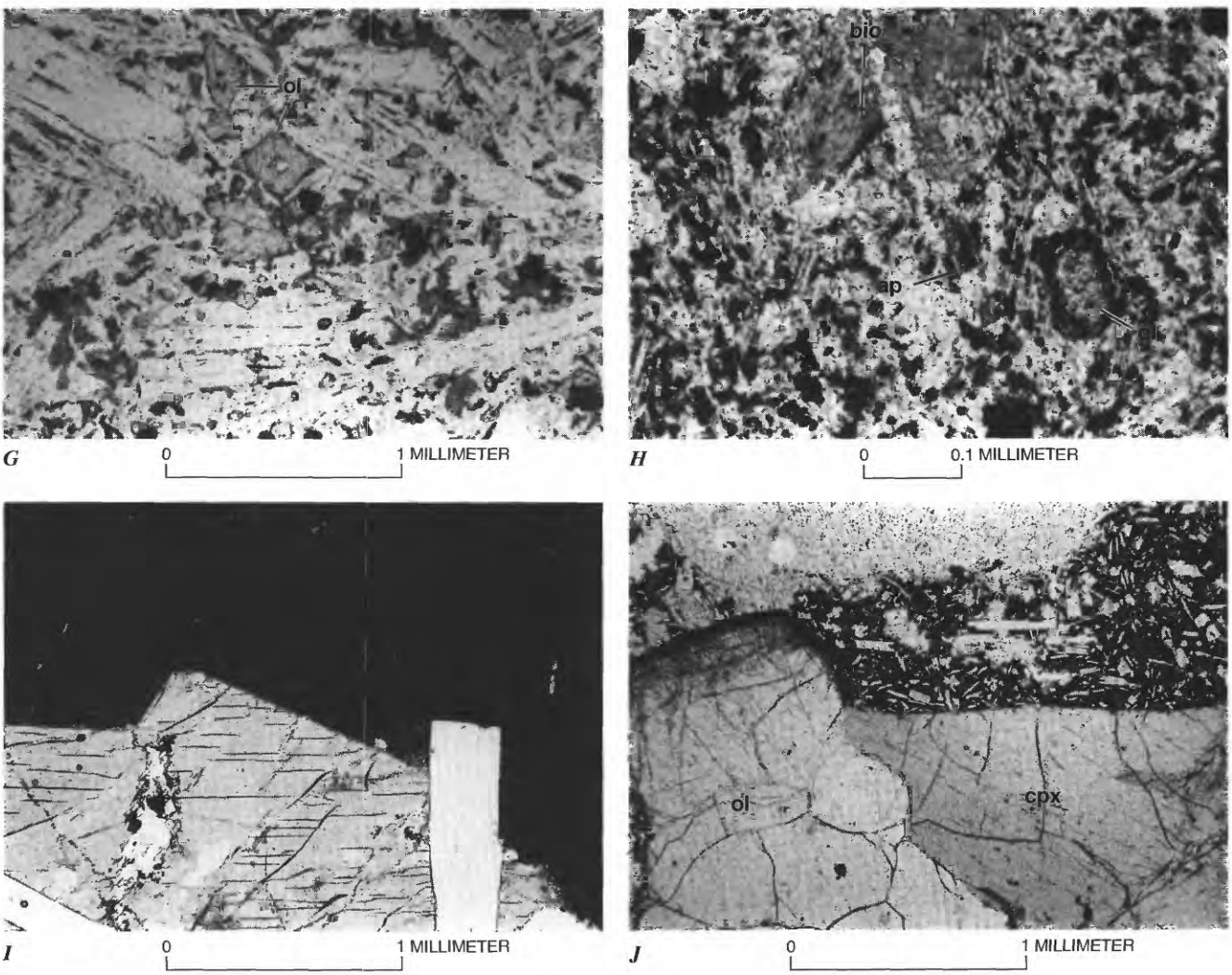

Figure 44. Continued.

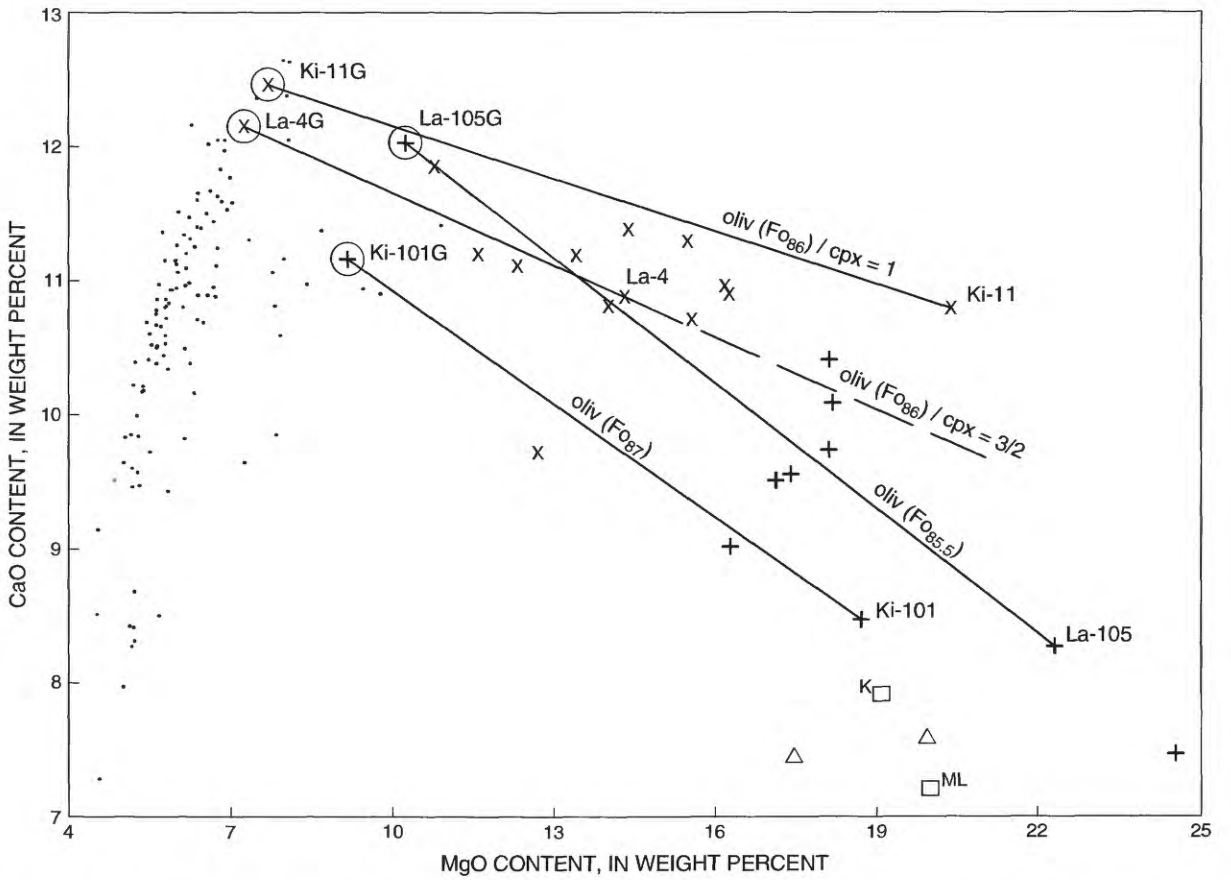

Figure 45. CaO versus MgO contents in ankaramite and picrite (see table 1) of the Hamakua Volcanics, in comparison with phenocryst-poor basalt (bs, table 1) of the Hamakua Volcanics and picrites from Hilo Ridge, Kilauea, and Mauna Loa. Solid lines (dashed where projected) are mineral or mineral-assemblage control lines (cpx, clinopyroxene; oliv, olivine) that connect related whole-rock and groundmass compositions (circled symbols indicate groundmass-separate samples; numbers refer to samples listed in table 1). Olivine compositions and olivine/clinopyroxene ratios represented by control lines were calculated from compositional differences between related whole-rock and groundmass-separate samples. Plotted whole-rock compositions: x's, ankaramite of the Hamakua Volcanics; pluses, high-Ca picrite of the Hamakua Volcanics; dots, phenocryst-poor basalt of the Hamakua Volcanics; triangles, tholeiitic picrite from Hilo Ridge; squares, average compositions of picrites from Kilauea (K) and Mauna Loa (ML) (Wilkinson and Hensel, 1988).

mineralogy and texture but lack ilmenite. A few basalts of the Liloe Spring Volcanic Member (for example, sample HQ–14, table 14) are distinctly more plagioclase phyric, containing 2- to 3-mm-diameter plagioclase phenocrysts in abundances as high as 3 to 5 volume percent, accompanied by less abundant olivine and augite.

The phenocrysts in most basalts of the Liloe Spring Volcanic Member exhibit reverse zoning on rounded cores, and, in a few samples, strings of glass inclusions decorate the core-rim boundary. These features show that early-formed phenocryst phases later became unstable, either by decompression of the magma or by the introduction of new magma into the chamber. Several basalts contain glomeroporphyritic clots of olivine, plagioclase, and augite, but discrete gabbroic xenoliths were found in only one of the most evolved basalts (sample HR–41, table 14). Edges of the xenolith crystals in contact with the host basalt are sharp and euhedral (fig. 44*I*), showing that the xenolith phases (table 8) are in equilibrium with their host basalt. Even though many phenocrysts show evidence of disequilibrium, possibly from magma mixing, these phases were fractionated from the magma to produce the evolved basalts.

The compositions of basalts of the Liloe Springs Volcanic Member are plotted in figure 53, which shows a distribution somewhat similar to those of the high-Ti basalts. The apparent trend of points on a plot of CaO versus MgO contents suggests a consistent removal of olivine, augite, and plagioclase. However, the scatter in terms of Al_2O_3 and SiO_2 contents shows that the fractionation sequence is substantially more complex. Projected onto the CS–MS–A plane (fig. 54), these compositions form a cluster above the 30-kbar phase boundary. The spread of points extends from slightly alkaline compositions to compositions more silica saturated than those of the high-Ti basalts. The lower-flank

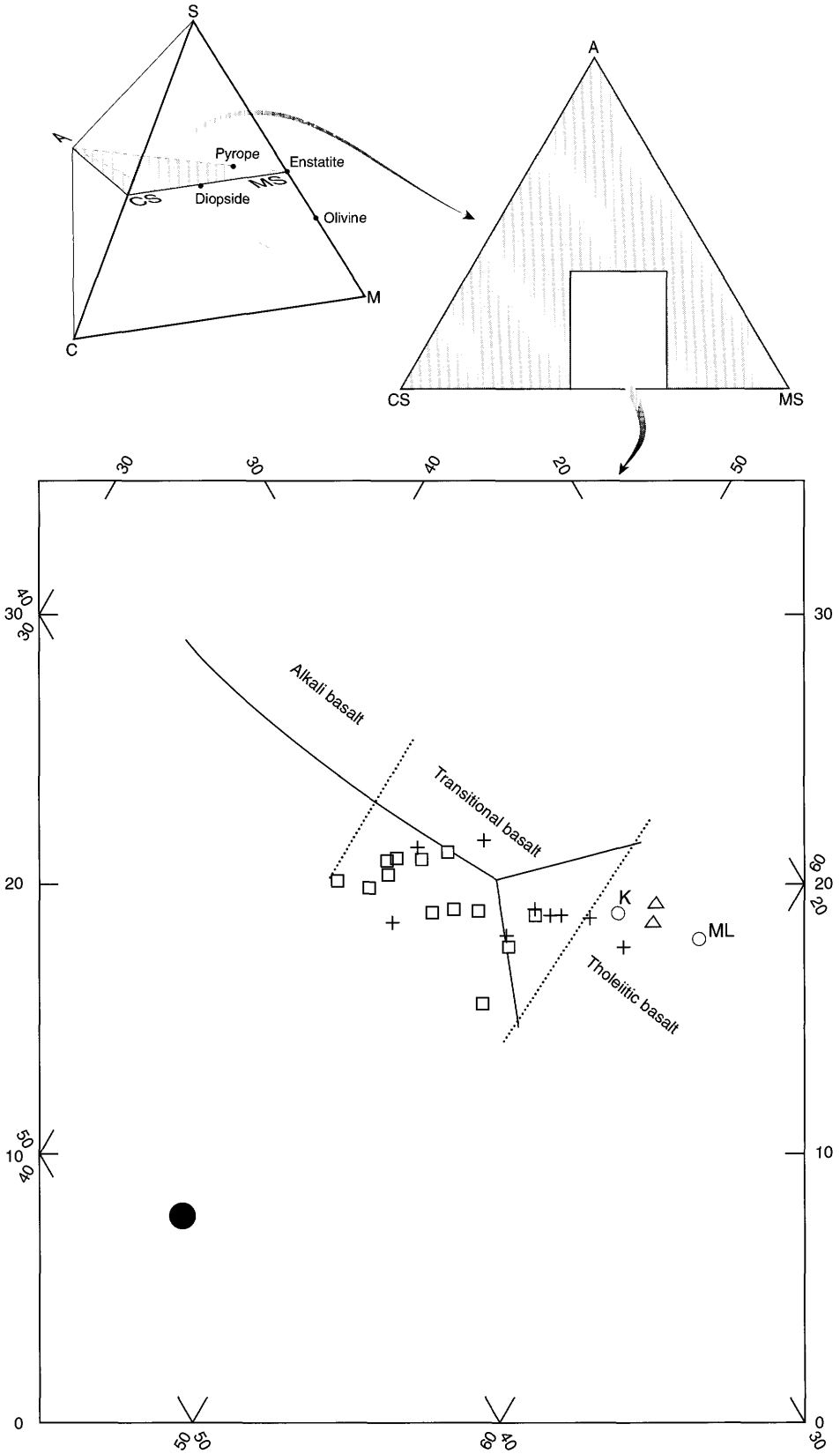

Figure 46. Selected compositions of picrite and ankaramite, projected from olivine onto CS–MS–A plane of the C–M–S–A tetrahedron of O'Hara (1968). See figure 40 for algorithm used to derive components of tetrahedron. Solid lines, 30-kbar phase boundaries of O'Hara (1968); dotted lines, boundaries between fields of alkali basalt, transitional basalt, and tholeiitic basalt. Plotted lava compositions: squares, ankaramite from Mauna Kea; pluses, high-Ca picrite from Mauna Kea; triangles, tholeiitic picrite from Hilo Ridge; circles, average compositions of picrites from Kilauea (K) and Mauna Loa (ML) (Wilkinson and Hensel, 1988); large dot, composition of clinopyroxene phenocryst in ankaramite of the Hamakua Volcanics (table 8).

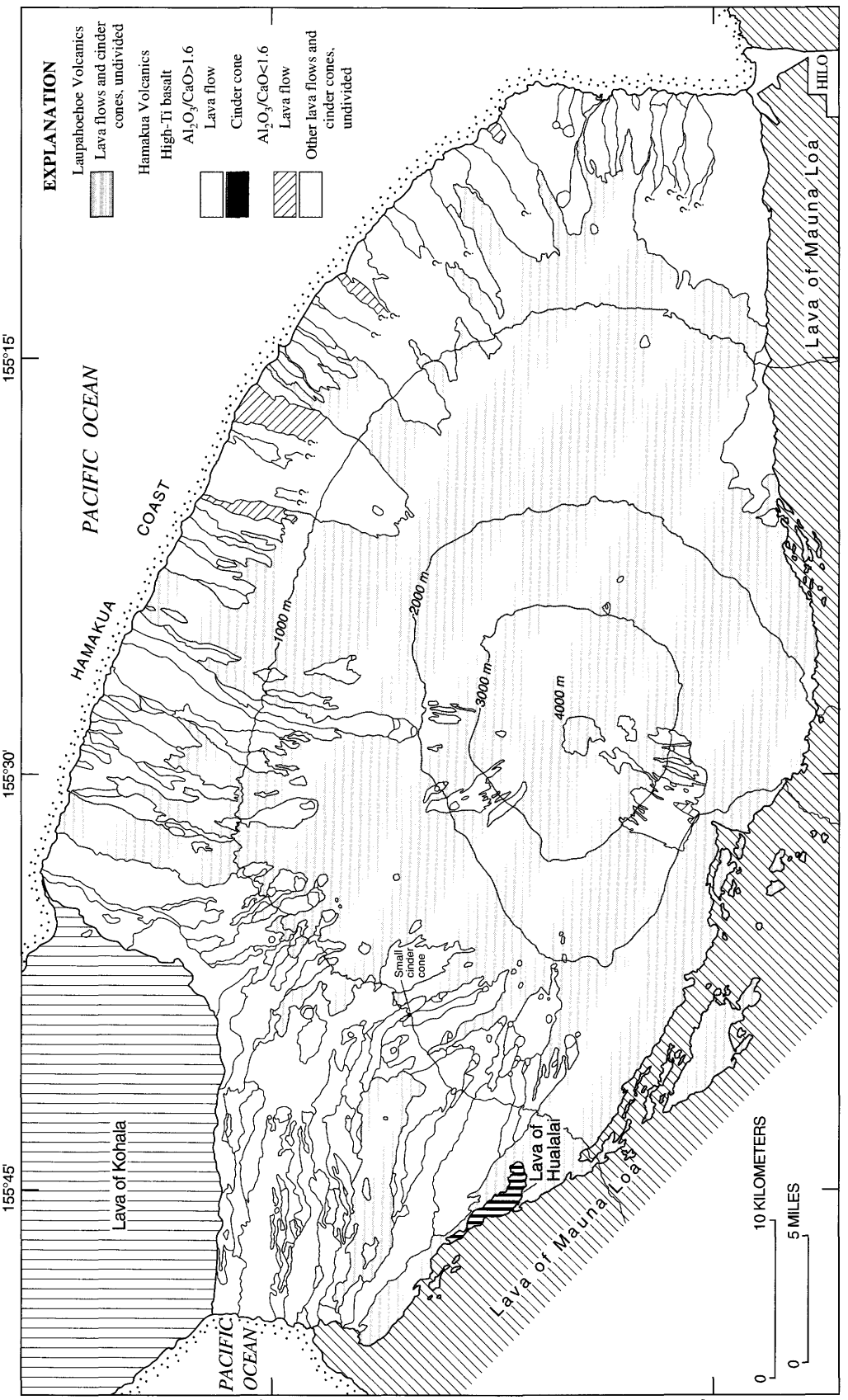

Figure 47. Geologic map of Mauna Kea, showing generalized distribution of two types of high-Ti basalt lava flows of the Hamakua Volcanics. Internal contacts distinguish individual lava flows and cinder cones. Queries mark limits of mapping at edge of dense rain forest. Geology simplified from plates 1 and 2 and Wolfe and Morris (1996).

Table 12. Major-oxide and normative-mineral compositions of high-Ti basalts of the Hamakua Volcanics

[Major-oxide compositions and Cross, Iddings, Pirsson, and Washington (CIPW) norms in weight percent; major oxides adjusted to 100 percent dry weight after partitioning of Fe to FeO and Fe_2O_3 in the ratio 88:12. See table 1 for original analyses and analysts]

	$Al_2O_3/CaO>1.60$			$Al_2O_3/CaO<1.60$		
Sample	IO-6	La-103	Mu-11	IT-7	JS-1	JS-2
Major oxides						
SiO_2	46.49	45.82	46.84	47.32	46.76	46.80
Al_2O_3	14.85	15.02	14.82	14.04	13.78	13.79
Fe_2O_3	1.93	1.99	1.91	1.74	1.83	1.86
FeO	12.73	13.13	12.63	11.50	12.09	12.26
MgO	5.13	5.01	5.22	5.21	5.30	5.18
CaO	8.42	7.96	8.69	10.23	9.83	9.60
Na_2O	3.38	3.45	2.94	3.17	3.28	3.17
K_2O	1.43	1.67	1.22	1.11	1.31	1.35
TiO_2	4.65	4.84	4.90	4.85	4.91	5.03
P_2O_5	.76	.89	.62	.63	.71	.75
MnO	.22	.22	.21	.20	.20	.21
CIPW norms						
q	0.00	0.00	0.00	0.00	0.00	0.00
or	8.45	9.87	7.21	6.56	7.74	7.98
ab	28.60	27.25	24.88	26.82	26.49	26.82
an	21.12	20.57	23.64	20.80	19.01	19.41
ne	.00	1.05	.00	.00	.68	.00
di	13.03	10.91	12.79	21.32	20.77	19.30
hy	.09	.00	10.70	2.47	.00	1.61
ol	15.30	16.22	7.28	8.83	11.68	10.90
mt	2.80	2.89	2.77	2.52	2.65	2.70
il	8.83	9.19	9.31	9.21	9.33	9.55
ap	1.80	2.11	1.47	1.49	1.68	1.78

Samples:

IO-6. Flow exposed in Kamakoa Gulch (see pls. 1, 4).

IT-7. Flow forming northwest rim of Maulua Gulch (see pl. 4 for location).

JS-1. Top flow of Kaawalii Gulch section (see fig. 13).

JS-2. Flow along southeast side of Kukaiau Gulch, Hamakua coast (see pl. 4 for location).

La-103. Flow near top of southeastern Laupahoehoe Gulch section (see fig. 13).

Mu-11. Flow near top of Maulua Gulch section (see fig. 13).

basalts with compositions similar to basalts of the Liloe Spring volcanic member would plot within this same cluster. All sampled basalts of the Liloe Spring Volcanic Member have compositions that have been affected by plagioclase and (or) augite fractionation (fig. 53).

The basalts of the Liloe Spring Volcanic Member must have evolved within a magma chamber sufficiently shallow in the volcano to feed vents at or near the summit during the later part of the basaltic substage. Because this magma system persisted over a period of several tens of thousands of years, it is important to determine the composition of the parental magma and the fractionation process. Because all the basalts of the Liloe Spring Volcanic Member contain less than 7.0 weight percent MgO, none was erupted without some fractionation. Therefore, we have no direct evidence of the parental-magma composition. Transitional basalt (sample IP–21) has a composition similar in degree of silica saturation to much of the Liloe Spring cluster. Mass-balance calculations, using this transitional basalt as a parental magma and various Liloe Spring basalts as daughter magmas, give moderately good fits (see table 15; liquid-descent line, fig. 53). Because results with these parents and various possible Liloe Spring daughters show fits that are better for some pairs than for others, there is probably not a

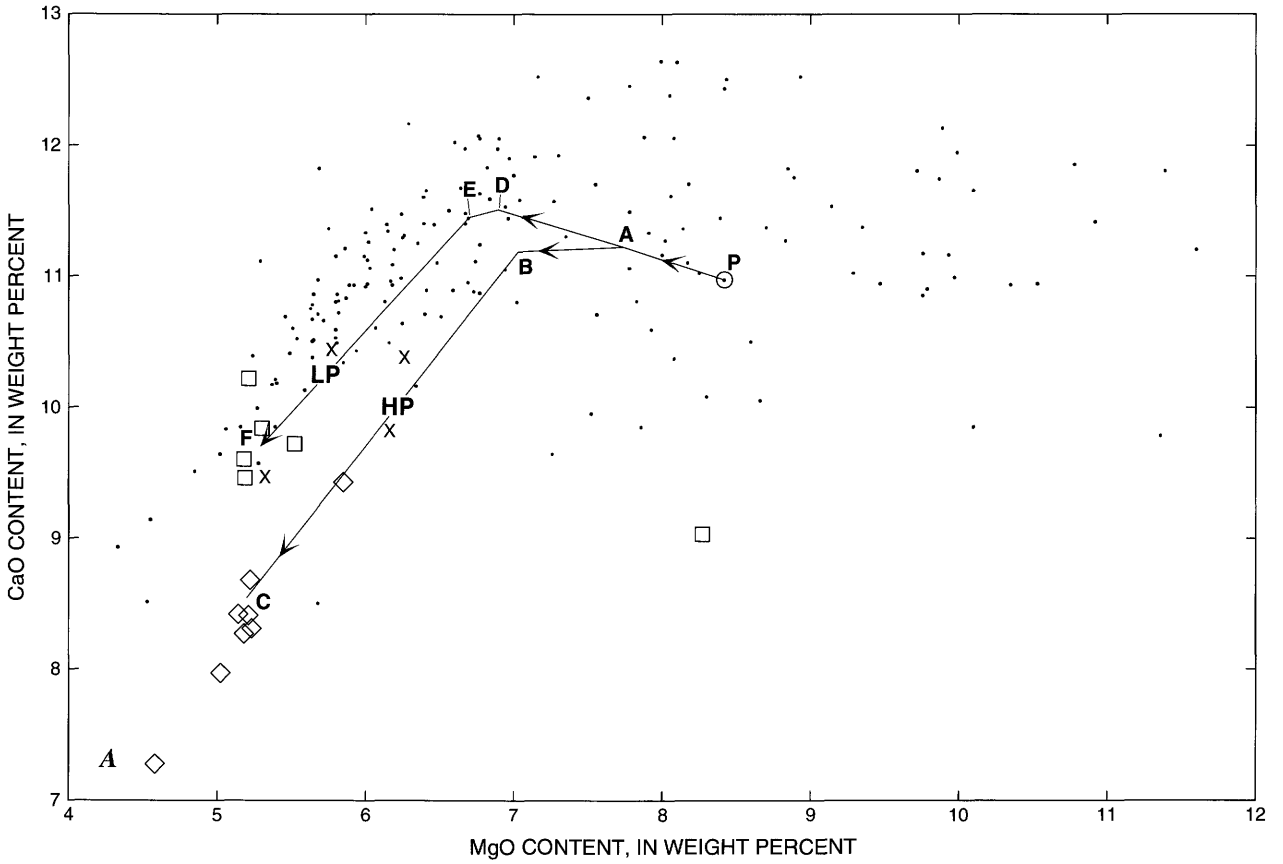
CaO CONTENT, IN WEIGHT PERCENT
MgO CONTENT, IN WEIGHT PERCENT
A
E
D
A
P
B
LP
HP
F
C

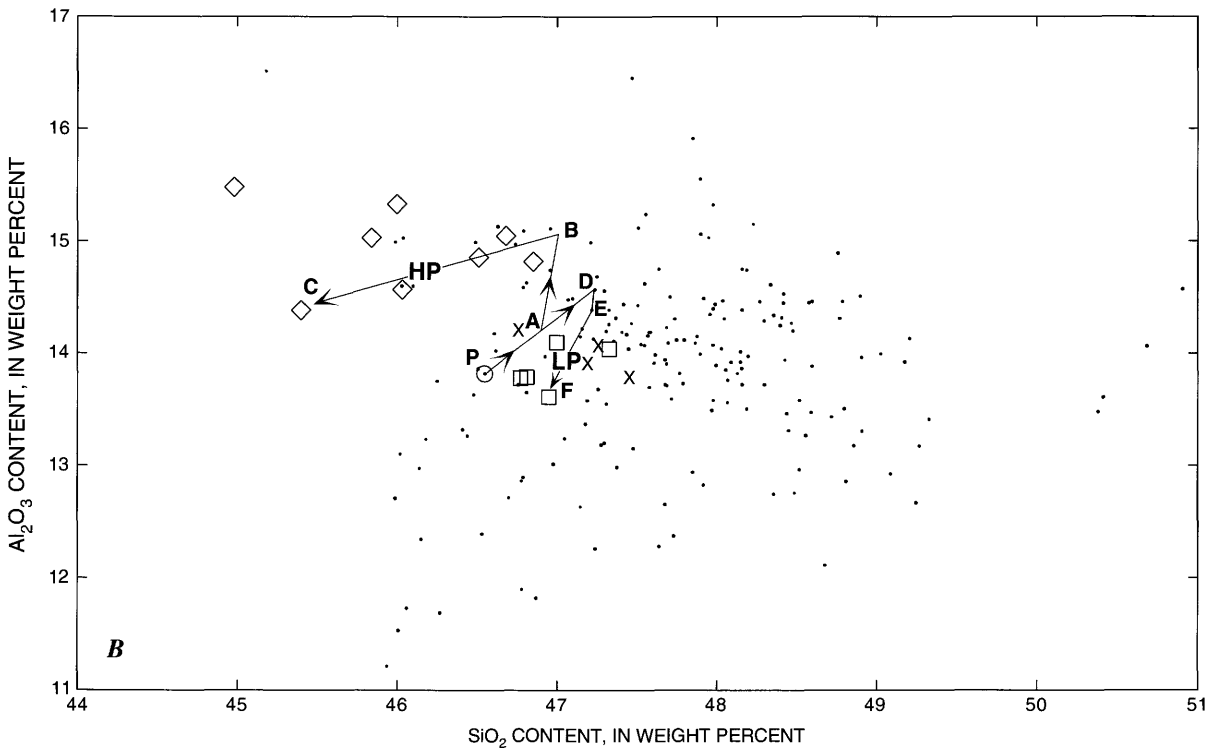
Al_2O_3 CONTENT, IN WEIGHT PERCENT
SiO_2 CONTENT, IN WEIGHT PERCENT
B
HP
C
D
E
A
P
LP
F
B

← **Figure 48.** Variation diagrams comparing high-Ti basalts (containing more than 4.5 weight percent TiO_2) with other basalts of the Hamakua Volcanics, showing hypothetical paths of magma evolution. *A*, CaO versus MgO contents. *B*, Al_2O_3 versus SiO_2 contents. Diamonds, high-Ti basalts with Al_2O_3/CaO ratios of >1.6; squares, high-Ti basalts with Al_2O_3/CaO ratios of <1.6; x's, basalts containing 4.0 to 4.5 weight percent TiO_2; circle, sample HP–13 (basalt of the Hamakua Volcanics), which is modeled as parental magma of high-Ti basalts (see table 13); dots, other basalts of the Hamakua Volcanics. On each diagram, two liquid-descent lines are shown; both start from point P, composition of hypothetical parental magma, but diverge at point A. Along lower-pressure path (LP), from point P to point D, only olivine is removed from magma; from point D to point E, olivine+plagioclase is removed; and from point E to point F, olivine+plagioclase+augite is removed. Along higher-pressure path (HP), from point P to point A, only olivine is removed; from point A to point B, olivine+augite is removed; and from point B to point C, olivine+augite+plagioclase is removed.

parental magma common to all basalts of the Liloe Spring Volcanic Member. Furthermore, several flows within the Liloe Spring Volcanic Member are alkaline in composition (fig. 54; for example, samples HQ–24, Wa–16, table 1) and evolved from parental magmas similar in composition to sample HP–13 (fig. 49).

Inconsistent results of calculations to test crystal fractionation between various pairs of basalts of the Liloe Spring Volcanic Member (for example, samples HR–8, HQ–14, table 15) show that few of these lavas are truly comagmatic. In contrast, samples of lavas shown to be from the same vent but with different lithologies and compositions (for example, samples HQ–13, HQ–14) do give the expected low residuals (see table 15; liquid-descent line, fig. 53.)

Our interpretation of the field and petrographic observations and the results of mass-balance calculations is that the basalts of the Liloe Spring Volcanic Member were erupted from a long-lived (approx 10^4–10^5 yr), relatively shallow magma chamber beneath the summit of the volcano. Magma batches of differing composition periodically fed this chamber and, after remixing of the new and residual magmas, cooled sufficiently to allow the separation of 5 to 20 percent of crystals before the next eruption. Some eruptions may have produced voluminous flows, which traveled as far as the lower flanks.

PLAGIOCLASE-RICH BASALTS

Basalts unusually rich in plagioclase phenocrysts (more than 8–10 volume percent) were erupted late in the basaltic substage (see pl. 1). The vents for these flows are concentrated on the west flank of the volcano, although several flows are on the surface of the northeast flank (fig. 55). Nearly 75 percent of the exposed vents on the west flank erupted plagioclase-rich basalts.

All of these plagioclase-rich basalts contain plagioclase phenocrysts (An_{77}–An_{82}) that are blocky, 3 to 4 mm across, and complexly twinned. Accompanying the plagioclase in subordinate amounts are olivine and augite phenocrysts, set in a pilotaxitic groundmass of plagioclase, augite, and magnetite (fig. 44*E*). Chemical compositions of these basalts generally show somewhat higher Al_2O_3 contents than in most other Hamakua basalts (see fig. 56; table 16), suggesting either the removal of clinopyroxene, as in the high-Ti basalts, or the addition of plagioclase.

Mass-balance calculations, using sample IP–20 (table 17) as a likely parental magma, suggest that plagioclase addition is important in at least some of the basalts (for example, samples IP–6, IQ–16). The plagioclase-rich basalts contain more phenocrysts of plagioclase relative to phenocrysts of olivine and augite than do other Hamakua basalts. Genesis of the plagioclase-rich basalts must have involved the emplacement of basaltic magma at a level within the volcano superstructure where slow crystallization of the three silicate phases proceeded. Some olivine and augite were removed from the magma, but plagioclase crystals, kept in suspension, were concentrated before eruption. It is tempting to speculate that all of the west-slope vents (fig. 55) represent eruptions from the same fractionating magma chamber under that part of the volcano during late Hamakua time.

A few lavas in this system were fractionated almost to the limit of the basalt field. Sample IP–2 (fig. 56; table 16) is a plagioclase-bearing basalt that is not as porphyritic as those described above; mass-balance calculations (table 17) suggest the removal of much more augite and plagioclase.

The plagioclase-rich basalts were erupted from numerous vents on the west flank of Mauna Kea, as well as at scattered localities elsewhere on the volcano (fig. 55). This basalt type, which appeared late in the basaltic substage, could have been erupted contemporaneously with the activity that produced the basalts of the Liloe Spring Volcanic Member. The plagioclase-rich basalts originated by crystal fractionation of a subalkaline parental magma slightly less silica saturated than basalts of the Liloe Spring Volcanic Member.

BASALTS OF THE HOPUKANI SPRINGS VOLCANIC MEMBER

The basalts of the Hopukani Springs Volcanic Member, which crop out on the upper south and east flanks of the volcano (pl. 2), represent eruptions from the summit region. The exposed lavas do not represent as long a timespan as those in the coastal gulches.

The Hopukani Springs lavas include picrite, ankaramite, olivine basalt, plagioclase basalt, and various weakly porphyritic, evolved basalts. The porphyritic basalts

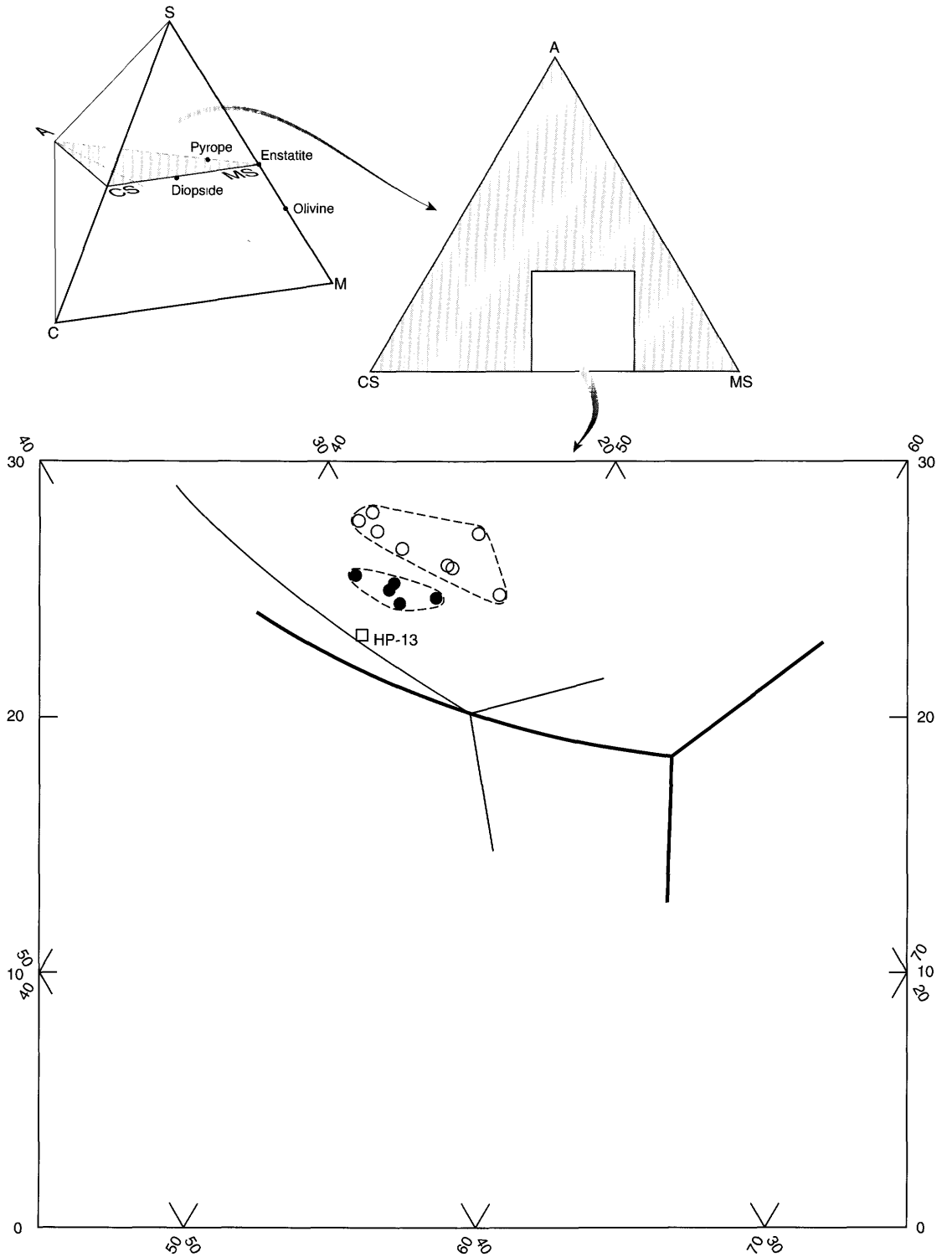

Figure 49. Selected compositions of high-Ti basalt of the Hamakua Volcanics, projected from olivine onto CS–MS–A plane of C–M–S–A tetrahedron of O'Hara (1968). See figure 40 for algorithm used to derive components of tetrahedron. Heavy lines, 1-bar phase boundaries of O'Hara (1968); light lines, 30-kbar phase boundaries of O'Hara (1968). Dashed lines delineate two groups of high-Ti basalt samples that are distinguished on the basis of Al_2O_3/CaO ratios (see table 12 for compositions of representative samples): dots, samples with ratios of <1.6 that are inferred to have fractionated at relatively low pressure; circles, samples with ratios of >1.6 that are inferred to have fractionated at relatively high pressure. Plots of two groups are displaced toward successively higher-pressure cotectic positions (cotectic lines not shown) of O'Hara (1968). Square, composition of sample HP–13 (basalt of the Hamakua Volcanics), which is modeled as parental magma of high-Ti basalts. See table 13 for mass-balance calculations.

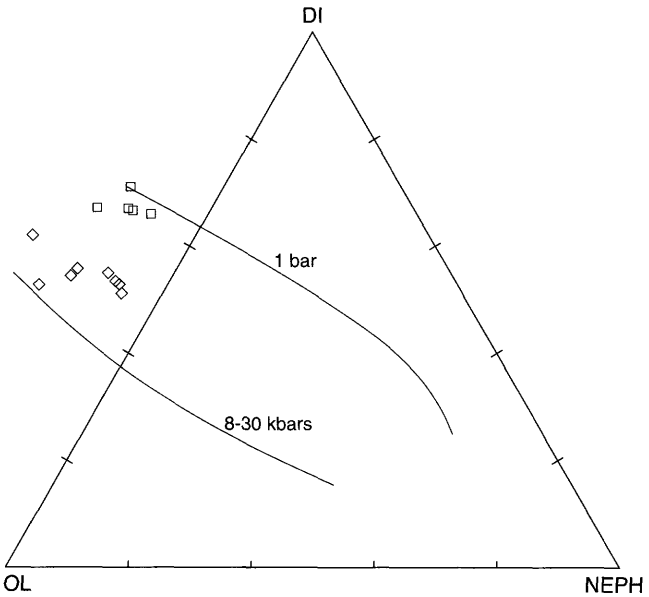

Figure 50. Selected compositions of high-Ti basalt of the Hamakua Volcanics, projected from plagioclase onto DI–OL–NEPH plane of Sack and others (1987). Components of triangular projection (see Sack and others, 1987, for full discussion of projection): DI, $(CaO+TiO_2+Na_2O+K_2O)-(Al_2O_3+Fe_2O_3)$; NEPH, $\frac{1}{4}(11Na_2O+11K_2O+3CaO+Al_2O_3+Fe_2O_3+FeO+MnO+MgO)-\frac{1}{2}(SiO_2+2TiO_2)$; OL, $\frac{1}{2}(FeO+MnO+MgO+Al_2O_3+Fe_2O_3-CaO-Na_2O-K_2O)$. Curves show cotectic lines at different pressures. Two groups of high-Ti basalts are distinguished on the basis of Al_2O_3/CaO ratios (see table 12): squares, samples with ratios of <1.6, which cluster near 1-bar cotectic line; diamonds, samples with ratios of >1.6, which plot closer to 8- to 30-kbar cotectic line, suggesting that they represent liquids derived at higher pressures.

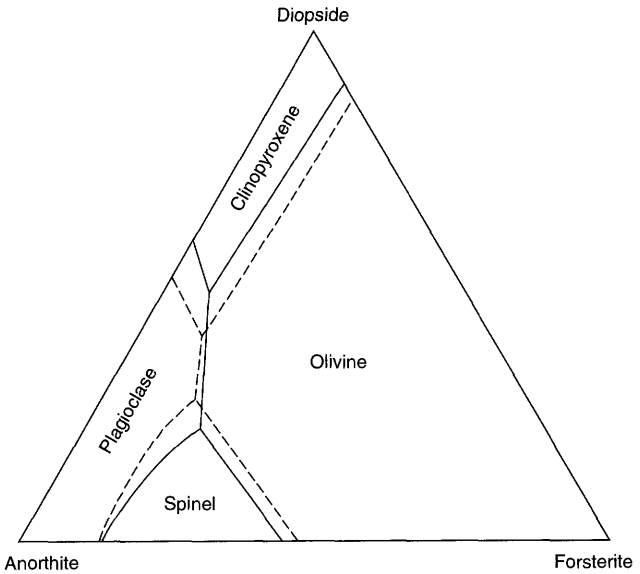

Figure 51. Liquidus boundaries in diopside-anorthite-forsterite system (from Presnall and others, 1978), showing different crystallization paths at different pressures. Solid lines, 1-bar phase boundaries; dashed lines, 3-kbar phase boundaries. Clinopyroxene field is larger at 3 kbars than at 1 bar; therefore, more clinopyroxene crystallizes before composition of liquid reaches boundary with plagioclase, causing higher augite/plagioclase ratios in fractionating crystals. See table 13 for mass-balance calculations.

contain plagioclase, olivine, and augite phenocrysts, 2 to 4 mm across. In some flows, these minerals also occur in clots that appear to be accumulations of fractionated phases. Where the groundmass for all of these basalts is nearly holocrystalline, it is pilotaxitic and consists of minor olivine, abundant plagioclase and augite, and scattered titanomagnetite and ilmenite.

The compositions of representative Hopukani Springs lavas are listed in table 18. Data for these and another 15 samples are projected onto the CS–MS–A plane in figure 57, where most data points are included within one of four groups (A–D) within which the lavas are related by composition and proximity. Each group was derived from a unique parental magma, and its members are probably related by crystal fractionation.

The samples in group A are unique among the Hamakua Volcanics because of their high CaO content (more than 12 weight percent) and SiO_2 content. All of these samples come from a section of olivine-bearing lavas exposed in Waikahalulu Gulch at 2,925-m (9,600 ft) elevation. A parental magma for group A is similar to sample Wa–8 (table 18).

The samples in group B were collected in both Pohakuloa and Waikahalulu Gulches. Several of these lavas contain more than 7 weight percent MgO (for example, sample HQ–16, table 18), but they are so phenocryst rich that their compositions may reflect accumulation of crystals and clots of crystals.

The three samples in group C are from exposures on the east side of the volcano near Waipahoehoe Gulch (pl. 2; for example, sample HR–59, table 18). Finally, the three samples in group D are from a sequence of flows in the uppermost part of Pohakuloa Gulch, at 3,700-m (12,400 ft) elevation (for example, sample HR–51, table 18).

Mass-balance calculations show that each of these groups is compositionally distinct. The compositions of the samples within each group are sufficiently similar to indicate that the lavas could be comagmatic. Comparison of the spread of points in figure 57 with those for the Hamakua Volcanics in general (fig. 40) shows some overlap, but the compositions of the samples in group A are unique. The parental magmas for all analyzed Hopukani Springs lavas were less alkaline than many of the Hamakua lavas, suggesting that the melts feeding vents near the summit resulted from higher degrees of partial melting than for many of the lavas erupted on the lower flanks.

Comparison of figures 54 and 57 shows that the samples in group B are similar in degree of silica saturation to many Liloe Spring lavas. However, we were unable to find a parental-magma composition from group B that yielded

Table 13. Mass-balance calculations testing the derivation of high-Ti basalts

[All values in weight percent, calculated to 100 percent dry weight]

	Parental magma (sample HP-13)	Daughter (sample La-103)			Daughter (sample JS-2)		
		Observed (a)	Modeled (b)	Residual (a-b)	Observed (a)	Modeled (b)	Residual (a-b)
SiO_2	46.61	45.93	45.97	-0.04	46.88	46.88	0.0
Al_2O_3	13.83	15.05	15.06	-.01	13.81	13.80	.01
Fe (as FeO)	12.89	14.93	14.96	-.03	13.97	13.99	-.02
MgO	8.43	5.02	5.02	.0	5.19	5.16	.03
CaO	10.99	7.98	7.97	.01	9.62	9.61	.01
Na_2O	2.51	3.46	3.40	.06	3.18	3.15	.03
K_2O	.83	1.67	1.64	.03	1.35	1.44	-.09
TiO_2	3.28	4.85	4.86	-.01	5.04	4.92	.12
P_2O_5	.42	.89	.89	.0	.75	.80	-.05
MnO	.20	.22	.25	-.03	.21	.25	-.04
Sum of the squares of residuals				.008			.029
Phases removed from parental magma in calculating modeled composition:							
Olivine (Fo_{74})				-6.12			-8.15
Clinopyroxene[1]				-24.13			-18.28
Plagioclase (An_{60})				-19.23			-21.36
Magnetite[1]				-2.87			-3.20
Total				-52.35			-50.99

[1]Augite composition: $Wo_{40}En_{48}Fs_{12}$, with 1.61 weight percent TiO2 and 3.62 weight percent Al_2O_3 (see table 8); magnetite composition: see table 8.

low residuals in mass-balance calculations to derive any Liloe Spring lava. An important feature of Hamakua lavas erupted from the summit region, in both the Hopukani Springs and Liloe Spring Volcanic Members, is the predominantly high degree of silica saturation. These lavas, erupted from the summit of the volcano above the inferred, earlier shield-stage summit reservoir (see subsection below entitled "Shield Stage"), appear to represent magmas that were generated with the highest degrees of melting of all those erupted during the postshield stage.

BASALT FROM KANOA

Basalt containing about 3 volume percent of small (1 mm diam) olivine phenocrysts was erupted northwest of Hilo from Kanoa and a nearby cone (fig. 12). These flows are older than the ankaramite flow from Kauku that wraps around the two cones. The composition of this basalt, which is unique on Mauna Kea, is listed in table 19; it shows some of the features of evolved Hamakua rocks and some of strongly alkaline basalts. The high TiO_2, total Fe, and alkali contents are similar to those of the high-Ti basalts, but the low SiO_2 and high MgO contents are similar to those of nephelinitic lavas of the Honolulu Volcanics (Macdonald, 1968), which have much lower Fe and TiO_2 contents. The high MgO content suggests that this composition most likely represents a magma that has not evolved owing to crystal fractionation. However, the high Fe, TiO_2, and alkali contents suggest a primitive melt with a very low degree of partial melting.

LAUPAHOEHOE VOLCANICS

INTRODUCTION

A major result of our mapping of the entire surface of Mauna Kea is recognition that the boundary between the Hamakua and Laupahoehoe Volcanics is petrologic as well as stratigraphic. As shown in figures 5 and 6, the lavas of these two formations are compositionally distinct. Wherever hawaiitic lavas are found in contact with basalt, the basalt is invariably older. Therefore, a striking conclusion is that hawaiitic lavas were erupted only after basalt production ceased at or earlier than approximately 70 ka.

A distinct compositional gap separates the Laupahoehoe and Hamakua Volcanics (figs. 5, 6). Although early interpretations of the hawaiitic lavas as "andesitic" differentiates (Daly, 1911; Washington, 1923) appears intuitively correct, the connection is far from straightforward. West

Table 14. Major-oxide and normative-mineral compositions of representative lavas of the Liloe Spring Volcanic Member and of a similar flow from the northwest flank of Mauna Kea

[Major-oxide compositions and Cross, Iddings, Pirsson, and Washington (CIPW) norms in weight percent; major oxides adjusted to 100 percent dry weight after partitioning of Fe to FeO and Fe_2O_3 in the ratio 88:12. See table 1 for original analyses and analysts]

	Liloe Spring Volcanic Member				Northwest Flank
Sample----- HQ-5	HQ-13	HQ-14	HR-8	HR-41	IO-13
Major oxides					
SiO_2 --------47.22	48.14	48.15	48.18	48.57	48.42
Al_2O_3 -------14.13	13.91	14.39	13.97	13.47	13.94
Fe_2O_3 ------- 1.82	1.83	1.66	1.66	1.84	1.79
FeO---------12.05	12.11	10.99	10.97	12.15	11.86
MgO--------- 5.80	5.48	6.24	7.00	5.16	5.64
CaO---------10.80	10.41	11.29	11.77	9.84	10.49
Na_2O -------- 2.91	2.71	2.60	2.30	3.05	2.55
K_2O --------- .72	.88	.79	.68	1.10	.97
TiO_2 -------- 3.91	3.83	3.31	2.91	4.07	3.66
P_2O_5 -------- .44	.47	.40	.36	.54	.48
MnO--------- .20	.21	.19	.19	.21	.20
CIPW norms					
q---------- 0.00	0.00	0.00	0.00	0.00	0.00
or---------- 4.25	5.20	4.67	4.02	6.50	5.73
ab----------24.62	22.93	22.00	19.46	25.81	21.58
an----------23.37	23.19	25.26	25.79	19.81	23.73
ne---------- .00	.00	.00	.00	.00	.00
di----------22.62	21.06	23.18	24.87	21.16	20.86
hy---------- 3.63	12.66	8.31	10.42	10.22	14.98
ol----------10.42	3.93	6.97	6.67	4.85	2.47
mt---------- 2.64	2.65	2.41	2.41	2.67	2.60
il---------- 7.43	7.27	6.29	5.53	7.73	6.95
ap---------- 1.04	1.11	.95	.85	1.28	1.14

Samples:

HQ-5. Nearly aphyric basalt from surface flow on slope above Pohakuloa Training Area (see pls. 2, 3).

HQ-13. Nearly aphyric basalt from cinder cone exposed in west wall of Pohakuloa Gulch (same cone as for sample HQ-14; see pls. 2, 3).

HQ-14. Plagioclase-phyric basalt from cinder cone exposed in west wall of Pohakuloa Gulch (same cone as for sample HQ-13; (see pls. 2, 3).

HR-8. Moderately porphyritic basalt from small gulch west of Waikahalulu Gulch (see pls. 2, 3).

HR-41. Aphyric basalt from fissure ridge west of Keanakakoi (adz quarry) (see pls. 2, 3).

IO-13. Weakly porphyritic basalt flow north of Kamakoa Gulch (see pls. 1, 4).

and others (1988) pointed out that fractionation trends in the two series are offset, suggesting that derivation of hawaiite from basalt is not likely to be a matter of low-pressure differentiation.

In this section, we review the petrologic features of Laupahoehoe lavas and discuss the origin of the group as a whole in the context of the development of the postshield stage of the volcano.

PREVIOUS INVESTIGATIONS

Several recent petrologic and geochemical studies have focused primarily on the origin of the Laupahoehoe Volcanics. Jackson and others (1982) and Fodor and Vandermeyden (1988) studied the mafic and ultramafic xenoliths that occur in 20 to 30 percent of the cinder cones and lava flows. Because these xenoliths are common in the hawaiitic lavas

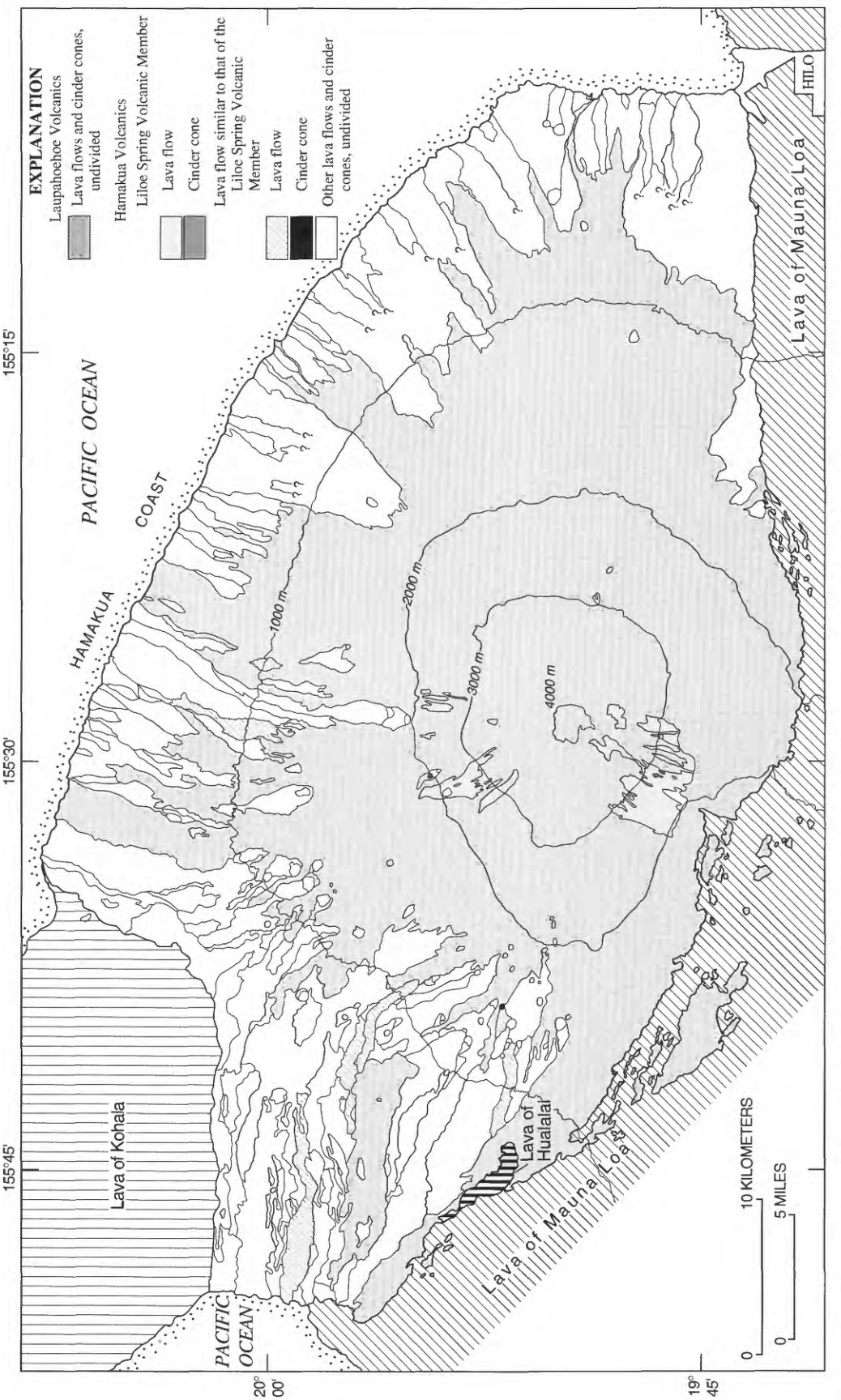

Figure 52. Geologic map of Mauna Kea, showing generalized distributions of basalts of the Liloe Spring Volcanic Member of the Hamakua Volcanics on upper flanks and of lavas of similar age and composition on lower flanks. Internal contacts distinguish individual lava flows and cinder cones. Queries mark limits of mapping at edge of dense rain forest. Geology simplified from plates 1 and 2 and Wolfe and Morris (1996).

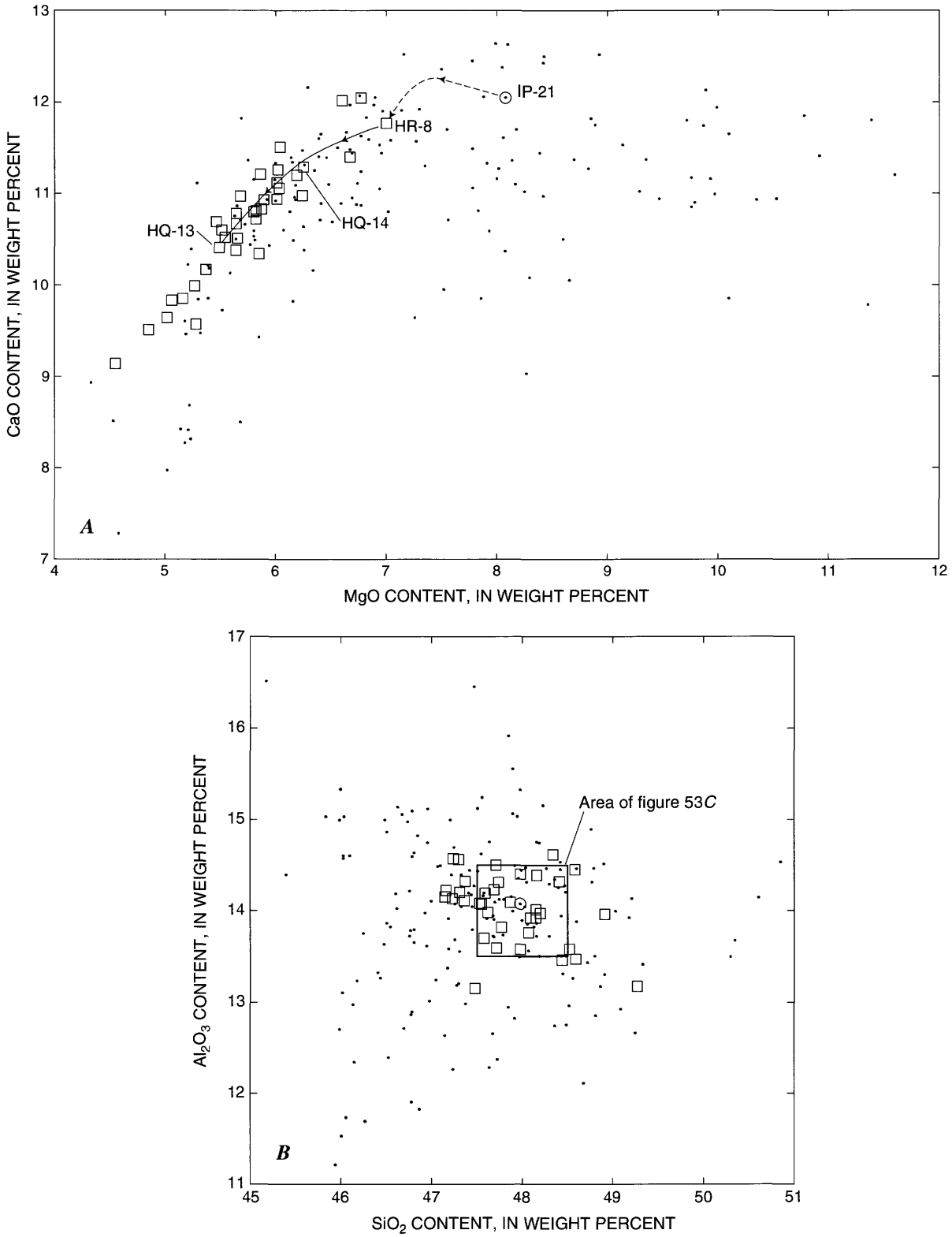

Figure 53. Variation diagrams comparing basalts of the Liloe Spring Volcanic Member of the Hamakua Volcanics (squares) with all other basalts of the Hamakua Volcanics (dots), showing hypothetical paths of magma evolution. *A*, CaO versus MgO contents. *B*, *C*, Al_2O_3 versus SiO_2 contents. Sample IP-21 (circle) is a hypothetical parental magma (see table 15), and liquid-descent lines (dashed where uncontrolled by compositions of specific samples) are shown for parent-daughter pairs listed in table 15. Scatter of data points in figure 53*B* reflects a range of parental-magma compositions, possibly a result of mixing in an open magma chamber.

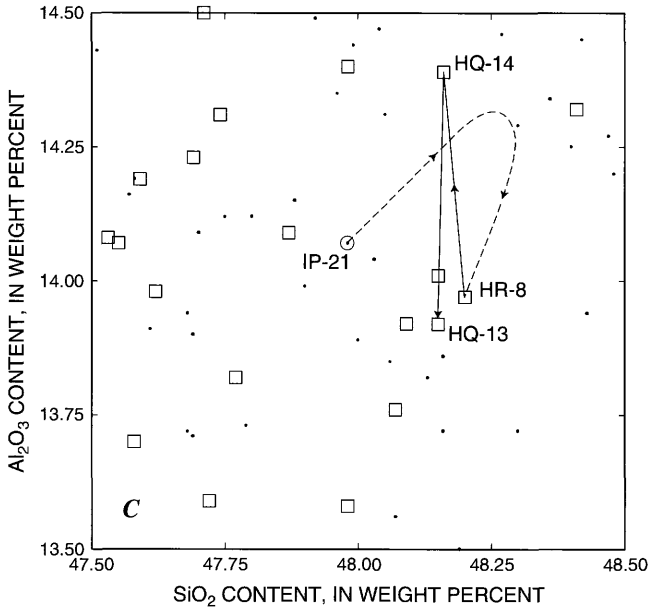

Figure 53. Continued.

but not in the underlying basalts, the gabbros were used by Fodor and Vandermeyden to model crystal fractionation from basalt to hawaiite.

Trace-element analysis of Hamakua basalts and Laupahoehoe hawaiites by Frey and others (1990) provides the basic model for the fractionation process. Frey and his colleagues noted that incompatible trace elements, such as P or Ce, are twice as abundant in the hawaiitic lavas as in the basaltic lavas, showing that hawaiitic magma represents residual liquid after crystallization of approximately half of a reasonable basaltic parental magma. However, Sr content also increases between the two series, exhibiting incompatible behavior. Because Sr is fractionated into plagioclase, Frey and others (1990) interpreted these observations to indicate that fractionation could not involve much, if any, plagioclase and thus would have to take place at a pressure sufficiently high to suppress plagioclase crystallization. The fractionation was modeled by Frey and others (1990) and Fodor and Vandermeyden (1988) with this high-pressure constraint.

West and others (1988) studied the compositional variation within a group of Laupahoehoe samples from the summit and south flank of Mauna Kea; they found neither temporal nor spatial control of the composition. Major- and trace-element variations were shown to result from crystal fractionation, which was interpreted as a likely result of crystal growth along conduit or magma-chamber surfaces over a range of pressures.

PETROGRAPHY

Laupahoehoe lavas, whether hawaiite, mugearite, or benmoreite, are typically aphyric. In hand specimen, they are dense, medium to dark gray, and contain very few discernible crystals. A few flows are weakly porphyritic,

Table 15. Mass-balance calculations illustrating the origin of some basalts of the Liloe Spring Volcanic Member

[All values in weight percent, calculated to 100 percent dry weight]

	Parental magma (sample IP-21)	Daughter (sample HR-8), using sample IP-21 as parent			Daughter (sample HQ-14), using sample HR-8 as parent			Daughter (sample HQ-13), using sample HQ-14 as parent		
		Observed (a)	Modeled (b)	Residual (a-b)	Observed (a)	Modeled (b)	Residual (a-b)	Observed (a)	Modeled (b)	Residual (a-b)
SiO_2	48.14	48.26	48.25	0.01	48.22	48.28	-0.06	48.23	48.20	0.03
Al_2O_3	14.06	13.99	13.98	.01	14.41	14.45	-.04	13.94	13.92	.02
Fe (as FeO)	11.47	12.50	12.49	.01	12.52	12.56	-.04	13.80	13.78	.02
MgO	8.07	7.01	7.01	.0	6.25	6.27	-.02	5.49	5.48	.01
CaO	12.04	11.79	11.79	.0	11.31	11.31	.0	10.43	10.43	.0
Na_2O	2.26	2.31	2.39	-.08	2.60	2.46	.14	2.72	2.75	-.03
K_2O	.58	.68	.66	.02	.79	.74	.05	.88	.93	-.05
TiO_2	2.87	2.92	2.90	.02	3.31	3.35	-.04	3.84	3.82	.02
P_2O_5	.34	.36	.39	-.03	.40	.39	.01	.47	.49	-.02
MnO	.17	.19	.18	.01	.19	.20	-.01	.21	.21	.0
Sum of the squares of residuals				.010			.032			.006
Phases removed from or added to parental magma in calculating modeled compositon:										
Olivine	(Fo_{78})			-3.30	(Fo_{78})		-1.06	(Fo_{78})		-1.69
Plagioclase	(An_{76})			-6.03	(An_{76})		-1.78	(An_{70})		-8.92
Clinopyroxene[1]				-4.68			-5.48			-6.97
Magnetite[2]				+.95[3]			-.95			-.45
Ilmenite[2]				-.95			+.75			-.03

[1]From gabbro xenolith; see table 8 for composition.
[2]See table 8 for composition.
[3]Addition of magnetite is an unreasonable crystal-fractionation process; none of the parental magmas of the Hamakua Volcanics had Fe contents sufficiently high to derive the composition of sample HR-8 without requiring the addition of iron as magnetite.

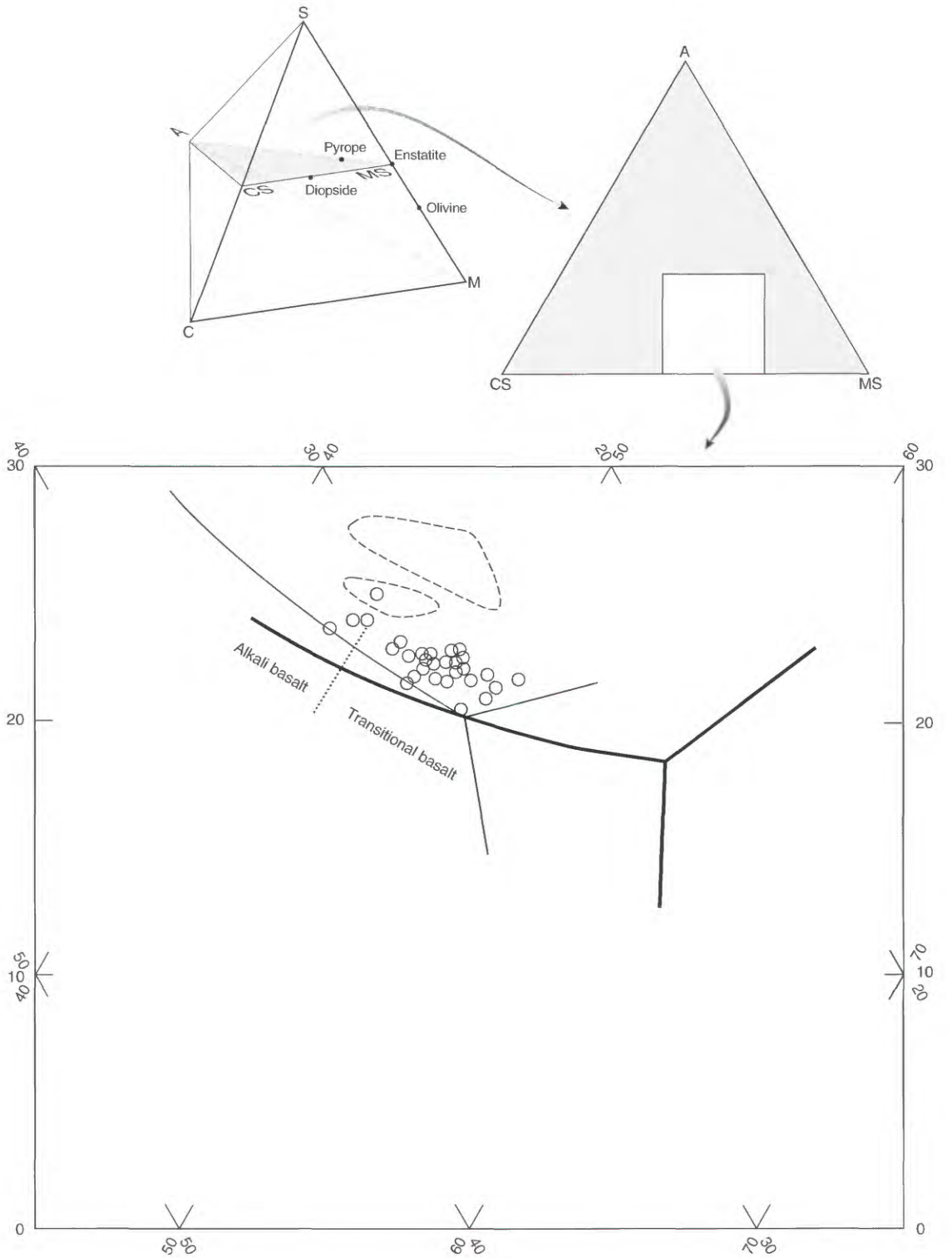

Figure 54. Selected compositions of basalt of the Liloe Spring Volcanic Member of the Hamakua Volcanics (circles), projected from olivine onto CS–MS–A plane of C–M–S–A tetrahedron of O'Hara (1968). See figure 40 for algorithm used to derive components of tetrahedron. Heavy lines, 1-bar phase boundaries of O'Hara (1968); light lines, 30-kbar phase boundaries of O'Hara (1968); dotted line, boundary between fields of alkali basalt and transitional basalt; dashed lines, boundaries of plots of two groups of high-Ti basalts from figure 49. Compositions of basalts of the Liloe Spring Volcanic Member are offset from those of high-Ti basalts toward greater silica saturation and plot closer to lower-pressure (1 bar) phase boundary.

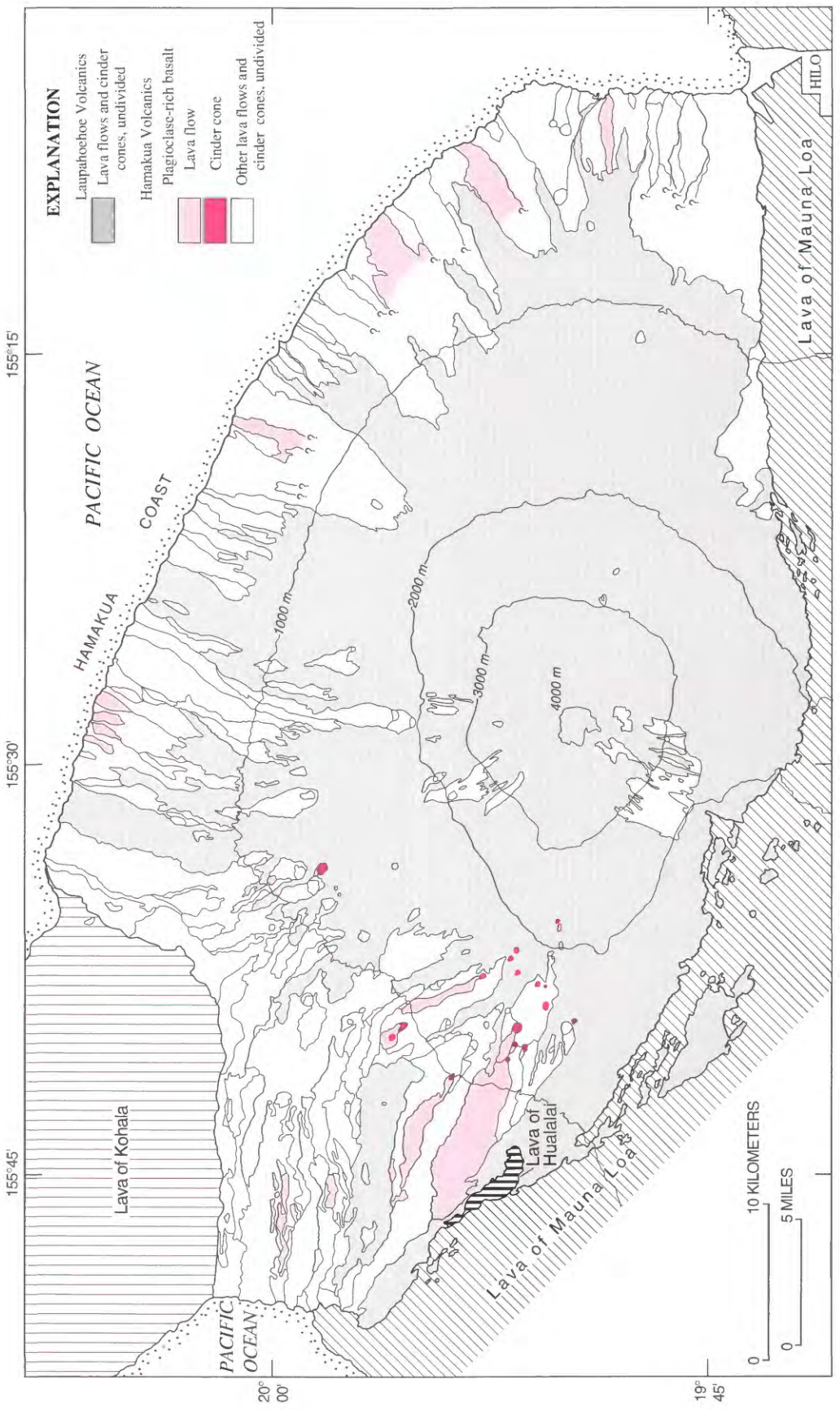

Figure 55. Geologic map of Mauna Kea, showing generalized distribution of plagioclase-rich (plagioclase phenocrysts >8 volume percent) basalt of the Hamakua Volcanics. Internal contacts distinguish individual lava flows and cinder cones. Queries mark limits of mapping at edge of dense rain forest. Geology simplified from plates 1 and 2 and Wolfe and Morris (1996).

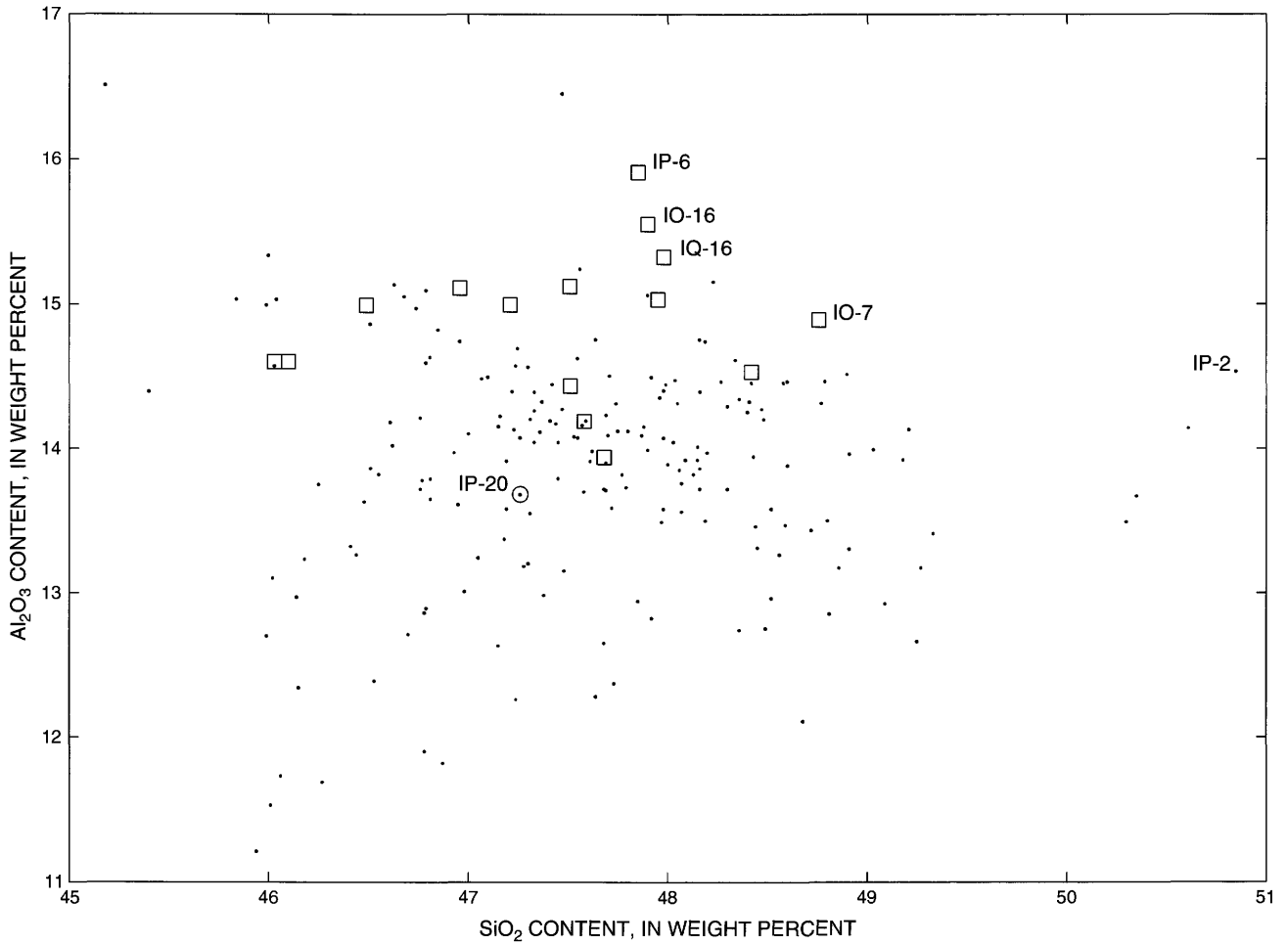

Figure 56. Al_2O_3 versus SiO_2 contents of plagioclase-rich basalts (squares) in comparison with other basalts of the Hamakua Volcanics (dots). Sample IP–20 (circle), hypothetical parental magma (see table 17); chemical analyses and normative-mineral compositions of other numbered samples are listed in table 16.

containing plagioclase phenocrysts and olivine microphenocrysts. Thin-section examination reveals a little more variation in texture and mineralogy. Several flows are characterized by plagioclase phenocrysts, thin (max 2–3 mm in longest dimension) plates, as high as 10 volume percent in abundance. Olivine and magnetite microphenocrysts, 0.2 to 0.5 mm long, are present in nearly every specimen. The groundmass of all specimens is plagioclase rich, with tiny augite grains filling interstices. Olivine and magnetite are scattered throughout; ilmenite and apatite occur in rare glass pools (fig. 44*G*). The texture of holocrystalline rocks from flow interiors is trachytic, tending toward pilotaxitic, whereas specimens collected near the surface of a flow are glassier and have hyalopilitic groundmass textures.

Benmoreite flows contain, besides the above-mentioned minerals, microphenocrysts of biotite (max 0.25 mm diam) and brown apatite (fig. 44*H*). The appearance of the apatite is similar to that in the benmoreites of Mount Etna described by Klerkx (1966), who noted that the dark color and pseudopleochroism is a result of minute inclusions of titanomagnetite or hematite.

Many Laupahoehoe lavas carried mafic and ultramafic xenoliths to the surface during eruption. A few of these flows contain abundant xenocrystic olivine, recognized by irregular shapes and, in a few examples, kink bands. Xenocrysts of plagioclase are much less common. Clinopyroxene is unstable in hawaiitic magma, as evidenced by extensive solution of xenolithic augite in contact with hawaiitic host (fig. 44*J*). Augite never occurs as phenocrysts and only rarely as xenocrysts.

Microprobe analyses of minerals from hawaiitic lavas were reported by West and others (1988). Phenocrysts and microphenocrysts of plagioclase range in composition from An_{57} to An_{60}, and olivine microphenocrysts are typically

Table 16. Major-oxide and normative-mineral compositions and phenocryst modes of representative plagioclase-rich basalts and porphyritic basalt

[Major-oxide compositions and Cross, Iddings, Pirsson, and Washington (CIPW) norms in weight percent; major oxides adjusted to 100 percent dry weight after partitioning of Fe to FeO and Fe_2O_3 in the ratio 88:12; phenocryst modes in volume percent. See table 1 for original analyses and analysts]

	Plagioclase-rich basalts				Porphyritic basalt
Sample	IO-16	IQ-16	IO-7	IP-6	IP-2
Major oxides					
SiO_2	47.89	47.97	48.75	47.84	50.84
Al_2O_3	15.55	15.32	14.88	15.91	14.53
Fe_2O_3	1.65	1.59	1.59	1.58	1.65
FeO	10.90	10.52	10.51	10.47	10.87
MgO	5.29	6.14	5.80	5.69	4.33
CaO	11.11	11.39	10.49	11.81	8.93
Na_2O	2.76	2.59	2.96	2.45	3.34
K_2O	.84	.80	.93	.73	1.37
TiO_2	3.41	3.10	3.44	2.99	3.16
P_2O_5	.40	.40	.47	.36	.76
MnO	.19	.18	.18	.17	.21
CIPW norms					
q	0.00	0.00	0.00	0.00	0.50
or	4.96	4.73	5.50	4.31	8.10
ab	23.35	21.92	25.05	20.73	28.26
an	27.56	27.81	24.57	30.26	20.61
ne	.00	.00	.00	.00	.00
di	20.65	21.47	20.10	21.45	15.62
hy	5.16	6.75	8.48	7.71	16.75
ol	7.41	8.21	6.38	6.73	.00
mt	2.39	2.31	2.31	2.29	2.39
il	6.48	5.89	6.53	5.68	6.00
ap	.95	.95	1.11	.85	1.80
Phenocryst modes					
plagioclase[1]	8.4	13.0	14.1	21.0	4.0
olivine	.3	2.0	4.7	3.9	.0
augite	.1	5.4	7.5	3.6	4.0

[1]Includes microphenocrysts.

Samples:

IO-7. Plagioclase-rich basalt flow in Kamakoa Gulch (see pls. 1,4).

IO-16. Plagioclase-rich basalt flow (see pls. 1,4).

IP-2. Porphyritic basalt flow north of Auwaiakeakua Gulch (see pls. 1,4).

IP-6. Plagioclase-rich basalt flow from Puu Papapa (see pls. 1,4).

IQ-16. Plagioclase-rich basalt of Puu o Kale (see pl. 4).

Fo_{75}. Typical groundmass-mineral compositions are listed in table 20. The compositions of coexisting magnetite and ilmenite from one hawaiite flow suggest that these minerals crystallized at temperatures near 1,060°C and an oxygen fugacity of $10^{-10.1}$ bar.

COMPOSITION

Individual flows have been mapped in most of the area covered by Laupahoehoe lavas. Samples collected from each of these flows have been analyzed for major elements

Table 17. Mass-balance calculations to derive the compositions of plagioclase-rich basalts and porphyritic basalt

[All values in weight percent, calculated to 100 percent dry weight]

	Parental magma (sample IP-20)	Daughter (sample IQ-16)			Daughter (sample IP-6)			Daughter (sample IP-2)		
		Observed (a)	Modeled (b)	Residual (a-b)	Observed (a)	Modeled (b)	Residual (a-b)	Observed (a)	Modeled (b)	Residual (a-b)
SiO_2	47.68	48.04	47.97	0.07	47.75	47.70	0.05	50.78	50.75	0.02
Al_2O_3	13.92	15.34	15.30	.04	15.95	15.92	.03	14.51	14.50	.01
Fe (as FeO)	12.14	11.98	11.93	.05	11.89	11.86	.03	12.35	12.33	.02
MgO	7.88	6.15	6.13	.02	5.68	5.66	.02	4.33	4.32	.01
CaO	11.05	11.41	11.40	.01	11.88	11.88	.03	8.92	8.92	.0
Na_2O	2.56	2.59	2.70	-.11	2.57	2.64	-.07	3.62	3.65	-.03
K_2O	.84	.80	.87	-.07	.76	.81	-.05	1.37	1.41	-.04
TiO_2	3.31	3.11	3.06	.05	2.98	2.95	.03	3.16	3.14	.02
P_2O_5	.44	.40	.47	-.07	.36	.42	-.06	.76	.77	-.01
MnO	.18	.18	.18	.0	.17	.17	.0	.21	.21	.0
Sum of the squares of residuals				.034			.017			.004
Phases removed from or added to parental magma in calculating modeled compositon:										
Olivine		(Fo_{85})		-3.50	(Fo_{85})		-4.44	(Fo_{74})		-7.29
Plagioclase		(An_{79})		+2.98	(An_{79})		+8.16	(An_{79})		-14.97
Clinopyroxene[1]				-2.36			+.25			-17.03
Magnetite[2]				+.75			+2.10			-1.46
Ilmenite[2]				-.97			-1.46			-1.77

[1]From ankaramite phenocryst; see table 8 for composition.
[2]See table 8 for composition.

(table 1); this set of 215 analyses is the basis for much of the following descriptions and discussion. A selection of analyses spanning the full compositional range is listed in table 21. MgO-variation diagrams of the full data set (fig. 58) show that Laupahoehoe lavas range in composition from hawaiite containing as much as 5.0 weight percent MgO to benmoreite containing about 2.2 weight percent MgO; however, most samples fall within a much narrower range between 3.5 and 4.5 weight percent MgO.

The compositional trends (fig. 58) clearly suggest crystal fractionation; their curvature reflects changes in the compositions of the fractionating phases, particularly plagioclase. The sharp inflection at approximately 3.0 weight percent P_2O_5 indicates that apatite fractionation occurred in the most evolved magmas.

The fractionation trend represented by the samples listed in table 21 also involves a steady increase in the degree of silica saturation. The most mafic hawaiites contain about 2 weight percent normative nepheline, whereas the benmoreites contain normative hypersthene.

The compositions of Laupahoehoe lavas have been plotted on the DI–OL–NEPH diagram of Sack and others (1987) and projected onto the CS–MS–A plane of O'Hara (1968) (figs. 59 and 60, respectively). Laupahoehoe lavas plot on the diagram of Sack and others between the trends of liquids on the olivine+orthopyroxene+clinopyroxene cotectic at 8 to 30 kbars and at 1 bar, suggesting that the magmas may represent liquids from a plagioclase+augite+olivine cotectic at elevated pressure. The displacement of points on O'Hara's projection from the low-pressure cotectic (fig. 60) also suggests fractionation at pressures higher than in shallow magma reservoirs.

ORIGIN OF THE MOST MAFIC HAWAIITE

Frey and others (1990) used trace-element abundances to argue that the most mafic hawaiites must be derived from basaltic magma by fractionation of a clinopyroxene-dominated assemblage. A plot of Sr versus P_2O_5 contents (fig. 61) shows the strong contrast between the Sr contents of Hamakua and Laupahoehoe lavas and the diverse trends. The positive slope of the Hamakua trend results from both olivine control and variation in the degree of silica saturation of the parental magmas; the most alkaline lavas have the highest Sr and P_2O_5 contents. The few Hamakua samples with higher P_2O_5 contents, offset from the main trend, reflect extensive fractionation, as in the formation of the high-Ti basalts. The negative slope of the Laupahoehoe trend reflects the predominance of plagioclase fractionation in the evolution of the hawaiitic magmas.

For a Hamakua basaltic magma to be parental to the most mafic hawaiite requires fractionation that would allow a twofold increase in Sr content. Comparison of the Al_2O_3/CaO ratios and Sc contents of basalts with those of the more mafic hawaiites suggests that clinopyroxene must dominate this fractionation (Frey and others, 1990). Furthermore,

Table 18. Major-oxide and normative-mineral compositions of representative basalts of the Hopukani Springs Volcanic Member

[Major-oxide compositions and Cross, Iddings, Pirsson, and Washington (CIPW) norms in weight percent; major oxides adjusted to 100 percent dry weight after partitioning of Fe to FeO and Fe_2O_3 in the ratio 88:12. See plate 3 for locations and table 1 for original analyses and analysts]

Sample	HQ-16	HR-44	HR-51	HR-59	Wa-8
			Major oxides		
SiO_2	48.55	47.62	47.62	46.80	49.24
Al_2O_3	13.26	10.60	14.75	13.65	12.66
Fe_2O_3	1.62	1.57	1.66	1.69	1.54
FeO	10.73	10.37	10.96	11.20	10.14
MgO	7.27	14.01	6.29	9.14	8.41
CaO	11.56	10.80	12.15	11.52	12.42
Na_2O	2.42	1.84	2.47	2.12	1.84
K_2O	.67	.43	.62	.26	.56
TiO_2	3.39	2.32	2.95	3.06	2.69
P_2O_5	.35	.26	.35	.36	.31
MnO	.18	.18	.19	.19	.18
			CIPW norms		
q	0.00	0.00	0.00	0.00	0.00
or	3.96	2.54	3.66	1.54	3.31
ab	20.48	15.57	20.90	17.94	15.57
an	23.34	19.39	27.33	26.96	24.63
ne	.00	.00	.00	.00	.00
di	25.97	26.16	25.29	22.70	28.50
hy	11.70	9.64	4.58	9.96	18.96
ol	4.96	19.41	9.43	11.80	.97
mt	2.35	2.28	2.41	2.45	2.23
il	6.44	4.41	5.60	5.81	5.11
ap	.83	.62	.83	.85	.73

Samples:

HQ-16. Olivine basalt in Pohakuloa Gulch.

HR-44. Ankaramite in upper part of Pohakuloa Gulch.

HR-51. Weakly porphyritic basalt in upper part of Pohakuloa Gulch.

HR-59. Plagioclase basalt in Waipahoehoe Gulch.

Wa-8. Olivine basalt in Waikahalulu Gulch.

to avoid depleting Sr, plagioclase fractionation must be minimal.

Frey and others (1990) used mass-balance calculations to model the derivation of a high-MgO hawaiite by removal of olivine and augite from several different Hamakua magmas. In making these calculations, they used a clinopyroxene containing 8.6 weight percent Al_2O_3, on the basis of the compositions experimentally determined by Mahood and Baker (1987) for basalt-to-hawaiite fractionation at 8 kbars. None of the clinopyroxenes from xenoliths on Hawaiian volcanoes (Kuno, 1969; Fodor and Vandermeyden, 1988) contains more than about 5 weight percent Al_2O_3. The derivation of our most MgO rich hawaiite from a slightly alkaline basalt (sample Mu–5), using three different clinopyroxenes, is illustrated in table 22. Clearly, the higher the Al_2O_3 content of the pyroxene, the less plagioclase is involved in the fractionation.

Fractionation dominated by aluminous clinopyroxene is a reasonable hypothesis for pressures higher than 5 to 7 kbars, which greatly expands the clinopyroxene field (Mahood and Baker, 1987). This effect is illustrated by the liquidus-phase relations in the system diopside-forsterite-anorthite (Presnall and others, 1978), which are summarized in figure 62. Elevated pressure enhances clinopyroxene crystallization, and the basaltic parental magma crystallizes olivine and augite before the melt composition reaches the three-phase cotectic with plagioclase. The composition of the liquid on this cotectic at 5 to 7 kbars is well within the low-pressure plagioclase field, and decreasing pressure during magma ascent shifts the three-phase cotectic from E to

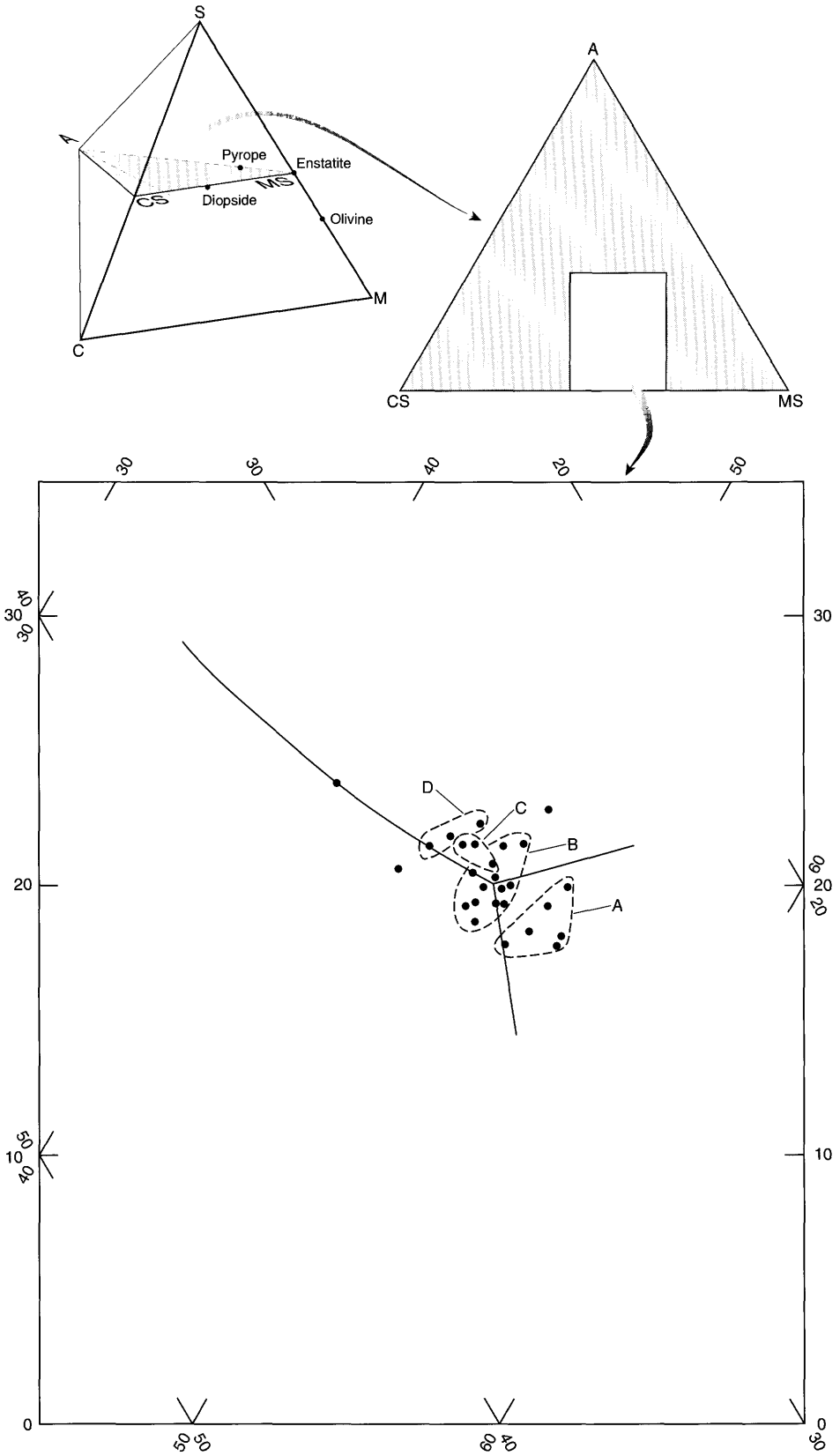

Figure 57. Selected compositions of basalt of the Hopukani Springs Volcanic Member of the Hamakua Volcanics (dots), projected from olivine onto CS–MS–A plane of C–M–S–A tetrahedron of O'Hara (1968). See figure 40 for algorithm used to derive components of tetrahedron. Solid lines, 30-kbar phase boundaries of O'Hara (1968); dashed lines, field boundaries for groups of compositionally distinct lavas (A–D) discussed in text.

Table 19. Major-oxide and normative-mineral compositions of basalt from Kanoa and nepheline basanite of the Honolulu Volcanics, Oahu

[Major-oxide compositions and Cross, Iddings, Pirsson, and Washington (CIPW) norms in weight percent. Values for sample HU-6 adjusted to 100 percent dry weight after partitioning of Fe to FeO and Fe_2O_3 in the ratio 88:12. See table 1 for original analysis and analysts of sample HU-6]

	Basalt from Kanoa (sample HU-6)	Nepheline basanite (Macdonald and Katsura, 1964, table 10, no. 2)
Major oxides		
SiO_2	40.58	44.33
Al_2O_3	13.33	12.80
Fe_2O_3	2.18	3.38
FeO	14.38	9.14
MgO	8.27	11.05
CaO	9.03	10.52
Na_2O	3.85	3.60
K_2O	1.29	.99
TiO_2	6.10	2.65
P_2O_5	.81	.43
MnO	.20	.15
CIPW norms		
q	0.00	0.00
or	7.62	6.12
ab	9.11	11.53
an	15.28	15.57
ne	12.71	10.22
di	19.83	27.18
hy	.00	.00
ol	18.84	17.60
mt	3.16	4.87
il	11.59	5.02
ap	1.92	1.01

E′ (fig. 62). Thus, plagioclase phenocrysts form in the ascending magmas, and clinopyroxene phenocrysts or xenocrysts dissolve in these magmas (see fig. 44*J*).

As recognized by Frey and others (1990), a serious difficulty remains with this model: It does not permit a sufficient increase in Sr content to match the Sr contents of hawaiitic lavas (West and others, 1988). Using Sr partition coefficients of 0.001 for olivine, 0.07 for clinopyroxene, and 1.7 for plagioclase, the bulk *D* value for the fractionation listed in table 22 is 0.342, which allows Sr content to increase from about 600 ppm in a parental magma to only 995 ppm in a derived mafic hawaiite. Other trace elements, such as Rb and Ba, also are insufficiently abundant in potential parental magmas (for example, sample Mu–5, table 22) to yield the abundances found in hawaiites.

We conclude from these arguments that although the hawaiitic magmas probably did fractionate from basaltic magma at a level below the base of the crust, the parental magma has not been erupted onto the surface of Mauna Kea. This parental magma must have an Sr content greater than that in any of the known basalts, at least 800 ppm, and other incompatible trace elements must also be about 20 percent more concentrated than in known basalts. Although increases in these trace-element abundances might occur through the incorporation of liquids derived from small degrees of partial melting of the lithosphere (Chen and Frey, 1985), no corresponding change is evident in the Sr-isotopic composition of Mauna Kea lavas (fig. 35).

FRACTIONATION WITHIN THE HAWAIITIC SUITE

The trends of major-oxide variation with respect to MgO (fig. 58) suggest that the compositional variation within the Laupahoehoe lavas is related to crystal fractionation of such phases as clinopyroxene and plagioclase (West and others, 1988). To assess the fractionation process and to understand the spread of points and changes in trend slopes, we used mass-balance calculations to model the evolution of magma compositions. Compositions of the minerals that are used in these calculations are based on electron-microprobe analyses of microphenocryst or groundmass-mineral phases (olivine, magnetite, ilmenite, apatite, biotite; see table 20) and on hypothetical compositions (plagioclase, clinopyroxene) that allow the best fits.

Selected analyses from across the compositional range were used to model a stepwise fractionation process from the most mafic hawaiite to benmoreite; the results are plotted in figure 63 and listed in table 23. Important features of this fractionation process are as follows. (1) Plagioclase, clinopyroxene, olivine, and magnetite are the most important phases, composing about 90 percent of the fractionating assemblage at each step. (2) The ratios among these four minerals are approximately constant across the full range of fractionation. (3) Biotite removal is necessary to accurately model the K_2O distribution, and biotite fractionation must occur across the full compositional range, even though biotite is observed only in the benmoreites. (4) Simple fractionation cannot account for the scatter of compositions along the trends shown for oxides in figure 58. For example, the high P_2O_5 contents of samples containing from 3.3 to 3.5 weight percent MgO cannot be derived by fractionation from the most mafic hawaiite; either apatite must have been added, or, more likely, the parental magma was slightly more enriched in P_2O_5.

Biotite fractionation accounts for some of the puzzling trace-element behavior observed by West and others (1988), mainly the limited enrichments of K, Rb, and Ba. The small (5–10 percent) decoupling of trace- and major-element abundances (West and others, 1988) could be a result of variation in parental magmas.

West and others (1988) suggested that the aphyric texture of the Laupahoehoe lavas might reflect crystallization on magma-chamber or conduit walls. Furthermore, they concluded that polybaric crystallization, which we assume would have been controlled by decreasing pressure during magma ascent, might account for the compositional varia-

Table 20. Electron-microprobe analyses of representative minerals in hawaiitic lavas of the Laupahoehoe Volcanics, and compositions of minerals used in mass-balance calculations

[All values in weight percent. grd, groundmass; mph, microphenocryst; phn, phenocryst; xen, xenocryst]

Plagioclase: Occurrence.	phn[1]	mph[2]	grd	grd	grd
SiO_2	53.66	53.70	53.64	54.25	56.07
Al_2O_3	29.26	29.07	29.86	28.90	27.67
Fe (as FeO)	.59	.47	---	---	---
CaO	11.40	11.33	11.46	10.62	9.93
Na_2O	4.44	4.98	4.99	5.40	6.16
K_2O	.29	.32	.31	.47	.45
Total	99.64	99.87	100.26	99.64	100.28
An	57.6	55.2	55.0	50.7	45.9
Ab	40.6	43.9	43.3	46.7	51.6
Or	1.8	1.9	1.7	2.6	2.5

Clinopyroxene: Occurrence.	grd[2]	grd[2]	cpx1[3,4]	cpx2[3,5]
SiO_2	47.89	46.68	48.36	50.3
Al_2O_3	4.07	4.40	8.56	4.1
Fe_2O_3	3.21	3.97	.00	2.63
FeO	7.26	7.43	6.80	3.13
MgO	11.96	11.53	13.31	15.7
CaO	21.67	21.39	20.00	22.0
Na_2O	.72	.73	.73	.38
TiO_2	3.05	3.67	2.24	1.1
MnO	.32	.34	.10	.07
Total	100.15	100.14	100.10	99.41
Wo	44.2	43.4	38.1	43.4
En	39.6	39.0	47.0	50.6
Fs	16.2	17.6	14.9	6.0

Magnetite: Occurrence.	grd	grd[3]	**Ilmenite:** grd	grd[3]
Al_2O_3	1.05	0.93	0.47	0.10
Fe_2O_3	23.66	23.40	8.95	7.30
FeO	48.90	49.38	40.34	39.76
MgO	1.93	1.28	1.21	1.98
TiO_2	23.38	22.98	48.34	49.07
MnO	1.08	.84	.91	.82
Total	100.00	98.81	100.22	99.03

Olivine: Occurrence.	mph[1]	grd	grd[2]	xen[1]
SiO_2	37.65	38.14	36.19	38.27
FeO	22.91	25.75	34.27	17.99
MnO	---	.45	.45	---
MgO	39.55	35.45	29.50	43.30
NiO	---	.09	.02	---
CaO	---	.31	.45	---
Total	100.11	100.19	100.88	99.56
Fo	75.5	71.1	60.9	81.1

Biotite: Occurrence.	mph[3]
SiO_2	40.3
Al_2O_3	12.1
Fe (as FeO)	9.04
MgO	20.5
CaO	.07
Na_2O	.98
K_2O	8.90
TiO_2	5.48
MnO	.16
Total	97.53

Apatite: Occurrence.	mph[3]
Fe (as FeO)	0.75
MgO	.48
CaO	53.88
MnO	.10
P_2O_5	40.92
Total	96.13

[1]West and others (1988).
[2]Perdue (1982).
[3]Used in mass-balance calculations in tables 22 and 23.
[4]Frey and others (1990); same as cpx1 of table 22.
[5]Fodor and Vandermeyden (1988, table 3, No. 9); same as cpx2 of table 22.

tion among Laupahoehoe lavas. However, we believe that the evidence does not support polybaric crystallization as a control on compositional variation. The data plotted in figures 59 and 60, which should show the effects of any polybaric crystallization, display no such effect. The most mafic Laupahoehoe hawaiite, sample HR–67, plots within the tight cluster of data points (fig. 59) between the 8- to 30-kbar and 1-bar cotectics on the DI–OL–NEPH plane of Sack and others (1987); there is no spreading away from this cluster toward the 1-bar cotectic of data points representing the more evolved Laupahoehoe lavas. Similarly, data points representing the full Laupahoehoe compositional range (fig. 60) are approximately equidistant from the 1-bar cotectic in the CS–MS–A plane of O'Hara (1968).

An additional line of reasoning also argues against polybaric crystallization as a significant cause of the compositional variation among Laupahoehoe lavas. As shown in figure 62, the most mafic hawaiitic liquid had reached a cotectic where it was in equilibrium with plagioclase, clinopyroxene, and olivine. This is, in fact, a quaternary cotectic involving magnetite as well. Decompression would displace the cotectic composition such that the liquid composition would lie in the plagioclase field, and increasingly greater amounts of plagioclase would have to be fractionated for the liquid to reach the lower-pressure cotectic composition. The calculations summarized in table 23, however, suggest that the ratios among the four major phases remain nearly constant as the liquid evolves; there is no indication

Table 21. Major-oxide and normative-mineral compositions of representative lavas of the Laupahoehoe Volcanics

[Major-oxide compositions and Cross, Iddings, Pirsson, and Washington (CIPW) norms in weight percent; major oxides adjusted to 100 percent dry weight after partitioning of Fe to FeO and Fe_2O_3 in the ratio 88:12. See table 1 for original analyses and analysts]

Sample -----	HP-11	HQ-4	HR-55	HR-67	HR-72	JQ-10
			Major oxides			
SiO_2 -------	50.12	52.79	49.44	48.75	51.76	55.86
Al_2O_3 ------	17.17	17.60	16.92	16.99	17.18	17.71
Fe_2O_3 ------	1.44	1.22	1.48	1.51	1.32	1.12
FeO --------	9.53	8.08	9.80	10.00	8.71	7.38
MgO --------	4.11	3.03	4.55	5.01	3.59	2.26
CaO --------	7.08	6.18	7.39	7.65	6.74	4.54
Na_2O -------	4.70	5.19	4.50	4.20	4.91	5.70
K_2O --------	1.86	2.36	1.76	1.65	2.06	2.79
TiO_2 -------	2.86	2.07	3.08	3.23	2.50	1.41
P_2O_5 -------	.90	1.25	.87	.81	1.02	1.00
MnO --------	.22	.23	.21	.20	.22	.23
			CIPW norms			
q ----------	0.00	0.00	0.00	0.00	0.00	0.00
or ---------	10.99	13.95	10.40	9.75	12.17	16.49
ab ---------	35.86	43.13	33.95	32.22	40.19	48.23
an ---------	20.29	17.76	20.77	22.63	18.75	14.50
ne ---------	2.12	.43	2.23	1.80	.74	.00
di ---------	7.47	3.97	8.46	8.29	6.69	1.26
hy ---------	.00	.00	.00	.00	.00	4.58
ol ---------	13.69	12.18	14.17	15.11	12.43	8.33
mt ---------	2.09	1.77	2.15	2.19	1.91	1.62
il ---------	5.43	3.93	5.85	6.13	4.75	2.68
ap ---------	2.13	2.96	2.06	1.92	2.42	2.37

Samples:

HP-11. Hawaiite flow from Puu Ka Pele (see pl. 4).

HQ-4. Mugearite scoria block from Puu Pohakuloa (see pl. 3).

HR-55. Hawaiite flow from Puu Makanaka (see pl.3).

HR-67. Hawaiite flow from Puu Kaiwiiwi (see pl. 3).

HR-72. Mugearite flow from Puu Poliahu (see pl. 3).

JQ-10. Benmoreite flow from Kaluamakani (see pl. 4).

of the enhanced plagioclase fractionation that should have occurred as a result of decompression. Therefore, we suggest that all the Laupahoehoe magmas originated at similar depth, in a deep magma chamber(s) in which the magmas evolved to varying extents. Little or no fractionation occurred upon ascent, although some of the magmas began to crystallize plagioclase before eruption.

The slight increase in silica saturation throughout the fractionation sequence of Laupahoehoe lavas (table 21) results from the 1.5- to 3-percent removal of magnetite and ilmenite for each step summarized in table 23.

MAFIC AND ULTRAMAFIC XENOLITHS

Useful evidence to help locate the magma chamber(s) in which the hawaiitic magmas evolved comes from the suite of mafic and ultramafic xenoliths contained in 20 to 30 percent of the Laupahoehoe flows and cinder cones. Xenoliths in Hawaiian lavas have been the subject of numerous studies (see review by Clague and Dalrymple, 1987, p. 24–27, and references therein). Those in Mauna Kea lavas were investigated by Fodor and Vandermeyden (1988), who made a careful study of gabbroic xenoliths from the summit

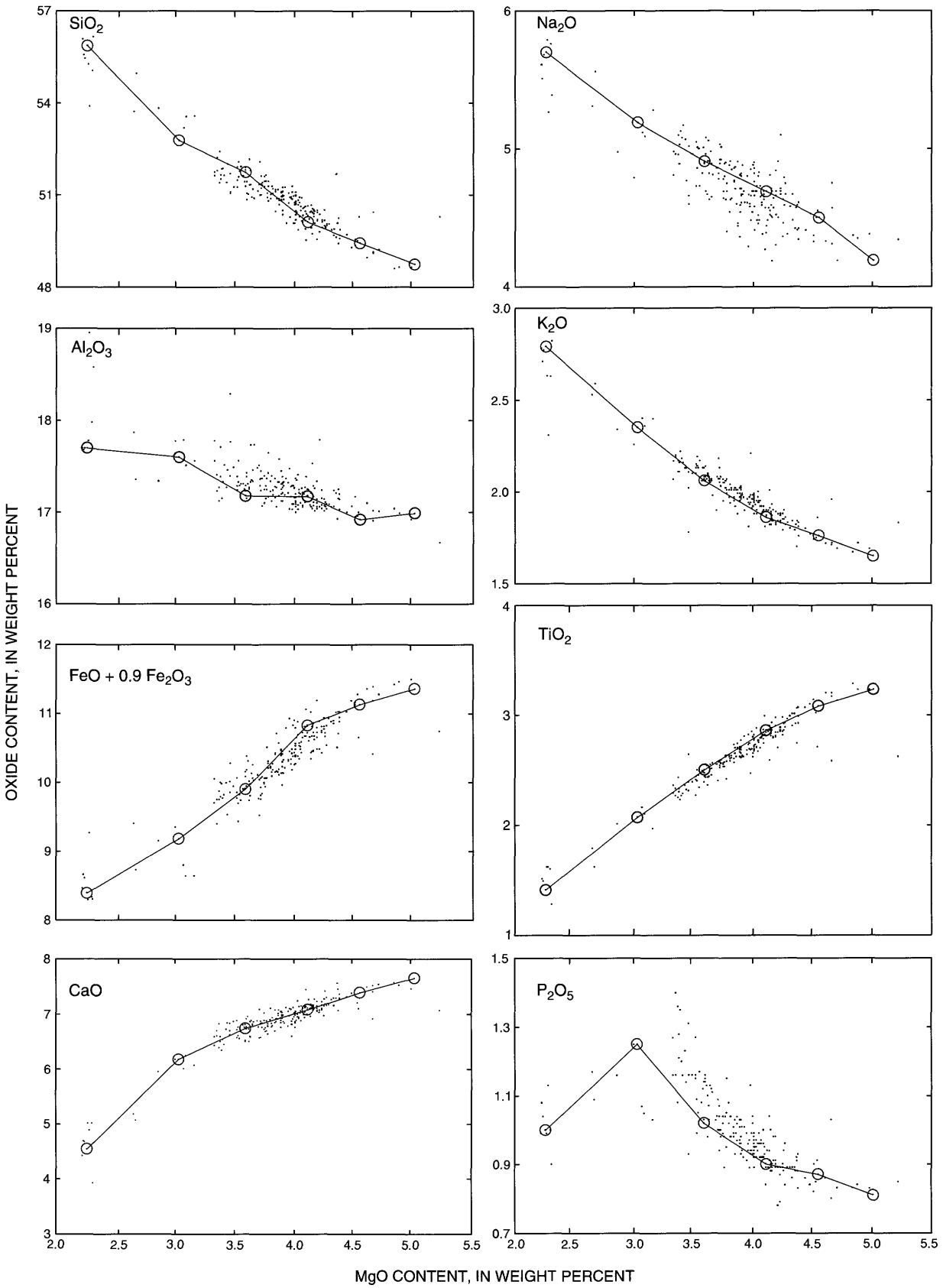

Figure 58. MgO-variation diagrams for lavas of the Laupahoehoe Volcanics. Circled data points represent lava compositions used for modeling in mass-balance calculations (see table 23); connecting line, viewed from right to left, approximates fractionation-controlled liquid-descent line.

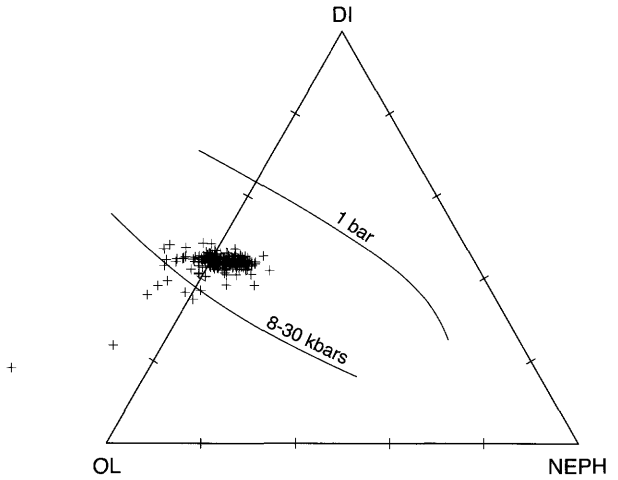

Figure 59. Compositions of lavas of the Laupahoehoe Volcanics (crosses), projected from plagioclase onto DI–OL–NEPH plane of Sack and others (1987). See figure 50 for algorithm used to derive components of triangular projection. Curves show cotectic lines at different pressures.

cone; by Jackson and others (1982), who reported field modes of occurrences from more than 35 cones and flows; and by H.G. Wilshire and J.E. Nielson (written commun., 1987), who made a careful study of xenoliths from Puu Haiwahine.

Xenoliths in Laupahoehoe lavas and cinder cones represent three lithologic groups, in order of abundance: gabbro, peridotite, and pyroxenite. The gabbros vary in grain size and modal composition, but they are uniformly composed of plagioclase (An_{81-86}), clinopyroxene ($Wo_{44}En_{46}Fs_{10}$), and olivine (Fo_{80}) (Fodor and Vandermeyden, 1988). Gabbro, two-pyroxene gabbro, and troctolite are the most common rock types. Grain size ranges from 0.5 to 5 mm, and many samples appear banded from inhomogeneous distribution of pyroxene and plagioclase. Microgabbros with very fine grained to fine-grained, equigranular textures commonly are compositionally banded. Some of these microgabbros contain crosscutting dikes and veins with similar minerals that differ from those of the host in grain size.

Dunite and wehrlite are the most common of the Mauna Kea ultramafic xenoliths (see Jackson and others, 1982); Cr-diopside lherzolites are comparatively rare, and some or them occur as composites with dunite. Many to most peridotites are deformed; the rocks are sheared, and grains exhibit kink bands. In most of the literature on Hawaiian xenoliths, such peridotites are termed "metamorphic"; they form significant proportions of the total xenolith assemblages. H.G. Wilshire and J.E. Nielson (oral commun., 1988) reported that some xenoliths of this type, including some dunites, have veins and dikes of gabbro and microgabbro, as much as about 1 cm thick; the finer grained dunites commonly contain net veins of microgabbro, 1 to 3 mm thick. Such textures suggest that the dunites could be from melt-extraction zones, possibly for midoceanic-ridge basaltic (MORB) magmas, and so are not "cumulates." The larger dikes cutting these dunites could be very much younger, possibly related to Mauna Kea shield-stage volcanism.

Fodor and Vandermeyden (1988) showed that the compositions of plagioclase in the gabbros are unlikely for plagioclase that crystallized from MORB-like magma. They suggested, instead, that the gabbroic xenoliths represent crystallization residues from Hamakua alkaline basalts which yielded evolved Hamakua hawaiites (our high-Ti basalts) or Laupahoehoe hawaiites. They hypothesized the crystallization of a large magma chamber in the superstructure of the volcano to account for the various types of xenoliths found in their study. Although we cannot rule out such a possible source of some xenoliths, the persistence of peridotite in the xenolith assemblage argues for an alternative source. Most xenoliths are bounded by planar surfaces, with as many as six differently oriented surfaces on a single fragment. The source of these xenoliths must be complexly jointed. Well-rounded xenoliths, possibly from loosely compacted accumulates, are fairly rare.

We agree with H.G. Wilshire and J.E. Nielson (oral commun., 1988) that the source for most, if not all, of the xenoliths is likely to be a zone of intensely injected and jointed peridotite at or somewhat below the base of the oceanic crust. An alternative suggestion to the view that the gabbro xenoliths represent residues from fractionating Hamakua basaltic magma (Fodor and Vandermeyden, 1988) is that most of these xenoliths, especially those with two pyroxenes, could represent tholeiitic dikes injected during building of the shield. Mineral compositions alone, however, are insufficient to distinguish whether a pyroxene and plagioclase assemblage was derived from tholeiitic magma or from transitional- to alkali-basalt magma.

ORIGIN OF LAUPAHOEHOE HAWAIITIC LAVAS

Interpretations of the major-element compositions of the hawaiitic lavas require extensive fractionation of an alkali-basalt parental magma. The first stage of this fractionation must have been dominated by removal of clinopyroxene at pressures of at least 5 to 7 kbars. This removal produced a hawaiitic liquid at a quaternary cotectic (olivine, clinopyroxene, plagioclase, magnetite). Varying degrees of fractionation of this cotectic assemblage produced more evolved magmas, ranging in composition to benmoreite.

These hawaiitic, mugearitic, and benmoreitic magmas apparently ascended to the surface without interruption, passing through the source region(s) of xenolith assemblages and entraining fragments. The spatial relations of the magma chamber, xenolith source, and ascent paths are illustrated in figure 64*D*.

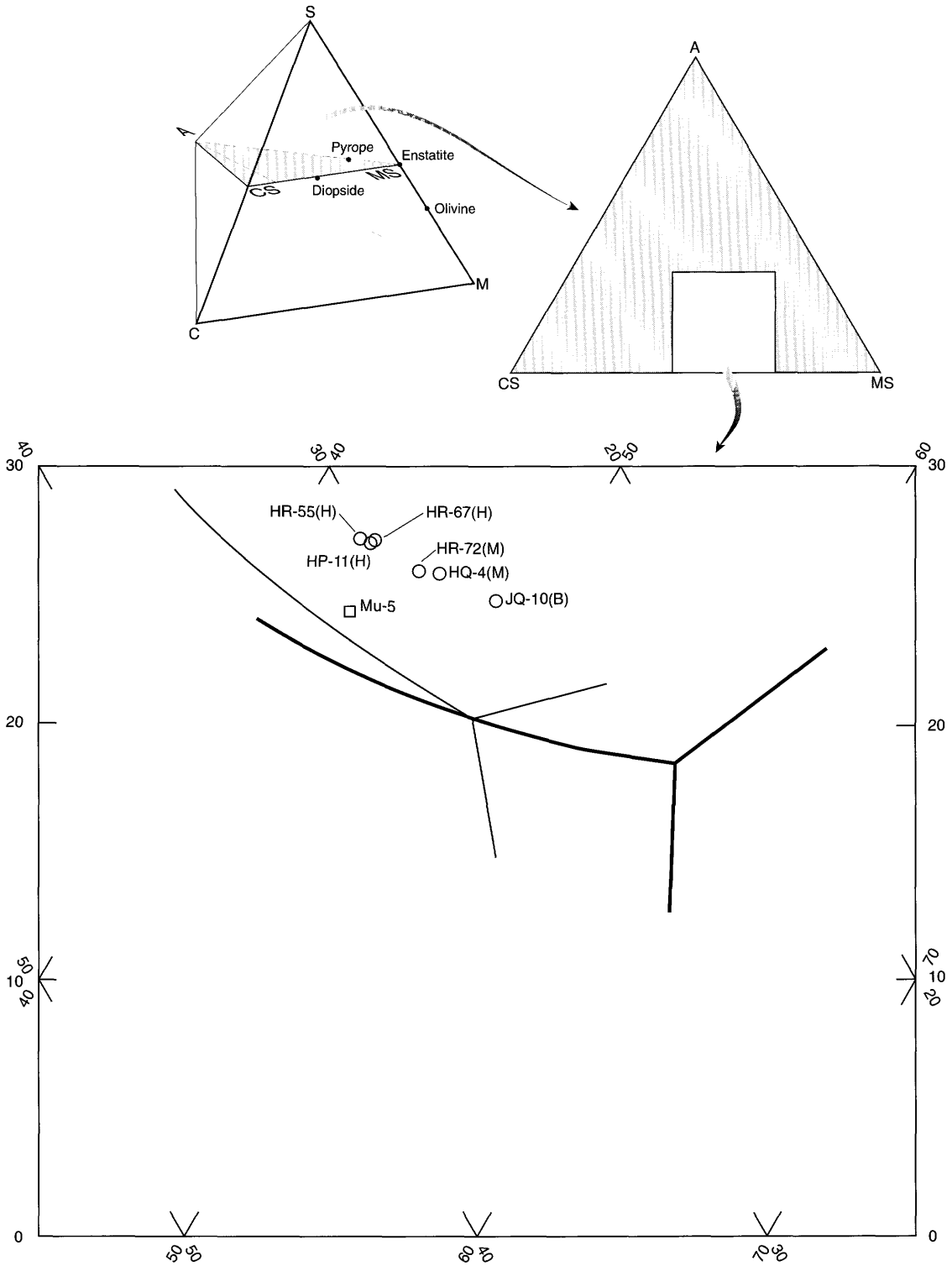

Figure 60. Selected compositions of lavas of the Laupahoehoe Volcanics projected from olivine onto CS–MS–A plane of C–M–S–A tetrahedron of O'Hara (1968). See figure 40 for algorithm used to derive components of tetrahedron. Heavy lines, 1-bar phase boundaries of O'Hara (1968); light lines, 30-kbar phase boundaries of O'Hara (1968). Circles, Laupahoehoe lavas, showing sample number and, in parentheses, lava type (B, benmoreite; H, hawaiite; M, mugearite); see table 21 for chemical analyses and normative-mineral compositions, and figure 58 for approximations of fractionation-controlled liquid-descent lines. Square, composition of sample Mu–5 (basalt of the Hamakua Volcanics), which is modeled as parental magma of sample HR-67 (most mafic hawaiite); see table 22 for mass-balance calculations. Sample HR–67 is modeled as parental magma of other Laupahoehoe lavas depicted here; see table 23 for mass-balance calculations.

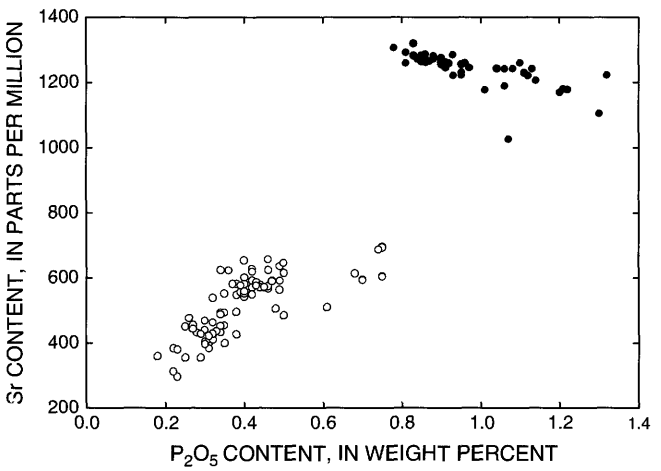

Figure 61. Sr versus P_2O_5 contents of lavas of the Hamakua Volcanics and the Laupahoehoe Volcanics (from Frey and others, 1990). Circles, Hamakua Volcanics; dots, Laupahoehoe Volcanics.

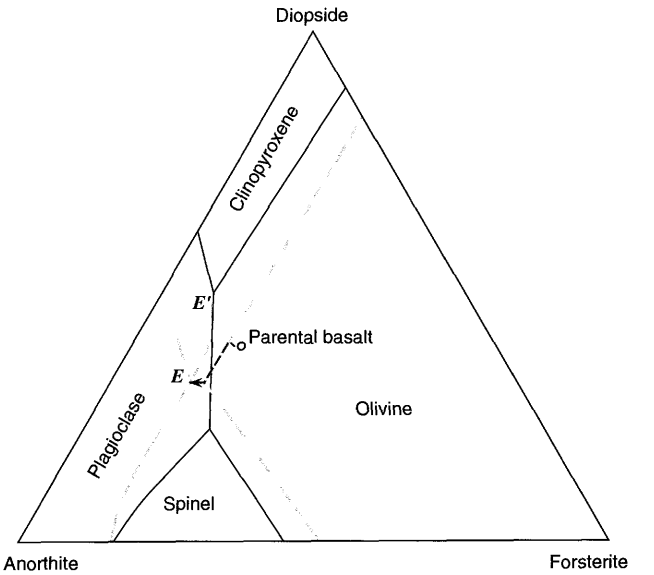

Figure 62. Liquidus boundaries in diopside-anorthite-forsterite system (from Presnall and others, 1978), showing effect of pressure on crystallization of alkali basalt to produce hawaiitic liquid. Solid black lines, 1-bar phase boundaries; solid red lines, 7-kbar phase boundaries. Circle indicates composition of alkali basalt, hypothetical parental magma of hawaiitic liquid. Dashed black line shows path of parental liquid during crystallization at 7 kbars; dashed red line shows trace of three-phase cotectic point (E to E') as magma is decompressed.

DEVELOPMENT OF MAUNA KEA VOLCANO— AN INTERPRETATIVE SUMMARY

INTRODUCTION

The geology and petrology of Mauna Kea Volcano provide a rich detail of activity during a particularly extensive postshield stage. That detail, combined with inferences on shield-stage activity, enables us to write a history of mantle melting and surface eruptions for this large Hawaiian volcano. In the following review of the development of Mauna Kea Volcano, we describe its growth through the first three stages—preshield, shield, and postshield—that are now recognized in the evolution of a typical Hawaiian volcano (Clague and Dalrymple, 1987).

The growth and evolution of Hawaiian volcanoes apparently results from continuous passage of the Pacific Plate over the Hawaiian hotspot, a relatively fixed source of ascending primitive mantle material (Clague and Dalrymple, 1987). However, volcano growth along the Hawaiian Chain is a discontinuous process. As indicated by Mauna Kea, once a conduit system is established as a pathway for ascending magma, it persists for possibly a million years (see fig. 4). During this time, production of tholeiitic magma increases to a rate as high as about 0.1 km^3/yr but averages somewhat less (Dvorak and Dzurisin, 1993). While eruptions and intrusions are completing construction of a shield with a volume of approximately 30,000 km^3, another, apparently independent conduit system is established 40 to 50 km to the southeast (fig. 64*C*). Eventually, magma production decreases by an order of magnitude, and the volcano enters the postshield stage.

The types of lava and length of activity of the postshield stage vary from volcano to volcano (Wright and Clague, 1989). The characteristic lava is hawaiite, an evolved alkalic basalt, but some volcanoes (such as Mauna Kea) pass through a transitional period during which the shield-stage tholeiitic lavas give way to transitional and alkali basalts before the appearance of hawaiite.

Comparison of basalt compositions with those of liquids obtained through high-pressure, dry-melting experiments by O'Hara (1968) (see fig. 40) and Falloon and others (1988) show that the range of lava compositions erupted during the preshield, shield, and postshield stages can originate from parental magmas generated by differing degrees of partial melting of garnet-bearing peridotite at pressures near 30 kbars. Although the precise cause of this melting is still unknown, the general view is that hot primitive mantle material ascends beneath the oceanic lithosphere underlying Hawaii and reacts with the lithosphere to produce the Hawaiian parental magmas (Clague and Dalrymple, 1987). Isotopic compositions of Hawaiian lavas (for example, Chen and Frey, 1985) indicate that the dominant contribution comes from undepleted primitive mantle, with smaller amounts from depleted lithospheric mantle. The magma-production history (rate, volume, and composition) of

Table 22. Mass-balance calculations to derive the compositions of the most mafic hawaiites of the Laupahoehoe Volcanics

[Major oxides and mineral compositions in weight percent, calculated to 100 percent dry weight; trace-element contents in parts per million (from Frey and others, 1990). Clinopyroxene compositions: cpx1, $Wo_{38}En_{47}Fs_{15}$, 8.56 weight percent Al_2O_3, and 2.24 weight percent TiO_2 (Frey and others, 1990) (see table 20 for microprobe analysis); cpx2, $Wo_{43}En_{51}Fs_6$, 4.10 weight percent Al_2O_3, and 1.10 weight percent TiO_2 (Fodor and Vandermeyden, 1988, table 3, no. 9) (see table 20 for microprobe analysis); cpx3, $Wo_{40}En_{48}Fs_{12}$, 3.62 weight percent Al_2O_3, and 1.61 weight percent TiO_2 (see table 8 for microprobe analysis)]

Parental magma (sample Mu-5)	Daughter (sample HR-67)						
	Observed (a)	Modeled (b)	Residual (a-b)	Modeled (c)	Residual (a-c)	Modeled (d)	Residual (a-d)
Major oxides							
SiO_2 ---------- 46.78	48.82	48.91	-0.09	48.97	-0.15	48.97	-0.15
Al_2O_3 -------- 14.59	17.02	17.06	-.04	17.08	-.06	17.07	-.05
Fe (as FeO)-- 12.37	11.38	11.43	-.05	11.47	-.09	11.47	-.09
MgO---------- 8.08	5.02	5.04	-.02	5.05	-.03	5.04	.02
CaO---------- 10.36	7.66	7.66	.00	7.66	.00	7.66	.00
Na_2O ---------- 2.85	4.21	4.15	.06	4.19	.02	4.20	.00
K_2O ---------- .90	1.65	1.53	.12	1.48	.17	1.47	.18
TiO_2 ---------- 3.34	3.24	3.30	-.06	3.33	-.09	3.33	-.09
P_2O_5 ---------- .42	.81	.74	.07	.71	.10	.71	.10
MnO---------- .17	.20	.19	.01	.18	.02	.19	.01
Trace elements							
Rb---------- 16.9	30	27.9	2.1	26.5	3.5	26.5	3.5
Sr---------- 603	1,300	995	305	946	354	944	356
Ba---------- 303	570	500	70	475	95	475	95
Ce---------- 61	100	100	0	95	5	96	4
Sum of the squares of residuals (major oxides only).			.042		.102		.100
Phases removed from or added to parental magma in calculating modeled composition:							
Olivine---------- (Fo_{74})			-5.12		-4.49		-5.02
Plagioclase---------- (An_{79})			-10.40		-4.72		-8.42
Clinopyroxene---------- (cpx1)			-19.80	(cpx2)	-23.27	(cpx3)	-18.16
Magnetite[1]----------			-3.11		-3.31		-3.58
Ilmenite[1]----------			-.51		+.28		-.23
Total			-38.94		-35.51		-35.41

[1]See table 20 for composition.

Mauna Kea places significant limiting constraints on this melting process.

PRESHIELD STAGE

Hawaiian preshield lavas are known only from Loihi Volcano (see fig. 1). Dredge samples from Loihi include tholeiitic and alkali basalts. Moore and others (1982) suggested that Loihi is in transition from production of early alkali basalts, reflecting low degrees of partial melting of the source rocks, to production of tholeiitic basalt, reflecting greater partial melting as shield building develops.

Preshield lavas, if present on Mauna Kea Volcano, are not exposed. Figure 3 shows an approximate volume of 500 km^3 of preshield lava, equivalent to the volume of Loihi as estimated from bathymetry (fig. 1). However, neither the ultimate volume of Mauna Kea preshield lava nor the duration of its production is known. We simply infer that a relatively small volume of alkali basalt was produced by low degrees of partial melting from the Mauna Kea source rocks during the earliest period of magma production.

SHIELD STAGE

Shield-stage lavas are not exposed on the subaerial part of Mauna Kea. Hilo Ridge, however, which has strong topographic definition at depths below 1.5 km (fig. 1), closely resembles in form the submarine extension of Kilauea's east rift zone. By analogy with Kilauea (see Decker, 1987, for a review of its structure and dynamics), we interpret Hilo Ridge as the east rift zone of Mauna Kea Volcano during the shield stage. We presume that, as at Kilauea, the rift-zone

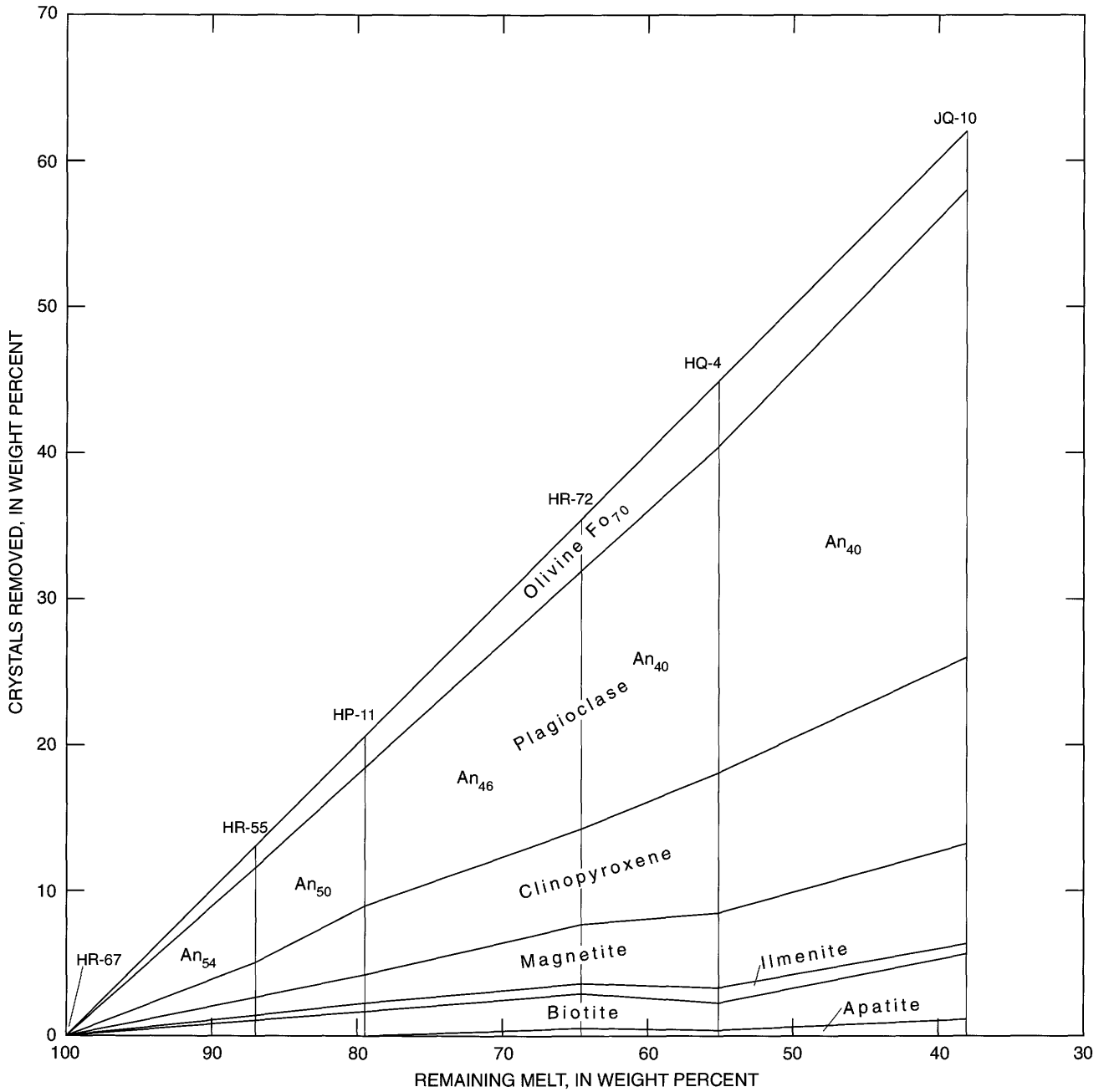

Figure 63. Schematic diagram illustrating stepwise fractionation of hawaiitic lavas of the Laupahoehoe Volcanics, showing evolution from most mafic hawaiite to benmoreite. Sample HR–67 (most mafic hawaiite) is modeled in successive mass-balance calculations as parental magma of sample JQ–10 (benmoreite); other sample numbers shown are modeled intermediate daughters (see table 23). Vertical lines represent individual samples; amount of each mineral removed is shown by vertical separation of mineral boundaries. Percentages of both crystals removed and melt remaining for each step are determined with respect to composition of sample HR–67. "An" (anorthite content, in weight percent) indicates calculated composition of plagioclase removed in each modeled step. See Spengler and Garcia (1988) for similar fractionation diagram for hawaiitic lavas of Kohala Volcano.

lavas of Mauna Kea were erupted along the ridge axis from shallow conduits supplied from a shallow central reservoir beneath the summit region of the volcano.

We view the shield stage as representing that period in the growth of the volcano characterized by voluminous eruption of fluid lava, much of which was pahoehoe. As noted above in the subsection entitled "Geologic Setting," surface slopes on actively growing Hawaiian shields are much steeper below sea level than above; a sharply defined break in slope occurs at the shoreline (Moore and Fiske,

Table 23. Mass-balance calculations illustrating fractionation in hawaiitic lavas of the Laupahoehoe Volcanics

[All values in weight percent, calculated to 100 percent dry weight]

	Parental magma (sample HR-67)	Daughter (sample HR-55), using sample HR-67 as parent			Daughter (sample HP-11), using sample HR-55 as parent		
		Observed (a)	Modeled (b)	Residual (a-b)	Observed (a)	Modeled (b)	Residual (a-b)
SiO_2	48.82	49.51	49.53	-0.02	50.18	50.18	0.0
Al_2O_3	17.02	16.95	16.95	.0	17.20	17.20	.0
Fe (as FeO)	11.40	11.15	11.16	-.01	10.86	10.86	.0
MgO	5.01	4.56	4.56	.0	4.11	4.11	.0
CaO	7.66	7.40	7.39	.01	7.09	7.09	.0
Na_2O	4.20	4.51	4.44	.07	4.71	4.71	.0
K_2O	1.65	1.76	1.76	.0	1.86	1.86	.0
TiO_2	3.23	3.09	3.10	-.01	2.87	2.87	.0
P_2O_5	.81	.87	.90	-.03	.91	.91	.0
MnO	.20	.21	.20	.01	.22	.21	.01
Sum of the squares of residuals				.0065			.0001
Phases removed from or added to parental magma in calculating modeled composition:							
Olivine		(Fo_{70})		-1.35		(Fo_{70})	-0.93
Plagioclase		(An_{54})		-6.61		(An_{50})	-3.38
Clinopyroxene[1]				-2.45			-2.61
Magnetite[1]				-1.27			-.76
Ilmenite[1]				-0.24			-.40
Phlogopite[1]				-1.11			-.50
Apatite[1]				-.05			-.10
Total				-13.08			-8.68
Original melt remaining				86.92			79.38

	Daughter (sample HR-72), using sample HP-11 as parent			Daughter (sample HQ-4), using sample HR-72 as parent			Daughter (sample JQ-10), using sample HQ-4 as parent		
	Observed (a)	Modeled (b)	Residual (a-b)	Observed (a)	Modeled (b)	Residual (a-b)	Observed (a)	Modeled (b)	Residual (a-b)
SiO_2 51.80	51.78	0.02	52.85	52.85	0.0	55.92	55.93	-0.01
Al_2O_3 17.20	17.19	.01	17.62	17.62	.0	17.72	17.73	-.01
Fe (as FeO) 9.92	9.91	.01	9.19	9.19	.0	8.40	8.40	.0
MgO 3.59	3.59	.0	3.03	3.03	.0	2.26	2.26	.0
CaO 6.75	6.76	-.01	6.19	6.19	.0	4.54	4.54	.0
Na_2O 4.92	5.00	-.08	5.20	5.22	-.02	5.70	5.68	.02
K_2O 2.06	2.07	-.01	2.36	2.36	.0	2.79	2.79	.0
TiO_2 2.50	2.49	.01	2.07	2.07	.0	1.42	1.42	.0
P_2O_5 1.02	.99	.03	1.25	1.24	.01	1.00	1.00	.0
MnO .22	.22	.0	.23	.23	.0	.23	.26	-.03
Sum of the squares of residuals	.0099				.0007			.0017
Phases removed from or added to parental magma in calculating modeled composition:								
Olivine (Fo_{70})		-1.72		(Fo_{70})	-1.49		(Fo_{70})	0.81
Plagioclase (An_{46})		-10.42		(An_{40})	-7.15		(An_{40})	-17.54
Clinopyroxene[1]		-2.30			-4.83			5.62
Magnetite[1]		-2.75			-1.59			-3.01
Ilmenite[1]		-.15			-.60			.62
Phlogopite[1]		-1.15			.94			-4.71
Apatite[1]		-.26			.09			-1.33
Total		-18.75			-14.63			-30.78
Original melt remaining		64.49			55.06			38.11

[1]See table 20 for composition.

1969). As long as the rate of upward growth due to volcanic resurfacing exceeds the rate of subsidence, the slope break is maintained at sea level. However, when production of voluminous fluid lava is curtailed, subsidence carries the fossil slope break below sea level. Figure 1 shows three successive slope breaks along the northeast flank of Hawaii: the first at approximately 1-km depth on Kohala Volcano; the second at approximately 0.4-km depth on Mauna Kea Volcano; and the third, south of Hilo, at sea level on Mauna Loa and Kilauea Volcanoes.

The submarine surface above the Mauna Kea slope break slopes 2.8° in the area of the cross section shown in figures 1 and 2. An identical slope occurs along the northeastern part of Kilauea's subaerial southeast flank; Kilauea's subaerial flank farther southwest has been steepened by faulting. Even gentler slopes (generally less than 2° and locally less than 1°) characterize the lower northeast sector of the combined Mauna Loa and Kilauea shields between Hilo and Cape Kumukahi. Thus, we believe that the gentle submarine slope between sea level and 400-m depth along the northeast flank of Mauna Kea approximately represents the fossil surface of the shield.

The subaerially exposed postshield lavas on the lower flank of Mauna Kea underlie appreciably steeper slopes, ranging from approximately 4° to 9°. However, the postshield flows have been truncated in the seacliffs of Mauna Kea's northeast coast, indicating that they at least partly bury shield-stage lavas on the nearshore submarine slope. Nevertheless, we conclude that the approximate boundary between shield and postshield flows is close below sea level at the shoreline.

K-Ar ages for some of the oldest visible basalts of Mauna Kea, exposed near sea level in deep gulches on the northeast flank of the volcano (figs. 12, 13), indicate that the shield stage had terminated by about 250 ka. We estimate the volume of the shield, including the large volume that has subsided beneath the level of the adjacent ocean floor (fig. 1*B*), at 32,000 km^3. Applying Swanson's (1972) estimate of 0.1 km^3/yr for Kilauea's magma-supply rate, we calculate a minimum duration of 320,000 yr for the shield stage. However, as indicated by Dvorak and Dzurisin (1993), that rate probably represents a maximum value, and Kilauea's average magma-supply rate is more likely between 0.01 and 0.1 km^3/yr. In addition, Mauna Kea's magma-supply rate probably accelerated during the early part of the shield stage and waned during the later part. Thus, appreciable uncertainty exists about the duration of the shield stage. A median average magma-supply rate, approximately 0.5 km^3/yr, gives a 650,000-yr duration for the shield stage, which we provisionally accept as a reasonable estimate (see fig. 4).

Figure 1 shows that Hilo Ridge loses its strong topographic definition at depths above 1,500 m and has no topographic expression above the slope break at 400-m depth or on the subaerial part of the volcano. The lavas on the crest of Hilo Ridge represent the youngest flows erupted during the active life of the east rift zone. Moore and Peck (1966) noted that the vesicularity of samples of pillow basalt dredged from Hilo Ridge was comparable to that of basalt at much shallower depths on the currently active rift zones of Kilauea and Mauna Loa. They concluded that approximately 1,000 m of subsidence had occurred since these dredged basalts were erupted on Hilo Ridge. At a subsidence rate of approximately 2.6 mm/yr, which Ludwig and others (1991) determined to have been fairly uniform since 475 ka for this part of Hawaii, this much subsidence would have required about 400,000 yr. Evidently, Mauna Kea's east rift zone was inactive during a later part of the shield stage. Apparently, rift-zone eruptions ceased, possibly as a result of waning magma production (see fig. 4), and shield lavas issued from the summit area or, possibly, from radial vents like those on the northwest flank of Mauna Loa (Lockwood and Lipman, 1987). Thus, subaerial Mauna Kea lacks the elongate-ridge form that, on its neighbors, reflects the influence of recurrent rift-zone eruptions.

Figure 64. Schematic cross sections of Mauna Kea, showing → its growth history and its relation to adjacent volcanoes along Kea locus (Jackson and others, 1972). Sections run approximately northwest to southeast (left to right). Interleaved lavas of Mauna Loa, to southwest along Loa locus (Jackson and others, 1972), are not shown. *A*, Middle shield stage, approximately 600 ka. Magma-supply rate is high, averaging 0.01 to 0.1 km^3/yr. Tholeiitic-basalt magma rises from upper-mantle source region through a central conduit to shallow reservoir beneath Mauna Kea's summit. Volcano develops active east rift zone (not shown), which is also supplied with magma from summit reservoir. Summit-reservoir drawdown that results from large rift-zone eruptions or intrusions causes formation and episodic rejuvenation of caldera (see Holcomb, 1987). Mauna Kea's volcanic edifice progressively subsides as its mass increases. Lava flows interfinger with those of Kohala, which is near end of its shield stage (Wolfe and Morris, 1996). *B*, Late shield stage, approximately 350 ka. Tholeiitic-basalt magma and, possibly, transitional-basalt magma continues to rise, although diminishing magma production had resulted in termination of rift-zone activity, and so caldera fills with lava and is not rejuvenated. Central conduit and summit reservoir are still active; shield lavas erupt at summit or, possibly, from radial vents supplied from summit reservoir. Flows interfinger with postshield lavas of Kohala. *C*, Postshield stage (basaltic substage), approximately 150 ka. Melting rate and, thus, degree of partial melting in source region are diminished, and so production of tholeiitic-basalt magma has ceased. Transitional-basalt magma from central part of source region maintains supply to central conduit and summit reservoir. Alkali-basalt magma from outer parts of source region rises in small batches into flanks of volcano, where it commonly fractionates in isolated ephemeral chambers before erupting at surface. Southeastward along Kea locus, Kilauea is in preshield stage, erupting alkalic-basalt lavas. *D*, Postshield stage (hawaiitic substage), approximately 30 ka. Alkali-basalt magma, generated in response to slow melting rate and, thus, low degree of partial melting in source region, collects in reservoirs in upper mantle near base of crust, where it fractionates into evolved magma (hawaiite, mugearite, or benmoreite) that rises to surface without undergoing further fractionation. Some evolved magma entrains gabbro, peridotite, and pyroxenite xenoliths either from upper mantle or from intrusive bodies within oceanic crust or volcanic edifice of Mauna Kea. To southeast, full tholeiitic-basalt magma production is now under way at Kilauea.

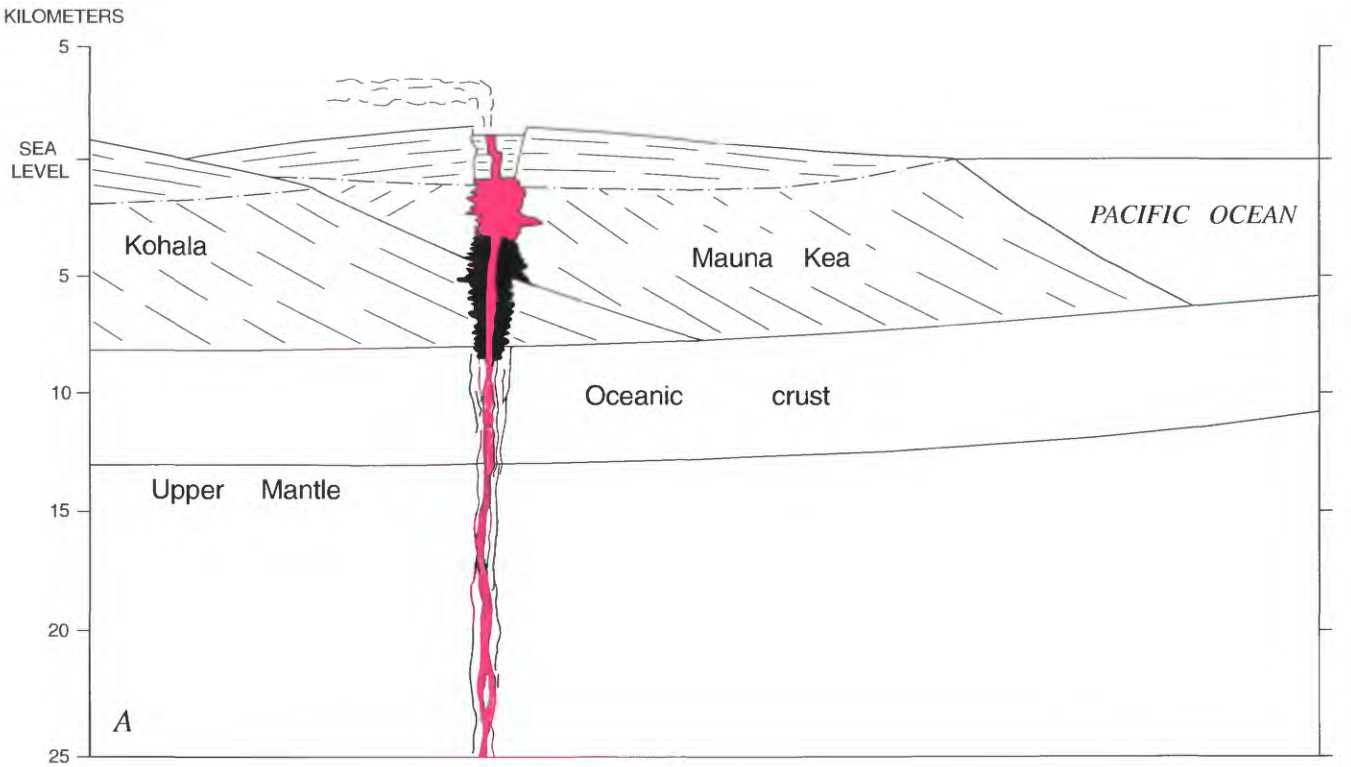
KILOMETERS
5
SEA LEVEL
5
10
15
20
25
Kohala
Mauna Kea
PACIFIC OCEAN
Oceanic crust
Upper Mantle
A

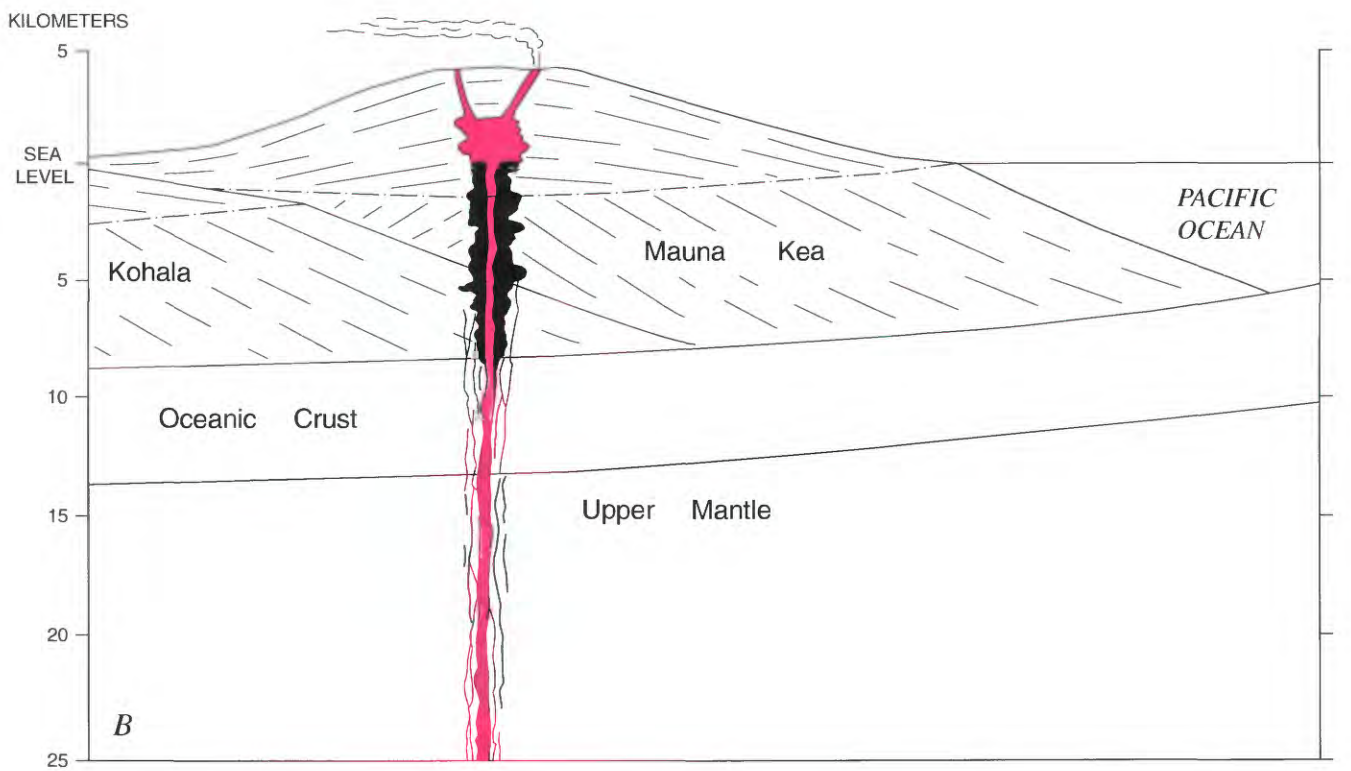
KILOMETERS
5
SEA LEVEL
5
10
15
20
25
Kohala
Mauna Kea
PACIFIC OCEAN
Oceanic Crust
Upper Mantle
B

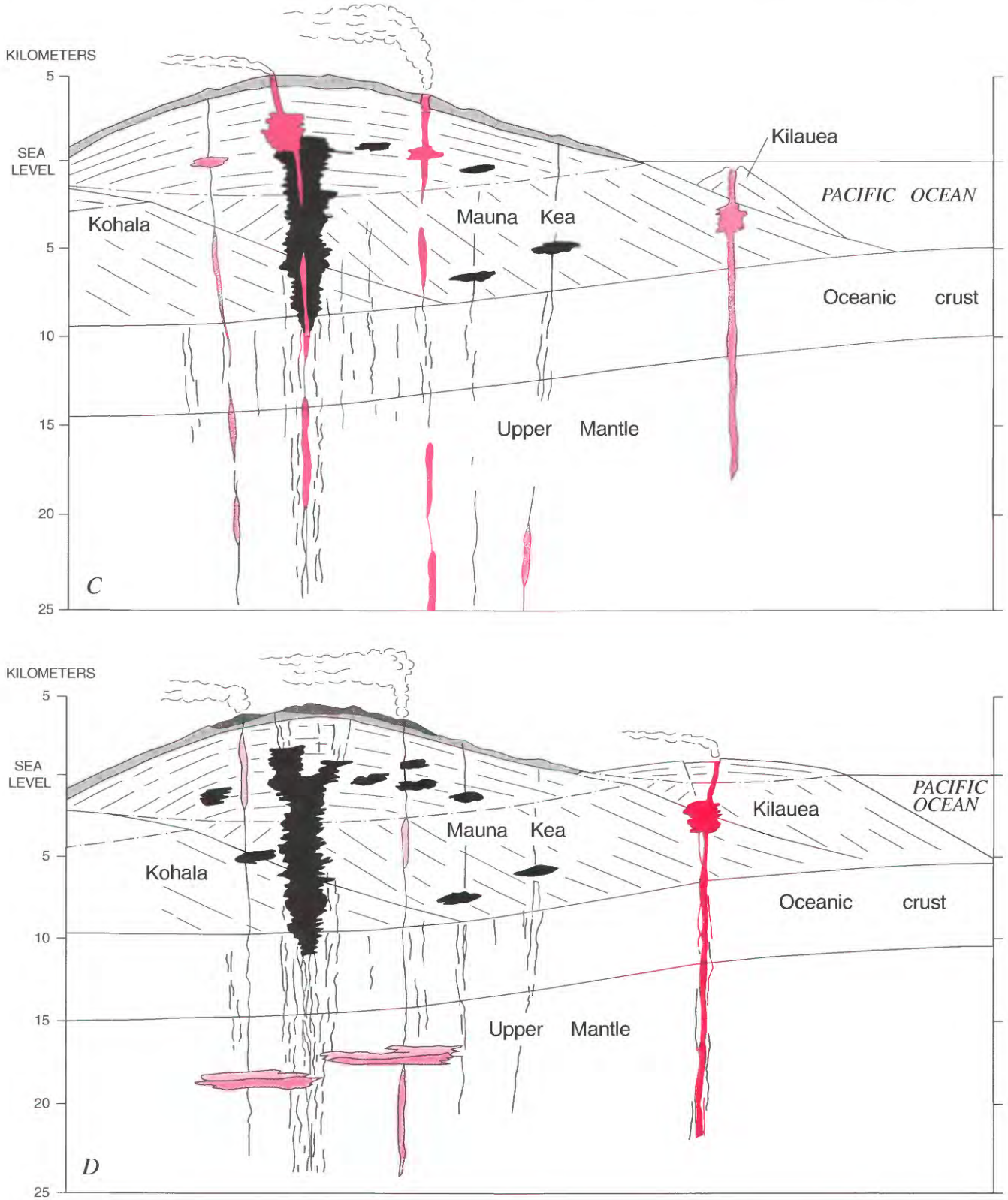

Figure 64. Continued.

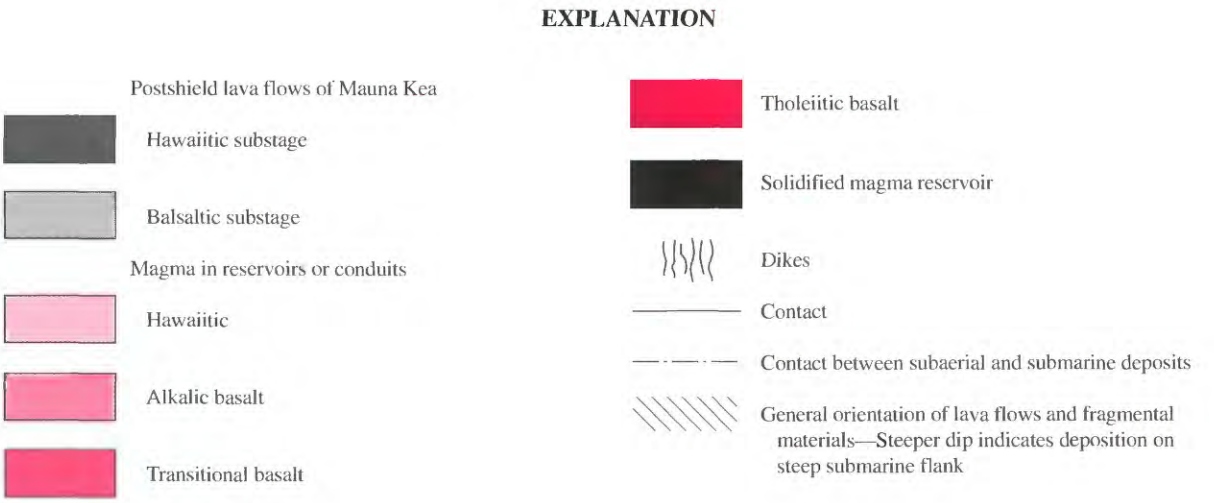

Figure 64. Continued.

Our compositional data set (table 1) for the Mauna Kea shield stage consists of analyses of three pillow-basalt samples dredged from Hilo Ridge, the same samples from which Moore and Peck (1966) inferred ridge subsidence. Two of the dredged samples, ER–20 and ER–21, are of picritic tholeiitic basalt collected from 1,650- and 2,750-m depth, respectively; the third sample, ER–22, is of transitional olivine basalt, collected from 3,200-m depth. As shown in figure 36, Kilauea lavas, though predominantly tholeiitic, include a few basalts similar in composition to the transitional basalts of Mauna Kea. This similarity indicates that such basalts are erupted at times during the shield stage, and sample ER–22 may represent an apparently similar occurrence in the shield stage of Mauna Kea. An alternative view is that sample ER–22 represents a period of transition, late in the shield stage, during which tholeiitic and alkalic basalt were both erupted. In support of such a view, Moore and Clague (1992) interpreted samples collected from the sea floor west of Hawaii as representative of Mauna Kea flows of both tholeiitic and transitional basalt that drape reefs with ages of 245 and 340 ka. They concluded from these observations that the transition from tholeiite to alkalic basalt was underway by 340 ka and was still incomplete by 245 ka.

POSTSHIELD STAGE

BASALTIC SUBSTAGE

The postshield, basaltic-substage lavas, which compose the Hamakua Volcanics, capped the entire subaerial surface of Mauna Kea (fig. 64*C*) before the hawaiitic capping lavas (Laupahoehoe Volcanics) were erupted. Nearly all of the Hamakua lavas are transitional or alkali basalt. We estimate the total volume of these postshield basalts at approximately 850 km^3. They were erupted from approximately 250 to 70 ka, giving an average lava-supply rate of about 0.005 km^3/yr, about a tenth of the median estimated supply rate during the shield stage. The decrease in production rate and silica saturation, in comparison with those of the tholeiitic shield lavas, reflects lower melt production and lower degree of partial melting in the mantle source region.

Hamakua basalts cover a broad compositional range, reflecting two separate controls: differing degrees of partial melting of the mantle source rocks to generate parental magmas of varying alkalinity (fig. 40) and subsequent crystal fractionation to produce various evolved daughter magmas from the parents. The Hamakua lavas include many evolved basalts (fig. 36) representing magmas fractionated by crystallization and separation of approximately 10 to 40 percent crystals of olivine, clinopyroxene, and plagioclase. Except for the small group of CaO-poor, high-Ti basalts that apparently fractionated relatively deep within the volcano, the evolved basalts fractionated at shallow levels, probably at pressures of about 1 to 2 kbars. Thus, we expect that many small plutons composed of these separated crystals plus crystallized unerupted magma are scattered beneath much of the volcano surface at about 3- to 6-km depth (fig. 64*C*).

Many of the Hamakua surface flows are no more than 150,000 yr old. The oldest flows, for which K-Ar data sug-

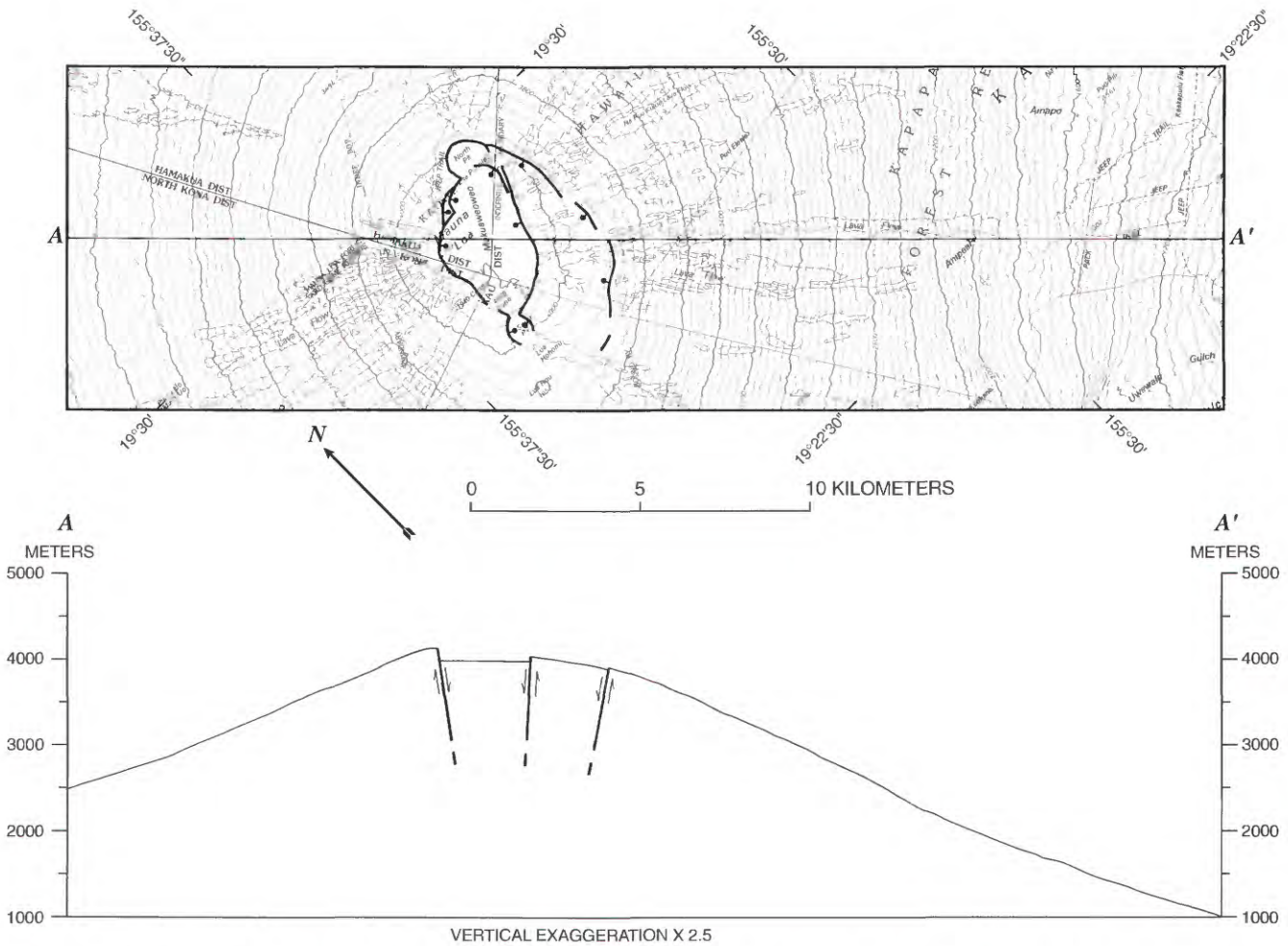

Figure 65. Comparison of topographic profiles of Mauna Loa and Mauna Kea Volcanoes. Base maps from U.S. Geological Survey 1:100,000, Hawaii County, Hawaii, Sheets 1 and 2, 1980; contour interval, 40 m. *A*, Profile of Mauna Loa, showing normal faults that bound or occur near summit caldera. Faults are dashed in cross section to indicate uncertainty about style and depth of downward projection. Ball and bar on downthrown block; arrows indicate directions of relative movement. *B*, Profile of Mauna Kea showing superimposed profile of Mauna Loa (dot-dashed line), which represents inferred contact between the postshield-stage Hamakua Volcanics and underlying shield-stage lavas. Contact with overlying Laupahoehoe Volcanics dashed where approximately located, queried where uncertain.

gest an age of approximately 200,000 to 250,000 yr, are exposed only in deep gulches that cut the northeast flank of the volcano (fig. 12). Two tholeiitic basalt flows interleaved with transitional basalt occur among these oldest lavas in Laupahoehoe Gulch, between sea level and 50-m elevation (fig. 13). We know of no other tholeiites exposed on the subaerial part of Mauna Kea. These relatively old lavas, with minor interlayered tholeiitic basalts and picrites, seem to represent the uppermost part of a transition zone between the tholeiitic shield and the overlying transitional and alkaline postshield basalts.

Hamakua basalt, which forms much of the present surface of the volcano, was erupted from vents near the summit and on the flanks of Mauna Kea. Lower-flank flows are predominantly elongate aa flows that issued during individual eruptions from scattered vents. Where not buried by younger lavas, these vents are generally marked by cinder cones. Three-quarters or more of the exposed Hamakua cones are on the northwest flank (fig. 12). This asymmetry partly reflects burial by younger lavas; Laupahoehoe lavas are more extensive over the east than the west half of the volcano. However, it also reflects a high concentration of plagioclase basalt cinder cones on the lower west flank (pl. 1), where repeated Hamakua eruptions built a prominent topographic bulge. Generally, each isolated cinder cone on the lower flanks probably represents the rise from the mantle of an individual magma batch. However, the abundance of numerous cones and flows of similar plagioclase basalt on the lower west flank leads us to speculate that these fea-

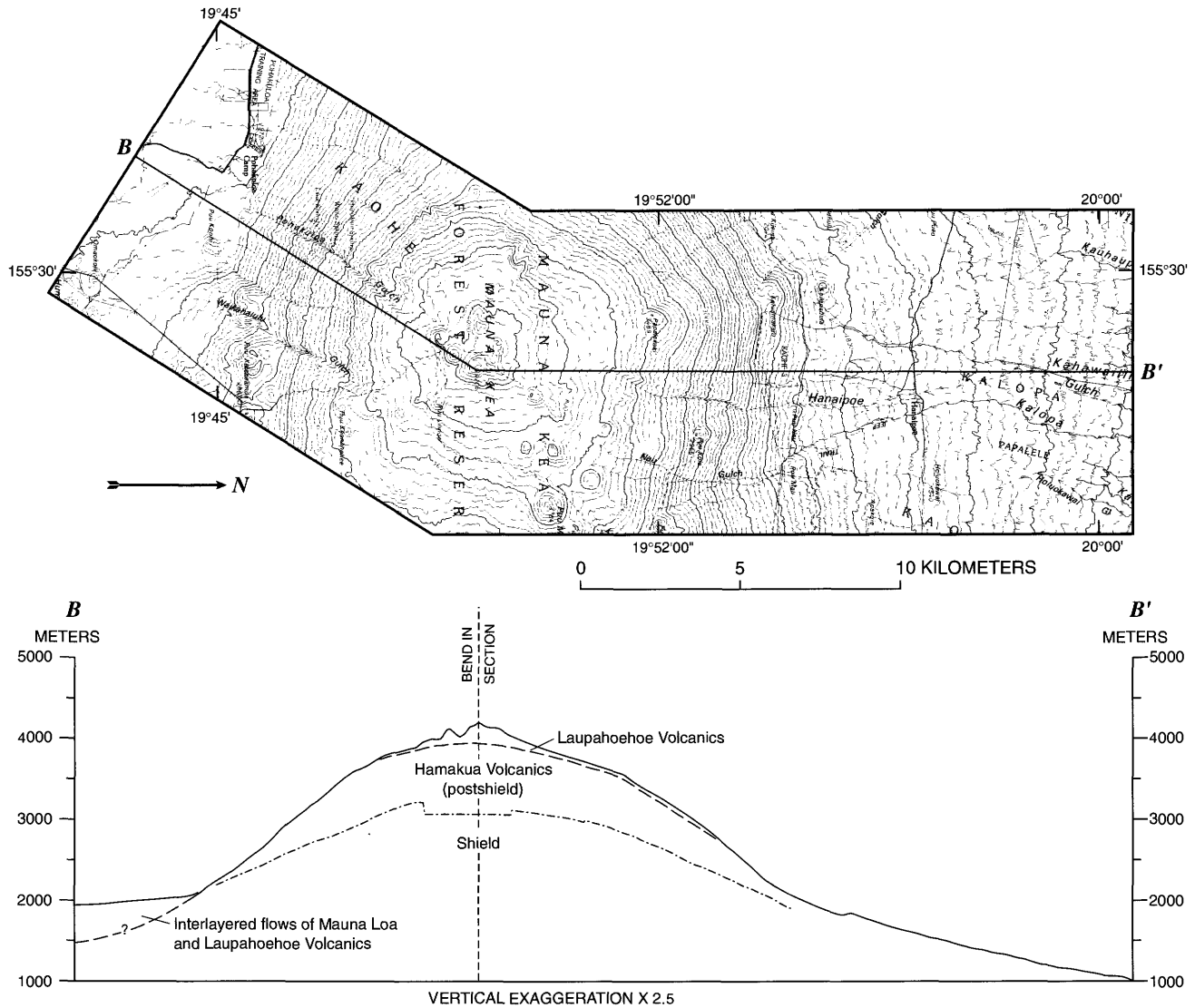

Figure 65. Continued.

tures could have been erupted from a common fractionating magma reservoir.

Upper-flank lavas of the Hamakua Volcanics record a somewhat different eruptive style from those on the lower flanks. Several lines of circumstantial evidence, which we review below, suggest to us that these upper-flank lavas may have been erupted from a long-lived, shallow magma-reservoir complex beneath the summit of Mauna Kea. Actively inflating and deflating summit reservoirs are fundamental elements in the dynamics of such shield-stage volcanoes as Kilauea and Mauna Loa (Decker, 1987).

In their limited gulch exposures, the older (approx 150,000–200,000 yr) upper-flank basalts, which compose the Hopukani Springs Volcanic Member, consist largely of thin-layered pahoehoe. Thus, morphologically they resemble the fluid basalts of the active shield volcanoes Kilauea and Mauna Loa more than they do the elongate aa flows on the lower flanks.

The younger (approx 70,000–150,000 yr) upper-flank basalts, which compose the Liloe Spring Volcanic Member, consist predominantly of stacked, thin aa flows of evolved basalt of fairly constant, phenocryst-poor lithology. Kipukas in the overlying Laupahoehoe Volcanics reveal that these Liloe Spring flows veneered at least the upper north, northwest, and south flanks of the pre-Laupahoehoe volcano (fig. 12). Repeated eruption of numerous flows of lithologically similar, evolved basalt from vents concentrated in a limited area near the summit of the volcano suggests that the Liloe Spring basalts fractionated in and were erupted from a long-lived, shallow, near-summit reservoir. Crystal zoning in these basalts, formed by rounding of phenocrysts by resorption, followed by development of overgrowths of differing

composition, provides evidence that the lavas were erupted from a reservoir periodically recharged by hotter, less evolved magma.

Exposures in the south-flank kipuka show that some of these Liloe Spring basalts were fed by dikes or erupted from fissure vents. The fissure vents and some of the dikes form a 120° arc (pl. 2) high on the upper south flank, centered near the summit, with a 1.5- to 2-km radius of curvature. We speculate that this arcuate feeder system represents Liloe Spring dikes emplaced along circumferential fractures related to cross-summit extension and summit subsidence.

Flows of Liloe Spring basalt on the north, northwest, and south flanks disappear upslope beneath a cover of younger lavas of the Laupahoehoe Volcanics. Although a few scattered basaltic cinder cones occur within the kipukas of Liloe Spring basalt on the north and south flanks, no basaltic cinder cones project upward as kipukas through the veneer of near-summit Laupahoehoe lavas. This observation suggests that the buried Liloe Spring vents may have been fissure vents which built only low spatter ramparts—as predominate on Kilauea and Mauna Loa—rather than point-source vents which built large cinder cones.

Comparison of the flank and summit topography of Mauna Kea with that of Mauna Loa may bear on the hypothesis that a shallow summit reservoir persisted at Mauna Kea throughout the postshield, basaltic substage. Profiles and topographic maps of the two volcanoes (fig. 65) show that (1) the summit area of each volcano includes a plateaulike surface which slopes less steeply than the flanks and (2) the upper flanks of Mauna Kea are approximately twice as steep as those of Mauna Loa.

A plateaulike surface surmounted by a veneer of Laupahoehoe cinder cones and lava flows forms the summit of Mauna Kea, contrasting markedly with the steep (approx 20°) upper flanks (figs. 65*B*). Extrapolation from outcrops of Liloe Spring basalt along or near the profile line (see pl. 2) indicates that the slope of the summit plateau before addition of the Laupahoehoe lavas was about 3°. The summit plateau, the slope break at its edge, and the steep upper flanks, therefore, predate the hawaiitic substage.

A remarkable analog of the buried Mauna Kea summit plateau is at the summit of Mauna Loa. Mokuaweoweo Caldera and a gently sloping (approx 3°) surface to the southeast form a summit plateau that is 5 km wide along the profile line (fig. 65*A*), contrasting sharply with the steeper slopes (approx 10°) of the upper flanks. The gently sloping lavas southeast of the caldera, as well as those underlying the steeper upper southeast and northwest flanks of Mauna Loa, are all part of a 750- to 1,500-yr-old, tube-fed pahoehoe complex erupted from a shield centered in the area of the present caldera (Lockwood and Lipman, 1987), which is a younger feature. Because the caldera walls are essentially the footwalls of high-angle normal faults, this Mauna Loa summit plateau is bounded by normal faults. We suggest that its low slopes and bounding faults are the surface expressions of extension and subsidence of the summit of Mauna Loa above a magma reservoir at about 3-km depth (Decker, 1987). Extending the analogy to Mauna Kea, we suggest that the gently sloping summit plateau of the basaltic substage, which is bounded by abruptly steepening slopes, is the now-buried surface expression of extension and subsidence of the summit of Mauna Kea above a shallow magma reservoir.

The arcuate fracture system indicated by dikes and fissure vents of the Liloe Spring Volcanic Member suggests that normal faults may have bounded the summit plateau at times during the basaltic substage. However, we have no evidence of a deep caldera like those, several hundred meters deep, that have existed in fairly recent times on Mauna Loa and Kilauea (Holcomb, 1987; Lockwood and Lipman, 1987). Holcomb suggested that large caldera-collapse events on Kilauea result from voluminous rift-zone eruptions. Extending that view to Mauna Kea, we believe that large caldera-forming summit collapses were unlikely on Mauna Kea during the basaltic substage or even during the later part of the shield stage after the termination of eruptive activity in the east rift zone.

The upper flanks of Mauna Kea are twice as steep (approx 20°) as those of Mauna Loa (approx 10°). Basalts of the Liloe Spring Volcanic Member dip essentially parallel to the surface slopes. Because there is no direct evidence of deformation of these flows, most probably they mantle slopes that were already steep when the Liloe Spring basalts were erupted. We suggest two mechanisms for steepening of the upper flanks: (1) emplacement of voluminous shallow intrusions that would steepen the upper flanks by deforming the volcanic edifice during the later part of the shield stage or early part of the postshield stage; and (2) greater viscosity of postshield lava flows than of shield-stage tholeiitic basalt, and thicker accumulation of vent deposits and lava flows on the upper than on the lower flanks. We know of no evidence other than steepening of the upper flanks for massive intrusion (mechanism 1). Increased viscosity, in combination with preferred concentration of vents on the upper flanks (mechanism 2), probably contributed to upper-flank steepening during the basaltic substage. Projection of the Mauna Loa profile shown in figure 65*A* into figure 65*B* illustrates a hypothetical cross section in which upper-flank steepening of Mauna Kea reflects only greater upper-flank thickness of the Hamakua Volcanics.

The K-Ar ages of postshield basalts from the upper and lower flanks indicate that the Liloe Spring and Hopukani Springs Volcanic Members on the upper flanks of Mauna Kea Volcano consist of flows which (1) may have been erupted from a long-lived summit reservoir and (2) accumulated during the same interval as the lower-flank flows which were erupted from scattered individual vents marked by cinder cones. A compositional difference accompanies the difference in eruptive styles between the broadly coeval upper- and lower-flank flows. The upper-flank flows are

almost all transitional basalt (silica saturated) and include some of the most silica saturated lavas of the postshield stage; only 4 of 63 analyzed samples (approx 6 percent) of Hamakua basalt from above 2,000-m (6,560 ft) elevation are alkalic (ne normative). The lower-flank flows are generally more alkaline, and alkali basalt (silica undersaturated) is common; 29 of 155 analyzed samples (approx 19 percent) of Hamakua basalt from below 2,000-m (6,560 ft) elevation are alkalic. Thus, transitional basalt, generated by higher degrees of partial melting in the upper-mantle source, sustained and was erupted from the summit reservoir, whereas alkali basalt, generated by lesser degrees of partial melting, was more commonly erupted from scattered individual vents on the lower flanks of the volcano. This compositional zoning of the volcano suggests that the source region was zoned with respect to degree of partial melting: Greater partial melting occurred in the central part of the source area, and lesser partial melting near its perimeter. Furthermore, this scenario implies that magma batches supplying the lavas of the volcano's flanks rose along individual vertical paths from the mantle source (fig. 64*C*).

HAWAIITIC SUBSTAGE

The postshield, hawaiitic-substage lavas, which compose the Laupahoehoe Volcanics, form a discontinuous, magmatically evolved cap on Mauna Kea Volcano (fig. 22). Approximately 10 percent of the lava is benmoreite, and 90 percent is hawaiite and mugearite. The volume of Laupahoehoe flows and pyroclastic deposits is about 25 km^3 (dense-rock equivalent). These lavas were erupted from approximately 65 to 4 ka, giving an average lava-supply rate of about 0.0004 km^3/yr. This rate, which is one-tenth the lava-supply rate for the basaltic substage, presumably reflects greatly diminished melting rates in the mantle source.

Most Laupahoehoe eruptions formed prominent cinder cones and elongate, rugged lava flows composed predominantly of aa. The vents are largely concentrated near the summit and on the upper flanks of the volcano. Laupahoehoe cones and flows provide the rugged local topographic irregularities that make the upper slopes and summit of Mauna Kea contrast so markedly with the much smoother slopes of the Mauna Loa shield.

Concentrations of Laupahoehoe cinder cones occur in sectors west, northeast, and south to southeast of the volcano's summit. Cone alignments and elongation of these clusters radial to the summit are distinct in the western cluster, less certain in the northeastern cluster, and unrecognizable in the south-to-southeastern cluster. Although Macdonald (1945) and Porter (1972b) referred to these clusters as having erupted along rift zones radial to the summit, we see no connection between the clusters and the rift-zone structure of the underlying tholeiitic shield. However, the cone distribution apparently reflects radial stress inhomogeneities in the volcanic edifice.

The Holocene record provides some evidence that Laupahoehoe eruptions may have occurred in sporadic bursts of activity, rather than being more or less evenly spaced over the past 65,000 yr. Radiometric dating (table 6) and field relations indicate that the line of cinder cones, representing at least seven separate vents (pl. 2) extending northeastward from Kalaieha through Puu Kole (south flank), formed between 6 and 4 ka. Virtually identical lava compositions along this alignment suggest that the group of aligned cones and their flows represent a single magma batch. ^{14}C ages indicate that at least three other flows were erupted elsewhere on the volcano during the same time interval; these eruptions occurred on the northeast flank at Puu Lehu and Puu Kanakaleonui and on the south flank near Hale Pohaku. Apparently, Mauna Kea has been quiescent during the past 4,000 yr. We have found no Laupahoehoe lavas younger than those erupted during this burst of eruptive activity between 6 and 4 ka.

Laupahoehoe eruptions produced voluminous ash that was distributed beyond the cinder cones and the local airfall deposits near some of the cinder cones. This ash is the dominant component of a host of eolian, fluvial, and colluvial deposits that now mantle parts of Mauna Kea's flanks.

Mass-balance modeling and consideration of phase equilibria at elevated pressure suggest that the hawaiitic Laupahoehoe magma was generated by fractionation of an alkali basalt parent at a pressure of at least 5 to 7 kbars. Production of the most mafic hawaiitic lava requires removal of 40 to 50 percent of the parent as a crystal assemblage dominated by clinopyroxene (approx 50 weight percent), with lesser amounts of plagioclase, olivine, and Fe-Ti oxides. Dominance of clinopyroxene in the assemblage reflects the expanded stability field of clinopyroxene at elevated pressure. Generation of more evolved Laupahoehoe lavas, ranging to benmoreite, requires increasing plagioclase fractionation.

Compositions of Laupahoehoe lavas plot between the trends of liquids on the olivine+orthopyroxene+clinopyroxene cotectic at 8 to 30 kbars and 1 bar on the DI–OL–NEPH diagram (fig. 59) of Sack and others (1987), as well as in a restricted cluster offset from the low-pressure cotectic projected onto the CS–MS–A plane (fig. 60) of O'Hara (1968). These results suggest that the Laupahoehoe magmas were all generated by fractionation at elevated pressure and that no additional low-pressure fractionation occurred. Furthermore, the essentially constant proportions of silicate phases fractionated during the evolution from the most mafic hawaiite to benmoreite (table 23) suggest that the liquids represented by this compositional range were produced by cotectic crystallization at similar pressures and did not fractionate further during ascent.

About 20 to 30 percent of Laupahoehoe lavas contain gabbroic and ultramafic xenoliths entrained in the ascend-

ing evolved magma. Mineralogies, structures, and fabrics of these xenoliths indicate that they probably came from a zone of injected and intensely jointed peridotite at and somewhat below the base of the oceanic crust. In accord with this observation and with the evidence from phase equilibria discussed above, we conclude that the suite of hawaiitic magmas originated by varying degrees of fractionation of alkali basalt magma in a reservoir(s) in the upper mantle near the base of the oceanic crust (fig. 64*D*). Batches of this magma then rose directly to the surface, passing through the crust and the volcanic edifice with no further fractionation.

Our mapping shows no interleaving of basalt (Hamakua Volcanics) and hawaiitic lava (Laupahoehoe Volcanics). Thus, an abrupt change from production of basalt to production of hawaiite, mugearite, and benmoreite occurred before approximately 65 ka. Laupahoehoe melt-production rates were greatly diminished from those associated with Hamakua volcanism, as indicated by the diminished average lava-supply rate. Furthermore, evidence suggests that only alkali basaltic magma was produced in the source region, indicating a lower degree of partial melting than that which produced transitional basaltic magma during Hamakua volcanism. The most remarkable—and enigmatic—change was that the basaltic parental magma of the Laupahoehoe Volcanics ponded and fractionated extensively in the upper mantle before ascending to the surface without further interruption. In marked contrast, basaltic parental magma of the Hamakua Volcanics was erupted without undergoing such extreme fractionation—it was still basalt—and most of it shows the petrologic imprint of low-pressure fractionation in either ephemeral or long-lived reservoirs within the volcano superstructure.

GLACIATION

The glacial record on Mauna Kea was a major focus of attention for S.C. Porter (for example, Porter, 1979a, b, c, d), and we accept many of his interpretations as authoritative. However, our mapping, stratigraphic interpretations, and new K-Ar dating have led to some important revisions, foremost among which is recognition that the glacial record extends back no more than to 200–150 ka, rather to nearly 300 ka, as indicated to Porter (1979c, d) by the K-Ar ages available to him. Two separate glacial episodes were recorded during the postshield, basaltic substage, and their deposits are mapped as the Pohakuloa and Waihu Glacial Members of the Hamakua Volcanics. The older, Pohakuloa Glacial Member overlies basalt dated at approximately 150 to 200 ka and is overlain by basalt flows dated within the range 100–150 ka. K-Ar results indicate that the age of the younger, Waihu Glacial Member is within the range of 70–150 ka; Dorn and others (1991) reported an exposure age of 60 to 70 ka.

We recognize a single additional glacial unit, the Makanaka Glacial Member, which was deposited between approximately 40 and 13 ka, during the hawaiitic substage. Accordingly, these deposits are mapped as a glacial member within the Laupahoehoe Volcanics. Although Porter (1979a, c) described deposits of two separate Makanaka glacial episodes, we have found the deposits largely indistinguishable and the separate units unmappable. Field evidence suggests that the Makanaka deposits represent a single glacial episode unbroken by an interglacial hiatus.

REFERENCES CITED

Basaltic Volcanism Study Project, 1981, Basaltic volcanism on the terrestrial planets: New York, Pergamon, 1,286 p.

Beeson, M.H., 1976, Petrology, mineralogy, and geochemistry of the East Molokai Volcano Series, Hawaii: U.S. Geological Survey Professional Paper 961, 53 p.

Bonhommet, Norbert, Beeson, M.H., and Dalrymple, G.B., 1977, A contribution to the geochronology and petrology of the Island of Lanai, Hawaii: Geological Society of America Bulletin, v. 88, no. 9, p. 1281–1286.

Bryan, W.A., 1916, Mauna Kea shows signs of ancient glacial scouring: Pacific Commercial Advertiser, July 17, p. 1, 9; August 30, p. 7.

———1918, Report on discovery of ancient glaciation on Mauna Kea, Hawaii: Science, new ser., v. 47, no. 1220, p. 492.

Bryan, W.B., Finger, L.W., and Chayes, Felix, 1969, Estimating proportions in petrographic mixing equations by least-squares approximation: Science, v. 163, no. 3870, p. 926–927.

Chase, T.E., Miller, C.P., Seekins, B.A., Normark, W.R., Gutmacher, C.E., Wilde, Pat, and Young, J.D., 1980, Topography of the southern Hawaiian Islands: U.S. Geological Survey Open-File Map 81–120, 3 sheets.

Chen, C.-Y., and Frey, F.A., 1985, Trace element and isotopic geochemistry of lavas from Haleakala Volcano, East Maui, Hawaii; implications for the origin of Hawaiian basalts: Journal of Geophysical Research, v. 90, no. B10, p. 8743–8768.

Clague, D.A., and Dalrymple, G.B., 1987, The Hawaiian-Emperor volcanic chain. Part I. Geologic evolution, chap. 1 *of* Decker, R.W., Wright, T.L., and Stauffer, P.H., eds., Volcanism in Hawaii: U.S. Geological Survey Professional Paper 1350, v. 1, p. 5–54.

Clague, D.A., and Dalrymple, G.B., 1989, Tectonics, geochronology, and origin of the Hawaiian-Emperor Chain, *in* Winterer, E.L., Hussong, D.M., and Decker, R.W., eds., The eastern Pacific Ocean and Hawaii, v. N *of* The geology of North America: Boulder, Colo., Geological Society of America, p. 188–217.

Clague, D.A., and Heliker, Christina, 1992, The ten-year eruption of Kilauea Volcano: Earthquakes and Volcanoes, v. 23, no. 6, p. 244–254.

Clague, D.A., Jackson, E.D., and Wright, T.L., 1980, Petrology of Hualalai Volcano, Hawaii; implications for mantle composition: Bulletin Volcanologique, v. 43, no. 4, p. 641–656.

Clague, D.A., and Moore, J.G., 1991, Geology and petrology of Mahukona Volcano, Hawaii: Bulletin of Volcanology, v. 53, no. 3, p. 159–172.

Coombs, D.S., and Wilkinson, J.F.G., 1969, Lineages and fractionation trends in undersaturated volcanic rocks from the East Otago volcanic province (New Zealand) and related rocks: Journal of Petrology, v. 10, pt. 3, p. 440–501.

Cruikshank, D.P., 1986, Mauna Kea; a guide to the upper slopes and observatories: Honolulu, University of Hawaii, Institute for Astronomy, 59 p.

Dalrymple, G.B., and Lanphere, M.A., 1969, Potassium-argon dating: San Francisco, W.H. Freeman and Co., 258 p.

Daly, R.A., 1910, Pleistocene glaciation and the coral reef problem: American Journal of Science, ser. 4, v. 30, no. 179, p. 297–308.

———1911, Magmatic differentiation in Hawaii: Journal of Geology, v. 19, no. 4, p. 289–316.

Dana, J.D., 1890, Characteristics of volcanoes: New York, Dodd, Mead, and Co., 399 p.

Decker, R.W., 1987, Dynamics of Hawaiian volcanoes; an overview, chap. 42 *of* Decker, R.W., Wright, T.L., and Stauffer, P.H., eds., Volcanism in Hawaii: U.S. Geological Survey Professional Paper 1350, v. 2, p. 997–1018.

Dorn, R.I., Phillips, F.M., Zreda, M.G., Wolfe, E.W., Jull, A.J.T., Donahue, D.J., Kubik, P.W., and Sharma, Pankaj, 1991, Glacial chronology of Mauna Kea, Hawaii, as constrained by surface-exposure dating: National Geographic Research and Exploration, v. 7, no. 4, p. 456–471.

Dvorak, J.J., and Dzurisin, Daniel, 1993, Variations in magma supply rate at Kilauea Volcano, Hawaii: Journal of Geophysical Research, v. 98, no. B12, p. 22255–22268.

Falloon, T.J., Green, D.H., Hatton, C.J., and Harris, K.L., 1988, Anhydrous partial melting of a fertile and depleted peridotite from 2 to 30 Kb and application to basalt petrogenesis: Journal of Petrology, v. 24, no. 6, p. 1257–1282.

Feigenson, M.D., 1984, Geochemistry of Kauai volcanoes and a mixing model for the origin of Hawaiian alkali basalts: Contributions to Mineralogy and Petrology, v. 87, no. 2, p. 109–119.

Feigenson, M.D., Hofmann, A.W., and Spera, F.J., 1983, Case studies on the origin of basalt; II. The transition from tholeiitic to alkalic volcanism on Kohala Volcano, Hawaii: Contributions to Mineralogy and Petrology, v. 84, no. 4, p. 390–405.

Fodor, R.V., and Vandermeyden, H.J., 1988, Petrology of gabbroic xenoliths from Mauna Kea Volcano, Hawaii: Journal of Geophysical Research, v. 93, no. B5, p. 4435–4452.

Foshag, W.F., and González R., Jenaro, 1956, Birth and development of Parícutin Volcano, Mexico: U.S. Geological Survey Bulletin 965–D, p. 355–489.

Frey, F.A., Garcia, M.O., Wise, W.S., Kennedy, A.K., Gurriet, P.C., and Albarede, Francis, 1991, The evolution of Mauna Kea Volcano, Hawaii; petrogenesis of tholeiitic and alkalic basalts: Journal of Geophysical Research, v. 96, no. B9, p. 14347–14375.

Frey, F.A., Wise, W.S., Garcia, M.O., West, H.B., Kwon, S.-T., and Kennedy, A.K., 1990, Evolution of Mauna Kea Volcano, Hawaii; petrologic and geochemical constraints on postshield volcanism: Journal of Geophysical Research, v. 95, no. B2, p. 1271–1300.

Green, D.H., and Ringwood, A.E., 1967, The genesis of basaltic magmas: Contributions to Mineralogy and Petrology, v. 15, no. 2, p. 103–190.

Greenland, L.P., 1987, Composition of gases from the 1984 eruption of Mauna Loa Volcano, chap. 30 *of* Decker, R.W., Wright, T.L., and Stauffer, P.H., eds., Volcanism in Hawaii: U.S. Geological Survey Professional Paper 1350, v. 1, p. 781–790.

Gregory, H.E., and Wentworth, C.K., 1937, General features and glacial geology of Mauna Kea, Hawaii: Geological Society of America Bulletin, v. 48, no. 12, p. 1719–1742.

Hill, D.P., and Zucca, J.J., 1987, Geophysical constraints on the structure of Kilauea and Mauna Loa Volcanoes and some implications for seismomagmatic processes, chap. 37 *of* Decker, R.W., Wright, T.L., and Stauffer, P.H., eds., Volcanism in Hawaii: U.S. Geological Survey Professional Paper 1350, v. 2, p. 903–917.

Hofmann, A.W., Feigenson, M.D., and Raczek, Ingrid, 1984, Case studies on the origin of basalt; III, Petrogenesis of the Mauna Ulu eruption, Kilauea, 1969–1971: Contributions to Mineralogy and Petrology, v. 88, no. 1–2, p. 24–35.

———1987, Kohala revisited: Contributions to Mineralogy and Petrology, v. 95, no. 1, p. 114–122.

Holcomb, R.T., 1987, Eruptive history and long-term behavior of Kilauea Volcano, chap. 12 *of* Decker, R.W., Wright, T.L., and Stauffer, P.H., eds., Volcanism in Hawaii: U.S. Geological Survey Professional Paper 1350, v. 1, p. 261–350.

Ingamells, C.O., 1970, Lithium metaborate flux in silicate analysis: Analytica Chimica Acta, v. 52, no. 2, p. 332–334.

Jackson, E.D., Beeson, M.H., and Clague, D.A., 1982, Xenoliths in volcanic rocks from Mauna Kea Volcano, Hawaii: U.S. Geological Survey Open-File Report 82–201, 19 p.

Jackson, E.D., Silver, E.A., and Dalrymple, G.B., 1972, Hawaiian-Emperor Chain and its relation to Cenozoic circumpacific tectonics: Geological Society of America Bulletin, v. 83, no. 3, p. 601–617.

Jaggar, T.A., Jr., 1925, The Daly glacier on Mauna Kea, *in* Fiske, R.S., Simpkin, Thomas, and Nielsen, Elizabeth, 1987, Volcano Letter, no. 43, p. 1: Washington, D.C., Smithsonian Institution Press [unpaginated].

Kennedy, W.Q., 1933, Trends of differentiation in basaltic magmas: American Journal of Science, ser. 5, v. 25, no. 147, p. 239–256.

Klerkx, Jean, 1966, La crystallization de l'apatite dans les lavas de l'Etna [The crystallization of apatite in the lavas of Etna]: Société Belge de Géologie Annales, v. 89B, p. 449–458.

Kuno, Hisashi, 1969, Mafic and ultramafic nodules in basaltic rocks of Hawaii, *in* Larsen, L.H., Prinz, Martin, and Manson, Vincent, eds., Igneous and metamorphic geology (Poldevaart volume): Geological Society of America Memoir 115, p. 189–234.

Langenheim, V.A.M., and Clague, D.A., 1987, The Hawaiian-Emperor volcanic chain, chap. 2 *of* Decker, R.W., Wright, T.L., and Stauffer, P.H., Volcanism in Hawaii: U.S. Geological Survey Professional Paper 1350, v. 1, p. 55–84.

Lanphere, M.A., and Frey, F.A., 1987, Geochemical evolution of Kohala Volcano, Hawaii: Contributions to Mineralogy and Petrology, v. 95, no. 1, p. 100–113.

Le Bas, M.J., Le Maitre, R.W., Streckeisen, Albert, and Zanettin, B.A., 1986, Chemical classification of volcanic rocks based on the total alkali-silica diagram: Journal of Petrology, v. 27, no. 3, p. 745–750.

Lipman, P.W., and Banks, N.G., 1987, Aa flow dynamics, Mauna Loa 1984, chap. 57 *of* Decker, R.W., Wright, T.L., and Stauffer, P.H., eds., Volcanism in Hawaii: U.S. Geological Survey Professional Paper 1350, v. 2, p. 1527–1567.

Lockwood, J.P., and Lipman, P.W., 1987, Holocene eruptive history of Mauna Loa Volcano, chap. 18 *of* Decker, R.W., Wright, T.L., and Stauffer, P.H., eds., Volcanism in Hawaii: U.S. Geological Survey Professional Paper 1350, v. 1, p. 509–535.

Ludwig, K.R., Szabo, B.J., Moore, J.G., and Simmons, K.R., 1991, Crustal subsidence rate off Hawaii determined from $^{234}U/^{238}U$ ages of drowned coral reefs: Geology, v. 19, no. 2, p. 171–174.

Maaloe, Sven, Pedersen, R.B., and James, D., 1988, Delayed fractionation of basaltic lavas: Contributions to Mineralogy and Petrology, v. 98, no. 4, p. 401–407.

Macdonald, G.A., 1945, Ring structures at Mauna Kea, Hawaii: American Journal of Science, v. 243, no. 4, p. 210–217.

———1949, Petrography of the Island of Hawaii: U.S. Geological Survey Professional Paper 214–D, p. 51–96.

———1968, Composition and origin of Hawaiian lavas, *in* Coats, R.R., Hay, R.L., and Anderson, C.A., eds., Studies in volcanology: Geological Society of America Memoir 116, p. 477–522.

Macdonald, G.A., Abbott, A.A., and Peterson, F.L., 1983, Volcanoes in the sea; the geology of Hawaii: Honolulu, University of Hawaii Press, 517 p.

Macdonald, G.A., and Katsura, Takashi, 1962, Relationship of petrographic suites in Hawaii, *in* Macdonald, G.A., and Kuno, Hisashi, eds., The crust of the Pacific Basin: American Geophysical Union Monograph 6, p. 187–195.

———1964, Chemical composition of Hawaiian lavas: Journal of Petrology, v. 5, pt. 1, p. 82–133.

Mahood, G.A. and Baker, D.R., 1987, Experimental constraints on depths of fractionation of mildly alkalic basalts and associated felsic rocks; Pantelleria, Strait of Sicily: Contributions to Mineralogy and Petrology, v. 93, no. 2, p. 251–264.

Mark, R.K., and Moore, J.G., 1987, Slopes of the Hawaiian Ridge, chap. 4 *of* Decker, R.W., Wright, T.L., and Stauffer, P.H., eds., Volcanism in Hawaii: U.S. Geological Survey Professional Paper 1350, v. 1, p. 101–107.

Martinson, D.G., Pisias, N.G., Hays, J.D., Imbrie, John, Moore, T.C., Jr., and Shackleton, N.J., 1987, Age dating and the orbital theory of the ice ages; development of a high-resolution 0 to 300,000-year chronostratigraphy: Quaternary Research, v. 27, no. 1, p. 1–29.

Moore, J.G., 1987, Subsidence of the Hawaiian Ridge, chap. 3 *of* Decker, R.W., Wright, T.L., and Stauffer, P.H., eds., Volcanism in Hawaii: U.S. Geological Survey Professional Paper 1350, v. 1, p. 85–100.

Moore, J.G., and Clague, D.A., 1992, Volcano growth and evolution of the Island of Hawaii: Geological Society of America Bulletin, v. 104, no. 11, p. 1471–1484.

Moore, J.G., Clague, D.A., and Normark, W.R., 1982, Diverse basalt types from Loihi Seamount, Hawaii: Geology, v. 10, no. 2, p. 88–92.

Moore, J.G., and Fiske, R.S., 1969, Volcanic substructure inferred from dredge samples and ocean-bottom photographs, Hawaii: Geological Society of America Bulletin, v. 80, no. 7, p. 1191–1201.

Moore, J.G., and Peck, D.L., 1966, Submarine lavas from the east rift zone of Mauna Kea, Hawaii [abs.], *in* Abstracts for 1965: Geological Society of America Special Paper 87, p. 218.

O'Hara, M.J., 1968, The bearing of phase equilibria studies in synthetic and natural systems on the origin and evolution of basic and ultrabasic rocks: Earth-Science Reviews, v. 4, p. 69–133.

O'Hara, M.J., and Yoder, H.S., Jr., 1967, Formation and fractionation of basic magmas at high pressures: Scottish Journal of Geology, v. 3, pt. 1, p. 67–117.

Perdue, E.A., 1982, The petrology and geochemistry of lavas from the west flank of Mauna Kea Volcano, Hawaii: Santa Barbara, University of California, M.S. thesis, 171 p.

Porter, S.C., 1971, Holocene eruptions of Mauna Kea volcano, Hawaii: Science, v. 172, no. 3981, p. 375–377.

———1972a, Buried caldera of Mauna Kea Volcano, Hawaii: Science, v. 175, no. 4029, p. 1458–1460.

———1972b, Distribution, morphology, and size frequency of cinder cones on Mauna Kea Volcano, Hawaii: Geological Society of America Bulletin, v. 83, no. 12, p. 3607–3612.

———1973, Stratigraphy and chronology of late Quaternary tephra along the south rift zone of Mauna Kea Volcano, Hawaii: Geological Society of America Bulletin, v. 84, no. 6, p. 1923–1939.

———1975, Late Quaternary glaciation and tephrochronology of Mauna Kea, Hawaii *in* Suggate, R.P., and Cresswell, M.M., eds., Quaternary studies: Royal Society of New Zealand Bulletin 13, p. 247–251.

———1979a, Geologic map of Mauna Kea Volcano, Hawaii: Geological Society of America Map and Chart Series, no. MC–30, scale 1:48,000.

———1979b, Quaternary stratigraphy and chronology of Mauna Kea, Hawaii; a 380,000-yr record of mid-Pacific volcanism and ice-cap glaciation; summary: Geological Society of America Bulletin, pt. 1, v. 90, no. 7, p. 609–611.

———1979c, Quaternary stratigraphy and chronology of Mauna Kea, Hawaii; a 380,000-yr record of mid-Pacific volcanism and ice-cap glaciation: Geological Society of America Bulletin, pt. 2, v. 90, no. 7, p. 980–1093.

———1979d, Hawaiian glacial ages: Quaternary Research, v. 12, no. 2, p. 161–186.

———1987, Pleistocene subglacial eruptions on Mauna Kea, chap. 21 *of* Decker, R.W., Wright, T.L., and Stauffer, P.H., eds., Volcanism in Hawaii: U.S. Geological Survey Professional Paper 1350, v. 1, p. 587–598.

Porter, S.C., Stuiver, Minze, and Yang, I.C., 1977, Chronology of Hawaiian glaciations: Science, v. 195, no. 4273, p. 61–63.

Powers, H.A., 1955, Composition and origin of basaltic magma of the Hawaiian Islands: Geochimica et Cosmochimica Acta, v. 7, no. 1–2, p. 77–107.

Presnall, D.C., Dixon, S.A., Dixon, J.R., O'Donnell, T.H., Brenner, N.L., Schrock, R.L., and Dycus, D.W., 1978, Liquidus phase relations on the join diopside-forsterite-anorthite from 1 atm to 20 kbar; their bearing on the generation and crystallization of basaltic magma: Contributions to Mineralogy and Petrology, v. 66, no. 2, p. 203–220.

Roeder, P.L., and Emslie, R.F., 1970, Olivine-liquid equilibrium: Contributions to Mineralogy and Petrology, v. 29, no. 4, p. 275–289.

Rubin, Meyer, Gargulinski, L.K., and McGeehin, J.P., 1987, Hawaiian radiocarbon dates, chap. 10 *of* Decker, R.W.,

Wright, T.L., and Stauffer, P.H., eds., Volcanism in Hawaii: U.S. Geological Survey Professional Paper 1350, v. 1, p. 213–242.

Sack, R.O., Walker, David, and Carmichael, I.S.E., 1987, Experimental petrology of alkalic lavas; constraints on cotectics of multiple saturation in natural basic liquids: Contributions to Mineralogy and Petrology, v. 96, no. 1, p. 1–23.

Spengler, S.R., and Garcia, M.O., 1988, Geochemistry of the Hawi lavas, Kohala Volcano, Hawaii: Contributions to Mineralogy and Petrology, v. 99, no. 1, p. 90–104.

Stacey, J.S., Sherrill, N.D., Dalrymple, G.B., Lanphere, M.A., and Carpenter, N.V., 1981, A five-collector system for the simultaneous measurement of argon isotope ratios in a static mass spectrometer: International Journal of Mass Spectrometry and Ion Physics, v. 39, no. 2, p. 167–180.

Stearns, H.T., 1945, Glaciation of Mauna Kea, Hawaii: Geological Society of America Bulletin, v. 56, no. 3, p. 267–274.

———1946, Geology of the Hawaiian Islands: Hawaii Division of Hydrography Bulletin 8, 105 p. [2d printing, 1967, with supplement, 112 p.].

Stearns, H.T., and Macdonald, G.A., 1942, Geology and groundwater resources of the Island of Maui, Hawaii: Hawaii Division of Hydrography Bulletin 7, 344 p.

———1946, Geology and ground-water resources of the Island of Hawaii: Hawaii Division of Hydrography Bulletin 9, 363 p.

Steiger, R.H., and Jäger, Emilie, compilers, 1977, Subcommission on Geochronology; convention of the use of decay constants in geo- and cosmochronology: Earth and Planetary Science Letters, v. 36, no. 3, p. 359–362.

Swanson, D.A., 1972, Magma supply rate at Kilauea Volcano, 1952–1971: Science, v. 175, no. 4018, p. 169–170.

Takahashi, Eiichi, and Kushiro, Ikuo, 1983, Melting of a dry peridotite at high pressures and basalt magma genesis: American Mineralogist, v. 68, no. 9–10, p. 859–879.

Tilley, C.E., 1950, Some aspects of magmatic evolution: Geological Society of London Quarterly Journal, v. 106, pt. 1, no. 421, p. 37–61.

Washington, H.S., 1923, Petrology of the Hawaiian Islands; I, Kohala and Mauna Kea, Hawaii: American Journal of Science, ser. 5, v. 5, no. 30, p. 465–502.

Wentworth, C.K., 1938, Ash formations of the Island of Hawaii: Hawaiian Volcano Observatory Special Report 3, 183 p.

Wentworth, C.K., and Powers, W.E., 1941, Multiple glaciation of Mauna Kea, Hawaii: Geological Society of America Bulletin, v. 52, no. 8, p. 1193–1217.

West, H.B., Garcia, M.O., Frey, F.A, and Kennedy, A.K., 1988, Nature and cause of compositional variation among the alkalic cap lavas of Mauna Kea Volcano, Hawaii: Contributions to Mineralogy and Petrology, v. 100, no. 3, p. 383–397.

Wilkinson, J.G.F., and Hensel, H.D., 1988, The petrology of some picrites from Mauna Loa and Kilauea Volcanoes, Hawaii: Contributions to Mineralogy and Petrology, v. 98, no. 3, p. 326–345.

Wise, W.S., 1982, A volume-time framework for the evolution of Mauna Kea volcano, Hawaii [abs.]: Eos (American Geophysical Union Transactions), v. 63, no. 45, p. 1137.

Wolfe, E..W., 1997, Major-oxide analyses for Mauna Kea Volcano, Hawaii: U.S. Geological Survey Open-File Report OF–97–84.

Wolfe, E.W., and Morris, Jean, 1996, Geologic map of the Island of Hawaii: U.S. Geological Survey Miscellaneous Investigations Series Map, I–2524–A, scale 1:100,000.

Wolfe, E.W., Ulrich, G.E., Holm, R.F., Moore, R.B., and Newhall, C.G., 1987a, Geologic map of the central part of the San Francisco volcanic field, north-central Arizona: U.S. Geological Survey Miscellaneous Field Studies Map MF–1959, scale 1:50,000.

Wolfe, E.W., Ulrich, G.E., and Newhall, C.G., 1987b, Geologic map of the northwest part of the San Francisco volcanic field, north-central Arizona: U.S. Geological Survey Miscellaneous Field Studies Map MF–1957, scale 1:50,000.

Wright, T.L., 1971, Chemistry of Kilauea and Mauna Loa in space and time: U.S. Geological Survey Professional Paper 735, 40 p.

———1973, Magma mixing as illustrated by the 1959 eruption, Kilauea Volcano, Hawaii: Geological Society of America Bulletin, v. 84, no. 3, p. 849–858.

———1984, Origin of Hawaiian tholeiite; a metasomatic model: Journal of Geophysical Research, v. 89, no. B5, p. 3233–3252.

Wright, T.L., and Clague, D.A., 1989, Petrology of Hawaiian lava, *in* Winterer, E.L., Hussong, D.M., and Decker, R.W., eds., The eastern Pacific Ocean and Hawaii, v. N *of* The geology of North America: Boulder, Colo., Geological Society of America, p. 218–237.

☆ U.S. GOVERNMENT PRINTING OFFICE: 1997 - 573-046 / 20071 REGION NO. 8

SELECTED SERIES OF U.S. GEOLOGICAL SURVEY PUBLICATIONS

Periodicals

Earthquakes & Volcanoes (issued bimonthly).
Preliminary Determination of Epicenters (issued monthly).

Technical Books and Reports

Professional Papers are mainly comprehensive scientific reports of wide and lasting interest and importance to professional scientists and engineers. Included are reports on the results of resource studies and of topographic, hydrologic, and geologic investigations. They also include collections of related papers addressing different aspects of a single scientific topic.

Bulletins contain significant data and interpretations that are of lasting scientific interest but are generally more limited in scope or geographic coverage than Professional Papers. They include the results of resource studies and of geologic and topographic investigations; as well as collections of short papers related to a specific topic.

Water-Supply Papers are comprehensive reports that present significant interpretive results of hydrologic investigations of wide interest to professional geologists, hydrologists, and engineers. The series covers investigations in all phases of hydrology, including hydrology, availability of water, quality of water, and use of water.

Circulars present administrative information or important scientific information of wide popular interest in a format designed for distribution at no cost to the public. Information is usually of short-term interest.

Water-Resources Investigations Reports are papers of an interpretive nature made available to the public outside the formal USGS publications series. Copies are reproduced on request unlike formal USGS publications, and they are also available for public inspection at depositories indicated in USGS catalogs.

Open-File Reports include unpublished manuscript reports, maps, and other material that are made available for public consultation at depositories. They are a nonpermanent form of publication that may be cited in other publications as sources of information.

Maps

Geologic Quadrangle Maps are multicolor geologic maps on topographic bases in 7 1/2- or 15-minute quadrangle formats (scales mainly 1:24,000 or 1:62,500) showing bedrock, surficial, or engineering geology. Maps generally include brief texts; some maps include structure and columnar sections only.

Geophysical Investigations Maps are on topographic or planimetric bases at various scales, they show results of surveys using geophysical techniques, such as gravity, magnetic, seismic, or radioactivity, which reflect subsurface structures that are of economic or geologic significance. Many maps include correlations with the geology.

Miscellaneous Investigations Series Maps are on planimetric or topographic bases of regular and irregular areas at various scales; they present a wide variety of format and subject matter. The series also includes 7 1/2-minute quadrangle photogeologic maps on planimetric bases which show geology as interpreted from aerial photographs. The series also includes maps of Mars and the Moon.

Coal Investigations Maps are geologic maps on topographic or planimetric bases at various scales showing bedrock or surficial geology, stratigraphy, and structural relations in certain coal-resource areas.

Oil and Gas Investigations Charts show stratigraphic information for certain oil and gas fields and other areas having petroleum potential.

Miscellaneous Field Studies Maps are multicolor or black-and-white maps on topographic or planimetric bases on quadrangle or irregular areas at various scales. Pre-1971 maps show bedrock geology in relation to specific mining or mineral-deposit problems; post-1971 maps are primarily black-and-white maps on various subjects such as environmental studies or wilderness mineral investigations.

Hydrologic Investigations Atlases are multicolored or black-and-white maps on topographic or planimetric bases presenting a wide range of geohydrologic data of both regular and irregular areas; the principal scale is 1:24,000, and regional studies are at 1:250,000 scale or smaller.

Catalogs

Permanent catalogs, as well as some others, giving comprehensive listings of U.S. Geological Survey publications are available under the conditions indicated below from USGS Map Distribution, Box 25286, Building 810, Denver Federal Center, Denver, CO 80225. (See latest Price and Availability List.)

"Publications of the Geological Survey, 1879-1961" may be purchased by mail and over the counter in paperback book form and as a set microfiche.

"Publications of the Geological Survey, 1962-1970" may be purchased by mail and over the counter in paperback book form and as a set of microfiche.

"Publications of the U.S. Geological Survey, 1971-1981" may be purchased by mail and over the counter in paperback book form (two volumes, publications listing and index) and as a set of microfiche.

Supplements for 1982, 1983, 1984, 1985, 1986, and for subsequent years since the last permanent catalog may be purchased by mail and over the counter in paperback book form.

State catalogs, "List of U.S. Geological Survey Geologic and Water-Supply Reports and Maps For (State)," may be purchased by mail and over the counter in paperback booklet form only.

"Price and Availability List of U.S. Geological Survey Publications," issued annually, is available free of charge in paperback booklet form only.

Selected copies of a monthly catalog "New Publications of the U.S. Geological Survey" is available free of charge by mail or may be obtained over the counter in paperback booklet form only. Those wishing a free subscription to the monthly catalog "New Publications of the U.S. Geological Survey" should write to the U.S. Geological Survey, 582 National Center, Reston, VA 22092.

Note.–Prices of Government publications listed in older catalogs, announcements, and publications may be incorrect. Therefore, the prices charged may differ from the prices in catalogs, announcements, and publications.